THE EFFECT OF CHRONIC INGESTION OF AFRIPLEX GRT™ ON MYOCARDIAL INSULIN RESISTANCE AND MITOCHONDRIAL FUNCTION – A PRECLINICAL STUDY.

by

Marlouw Kroukamp

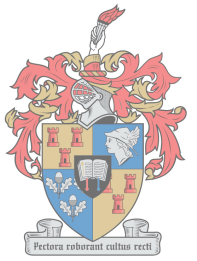

UNIVERSITEIT
iYUNIVESITHI
STELLENBOSCH
UNIVERSITY

Thesis presented in fulfilment of the requirements for the degree of Master of Science in Medical Sciences in the Faculty of Medicine and Health Sciences at Stellenbosch University

Supervisor: Prof. Barbara Huisamen

March 2018

DECLARATION

By submitting this thesis electronically, I declare that the entirety of the work contained therein is my own original work, that I am the authorship owner thereof (unless to the extent explicitly otherwise stated), that reproduction and publication thereof by Stellenbosch University will not infringe any third party rights and that I have not previously in its entirety or in part submitted it for obtaining any qualification.

Signature:

Date: 25 January 2018

ABSTRACT

Introduction: Obesity is an excessive fat accumulation in the body, known to be a significant precursor to insulin resistance and type 2 diabetes. Complications associated with obesity can contribute to the development of cardiovascular disease which, in turn, is associated with abnormal mitochondrial energetics. Rooibos (*Aspalathus linearis*) has known antidiabetic, anti-obesity and cardiovascular benefits. We investigated these properties with a focus on mitochondrial function, using an aspalathin-rich green rooibos extract, Afriplex GRT Extract.

Aims: (i) To determine whether Afriplex GRT Extract ingestion can improve the insulin resistance state elicited by a high fat diet using a rat model. (ii) To determine whether Afriplex GRT Extract ingestion has any effects on myocardial mitochondrial oxidative phosphorylation potential and the process of mitophagy

Methods: Male Wistar rats were fed either a control or a high fat diet (HFD) for 16 weeks. Half of each group was treated with Afriplex GRT Extract (60mg/kg/day) from weeks 11 to 16. Body weight, food and water intake were monitored, and liver- and intraperitoneal fat (IP) weighed at sacrifice. After sacrifice, myocardial mitochondria were isolated. Half of these were used to measure respiration on an oxygraph and the other half for Western Blot analysis of proteins involved in mitophagy. In addition, hearts were freeze clamped immediately after sacrifice and used to determine levels of insulin signalling proteins.

Results: The HFD caused increased body weight-, liver- and IP fat gain, and elevated leptin levels while it decreased insulin signalling protein expression (GLUT4, tAkt/PKB and tAMPK). Ingestion of Afriplex GRT Extract diminished the weight gain, liver weight gain, IP fat weight gain and leptin in HFD animals. Moreover, it improved oral glucose tolerance in control animals and, according to a borderline significance in a HOMA-IR calculation, insulin resistance in the control animals. However, an increased basal glucose level was seen in HFD animals treated with Afriplex GRT Extract. Afriplex GRT Extract improved mitochondrial coupling efficiency in HFD animals and oxidative phosphorylation in control animals. Afriplex GRT Extract decreased mitochondrial p62 and cytosolic Beclin-1 levels and BNIP3 dimerization in the mitochondria of the control animals, while increasing autophagic flux (LC3-II expression) in hearts from HFD animals. A decrease in Sesn2 levels indicated possible anti-oxidant effects.

Conclusion: We conclude that Afriplex GRT Extract resulted in less weight gain in HFD animals, improved whole-body insulin sensitivity and enhanced mitochondrial function. At the dose used, no detrimental effects were observed.

OPSOMMING

Inleiding: Vetsug is ‘n oormatige vet akkumulasie in die liggaam en ‘n belangrike oorsaaklike faktor vir insulien-weerstandigheid en tipe 2 diabetes. Komplikasies geassosieer met vetsug kan bydra tot die ontwikkeling van kardiovaskulêre siektes, wat weer geassosieer word met abnormale mitochondriale funksie. Rooibos (*Aspalathus linearis*) is bekend vir anti-diabetiese, anti-vetsug en kardiovaskulêre voordele. Ons het hierdie eienskappe ondersoek met ‘n fokus op mitochondriale funksie, deur die gebruik van ‘n aspalatien-ryk groen rooibos ekstrak, Afriplex GRT Ekstrak.

Doelstellings: (i) Om te bepaal of die inname van Afriplex GRT Ekstrak insulien-weerstandigheid, geïnduseer deur ‘n hoë vet dieet in ‘n rotmodel, kan verbeter. (ii) Om te bepaal of die inname van Afriplex GRT Ekstrak enige effek het op miokardiale mitochondrale oksidatiewe fosforilasie potensiaal en die proses van mitofagie.

Metodes: Manlike Wistar rotte is gevoer met óf ‘n normale kontrole dieët (standaard rotkos) óf ‘n hoë vet dieët (HFD) vir 16 weke. Die helfte van elke groep is behandel met Afriplex GRT Ekstrak (60mg/kg/dag) vanaf weke 11 tot 16. Liggaamsgewig, kos- en water inname was gemonitor en die lewergewig en intra-peritoniele (IP) vet gemeet na terminasie. Miokardiale mitochondria is geisoleer: een helfte van die preparaat was gebruik om respirasie te meet in ‘n oksigraaf, en die ander helfte vir Westerse klad analise van mitofagie geassosieerde proteïene. Harte is ook onder basale omstandighede gevriesklamp en gebruik om die vlakke van die insulien seintransduksiepad proteïene te bepaal.

Resultate: Die HFD het ‘n verhoging veroorsaak in liggaamsgewig-, lewer- en IP vet toename, sowel as in leptien vlakke teweeggebring. Daar was ook ‘n afname in insulienseintransduksie proteïene (GLUT4, tAkt/PKB, en tAMPK). Die inname van Afriplex GRT Ekstrak het die gewig toename sowel as die lewer, IP vet toename en leptien vlakke in die HFD diere verlaag. Afriplex GRT Ekstrak het die orale glukose toleransie in kontrole diere en, volgens ‘n grensgeval beduidendheid van ‘n HOMA-IR berekening, insulien weerstandigheid in die kontrole diere verbeter. Daarteenoor is verhoogde basale glukose vlakke in die HFD diere wat behandel was met Afriplex GRT Ekstrak, waargeneem. Afriplex GRT Ekstrak behandeling het die mitochondriale koppeling in die HFD diere en oksidatiewe fosforilasie in die kontrole diere verbeter. Dit het ook ‘n afname veroorsaak in mitochondriale p62, sitosoliese Beclin-1 vlakke en BNIP3 dimerisering in die harte van kontrole diere, terwyl dit ‘n verhoogte autofagie-fluks (LC3-II uitdrukking) in die harte van die HFD groepe veroorsaak het. Verlaagde Sesn2 uitdrukking dui moontlike anti-oksidatiewe effekte aan.

Gevolgtrekking: Afriplex GRT Ekstrak het gewigsverlies in HFD diere teweeggebring en insulien-weerstandigheid en mitochondriale funksie verbeter. Met die dosis gebruik was daar geen nadelige effekte waargeneem nie.

ACKNOWLEDGEMENTS

- I would firstly like to acknowledge the Division of Medical Physiology for the opportunity and privilege to partake in this research project, and my Supervisor, Professor Barbara Huisamen, for her guidance, advice, encouragement and endless support throughout my research project.

- A very special thank you to my colleagues in the Division of Medical Physiology, especially to Mignon Van Vuuren, Zimvo Maqeda and Yolandi Espach for their friendship, patience and encouragement.

- Another special thank you to my fiancé (Jarrett Engelbrecht), my two amazing parents (Hans and Martha Kroukamp), my brother (Tian Kroukamp) and the rest of my family and friends for their love, support and encouragement. Another very special thank you to my god-parents, Belinda and Tim Wilkes, whom have carried me throughout all my studies.

- A special thank you to the National Research Foundation, the Harry Crossley Foundation and the University of Stellenbosch for funding throughout my MSc studies.

- A part of this thesis has been presented as a poster at the PSSA Conference 2017 in Pretoria, where I have obtained third place in the Johnny van der Walt Poster Competition.

- Lastly, I would love to give praise and thank my Heavenly Father for giving me the ability and strength to complete my master's degree.

DEDICATIONS

I would like to dedicate my work to my grandmother Isabel Kroukamp (08-07-1932 – 30-11-2016), who always loved and supported me, especially throughout my studies. She is missed dearly, every day.

DISCLOSURE OF INTEREST

I have no interests to disclose.

Signed on the ...25th..... day of …January…….. 2018

at ……Tygerberg……..……..

.

…….. ……..

(Prof. B. Huisamen) (Marlouw Kroukamp)

TABLE OF CONTENTS

LIST OF FIGURES

CHAPTER 1

CHAPTER 2

CHAPTER 3……

LIST OF TABLES

LIST OF ABBREVIATIONS

°C	Degree Celsius
µl	Microliter
2DG	2-Deoxy-D-^{3}[H] glucose
AAC	ADP-ATP carrier
Acetyl-CoA	Acetyl-coenzyme A
ADH	Antidiuretic hormone
ADP	Adenosine diphosphate
AMPK	AMP-activated protein kinase
ANOVA	Analysis of Variance
ANT	Adenine nucleotide translocator
AS160	Akt substrate of 160 kDa
ATG	Autophagy related proteins
ATM	Ataxia-telangiectasia mutated
ATP	Adenosine triphosphate
Bax	Bcl-2-associated X protein
Bcl-2	B-cell lymphoma 2
BDM	2,3-butanedione monoxime
BMI	Body mass index
BNIP3	Bcl-2/adenovirus E1B 19-kDa protein-interacting protein 3
BSA	Bovine serum albumin
Ca^{2+}	Calcium
$CaCl_2$	Calcium Chloride
CAP	Catabolite Activator Protein
CD36	Cluster of differentiation 36
cm	Centimeter
CoQ	Coenzyme-Q

CPT-1	Carnitine palmitoyl-transferase 1
CPT-2	Carnitine palmitoyl-transferase 2
CsA	Cyclosporine A
$CuSO_4$	Copper (II) sulphate
CVD	Cardiovascular disease
Cyp-D	Cyclophilin-D
DAN	Diabetic autonomic neuropathy
DCM	Diabetic cardiomyopathy
dH_2O	Distilled water
DHAP	Dihydroxyacetone phosphate
DNA	Deoxyribonucleic acid
DPM	Disintegrations per minute
DPP-4	Dipeptidyl peptidase-4 inhibitor
DPPH	2,2-diphenyl-1-picrylhydrazyl
DTNB	5.5'-Dithiobis-(2-nitrobenzoic acid)
ECL	Enhanced chemiluminescence
EDTA	Ethylenediaminetetraaetic acid
EGTA	Ethylene glycol tetraacetic acid
ELISA	Enzyme-linked immunosorbent assay
ERK	Extracellular signal-regulated kinase
ET-1	Endothelin-1
ETC	Electron transport chain
F1F0-ATPase	ATP synthase
F6P	Fructose-6-phosphate
FAD	Flavin adenine dinucleotide
FAT/CD36	Fatty acid translocase CD36
FBP	Fructose-1,6-bisphosphate
FFA	Free fatty acids

FoxO1	Forkhead box protein O1
FRE	Fermented rooibos
FUNDC1	FUN14 Domain Containing 1
g	Grams
G6Pase	Glucose 6-phosphate
GAP	Glyceraldehyde-3-phosphate
GAPDH	Glyceraldehyde-3-phosphate dehydrogenase
GLP-1	Glucagon-like peptide-1
GLUT4	Glucose transporter 4
GRB2	Growth factor receptor-bound protein 2
GSH	Glutathione
GSK-3β	Glycogen synthase kinase-3β
GTPase	Small GTP-binding proteins
H^+	Hydrogen
HCl	Hydrochloric acid
Hepes	4-(2-hydroxyethyl)-1-piperazineethanesulfonic acid
HFD	High fat diet
HIF-1	Hypoxia-inducible factor-1 responsive element
HRP	Horse radish peroxidase
IL-6	Interleukin-6
IMM	Inner mitochondrial membrane
IP fat	Intraperitoneal fat
IR	Insulin receptor
IRS	Insulin receptor substrate
IRS-2	Insulin receptor substrate 2
JNK	c-Jun N-terminal kinase
KCl	Potassium chloride
kDa	Kilo Dalton

kg	Kilogram
LC3	Protein 1A/1B-light chain 3
LDL	Low density lipoprotein
m	Meter
M	Molar
MAPK	Mitogen-activated protein kinase
MCU	Mitochondrial Ca^{2+} uniporter
MEK1	Mitogen-activated protein kinase kinase
Mfn2	Mitofusin 2
mg	Milligram
$MgSO_4$	Magnesium sulfate
min	Minutes
ml	Milliliter
mm	Millimeter
mPTP	Mitochondrial permeability transition pore
mTOR	Mammalian target of rapamycin
mTORc1	mTOR complex 1
Na	Sodium
Na_2HPO_4	Di-Sodium hydrogen phosphate
$Na_2S_2O_4$	Sodium dithionite
Na_3VO_4	Sodium orthovanadate
NaCl	Sodium chloride
NAD^+	Nicotinamide adenine dinucleotide
NADH	Nicotinamide adenine dinucleotide
NaH_2PO_4	Sodium dihydrogen phosphate
NaOH	Sodium hydroxide
NBR1	Neighbour of BRCA1 gene 1
nM	Nano Molar

Nm	Nanometres
NO	Nitric oxide
NOS	Nitric oxide synthase
O_2	Oxygen
O-G1cNAc	O-linked N-acetylglucosamine
OGTT	Oral glucose tolerance test
OMM	Outer mitochondrial membrane
p62	Sequestosome-1
PAI-1	Plasminogen activator inhibitor 1
PDH	Pyruvate dehydrogenase
PDK	Pyruvate dehydrogenase kinase
PDK1	3-phosphoinositide-dependent protein kinase 1
PDK4	Pyruvate dehydrogenase kinase 4
PDP	Pyruvate dehydrogenase phosphatase
PEP	Phosphoenolpyruvate
PGC-1α	Peroxisome proliferator-activated receptor gamma coactivator-1α
PGK	Phosphoglycerate kinase
PGM	Phosphoglycerate mutase
PH	Pleckstrin homology domain
P_i	Inorganic phosphate
PI3K	Phosphoinositide 3-kinase
PINK1	PTEN-induced putative kinase protein 1
PIP2	Phosphoinositide 3,4-biphosphate
PIP3	Phosphoinositide (3,4,5) triphosphate
PKB	Protein kinase B
pmol	Picomol
PMSF	Phenylmethyl sulfonyl fluoride
PPAG	Phenylpropenoic acid glucoside

PPARα	Peroxisome proliferator-activated receptor alpha
PPARγ	Peroxisome proliferator-activated receptor gamma
PTB	Phosphotyrosine binding
PTEN	Phosphatase and tensin homolog
PVDF	Polyvinylidene fluoride
QO2	Mitochondrial oxygen consumption
RCI	Respiratory control index
RHEB	Ras homolog enriched in brain
ROS	Reactive oxygen specie
rpm	Revolutions per minute
SDS	Sodium dodecyl sulfate
SDS-PAGE	Sodium dodecyl sulfate-polyacrylamide gel electrophoresis
sec	Seconds
SEM	Standard Error of the Mean
Sesn2	Sestrin2
SGLT2	Sodium-glucose co-transporter 2
SH-2	Src homology 2
SHC	SHC-transforming protein 1
SMAC/Diablo	Second mitochondria-derived activator of caspases
SOS	Son of sevenless homolog 1
STZ	Streptozotocin
SU	Sulfonylureas
T1D	Type 1 diabetes
T2D	Type 2 diabetes
TBC1D1	TBC1 domain family member 1
TBS	Tris-buffered saline
TCA	Trichloracetic acid
TIM	Translocase of inner membrane

TMB	3,3’,5,5’-Tetramethylbenzidine substrate
TNF-α	Tumor necrosis factor-alpha
TOM	Translocase of outer membrane
TSC1	Tuberous sclerosis 1
TSC2	Tuberous sclerosis 2
UbI	Ubiquitin-like
ULK1	Unc-51 Like autophagy activating Kinase 1
VDAC	Voltage-dependent anion channels
Vps	Vacuolar protein sorting
vWF	von Willebrand factor
WC	Waist circumference
WHO	World Health Organization
WHR	Waist to hip ratio
WHtR	Waist to height ratio

CHAPTER 1: Literature Review

Rooibos, an indigenous plant to South Africa, is source to a famous and well-loved traditional tea. Afriplex GRT Extract is a spray dried, laboratory standardized extract made from green rooibos and has a high aspalathin content. Aspalathin is a potent anti-oxidant that is said to have positive effects on diabetic patients (Koza, 2013). With the increasing interest in natural products, the modern society always searches for more plant-based medicines and diets. In this thesis, it will be discussed how obesity can lead to cardiovascular diseases (CVDs), through insulin resistance and diabetes. With a focus on mitochondrial energetics, fat metabolism, glucose metabolism and insulin signalling, the effects of Afriplex GRT Extract will be investigated.

1. From Obesity to Diabetes

Obesity is an excessive accumulation of fat in the body (Hebebrand, et al., 2017). It is currently so common in the human population that it is seen as the most significant contributor to ill health, more so than undernutrition and infectious diseases (Kopelman, 2000). Obesity has been recognized as an epidemic that causes a rise in diabetes; and the notion that obesity is a significant and very common precursor to diabetes has been proved and demonstrated by previous research (Morris, et al., 1989).

In an interview with Dr. Vash Mungal-Singh (CEO of the Heart and Stroke Foundation of South Africa), she explained why South Africa is facing this “obesity epidemic” (Pan American Health Organization, 2012). She explains that South Africans “eat too much, drink too much alcohol, and don’t move enough.” Obesity does not only lead to diabetes, but it can cause a plethora of health problems such as insulin resistance, joint pain, hypertension, strokes, cardiovascular disease and some cancers (Kopelman, 2000; Formiguera & Cantón, 2004).

According to The World Health Organization (2016), since 1980, obesity has more than doubled (The Heart and Stroke Foundation South Africa, 2016). Out of 1.9 billion overweight people, 600 million were classified as obese. In 2014, 39% of adults (18 years and above) were overweight and 13% obese. More concerning is that 41 million children (under the age of 5) were already overweight/obese in 2014. South Africa has

the highest overweight and obesity rate across sub-Saharan Africa. A third of our men and 70% of our women are classified as overweight or obese (The Heart and Stroke Foundation South Africa, 2016). Amongst children between the ages of 2 and 14 years, 1 in 4 girls and 1 in 5 boys are either overweight or obese.

Obesity is driven by a change in eating habits and a decrease in physical activity of the human population. Dr. Mungal-Singh clarifies that, due to the increase in urbanisation and 'faster paced lifestyles,' people rely more and more on fast foods and Westernised diets (high in sugar, salt and unhealthy fats) (The Heart and Stroke Foundation South Africa, 2016). Obesity occurs when energy intake (mainly stored as triglycerides) is greater than energy output (Spiegelman & Flier, 2001). Due to this rise in energy intake, body-weight increases to an extent where there are substantial health consequences .

Adipose tissue is the main storage site for triglycerides (Ashrafi, 2007). In mammals, this connective tissue comes in two types namely; white and brown adipose tissue (Eder, et al., 2009). For this thesis, focus will be shifted solely to white adipose tissue. Not only does white adipose tissue serve as a source of energy, but it has functions in both heat insulation and mechanical cushion. Adipose tissue can be found subcutaneously, where its function as heat insulator is utilized. By surrounding internal organs, adipose tissue can also prevent physical shock to these organs (such as the kidneys) (Ashrafi, 2007).

White adipose tissue, especially visceral adipose tissue, is recognized as an endocrine organ and secretes many protein hormones such as; leptin (which is a cytokine-like hormone secreted in proportion to fat mass), adipokines (such as interleukin-6 (IL-6)) and adiponectin (Maffei, et al., 1995; Trayhurn & Bing, 2006; Eder, et al., 2009). The pancreas produces insulin, which is also secreted in proportion to fat mass (Friedman & Halaas, 1998). Insulin is one of the regulators that sustain energy balance and, along with leptin, cause inhibitory effects on energy intake (Ashrafi, 2007).

Adiponectin is the most profusely secreted protein by white adipose tissue (Brochu-Gaudreau, et al., 2010). Adiponectin has anti-inflammatory, insulin-sensitizing and anti-atherosclerotic properties. The insulin-sensitizing properties of adiponectin is regulated by its activation of AMP-activated protein kinase (AMPK), p38 mitogen-activated protein kinase (MAPK) and PPARα (peroxisome proliferator-activated

receptor aplha) (Deepa & Dong, 2009). Adiponectin is also a direct regulator of IL-6, which is a pro-inflammatory factor and a key regulator in inflammation, haematopoiesis and immune responses (Akira, et al., 1993). Decreased serum levels of adiponectin can be seen in obesity and type 2 diabetes (T2D) (Li & Wu, 2012). Furthermore, adiponectin levels are inversely correlated with cardiovascular disease development (Shibata, et al., 2009).

1.1. Assessing Obesity

1.1.1. Body Mass Index (BMI)

To calculate a person's BMI, the patient's weight (kg) is divided by the square of the height (m^2) (Department of Health and Human Services USA, n.d.) (Kopelman, 2000).

A body-mass index (BMI) of 30 kg m^{-2} or more indicates obesity in humans. However, when the BMI is between 25 kg m^{-2} and 29.9 kg m^{-2}, the person is considered overweight (Hu, 2008).

While BMI is an easy and inexpensive way of assessing obesity, many say that it is not the most accurate way of measuring obesity. In Medical News Today, an article was published by Christian Nordqvist stating that BMI does not take muscle mass, bone density, body composition, racial differences or gender differences into account (Nordqvist, 2013).

1.1.2. Waist-to-height Ratio (WHtR)

Waist-to-height ratio is a better measuring tool than BMI (Ashwell, et al., 2014). It is much simpler, because it uses the waist circumference and height. It is also a better method because, unlike BMI that does not consider lean body mass versus body fat, it includes the waist. The waist is a prime spot for abdominal fat to accumulate.

The waist-to-height ratio stipulates that the waist circumference should be less than half the height.

1.1.3. Waist Circumference (WC)

To measure the WC is also easy and inexpensive. The WC is measured either at the waist, belly button, or the smallest point of the midsection (Hu, 2008). Using WC as an indicator of obesity is suitable because of its simplicity and the direct relationship between the WC and the abdominal fat mass (Pouliot, et al., 1994). Men with a WC of

120 cm (or more) and women with a WC of 88 cm (or more) are normally considered to be at risk for cardio-metabolic disease (Wang, et al., 2005).

1.1.4. Waist-to-hip Ratio (WHR)

The WHR is the ratio of the circumference of the waist to the circumference of the hip. The WHR measures the abdominal obesity, similarly to the WC. The WHR is calculated by measuring the waist- and hip circumference, followed by the dividing of the waist measurement by the hip measurement (Hu, 2008). A WHR of more than 0.8 (in women) and 0.9 (in men) is considered excess abdominal fat distribution, according to a report from the WHO (World Health Organization, 2008).

1.1.5. Skinfold Thickness

To measure the skinfold thickness, a special calliper is used to pinch the skin and fat underneath it. This is done in certain areas of the body, such as the trunk, thighs and parts of the upper arm. Predictions of the body fat percentage is calculated with specific equations (Hu, 2008). To measure the skinfold thickness is convenient, safe, inexpensive and easy. It is, however, not very accurate or reproducible (Hu, 2008).

1.2. Insulin Resistance

Obesity is a leading risk factor for developing insulin resistance (National Institute of Diabetes and Digestive and Kidney Diseases, 2009). Insulin is secreted post-prandial and is the main hormone regulating high blood glucose levels. Insulin stimulates peripheral insulin sensitive tissue such as the liver, fat, heart and muscle to take up glucose from the circulation into the cells (see *'2.3 Insulin Metabolism'*) (Roland, 2016). When a person is insulin resistant, the peripheral tissue becomes resistant to the action of insulin to an extent that it cannot stimulate the cells effectively anymore. In other words, the body does produce insulin, but it is not used efficiently (Cefalu, 2001). Because the cells are not able to absorb the glucose efficiently, it causes a high glucose content in the blood.

Insulin resistance can thus lead to damaged blood vessels, increasing the risk for heart diseases and strokes (National Institute of Diabetes and Digestive and Kidney Diseases, 2009). Endothelial cells of the blood vessels secrete vasoconstrictors and vasodilators that regulate the microvascular flow (Lewis, 1998). Hyperglycaemia

causes an inhibition of and decrease in the production of the vasodilator, nitric oxide (NO), in arterial endothelial cells (Williams, et al., 1998; Brownlee, 2001; Brochu-Gaudreau, et al., 2010). High blood pressure and an eventual narrowing of the blood vessels are caused by this decrease (Vallance & Norman, 2001; Hoshiyama, et al., 2003; Koh, et al., 2005).

When there is a high blood glucose level for an extended period, the blood vessels are not able to relax or dilate properly (Koh, et al., 2005). The phosphorylation of nitric oxide synthase results in the production of NO. Excess glucose causes high levels in the glucose derived monosaccharide O-linked N-acetylglucosamine (O-G1cNAc) (Liu, et al., 2000). High O-G1cNAc levels inhibit this phosphorylation, thus decreasing nitric oxide production (Karunakaran & Jeoung, 2010). Without sufficient nitric oxide levels, the blood vessels are constantly contracted and would ultimately negatively influence the passage of blood through these vessels. This poor circulation will increase the risk of strokes and heart attacks (more under *'2.6. Pathophysiology of Diabetes'*).

Developing T2D is another risk of insulin resistance (Balarini & Braga, 2016). The link between insulin resistance and prediabetes or T2D is evident. Since insulin resistance already places a high demand on the β-cells for insulin secretion, T2D can develop. When a person is prediabetic, the blood glucose levels are normal because the β-cells can still produce necessary insulin to overcome the insulin resistance (see Figure 1.1 below) (Bell, 2003; Tabák, et al., 2012). Insulin levels are, however, higher than normal. This stress on the pancreas leads to an unceasing loss of β-cell function, resulting in the development of T2D. This is the tipping point where the pancreas is unable to secrete enough insulin, therefore blood glucose levels rise above normal. It has been shown that prediabetic persons are prone to develop T2D within 10 years, if they do not change their lifestyle by losing weight and increasing physical activity (National Institute of Diabetes and Digestive and Kidney Diseases, 2009).

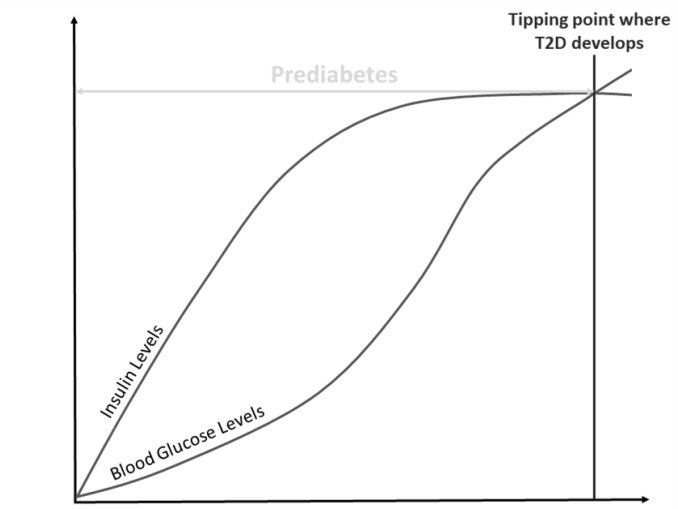

Figure 1.1 *The progression of prediabetes to type 2 diabetes (T2D) (Bell, 2003; Tabák, et al., 2012).*

1.2.1. Assessing insulin resistance

1.2.1.1. Oral Glucose Tolerance Test

An Oral Glucose Tolerance Test (OGTT) is a procedure used to diagnose insulin resistance or prediabetes (Center for Young Women's Health, 2016). This test determines how efficiently the body metabolises sugar or carbohydrates. When doing an OGTT on a human, the patient is given a concentrated sugary drink when in a fasting state. The blood glucose level is tested at basal level (before ingestion of the drink) and at different intervals thereafter up to 120 min. Diabetic persons will have a blood glucose level of more than 10.0 mmol/L at 2 hours, whereas a non-diabetic person will have a blood glucose level of less than 7.8 mmol/L (American Diabetes Association, 2006).

In rodents, sucrose, at a concentration of 1 g/kg, is given to the rats after an overnight fast by oral gavage. Accordingly, the blood glucose levels are measured at basal level and at different intervals up to 120 min.

1.2.1.2. The HOMA-IR Index

Another way of assessing insulin resistance and β-cell function is the HOMA-IR (homeostatic model of insulin resistance) assessment. This is calculated from fasting glucose and insulin or C-peptide concentrations (Matthews, et al., 1985).

The equations to calculate the HOMA-IR and HOMA-β can be seen below:

$$HOMA - IR = {Glucose\ \left(\frac{mmol}{L}\right) \times Insulin\left(\frac{mU}{L}\right)} \Big/ {22.5}$$

$$HOMA - \beta = {20 \times Insulin\left(\frac{mU}{L}\right)} \Big/ {Glucose\ \left(\frac{mmol}{L}\right) - 3.5}\ \%$$

The HOMA-β calculates the β-cell function, whereas HOMA-IR calculate insulin resistance. For the purpose of this thesis, we will only be calculating the HOMA-IR index, because insulin resistance is the point of interest in this case.

1.3. Diabetes

Obesity is a preventable disease and so is T2D. Koza (2013) states that, according to the Human Sciences Research Council's 2013 health and nutrition survey, one in 10 South Africans live with diabetes; and a quarter of people (between ages 55 and 64) are on their way to developing diabetes because of their extremely high blood sugar levels. People that develop T2D later in life have very high sugar levels because their bodies cannot utilize the amount of sugar that they ingest fast enough. An approximation that the prevalence of diabetes will increase to 552 million by 2030 was made by The International Diabetes Federation. It is said that 95% of that 552 million is associated with T2D (WHO Fact Sheet No: 311 , 2016).

Of diabetic people above the age of 65, at least 68 % die from some form of a heart disease. Another statistic stated by the American Heart Association (2015) declares that diabetic adults are more likely to develop heart disease than non-diabetic people. Thus, it is said that diabetes is one of the seven major controllable risk factors for CVD.

Diabetes is a condition of hyperglycaemia (Rother, 2007). There are currently 3 types of diabetes; recognized by either pancreatic β-cells that are not able to maintain sufficient insulin secretion, or because the insulin is no longer used efficiently by the body. (i) Type 1 diabetes (T1D) is a T-cell mediated autoimmune response against the β-cells that can be influenced by environmental factors and genetics. This causes

destruction of the β-cells, thus producing insufficient insulin for the body to use. T1D is an incurable disease that needs insulin treatment.

(ii) In T2D, either insulin resistance or decreased β-cell function can be the cause (Rother, 2007). The insulin sensitivity is decreased in liver, adipose and muscle tissue, resulting in over secretion of insulin in the body. It prevents the body from clearing the blood glucose efficaciously. Refer to Figure 1.2 for the effects of T2D on the insulin signalling pathway (more discussed in '*2.3.1. Insulin Signalling*'). As previously mentioned under '*1.2. Insulin Resistance,'* we know T2D patients have high levels of blood glucose that can eventually lead to heart disease, stroke, kidney failure and many more complications (National Institute of Diabetes and Digestive and Kidney Diseases, 2009).

(iii) In pregnant women, gestational diabetes occurs when the woman suddenly becomes glucose intolerant (National Institute of Diabetes and Digestive and Kidney Diseases, 2009). This condition normally reverses after pregnancy.

Healthy eating, exercise, blood sugar monitoring and pharmacotherapy are involved in the management of T2D. The goal for treating diabetes is to maintain the blood sugar levels within the normal range (between 3.9 and 5.5 mmol/L) (Defronzo, 2009; Chatterjee & Davies, 2015; Spero, 2016). A high-fiber, low-fat diet is recommended for diabetes, as well as regular aerobic exercise. If diet and exercise do not improve blood sugar levels, diabetes medications or insulin therapy can be used. Possible treatments for T2D include metformin, meglitinides, sulfonylureas (SU), thiazolidinediones, DPP-4 inhibitors, glucagon-like peptide-1 (GLP-1) receptor agonists, SGLT2 inhibitors and insulin therapy. Metformin is, however, the most recommended treatment for T2D (National Institute of Diabetes and Digestive and Kidney Diseases, 2009).

Metformin (an AMPK activator) acts by reducing the glucose levels in plasma (Zhou, et al., 2001; Madiraju, et al., 2014). Metformin also reduces gluconeogenesis, glucose secretion in the liver and endogenous glucose production. Moreover, metformin helps the body to utilize insulin more efficiently (similarly to thiazolidinediones). Thiazolidinediones improves insulin sensitivity and reduces β-cell failure by causing a decrease of free fatty acid accumulation and inflammatory cytokines; as well as an

increase in adiponectin levels and β-cell structure and function preservation (Consoli & Formoso, 2013). Metformin and thiazolidinediones are insulin sensitizers.

Meglitinides and SU are insulin secretagogues that help the body to secrete more insulin (Johnson, 2015). GLP-1 receptor agonists activate GLP-1 receptors in the small intestine to slow down digestion and pancreatic receptors to induce insulin secretion (Deacon, et al., 2012). Normally, GLP-1 is secreted by the L-cells of the gut on ingestion of a meal. It acts as an incretin hormone to decrease glucagon secretion and induce glucose-dependent insulin secretion from the pancreas even before the rise in plasma glucose or fatty acid levels (Lim & Brubaker, 2006; Marathe, et al., 2011). It has been shown that T2D patients have low levels of GLP-1 (Lastya, et al., 2014). GLP-1 is a protein therefore needs to be injected by the patient.

DPP-4 inhibitors inactivate the DPP-4 enzyme that usually breaks down GLP-1. DPP-4 inhibitors can be taken orally. DPP-4 inhibitors function and improve insulin secretion similarly to GLP-1 receptor agonists. SGLT2 inhibitors prevent the kidneys from reabsorbing glucose into the blood (Tahrani, et al., 2013). SGLT2 is found on the nephron and is responsible for more than 90 % of glucose reabsorption from the urinary filtrate. When SGLT2 is inhibited, this reabsorption is decreased and leads to increased glucose excretion in urine. As a last option, insulin therapy is sometimes needed in patients with T2D. Insulin cannot be taken orally, because insulin is a protein and will be broken down by the digestion system. Therefore, insulin is taken by injection.

To control blood glucose levels is a big challenge; and the use of plant derived nutraceuticals (along with current therapies that improve metabolic disturbances) can be helpful and promising (Rother, 2007; Dludla, et al., 2014). In Canada, for example, the increase in diabetes leads to the search for ways to manage T2D by plant-based diets. These are diets that discourage meat, eggs, diary and processed foods (Rinaldi, et al., 2016). Rinaldi et al., (2016) concludes that plant-based diets manage and prevent T2D by weight-loss properties and the ability to decrease cholesterol levels.

Medicinal plants have anti-hyperglycaemic effects because of their capability to restore pancreatic tissue function by either increasing insulin production, reducing glucose absorption in the intestines or facilitating metabolites in the insulin processes

(Malviya, et al., 2010). Researchers argue that plant derived medicines are low cost, less toxic and free from the side effects that come with synthetic drugs (Parikh, et al., 2014). Although this is not entirely true, the vast majority of indigenous people prefer natural products, and to a large portion of the South African population, it is all that is available to them. These are some of the reasons why the modern consumer prefers more natural products.

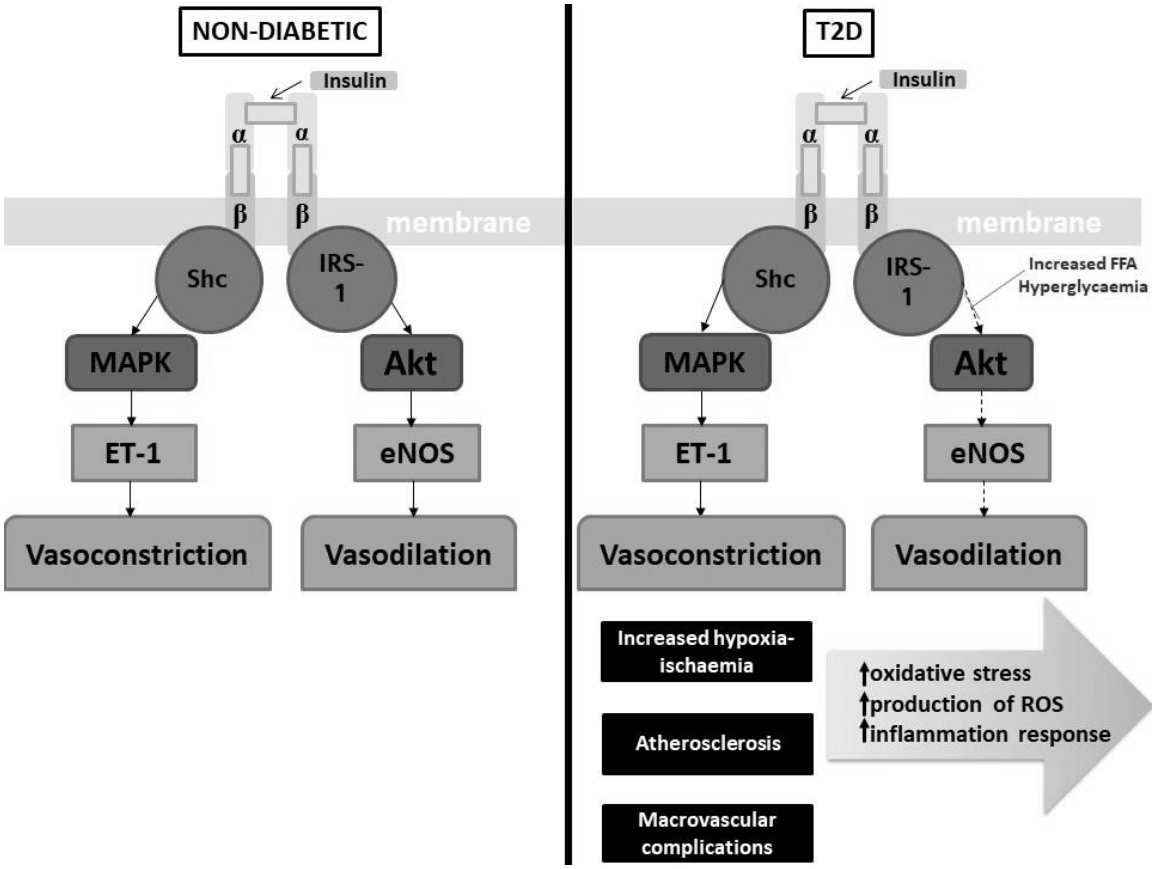

Figure 1.2 *A diagram showing the effects of T2D on insulin signalling (adapted from Aulston, et al., (2013)). The dotted lines indicate inhibition of the Akt pathway by increased FFA levels and hyperglycaemia. The solid lines indicate that the respective pathways are unaffected.*

1.4. Cardiovascular Disease

People with diabetes may suffer from certain conditions or complications that contribute to the development of CVD (Muhlestein, et al., 2003). These conditions include hypertension, abnormal cholesterol levels, high levels of triglycerides, obesity, absence of physical activity, and smoking (Dokken, 2008; American Heart Association, 2015).

Because of the high energy requirements of the heart, it can use fatty acids, carbohydrates, amino acids and ketone bodies as sources of energy (Lopaschuk, et al., 2010; Boundless, 2016). Under normal conditions, it will utilize fatty acids as the energy substrate of choice. Beta-oxidation of long-chain fatty acids provides energy to maintain the constant contractile activity of the heart (Lopaschuk, et al., 2010) (see *'2.1. Cardiac Metabolism'* for a detailed discussion). This oxidation is a complex metabolic process and ensures that the energy demands of the heart are met. Fatty acid metabolism is affected by alterations in contractile work, changes in hormone levels, limited oxygen supply and the presence of substrates such as glucose (Lopaschuk, et al., 2010). Alterations in the metabolism and excessive uptake and β-oxidation of fatty acids (as in obesity and diabetes) may negatively affect cardiac function (Lopaschuk, et al., 2010) (discussed in *'2.6.6. Heart Failure'*).

2. The Human, the Heart and its systems

2.1. Cardiac Metabolism

The heart is a vital organ that pumps not only blood, but nutrients and oxygen to the cells in our bodies (Stefan, 2015). With the cardiovascular system, the heart also has a waste removal function via the blood and vessels. The heart's wellbeing and health is of high importance and dysfunction in this organ can lead to major complications such as fatigue, an irregular heartbeat and much more. Lifestyle choices, genetics and age are only three of many factors that may compromise cardiac health.

Cardiomyocytes are terminally differentiated muscle cells (Woodcock & Matkovich, 2005). Cardiomyocytes are striated and contain actin and myosin filaments which are essential for the contractile activity of the heart. When these filaments slide over each other, the heart contracts. For this to happen, biochemical processes that require adenosine tri-phosphate (ATP) are necessary. ATP is the high-energy molecule ultimately responsible for contraction of the cardiomyocytes.

First, the ATP is bound to myosin allowing the myosin to move to a high-energy state. ATPase then converts ATP to ADP (adenosine diphosphate) and inorganic phosphate (P_i) (Figure 1.3) (Duke, 1999; Boundless, 2016). This energy release allows the myosin head to change position, rendering it ready to bind actin. ADP and P_i are still attached and myosin is still in a high energy state configuration. When calcium ions

attach to troponin (a protein complex), muscle contraction cycle is triggered. Consequently, active-binding sites on the actin is exposed. The myosin bridges the gap by attaching to the exposed actin-binding site. When the myosin binds to the actin, P_i is released, causing myosin to undergo a confirmation change to a lower energy state. As the energy is used by myosin, it pulls the actin-filament towards the M-line. The sarcomere will eventually shorten and cause the muscle to contract. This conformational change in myosin and pulling of the actin-filament is called the power stroke. The myosin is in a low-energy state after this power stroke.

Even though ADP is released after the power stroke, the bridge between myosin and actin is still in position. ATP moves the myosin to another high-energy state when it binds to it again, releasing the myosin head from the actin-filament (Lymn & Taylor, 1971). This muscle contraction cycle can then be repeated as soon as ATP is attached to myosin again. Without ATP, muscles would constantly be in their contracted state (hypercontracture).

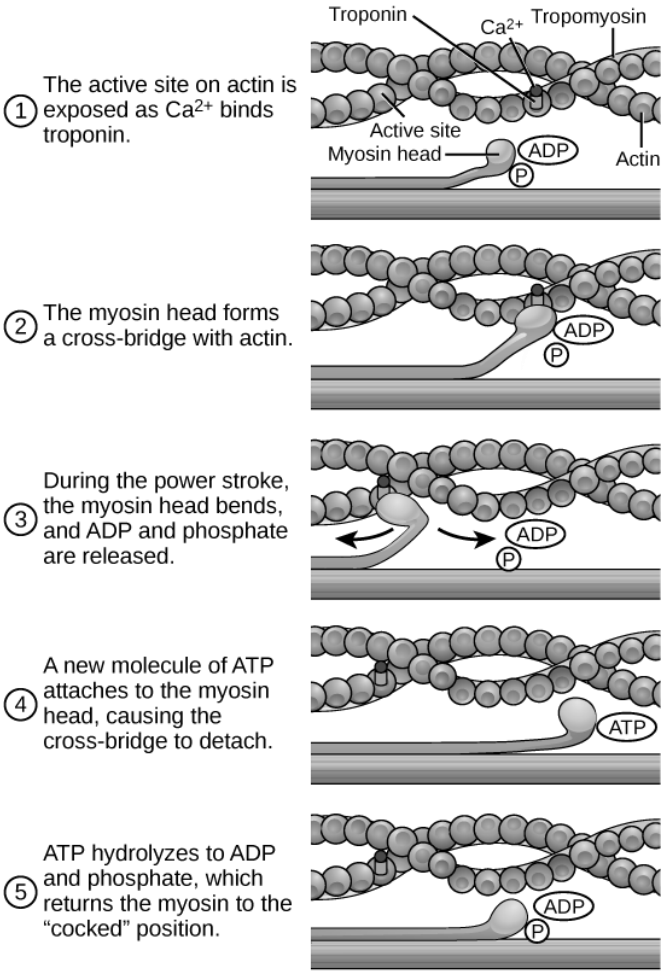

Figure 1.3 *The cross-bridge muscle contraction cycle (Boundless, 2016).*

It is well established that cells use ATP as a direct source of energy to accomplish different cellular tasks. These tasks include cellular division and substance transportation across the membrane. The latter statement makes it evident that ATP and its availability influences the survival or death of a cell. Unlike other organs, the heart does not have a large energy reserve and relies on external substrates to enter the heart and source ATP. Even though the mitochondrial ATP synthase enzyme (F_1F_0-ATPase) is the main synthesizer of ATP, it is also produced from the metabolism of substrates such as glucose, free fatty acids and lactate (Depre, et al., 1999). The heart is a constantly contracting organ, thus demanding continuous supply of ATP (Nagoshi, et al., 2011).

In the fed state, the heart preferentially uses carbohydrates as source of ATP because insulin levels are high. Contrastingly, in the fasted state, free fatty acids are the major ATP source of choice (Opie, 2004). As mentioned earlier, when ketone bodies and amino acids are abundant, the heart can also utilize these as sources of ATP. In the heart, more than 95% of ATP formation comes from the oxidative phosphorylation process in the mitochondria. The remaining ATP is generated by glycolysis and GTP formation in the citric acid cycle (also called Krebs cycle or TCA cycle).

(1) Glucose transporters (GLUT1 and GLUT4) transfer glucose into a cell (see '*2.2.3.2 Glycolysis*' for a detailed description) (Bonen, et al., 1990; Van Den Brom, et al., 2013). Glucose is converted to pyruvate through the glycolytic pathway in the cell cytoplasm (Nelson & Cox, 2004). The pyruvate dehydrogenase (PDH) complex, spanning the mitochondrial inner and outer membrane, is involved in the transformation of pyruvate to acetyl-CoA that will enter the citric acid cycle and electron transport chain (ETC) to produce ATP (Figures 1.4 and 1.5). PDPs (PDH phosphatases) and PDKs (PDH kinases) regulate PDH activity, and PDH is dephosphorylated in its active state.

(2) As mentioned earlier, free fatty acids are abundant in the blood when the body is in a fasted state, causing high free fatty acid intake into the heart (Bonen, et al., 2004; Opie, 2004). These free fatty acids are then used for oxidative metabolism. Passive diffusion or protein channels (cluster of differentiation 36 (CD36)) can transport the long chain fatty acids from the plasma into the cardiomyocytes (see *'2.2.2. Fatty Acid Metabolism'*). The free fatty acids (that have entered the cell) will then bind to the

intracellular fatty acid binding protein and be activated by coenzyme A (CoA) to form fatty Acyl-CoA derivatives.

Extra fatty Acyl-CoA can be stored as triglycerides. The CPT (carnitine palmitoyl transferase) system consist of CPT-1 and CPT-2 (McGarry & Brown, 1997). CPT-1 is an integral protein that converts long-chain fatty acids to acylcarnitine and shuttles it across the membrane to undergo β-oxidation and eventually produce acetyl-CoA. NADH (nicotinamide adenine dinucleotide) and acetyl-CoA are both coenzymes and by-products of β-oxidation (Stanley, et al., 2005). Acetyl-CoA is metabolised in the mitochondrial matrix through the citric acid cycle. NADH fuels the ETC and plays a role in ATP synthesis (more under '*2.2.1.1. Oxidative Phosphorylation*') (Stanley, et al., 2005).

Citrate synthase is one of the citric acid cycle enzymes and produces citrate by condensing acetyl-CoA and oxaloacetate (Stanley, et al., 2005; Van Den Brom, et al., 2013). Isomerization of citrate then takes place, followed by different conversion reactions that will eventually produce malate. These conversion reactions are the source of the by-products of the citric acid cycle, NADH and $FADH_2$. Oxaloacetate and NADH are produced when malate is dehydrogenated. The cycle repeats itself when oxaloacetate reacts with acetyl-CoA. A schematic representation of fatty acid and glucose metabolism in the cardiomyocyte can be seen in Figure 1.4 (Lopaschuck, et al., 2010; Van Den Brom, et al., 2013).

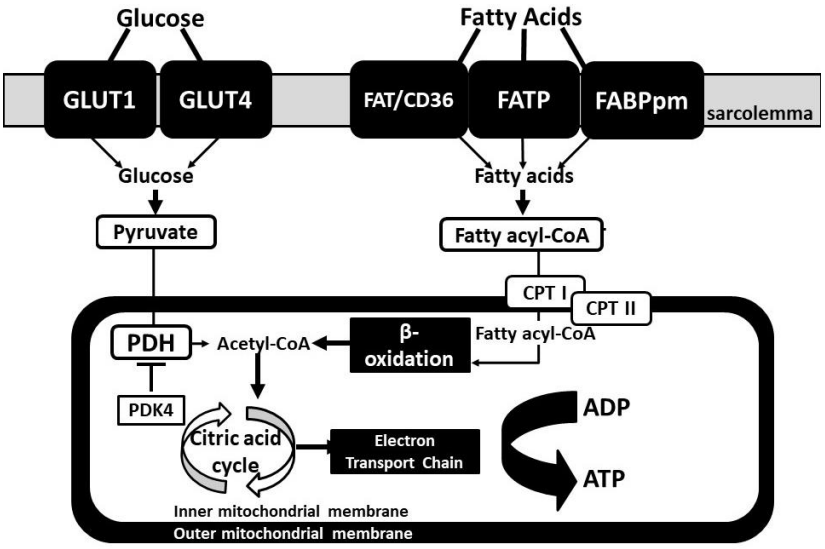

Figure 1.4 *A schematic of glucose and fatty acid metabolism in a cardiomyocyte (adapted from Van Den Brom, et al., (2013)).*

2.2. Energy metabolism

A key regulator in energy metabolism is PGC-1α (Liang & Ward, 2006). PGC-1α (PPARγ coactivator-1α) interacts with the transcription factors that are pivotal in glucose- and fat metabolism, thermogenesis, heart development, fiber type switching in skeletal muscle and mitochondrial biogenesis (Puigserver & Spiegelman, 2003; Gambino, et al., 2011).

These transcription factors are known as PPARs (peroxisome proliferator-activated receptors) and are lipid sensors that act in response to dietary lipid intake (Michalik, et al., 2006). They regulate lipid metabolism and storage. More specifically, PPARγ (peroxisome proliferator-activated receptor gamma) is a ligand-activated transcriptional factor that control genes regulating glucose- and lipid metabolism (Desvergne & Wahli, 1999). PPARγ is mainly involved in lipid metabolism, carbohydrate metabolism and adipocyte differentiation. The activation of PPARγ is linked to decreased blood glucose levels.

PGC-1α promotes cardiac mitochondrial biogenesis and is thus essential for the heart and its unceasingly high demand for ATP (Lehman, et al., 2000). Increased PGC-1α expression stimulates hepatic gluconeogenesis and fatty acid oxidative metabolism, and is therefore increased in fasting states (Yoon, et al., 2001; Kim, et al., 2005).

PGC-1α is also known to increase glucose uptake by upregulating GLUT4 expression in skeletal muscle and cultured muscle cells (Michael, et al., 2001; Evans, et al., 2004). In the muscles of T2D, reduced and compromised PGC-1α levels have been observed (Liang & Ward, 2006). It has been shown that T2D patients have downregulated PGC-1α levels in the muscles or a polymorphism on the PGC-1α gene (Gly482Ser) (Hara, et al., 2002; Mootha, et al., 2003).

2.2.1. Mitochondria

2.2.1.1. Oxidative Phosphorylation

During aerobic respiration, oxidative phosphorylation is the final step that occurs in the inner membrane of the mitochondria to produce ATP (Figure 1.5) (Alberts, et al., 2002; Stanley, et al., 2005; Vos, et al., 2015). Electrons from NADH and $FADH_2$ (which are by-products formed in the citric acid cycle from glycolysis and fatty acid oxidation) pass along mobile electron carrier molecules (see *'2.1. Cardiac Metabolism'*). Two carrier

molecules (coenzyme-Q (CoQ) and cytochrome c) are embedded in the inner mitochondrial membrane (IMM), along with four enzyme complexes (I, II, III, IV) that are involved in oxidative phosphorylation (Lesnefsky, et al., 2001; Berg, et al., 2002). The complexes include NADH dehydrogenase (complex I), succinate dehydrogenase (complex II), cytochrome c oxidoreductase (complex III), and cytochrome c oxidase (complex IV). The transfer of these electrons through a series of oxidation/reduction reactions from one complex to the next, is referred to as the ETC (as mentioned previously).

The reduction of NAD^+ provides two electrons to complex I. This reduction is fuelled by the substrates pyruvate, glutamate and malate. Malate is converted to oxaloacetate, that will, in turn, condense with acetyl-CoA to form citrate. Citrate is then metabolised in the citric acid cycle. The translocation of protons via complexes I, II and IV takes place from the mitochondrial matrix to the inner-membrane space (Chan, 2006).

Complex II, located in the IMM, is also involved in the citric acid cycle (Tzagoloff, 1982). The conversion of succinate to fumarate transfers electrons to the non-haem group on complex II. Hereafter the substrate is transferred to CoQ. Complex III is involved in the electron transfer between reduced CoQ to oxidized cytochrome c. Complex IV (IMM) transfers the electrons to oxygen to form water.

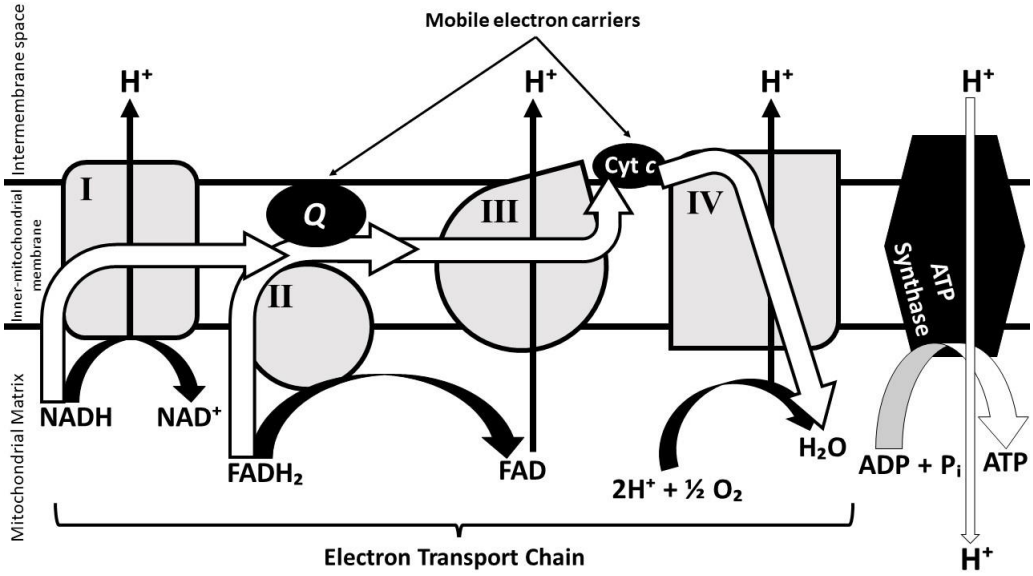

Figure 1.5 *A schematic of oxidative phosphorylation, with the focus on the electron transport chain (adapted from Vos et al., (2015), Alberts et al., (2002) and Nelson & Cox (2004).*

As mentioned earlier, oxidative phosphorylation is the main pathway that synthesizes ATP (Okuno, et al., 2011). The final reaction, where ADP and inorganic phosphate (P_i) form ATP, is catalysed by F_1F_0-ATPase. F_1F_0-ATPase does this by utilizing the protons that create an electrochemical potential across the inner membrane (Rines & Ardehali, 2014). The oxidative phosphorylation rate is influenced by the rate of myocyte energy demand and ATP utilisation (Stanley, et al., 2005).

ATP formed from oxidative phosphorylation is transferred to the cytoplasm from the mitochondrial matrix (Berg, et al., 2002; Klingenberg, 2008; Vos, et al., 2015). The transporter proteins responsible for facilitating this are known as ADP/ATP translocases of ADP-ATP carrier (AAC) (Adrian, et al., 1986; Klingenberg, 2008). Normally, some ATP molecules will re-enter the mitochondria (as ADP) to be recharged and thus maintain the ATP concentration in the cell to be higher than the ADP concentration. The rest of the ATP is used to drive other cellular processes (Alberts, et al., 2002).

To experimentally determine the bioenergetics in oxidative phosphorylation, the oxygen consumption of mitochondria must be determined. This can be done with a classic standard Clark-type oxygen electrode devised by Chance and Williams (Chance & Williams, 1955). Generally, State 1 respiration is the rate at which mitochondria consume oxygen in the presence of P_i (Brand & Nicholls, 2011). State 2 measures ADP independent respiration but in the presence of substrates (glutamate-malate or palmitoyl-malate). This is a measure of mitochondrial oxygen leak or uncoupled mitochondria. As soon as ADP is added (state 3), F_1F_0-ATPase function is activated, and mitochondria rapidly consumes oxygen to form ATP from ADP. This increase in ADP and energy demand enhance phosphorylation, thus increasing formation of ATP. State 4 respiration is when all the ADP is converted to ATP and phosphorylation is decreased. Respiration then reaches an equilibrium and respiration rate is decreased. This allows the mitochondria to respire as if they were in the resting state (or state 2). Again, a high respiration rate in the absence of ADP, is indicative of uncoupled mitochondria or an oxygen leak.

ATP turnover and substrate oxidation controls state 3 (Brand & Nicholls, 2011). Thus, a decrease in the state 3 respiration means that there is an inhibition in either the substrate metabolism, processing enzymes or enzymes involved in the ETC. Proton

leaks and agents that can cause F_1F_0-ATPase to recycle ATP to ADP, affect the state 4 respiration.

Conventionally, functional mitochondria should be able to make ATP as needed to meet energy demands (Brand & Nicholls, 2011). As measure of mitochondrial function, the RCI (respiratory control index) is used. The RCI is calculated by dividing the state 3 respiration by state 4 respiration. A high RCI value shows that the mitochondria display a high capacity for substrate oxidation and formation of ATP. A low RCI value because of high state 4 respiration indicates uncoupling of the mitochondria. This is usually because of leakage of H^+ from the inner membrane space into the matrix, thereby dispersing the electrochemical gradient without producing ATP. A high expression of uncoupling proteins will result in such a H^+ leak. RCI values can vary and be influenced by how the substrates have been utilized and from which tissues the mitochondria were isolated from. Despite the latter, the RCI is still a dependable parameter to measure mitochondrial function, because it is influenced by any change in the oxidative phosphorylation process.

The ADP/O ratio is the number of ATP molecules produced by the ETC, where two electrons move through the ETC (Brand & Nicholls, 2011). When there is an uncoupling (or disconnection) of the mitochondria proton translocation for ATP synthesis, the ADP/O ratio will be affected; indicating reduced coupling efficiency of the mitochondria. The function and mitochondrial oxidative capacity can thus be easily and reliably calculated by experimentally investigating the respiratory rates and ADP/O ratio.

The oxidative phosphorylation rate is another index to be used for evaluation of mitochondrial function and can be calculated for state 3 to determine the number of moles ATP produced per milligram mitochondria protein per minute. This is done by multiplying state 3 with the ADP/O ratio.

2.2.1.2. Autophagy and Mitophagy

Not only are mitochondria vital for cell metabolism, but they also regulate cell death. Stressors that can induce cell death include DNA damage, nutrient deficiency, growth factor loss, hypoxia, ischaemia/reperfusion, caloric restriction and oxidative stress (Høyer-Hansen, et al., 2007; Fulda, et al., 2010; Mihaylova & Shaw, 2012).

Cell death can occur by necrosis, apoptosis or autophagy (Fulda, et al., 2010). Necrosis is a non-apoptotic, passive and accidental cell death and results from environmental distress with uncontrolled release of inflammatory contents (Fink & Cookson, 2005).

In contrast, apoptosis is defined as an active and programmed process of cellular death to avoid inflammation (Fink & Cookson, 2005). Apoptosis can be introduced by either intrinsic (mediated by mitochondrial factors) or extrinsic factors (mediated by death receptor ligation). Both these pathways lead to the activation of apoptosis via caspase-3 and caspase-7 (Ichim & Tait, 2016). Either (1) B-cell lymphoma 2 (Bcl-2) family proteins (located on outer mitochondrial membrane (OMM)) or (2) mPTP (mitochondrial permeability transition pore) opening can mediate intrinsic apoptosis (Hengartner, 2000; Fulda & Debatin, 2006).

(1) There are two types of proteins in the Bcl-2 family, namely; pro-apoptotic and anti-apoptotic. Bcl-2/adenovirus E1B 19-kDa protein-interacting protein 3 (BNIP3), from the BH3 proteins family, is a pro-apoptotic protein (Burton & Gibson, 2009). Stress indicators from the cytosol 'activate' these pro-apoptotic proteins that will, in turn, transduce the stress signals to the mitochondria to initiate cell-death. The pro-apoptotic proteins (e.g. Bax) bind to the anti-apoptotic proteins (Bcl-2) to neutralize them (Chipuk, 2008). Cytochrome C and second mitochondria-derived activator of caspase (SMAC/Diablo) are then released into the cytosol to form an apoptosome that will allow the cell to undergo the programmed cell death (Cory & Adams, 2002).

(2) As mentioned previously, the electrochemical gradient is essential for the normal formation of ATP. Therefore, the IMM must be well maintained. Two essential factors for this maintenance include the mPTP and mitochondrial Ca^{2+} uniporter (MCU). The MCU is a selective ion channel that regulates Ca^{2+} uptake through the IMM (Tsai, et al., 2016). Different signals cause change in the IMM that can lead to the opening (or formation) of the mPTP (Halestrap, 2009). Inhibitors of the mPTP include adenine nucleotides, whereas increased matrix Ca^{2+} and ROS induce opening of the mPTP (Murphy & Steenbergen, 2008). When the pore opens, cytochrome C can leak out of the mitochondria to induce apoptosis. Furthermore, a loss in the electrochemical gradient occurs, leading to the destruction of the ETC causing inhibition in ATP synthesis and reversal of F_1F_0-ATPase occur because of this destruction of the ETC,

thus causing ATP depletion and cell death (Halestrap & Richardson, 2015). The mitochondria can also swell and burst due to the constant influx of solutes through the open pore (Newmeyer & Ferguson-Miller, 2003). Oxidative stress, phosphate levels, membrane potential and alteration in the mPTP's Ca^{2+} sensitivity can control the opening of the pore. Thus, an increase in Ca^{2+} uptake in the mitochondria can be pathological and initiate cell death. The immunosuppressant drug cyclosporine A (CsA) can limit mPTP opening (Crompton, et al., 1988).

According to Halestrap. et al., (2004), the mPTP consists of adenine nucleotide translocator (ANT), Cyclophilin-D (Cyp-D), F_1F_0-ATPase and mitochondrial proteins that are utilized as pore modulators (Halestrap, et al., 2004). According to other studies, other proteins have been identified as part of the mPTP, such as voltage-dependent anion channels (VDACs), hexokinase II (HK), the inorganic phosphate carrier (PiC), peptidyl prolyl isomerase F (PPIF), the peripheral benzodiazepine receptor (TSPO) and several members of the Bcl-2 family (Szabó, De Pinto, & Zoratti, 1993; Beutner, Rück, Riede, & Brdiczka, 1998; Vander Heiden, et al., 2001; Basso, et al., 2005; Chiara, et al., 2008; Sileikyte, et al., 2011; Varanyuwatana & Halestrap, 2012). Cyp-D is believed to help regulate and increase Ca^{2+} permeability, thus opening the pore. CsA inhibits mPTP opening by inhibiting binding of Cyp-D to the ANT (Clarke, et al., 2002; Liu, et al., 2011). Inorganic phosphates also have an important role in the pore's opening (Leung, et al., 2008). GNX-4975 is a novel inhibitor of the mPTP that has recently been identified (Richardson & Halestrap, 2016).

When harmful substances and malformed proteins need to be eliminated, or when compensation is needed for a loss of nutrients, autophagy is the intracellular process of degradation to maintain a positive energy balance (Yorimitsu & Klionsky, 2005). In healthy cells, autophagy is also used to help them survive (Lamb, et al., 2013). Autophagy removes cytoplasmic components such as pathogens and dysfunctional mitochondria. Autophagy can be (1) chaperone-mediated, which has limited degradation capacity because only cytosolic proteins with a certain peptide sequence motif are degraded (Majeski & Dice, 2004). Two other processes include (2) microautophagy (by means of direct lysosomal engulfment of the cytosolic cargo) and (3) macroautophagy which can also for example remove damaged mitochondria by means of the formation of an autophagosome (Reggiori & Klionsky, 2002).

Autophagy involves autophagy receptors that are classified according to their cargo binding domains (Behrends & Fulda, 2012). In vesicle biosynthesis, ubiquitin-like (UBL) systems are vital. They are activated by AMPK (a cellular energy sensor) and mTORc1 (mTOR complex 1, a nutrient sensor) (Lamb, et al., 2013). Ubiquitin binding domains utilize protein specific interactions. In the formation of the autophagosome, an isolated membrane (in the cytosol) is elongated around the cargo destined for elimination (see Figure 1.6) (Eskelinen, 2005; Hamacher-Brady, 2012; Kruppa, et al., 2016).

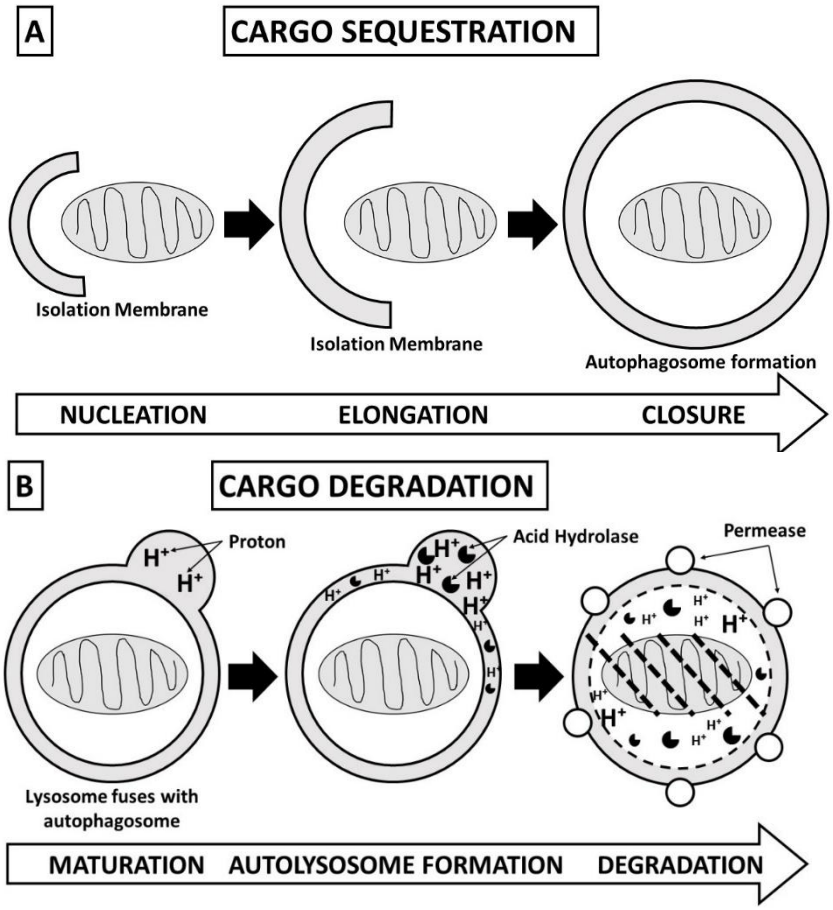

Figure 1.6 *A representation of the autophagic process (adapted from Hamacher-Brady (2012)).*

The membrane elongates and matures until the cargo is fully engulfed and enclosed (Lamb, et al., 2013). Ubiquitination reactions allow for this elongation and protein 1-light chain protein 3 (LC3-I) is essential for this process (Tanida, et al., 2008). LC3-II (formed when LC3-I conjugates with phosphatidylethanolamine in the membrane) plays a role in the elongation of the outer membrane of the autophagosome. LC3-II remains on the autophagosome until it is removed by deconjugation and the autophagosome becomes an autophagolysosome. The LC3-II present inside the inner vesicle, however, stays associated with the complete autophagosome allowing

investigators to associate LC3-II levels to autophagosome number (Klionsky, et al., 2012). Fusion of the autophagosome to the endosomes and lysosomes take place to form the autophagolysosome that will finally degrade the cargo (Shen & Mizushima, 2014; Kruppa, et al., 2016).

There are several proteins involved in the regulation of autophagy. More specifically, ATG (autophagy related) proteins that regulate the autophagosome formation (Mizushima, et al., 2003). Three ATG groups are involved. There is the (1) Atg9 system that is essential for expansion of the phagophore (Feng & Klionsky, 2017). The (2) PI3K (phosphoinositide 3-kinase) complex that consists of Beclin-1 and Vps (vacuolar protein sorting) 34 and 15 (Itakura, et al., 2008). Lastly is the (3) Ubl (ubiquitin-like) protein system with Atg8 (LC-3), Atg12, enzymes and proteases (Nakatogawa, 2013).

Autophagy is regulated by class I PI3Ks and class III PI3Ks (Katayama, et al., 2007). The former negatively regulates autophagy, whereas class III PI3K positively regulates autophagy. Not only does mTOR (mammalian target of rapamycin, a downstream target of class I PI3K/Akt) regulate cell growth and proliferation, but it can sense changes in energy and stress levels too (Cuyàs, et al., 2014). Growth can be promoted by mTOR by inhibiting autophagy and activating RNA translation (Kim, et al., 2011). In contrast, when nutrient levels are low, mTOR is inhibited and autophagy is continued.

Dephosphorylation of mTOR allows its detachment from the Atg13 complex and initiates autophagosome formation and cell death by autophagy (Jung, et al., 2009). When class III PI3K associates with Beclin-1 (which is involved in autophagosome formation) the PI3P (phosphatidylinositol 3-phosphate) complex is formed to allow for autophagy to be initiated (Komatsu, et al., 2007; McKnight & Zhenyu, 2013).

Autophagy can be quantified by many techniques, including Western blotting (more explained under *'8. Western Blots'*). Western blotting that aims to quantify autophagy focusses on the levels of LC3-II (Sharifi, et al., 2015). The conversion of LC3-I to LC3-II is taken as a good measure of autophagic flux, therefore the amount of autophagy that has occurred in a certain time span. The focus on LC3-II is because it is permanently associated with the autophagosome at its inner membrane, until it is degraded. The protein p62 (p62/SQSTM1 also known as sequestosome) is a ubiquitin scaffold protein and functions by enabling autophagic degradation of aggregated

ubiquitinated protein. It is also used as an indicator of autophagy progression because of its role as an adaptor protein and ubiquitin binding cargo receptor (Sharifi, et al., 2015). To summarise, autophagy can be identified by certain indicators namely; increased LC3-II, Beclin-1 and decreased p62 levels (Komatsu, et al., 2007; Meyer, et al., 2013).

As mentioned earlier, autophagy can be selective by targeting a specific organelle. This selective autophagy is mediated by membrane embedding and an example thereof is mitophagy (autophagy of the mitochondria) (Behrends & Fulda, 2012). The quality of a cell's mitochondria is vital for its viability and this mechanism is maintained by mitochondrial autophagy. Mitochondrial autophagy (or mitophagy) recognizes a damaged mitochondrion, thus allowing it to be engulfed by autophagosomes (Saito & Sadoshima, 2015).

Mitophagy is most commonly mediated by PINK1 (PTEN-induced putative kinase protein 1) that contains a mitochondria-targeting signal and Parkin (cytosolic E3 ubiquitin ligase) (Lazarou, 2015). In normal, polarized mitochondria, PINK1 is translocated into the mitochondria via TOM (translocase of outer membrane) and TIM (translocase of inner membrane). PINK1 is then attached to the IMM (Lazarou, et al., 2012). PINK1 is degraded by the N-end rule pathway, where the proteasome is degraded by N-terminal processing (Yamano & Youle, 2013). The N-end rule pathway degrades proteins by identifying the stability of a protein by its N-terminal residue (Varshavsky, 1996).

This import of PINK1 to the IMM is repressed in depolarized mitochondria, thus resulting in accumulation of PINK1 at the OMM (Jin, et al., 2010). This then causes the formation of a complex between TOM and PINK1 (700 kDa) that autophosphorylates at Ser 228 and Ser 402. Increased unfolded protein in the mitochondria also leads to PINK1 accumulation on the OMM.

Subsequently, PINK1 will then phosphorylate S65 on Ubiquitin and the ubiquitin-like domain of Parkin. As a result, Parkin ubiquitinates mitochondrial substrates on the OMM to recruit p62 which can associate with LC3 (refer to Figure 1.7) (Shires & Gustaffson, 2015).

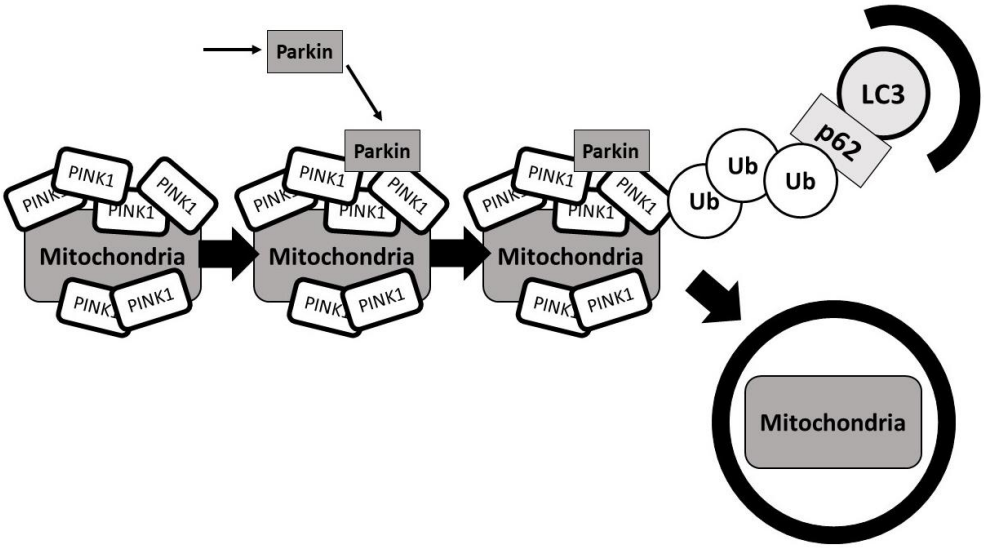

Figure 1.7 *A representation of mitophagy (adapted from Shires & Gustaffson (2015)).*

Mfn2 (mitofusin 2) is a substrate found on the OMM that is phosphorylated by the PINK1 accumulating on the OMM (Chen & Dorn, 2013). PINK1 accumulation also ameliorates the recruitment of Parkin to the phosphorylated Mfn2 on the damaged mitochondria surface (in cardiomyocytes, Mfn2 serves as a mitochondrial receptor for Parkin) (Saito & Sadoshima, 2015). Other proteins that also recruit Parkin to damaged mitochondria include VDACs (voltage-dependent anion channels) (Su, et al., 2012). LC3 proteins are bound to phagophores and recruited to the OMM via autophagy adaptors such as p62 and NBR1 (neighbour of BRCA1 gene 1) (Kirkin, et al., 2009). Kirkin, et al., (2009) states that NBR1 and p62 promotes autophagic degradation. These phagophores then expand and engulf the mitochondrion, forming an autophagosome (as discussed previously).

Beclin-1 not only plays a pivotal role in autophagy, but in tumor-suppression as well (Kang, et al., 2011). Beclin-1 is a component of the class III PI3K complex that mediates vesicle-trafficking processes and autophagosome formation in macroautophagy. On the other hand, it can also associate with Bcl-2 (an anti-apoptotic protein) to inhibit autophagy (Marquez & Xu, 2012; Galluzzi & Kroemer, 2013).

As mentioned earlier, BNIP3 is another pro-apoptotic protein that can be found on the mitochondrial membrane. BNIP3 can activate the downstream effectors of Bax/Bak by associating with Bcl-2 (Walls, et al., 2009; Marquez & Xu, 2012). This protein is a weak inducer of cell death, compared to that of other family members. BNIP3 can cause cell death in three different ways including apoptosis, necrosis and autophagy. BNIP3

(inserted into the mitochondrial membrane) transcription is activated by HIF-1 (a hypoxia-inducible factor-1 responsive element) under hypoxic conditions. In a study by Quinsay et al. (2010), they proved that, in cardiomyocytes, extensive autophagy is associated with an overexpression of BNIP3. Moreover, they also demonstrated that BNIP3 prompts and induces autophagy irrespective and independent of ROS generation, Ca^{2+} and mPTP opening (Quinsay, et al., 2010).

A third process whereby mitophagy can be regulated is by ULK1 (Unc-51 Like autophagy activating Kinase 1) (Wu, et al., 2014). When phosphorylated by AMPK, ULK1 connects cellular sensing to mitophagy (Egan, et al., 2011; Jeon, 2016). It has been reported that FUNDC1 (FUN14 Domain Containing 1) is a mitophagy receptor and that ULK1 translocates to damaged mitochondria and phosphorylates FUNDC1 at Ser17 (Liu, et al., 2012; Wu, et al., 2014). This phosphorylation at Ser17 enhances FUNDC1 binding to LC3 whereas ULK1-binding-deficient mutant of FUNDC1 prevents this translocation of ULK1 to mitochondria, thus inhibiting autophagy. A phosphorylation-mimetic mutant of FUNDC1 (S17D) and kinase-active ULK1 enhances LC3 interaction to form the autophagosome in cells without ULK1, thus enhancing mitophagy (Wu, et al., 2014).

2.2.2. Fatty acid metabolism

It is evident that energy supplies need to be managed sufficiently in all living organisms. The regulation of the uptake of fatty acid (FA) across the plasma membrane from the heart and skeletal muscles, is maintained by fatty acid translocase FAT/CD36 (see Figure 1.4) (Bonen, et al., 2004). The uptake of FA into the myocyte can be regulated in two ways, according Bonen et al. (2004). Regulation can be by either increasing the FAT/CD36 plasmalemmal content or by relocation of FAT/CD36 to the plasma membrane. The FA transport rate is reduced when FAT/CD36 is repressed. On the other hand, as soon as exposure to insulin or muscle contraction takes place, FAT/CD36 translocation to the cell surface is induced and FA transport increases (Bonen, et al., 2004).

FAT/CD36 is also located on the mitochondrial membrane and is said to be involved in mitochondrial FA oxidation (Bonen, et al., 2004). Parkin can stabilize CD36 by

ubiquitination in hepatocytes, thus regulating CD36 stability and maintaining FA uptake (refer to '*2.2.1.2 Autophagy and mitophagy*') (Saito & Sadoshima, 2015).

2.2.3. Glucose metabolism

In mammals, most tissues depend solely on glucose for metabolic energy, but the heart and skeletal muscle prefer fatty acids (Holloway, et al., 2010). Glucose homeostasis and metabolism is maintained and controlled by the interaction of insulin, glucagon, amylin and incretin hormones (refer to Figure 1.8) (Moore & Cooper, 1991; Näslund, et al., 1999; Ward, 2016). Insulin is a hormonal regulator of glucose in the circulation, where it controls both the release and utilization of glucose. In a hyperglycaemic state, insulin is released by the β-cells of the pancreas to decrease the blood glucose concentration by stimulating glucose uptake by peripheral insulin sensitive tissue (Aronoff, et al., 2004). Initially, insulin has been thought of being the only regulator of diabetes and insulin deficiency, but there has been an expansion in the understanding of glucoregulation where additional hormones have been discovered (Aronoff, et al., 2004; Nelson & Cox, 2004).

Also in the pancreas, are α-cells that release glucagon when blood glucose concentration drops below certain threshold values (hypoglycaemia) (Aronoff, et al., 2004). This discovery was made in the 1950s and it led to a better understanding of the associations between insulin and glucagon. In diabetes, the inappropriate increase in α-cell function leads to hyperglucagonaemia. Accordingly, hyperglucagonaemia can also contribute to the hyperglycaemic state (by stimulation of hepatic glucose production) seen in diabetic patients (Unger, et al., 1970).

Amylin is thought to be associated with insulin and, just like insulin, is also deficient in diabetic persons (Moore & Cooper, 1991; Aronoff, et al., 2004). Glucagon-like peptide-1 (GLP-1) is an incretin hormone, released by the L-cells of the gut, that stimulates the secretion of insulin after a meal. GLP-1 is also an important contributor to glucose homeostasis maintenance (Aronoff, et al., 2004).

Blood glucose levels are increased after a meal, especially a carbohydrate-rich meal (Radziuk, et al., 1978; Bacha, et al., 2010). This excess glucose can be stored in either cardiac myocytes and skeletal muscle, or adipocytes (Berg, et al., 2002). In cardiac myocytes, skeletal muscle and liver, glucose is stored in the form of glycogen. In

adipocytes, the glucose is converted to triacylglycerols (Berg, et al., 2002; Nelson & Cox, 2004).

Excess glucose can be converted into different forms: glycogen or fatty acids (Acheson, et al., 1988; Nelson & Cox, 2004). The (1) glycogenesis pathway converts glucose to glycogen (which is the glucose storage polymer). (2) Glycolysis converts glucose 6-phosphate to pyruvate. Pyruvate can then be converted to fatty acids or it can be metabolized to produce more ATP (by entering the citric acid cycle) (Näslund, et al., 1999; Ward, 2016).

When acetyl-CoA enters the pathway of lipid metabolism (instead of the citric acid cycle), glucose is converted to fatty acids. When energy is needed (hypoglycaemia), acetyl-CoA enters the citric acid cycle to release the stored energy derived from carbohydrates, fats and proteins (Näslund, et al., 1999; Berg, et al., 2002).

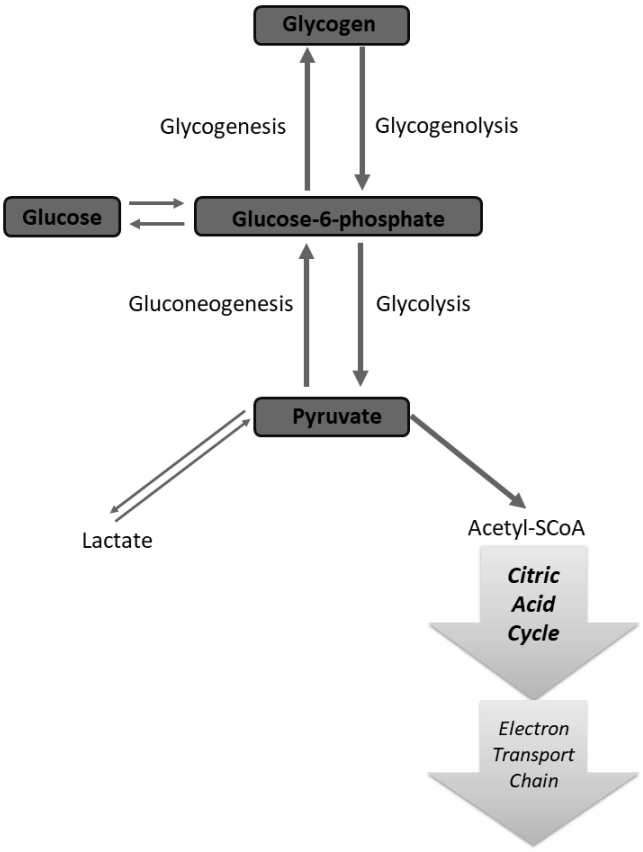

Figure 1.8 *A representation of glucose metabolism (adapted from Ward (2016)).*

2.2.3.1. Glucose Transport

Glucose transporters (GLUTs), are the proteins involved in mediating and controlling glucose transport into cells (Thorens & Mueckler, 2009). Of the 14 GLUT genes in the human genome, the protein production of only 2 will be further discussed in this review. GLUT1 is the basal glucose transporter that is present in most cells (Scheepers, et al., 2004). GLUT1 allows most tissues to be able to take up glucose at basal levels (Mueckler, 1990). GLUT4 is the insulin-responsive transporter that is present in muscle, cardiac- and fat cells. Insulin regulates the level of GLUT4 on the surface of muscle and fat cells.

In myocytes and adipocytes, glucose uptake is facilitated by GLUT4. GLUT4 is mostly retained in small intracellular vesicle membranes between meals, but some of the GLUT4 molecules can be found in the plasma membrane (Nelson & Cox, 2004). High levels of blood glucose activate the release of insulin from the pancreas (Leto & Saltiel, 2012). The insulin then prompts the intracellular vesicles to move to the plasma membrane. It is here where the vesicles fuse with the plasma membrane and expose the GLUT4 molecules on the outer surface of the cell. This movement and exposure of the GLUT4 molecules increase the rate of glucose uptake. As soon as the blood glucose levels are normalized, the release of insulin slows down and most of the GLUT4 molecules are internalized from the plasma membrane and stored in vesicles (Nelson & Cox, 2004). The signalling processes involved in this, will be discussed in Figure 1.9 below.

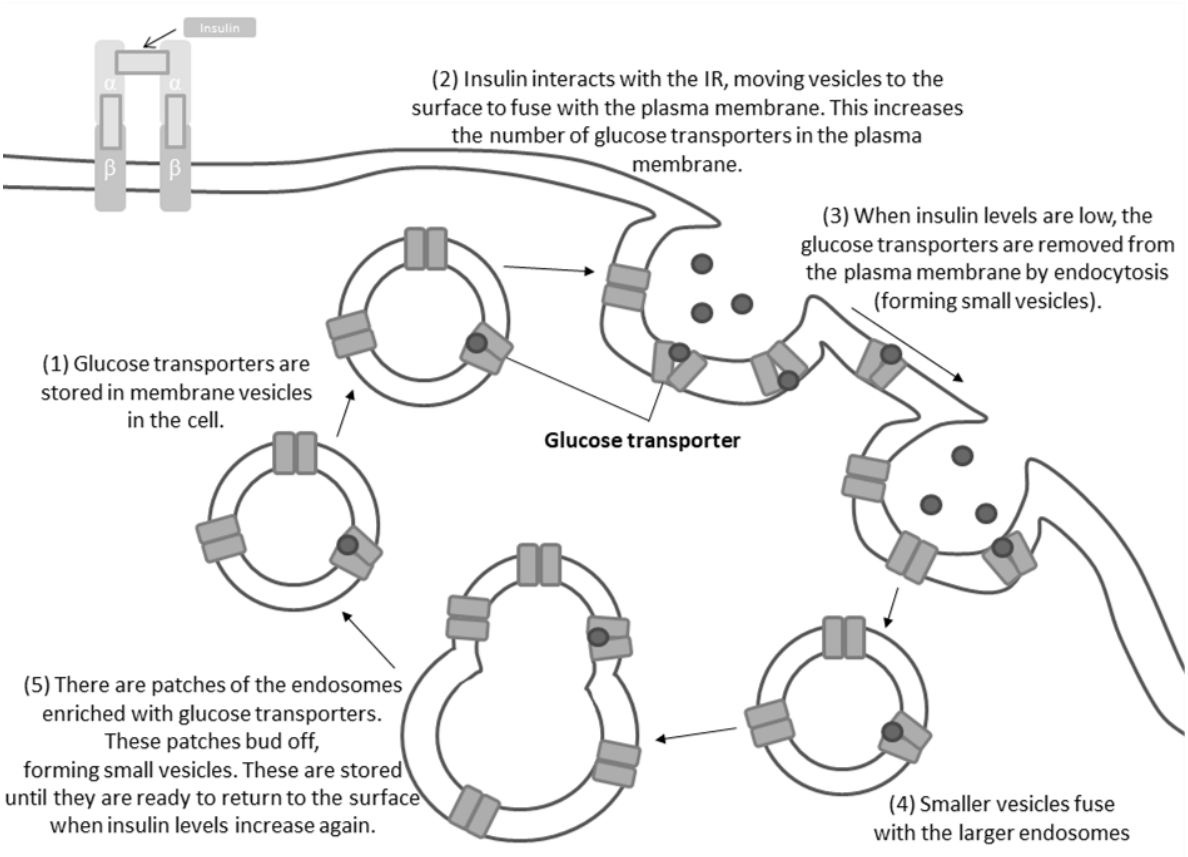

Figure 1.9 *How insulin regulates glucose transport by GLUT4 into a myocyte (adapted from Nelson & Cox (2004).*

2.2.3.2. Glycolysis

Through glycolysis, glucose molecules are broken down to form pyruvate by means of enzyme-catalyzed reactions (Nelson & Cox, 2004; Gargani, et al., 2012). Figure 1.10 shows the enzymes involved in the metabolism of glucose to pyruvate. The first part of the glycolysis pathway breaks the glucose down. Step 1 in the glycolysis pathway is catalyzed by hexokinase. This pathway starts with a glucose molecule that is phosphorylated to produce glucose-6-phosphate. Phosphorylation adds a phosphate group to a molecule, thus using one ATP molecule at this step. In the second step, phosphoglucose isomerase (PI) converts glucose-6-phosphate to fructose-6-phosphate (F6P). At the third step, another ATP molecule is used to provide a phosphate group to the F6P; producing fructose-1,6-bisphosphate (FBP). Phosphofructokinase catalyzes this conversion. Aldolase then converts FBP to produce glyceraldehyde-3-phosphate (GAP) and dihydroxyacetone phosphate (DHAP). GAP continues to the glycolytic pathway, but DHAP is reacted on by triphosphate isomerase to produce GAP at a later stage.

GAP is now phosphorylated and oxidized by NAD^+ (Nelson & Cox, 2004; Gargani, et al., 2012). Glyceraldehyde-3-phosphate dehydrogenase (GAPDH) is responsible for this reaction. A NAD^+ molecule is converted to NADH when it 'pulls' a hydrogen atom from the GAP. In this reaction, the GAP molecule then yields 1,3 biphosphoglycerate. NADH and hydrogen. Phosphoglycerate kinase (PGK) comes in to play next. PGK converts 1,3 biphosphoglycerate to 3-phosphoglycerate, and causes the loss of a phosphate group. This phosphate group is transferred to an ADP molecule to yield an ATP molecule.

At this stage, the position of the phosphate group on the 3-phosphoglycerate is rearranged (Nelson & Cox, 2004). This is made possible by phosphoglycerate mutase (PGM) that converts 3-phosphoglycerate to 2-phosphoglycerate. Enolase will subsequently convert 2-phosphoglycerate to phosphoenolpyruvate (PEP) by dehydrating the 2-phosphoglycerate. The final step entails the conversion of phosphoenolpyruvate to pyruvate. This is made possible by pyruvate kinase. A phosphate group from the PEP is transferred to an ADP molecule to produce an ATP molecule. Note that there are two PEP molecules, thus yielding two ATP molecules. This pathway consumes two ATP molecules and generates three ATP molecules.

The metabolic conditions and oxygen levels influence what happens next to the pyruvate molecules next (Nelson & Cox, 2004). In aerobic conditions, the PDH complex converts the pyruvate to acetyl-CoA in the mitochondria. Acetyl-CoA will then enter the citric acid cycle to aid in ATP synthesis (refer to *'2.2.1.1. Oxidative Phosphorylation')* (Hashimoto, et al., 2006). In contrast, in anaerobic conditions, the electron transport slows down and pyruvate is transformed into lactate (Nelson & Cox, 2004; Rogatzki, et al., 2015). This inhibits the glycolytic pathway because of an increase in the NADH concentration and decrease in NAD^+ (Stryer, 1995). Glycolysis is essential because it is a major source of ATP that can still to a certain extent, take place in anaerobic conditions. The reduction of pyruvate to lactate re-oxidizes NADH and allows the glycolysis pathway to continue.

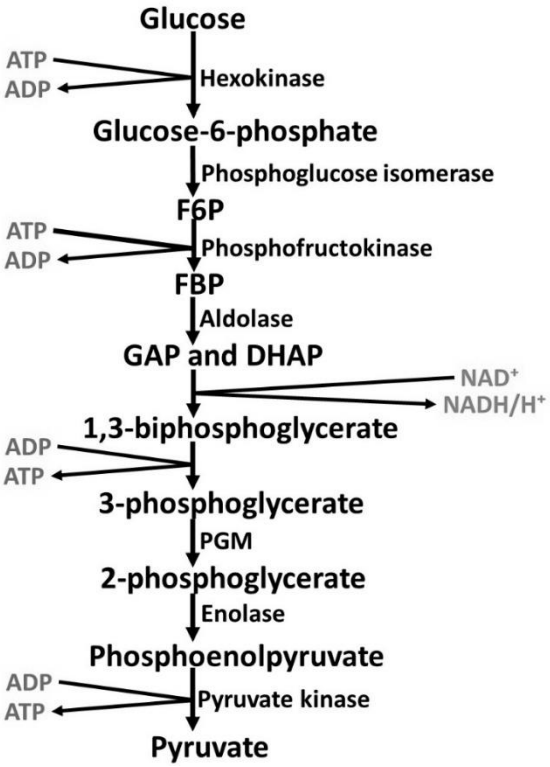

Figure 1.10 *The glycolytic pathway (modified from Gargani et al. (2012)).*

2.2.3.3. Gluconeogenesis

The opposite of glycolysis is gluconeogenesis ("the formation of a new sugar) (Nelson & Cox, 2004). This metabolic pathway converts pyruvate and carbon compounds to glucose, thus generating/synthesizing glucose from non-carbohydrate substrates (lactate, citric acid, amino acids and glycerol) (Nordlie, et al., 1999). Gluconeogenesis comes in to play when the supply of glucose is depleted; such as in periods of intense exercise, fasting, starvation and low-carbohydrate diets. The liver, and sometimes the cortex of the kidneys, serves as the sites at which gluconeogenesis occurs, but this does not play an important role in heart muscle metabolism (Exton & Park, 1968; Nelson & Cox, 2004).

2.2.3.4. Glycogenolysis

Gluconeogenesis is not the only mechanism by which humans and some animals prevent hypoglycaemia. Glycogenolysis degrades glycogen to glucose, as opposed to gluconeogenesis (Hers, 1976; Nelson & Cox, 2004). Glycogen functions as energy storage in the muscle and liver. When glucose is suddenly in need, glycogen can

quickly be metabolized to produce it. Glycogenolysis is stimulated when an adrenaline-induced fight-or-flight response is needed (McCorry, 2007).

2.2.3.5. Glycogenesis

When glucose and ATP levels are too high, glycogenesis converts glucose to glycogen (Bonen & McDermott, 1990; Nordlie, et al., 1999). This process also occurs in the liver and muscle cells. One ATP molecule per glucose unit (in the glycogen structure) is required for this synthesis of glycogen (Nelson & Cox, 2004).

2.3. Insulin Metabolism

The hormone insulin, that was briefly discussed earlier, is produced in the pancreas and secreted into the blood (Brownlee, 2001; Bevan, 2009). It tightly regulates the human metabolism. After food intake, the digestive tract will break down the carbohydrates into glucose, leading to insulin secretion by the pancreas (Saltiel & Kahn, 2001). Insulin then controls and stimulates the cells in the body to absorb the glucose and use it for energy (National Institute of Diabetes and Digestive and Kidney Diseases, 2009).

2.3.1. Insulin Signalling

Insulin in the circulation binds to the α-subunits of the insulin receptor (IR) on insulin sensitive peripheral tissues (Lizcano & Alessi, 2002). A schematic of the IR can be seen in Figure 1.11 (Voet, et al., 2006). The IR comprises of two α-subunits and two β-subunits (Voet, et al., 2006). Each α-subunit is linked to a β-subunit and the two α-subunits are in turn linked to each other by disulfide bonds. The α-subunits contain insulin binding sites and are located on the outside of the cell. The intracellular β-subunit contains the insulin-regulated tyrosine protein kinase (Cell Signaling Technology, 2016). Insulin binding activates the intrinsic tyrosine kinase activity of the β-subunits and will phosphorylate the insulin receptor substrate (IRS) proteins. IRS-1 and IRS-2 are the main substrate proteins in the heart. Proteins that have the Src Homology 2 (SH-2) domains in their structure can recognize the phosphotyrosine binding (PTB) domains on IRS1 (White, 1997).

The insulin signalling pathways control many processes such as glucose uptake (GLUT4 vesicle translocation), enzyme activation/inactivation, mitogenic responses, lipid synthesis and protein synthesis (White, 1997; Nelson & Cox, 2004). Insulin promotes protein synthesis by stimulating amino acid uptake into cells. Moreover, insulin also inhibits protein degradation, thus enhancing protein synthesis. The synthesis of lipids, inhibition of lipolysis and uptake of fatty acids can also be enhanced by insulin (Saltiel & Kahn, 2001).

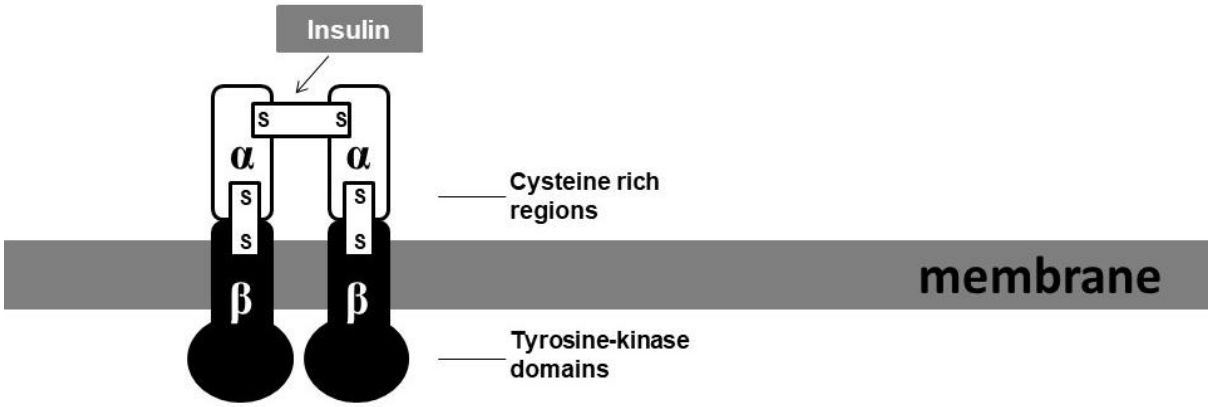

Figure 1.11 *A schematic diagram of the IR (adapted from Voet et al. (2006)).*

2.3.1.1. The PI3K-dependent pathway

The activation of PI3K is fundamental for insulin stimulated glucose uptake (Zhu, et al., 2013). The PI3K/PKB pathway mediates the metabolic effects caused by insulin. The serine/threonine kinase Akt is also known as protein kinase B or PKB (from here on will be referred to as Akt/PKB) (Cong, et al., 1997). In the PI3K-dependent pathway, the IRS-1 protein is the main link between the IR and PI3K (with SH-2 domains in the p85 regulatory subunit) (Rondinone, et al., 1997).

IRS-1 proteins have functions in glucose uptake in cardiac, skeletal muscle and adipose tissue; whereas IRS-2 is involved in glucose and insulin production in the liver and pancreatic β-cells respectively (Hers, et al., 2011; Hardin, et al., 2015). However, when IRS-1 levels are low (for example in non-insulin dependent diabetes mellitus or insulin resistance), IRS-2 takes over the role as main docking site for PI3K. For IRS-2 to bind to PI3K (in a similar way that IRS-1 does), a higher insulin concentration is required (Rondinone, et al., 1997).

To initiate the Ras/MAPK pathway, IRS-1 activates it by forming a complex with GRB2 (refer to Figure 1.12 (Hemmings & Restuccia, 2012)) (discussed under '2.*3.1.2.1. Ras/MAPK pathway*').

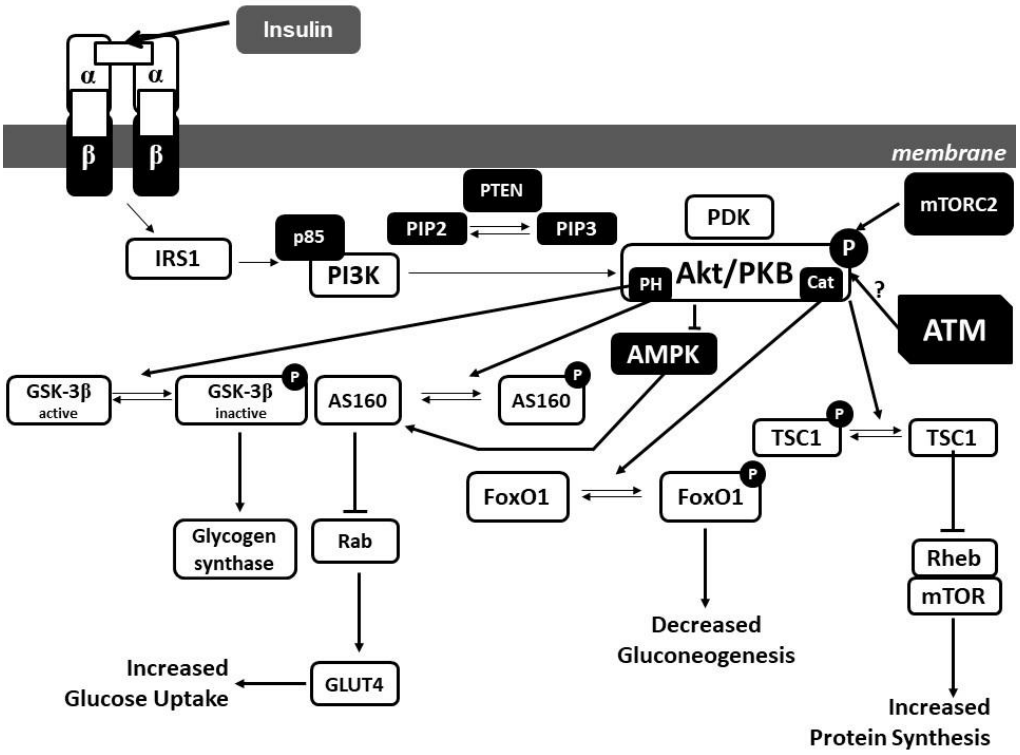

Figure 1.12 *A representation of the PI3K-dependent pathway (adapted from Hemmings & Restuccia (2012), Jeon (2016) and Sakamoto & Holman (2008)).*

The activation of PI3K by IRS-1 converts PIP2 (phosphatidylinositol 4,5-bisphosphate) to PIP3 (phosphatidylinositol (3,4,5) triphosphate) by phosphorylating the membrane lipid bound PIP2 (Hemmings & Restuccia, 2012). The level of PIP3 is regulated by PTEN (a protein tyrosine phosphatase that preferentially dephosphorylates phosphoinositide substrates, such as PIP3). PTEN downregulates intracellular levels of PIP3, thus down-regulating Akt/PKB signalling pathways (Hers, et al., 2011).

These polyphosphoinositides perform like "docking sites" on the plasma membrane (Hers, et al., 2011). Proteins containing pleckstrin homology (PH) domains can bind to these docking sites. This includes mTORc2 (mTOR complex 2), Akt/PKB and PDK1 (3-phosphoinositide-dependent protein kinase 1). The latter explains that Akt/PKB is not directly activated by PIP3 but rather recruited by it to the plasma membrane and

brought in close proximity to the enzymes that will phosphorylate it to be activated (Cell Signaling Technology, 2016).

In the PI3K/PKB pathway, PIP3 binds to Akt/PKB; aiding in the phosphorylation of key proteins (which can then be activated by other kinases) (Bevan, 2009; Hemmings & Restuccia, 2012). PIP3 changes the Akt/PKB conformation to allow for subsequent phosphorylation by PDK1 or mTORc2 (Song, et al., 2005).

PDK1 phosphorylates Akt/PKB at Thr308 (partial activation of Akt/PKB). When Akt/PKB is phosphorylated by mTORc2 at Ser473, full enzymatic activity is stimulated (full activation of Akt/PKB) (Bevan, 2009; Hemmings & Restuccia, 2012). Members of the PI3K-related kinase family are also able to phosphorylate Akt/PKB at Ser473 (Calleja, et al., 2007) (Hers, et al., 2011). When Akt/PKB is active, it can follow different signalling paths (see schematic Figure 1.12). Golding, *et al.* (2009) suggests that ATM (ataxia-telangiectasia (A-T) mutated) can also act on and regulate Akt/PKB phosphorylation (Halaby, et al., 2008; Golding, et al., 2009). ATM plays an important role in DNA repair and cell cycle checkpoints (Lavin & Shiloh, 1997).

Activation of Akt/PKB at the PH domain results in the initiation of at least two pathways. Firstly, Akt/PKB enters the cytoplasm where GSK-3β (glycogen synthase kinase-3β) can be phosphorylated and inactivated. This phosphorylation can lead to an increase in glycogen synthase activity, thus upregulating glycogen synthesis (Cross, et al., 1995). Secondly, Akt/PKB can phosphorylate AS160 (Akt substrate of 160kDa) and therefore recruit GLUT4 (glucose transporter 4) to the membrane, increasing glucose uptake (Cong, et al., 1997; Sakamoto & Holman, 2008).

Furthermore, activation of Akt/PKB at the catalytic (Cat) domain leads to activation of two more pathways (Manning & Cantley, 2007). Firstly, Akt/PKB can activate mTOR to induce protein synthesis. This happens when Akt/PKB inactivates the RHEB (Ras homolog enriched in brain) protein via TSC1 (tuberous sclerosis 1). Secondly, Akt/PKB can monitor cell survival by inhibiting the pro-apoptotic agent, FoxO1 (Forkhead box protein O1) (Tran, et al., 2003; Accili & Arden, 2004). When Akt/PKB phosphorylates FoxO1, gluconeogenesis is decreased. The latter occurs when insulin activates Akt/PKB in the liver and translocates to the nucleus, where FoxO1 is located. It is here where FoxO1 is phosphorylated at Ser256, Ser319 and Thr24. This results

in the relocation and degradation of FoxO1, thus decreasing G6Pase transcription; leading to the reduced gluconeogenesis mentioned earlier (Cell Signaling Technology, 2016).

AMPK, on the other hand, controls cellular and organismal metabolism in eukaryotic organisms (Nelson & Cox, 2004; Jeon, 2016). AMPK has a plethora of metabolic functions. It is a fuel-sensing enzyme that is stimulated by low intracellular ATP levels; and can also inhibit cellular growth (as a metabolic checkpoint) when nutrients are low (Ruderman, et al., 2013). AMPK can enhance glucose uptake (by phosphorylating TBC1D1, also known as AS160) and autophagy (via inhibition of mTORC1) (Jeon, 2016). As mentioned previously, AMPK can also stimulate autophagy by activating ULK (see *'2.2.1.2. Autophagy and Mitophagy*). This enzyme additionally plays a role in activating both glycolysis and fatty acid oxidation and uptake (via CD36 translocation and CPT-1 activation) (Mihaylova & Shaw, 2012; Jeon, 2016). In addition, FoxO and PGC1α can be activated by AMPK, thus mediating many other metabolic processes (Jeon, 2016).

The growth and mitogenic effects of insulin signalling is mediated by both the Akt/PKB and Ras/MAPK pathways. In the CAP/Cbl pathway, IR activation causes the phosphorylation of Cbl (more will be explained under '*2.3.1.2.2. CAP/Cbl pathway'*) (Lizcano & Alessi, 2002; Hers, et al., 2011). Diabetes, cancer and cardiovascular diseases result from a dysregulation of the PI3K/PKB pathway (Hers, et al., 2011). Abnormal gain or loss in Akt/PKB activation can cause many of the pathophysiological properties of type-2 diabetes and cancer.

2.3.1.2. The PI3K-independent pathway

When insulin activates IRS1 by binding to the IR, it can activate more pathways than just the PI3K-dependent pathway. When IRS1 and GRB2 (an adaptor protein) interact, the Ras/MAPK pathway is activated (Bevan, 2009; Boucher, et al., 2014). The translocation of the CAP/Cbl complex to the lipid rafts in the plasma membrane, activates the CAP/Cbl pathway; resulting in increased glucose uptake (refer to Figure 1.13) (Molina & Adjei, 2006; Watson & Pessin, 2006). The Ras/MAPK and CAP/Cbl pathways are both activated by PI3K-independent signalling.

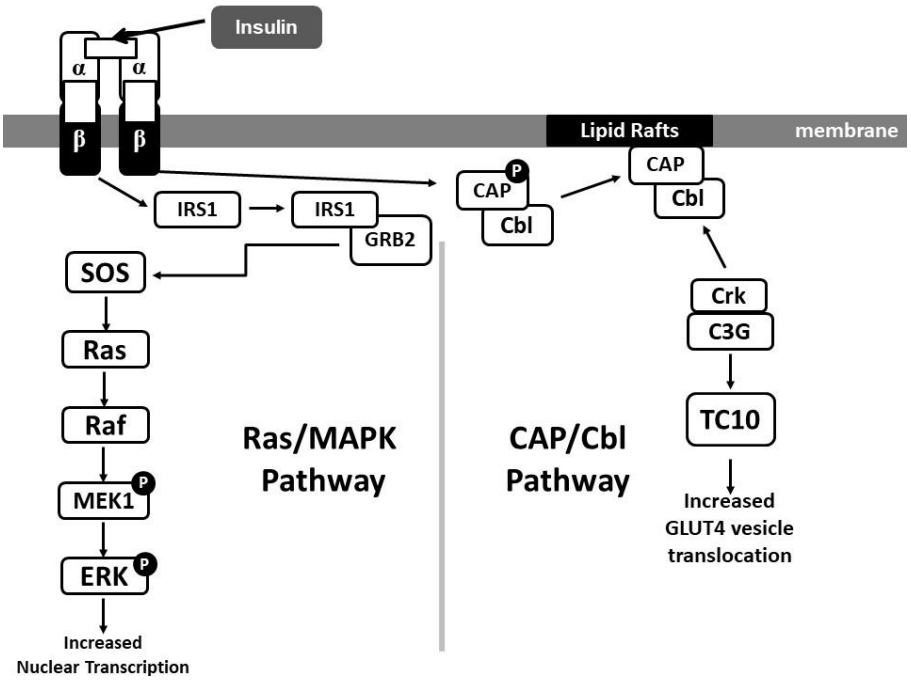

Figure 1.13 *A representation of the PI3K-independent pathways (adapted from Molina & Adjei (2006) and Watson & Pessin (2006)).*

2.3.1.2.1. Ras/MAPK pathway

The Ras/MAPK pathway is a cascade that activates mitogen-activated protein kinases (MAPK's); along with mitogenic responses by means of gene transcription (Bevan, 2009). This pathway is activated when IRS-1 associates with GRB2, thus directing the growth, proliferation, differentiation and survival of cell types. MAPK's include three groups of serine/threonine kinases namely; extracellular signal-regulated kinases (ERK1, ERK2 and ERK3), c-Jun amino-terminal kinase (JNK), and p38 MAPK's. The Ras/MAPK pathways can also be activated without IRS-1 (Orton, et al., 2005; Hardin, et al., 2015). This happens by the association between SHC and GRB2; but for the purpose of this literature review we will not be focusing on the latter.

Ras (which is a small GTPase) is activated at the proximal part of the Ras/MAPK pathway (Kolch, 2000). Receptor tyrosine kinases, G-protein-coupled receptors and/or integrins can bind to their respective receptors to activate Ras. These membrane proteins form large signalling complexes that convert Ras into its activated form (Orton, et al., 2005). This is accomplished by inducing the exchange of Ras-bound GDP with GTP. The interaction between Ras and SOS (son of sevenless homolog 1), a GDP/GTP-exchange factor, controls this process. GAPs (GTPase-activating

proteins) de-activate Ras and significantly enhance very low GTPase activity of Ras. Thus, it effectively optimizes the hydrolysis of GTP to GDP (Orton, et al., 2005).

GRB2 associates and binds to SOS, thus activating Ras. When Ras is activated, the small G-proteins recruit c-Raf to the plasma membrane (Bevan, 2009). This is where Raf is activated, in turn activating MEK1 by phosphorylating two serine residues of the protein. MEK1 phosphorylates ERK1/2 (serine/threonine kinase) at threonine and tyrosine residues. By directly phosphorylating transcription factors or indirectly targeting substrates such as p90-RSK family kinases (which has the ability to modify histones and transcription factors), activated ERK can regulate gene expression (Kolch, 2000; Orton, et al., 2005).

2.3.1.2.2. CAP/Cbl pathway

For the purpose of the current thesis, this pathway will only be discussed briefly. Glucose uptake is also mediated by this pathway by means of the recruitment of GLUT4 translocation to the plasma membrane (Bevan, 2009). Cbl is recruited to the IR by CAP (Baumann, et al., 2000). The CAP-Cbl complex dissociates from the IR and moves to lipid rafts in the plasma membrane. CAP-Cbl and Crk, which is associated with C3G (the Rho-family guanine nucleotide exchange factor) will then interact, activating TC10 (a GTP-binding protein). The CAP-Cbl pathway is involved in the movement of the GLUT4 vesicles on the actin cytoskeleton to the cell membrane.

2.4. Cellular Stress

Stress is a reaction to a threat or demand the body is faced with. Stress of the human body can lead to many unhealthy conditions, such as high blood pressure and heart disease (WebMD, 2016).

Chronic stress induces an increased and consistent heart rate, elevated stress hormones, high blood pressure, and an increased risk for heart attack and stroke (Torpy, et al., 2007). Stress hormones, such as catecholamines like adrenaline, can cause damage to the heart if exposed to elevated levels of these hormones for an extended period. The increased blood pressure and heart rate causes the heart to work harder to keep up with the blood flow demand.

The physiological effect of stress can be counteracted by sestrins (Sesns) (Budanov, et al., 2010). Sesns are stress-responsive proteins that are transcriptionally regulated by p53 (a tumor suppressor) and FoxO. Sesn2 (the cardiac isoform of sestrin) is mainly regulated by p53 (Budanov, et al., 2010; Dong, et al., 2017). Sesn2 is also known as hypoxia-inducible gene 95 (Hi95), indicating that it is stress-responsive and induced by oxidative stress, hypoxia or DNA damage (Lee, et al., 2013; Rhee & Bae, 2015). These regulators have functions such as oxidative stress inhibition, insulin resistance regulation, age attenuation and tumour suppression (Lee, et al., 2013).

Sesn2 can suppress oxidative stress by (1) operating as an alkylhydroperoxide reductase to rescue the peroxidase activity of overoxidized peroxiredoxins, or (2) by activating Nrf2 to upregulate anti-oxidant enzymes (Budanov, et al., 2004; Bae, et al., 2013; Yang, et al., 2014). Sesn2 also inhibits mTOR signalling by interacting with GATOR2 and phosphorylating TSC2 (Parmigiani, et al., 2014) (Budanov & Karin, 2008). In a study by Dong, et al. (2017), the effects of Sesn2 on cardiomyocyte hypertrophy was investigated. They concluded that Sesn2 can protect cardiomyocytes from hypertrophy induced by phenylephrine. Sesn2 does this by inhibiting ERK1/2 signalling.

Normally Sestrins inhibit mTORc1 by activating AMPK, thus preventing autophagy (Budanov, et al., 2010). This process is valuable and advantageous for the prevention of aging and age-associated pathologies. Consequently, when Sestrins are inhibited and mTOR activity increased, autophagy can be promoted (Wullschleger, et al., 2006).

2.5. The Physiological difference between Humans and Rodents

As previously discussed, T2D develops because of glucose homeostasis dysregulation. As a worldwide diabetic epidemic is rising, research needs to be performed to investigate and try to understand the pathophysiology of T2D (Chandrasekera & Pippin, 2013). The pathophysiology seen in obesity in humans can be mimicked by a popular animal model (Sumiyoshi, et al., 2006). This is the diet-induced obesity model that entails the intake of fat that comprises the diet to be of high caloric value. This model can lead to an increase in fat and insulin resistance in the animal.

Short lifespans and breeding periods, low maintenance and cost, ease of handling and easy genetic manipulation are all factors contributing to the preference of rodent species in T2D research. The development of hypothesis formation to data acquisition is managed with relative ease and in a short timeframe (Chandrasekera & Pippin, 2013). These animal models all elicit different phenotypic manifestations of T2D in humans; ranging from variations in severity, penetrance and duration (Chatzigeorgiou, et al., 2009).

Rodent models do have similarities with the human diabetic condition because the phenotype in these animals are also dependent on genetics, sex and age (Neubauer & Kulkarni, 2006). Furthermore, rodent models allow researchers to study the molecular mechanisms behind diabetes and to follow all the stages of the disease (Cefalu, 2006). Genetic manipulation is easy in rodents, and they have a relatively short breeding span. Rodents also allow researchers to gain access to physiological and invasive testing.

There are, however, limitations to the use of rodent models (Cefalu, 2006). Most rodent models cannot fully represent the natural pathophysiological mechanisms involved in the complex T2D state in the human. In rodents, the inability to increase β cells mass in response to obesity-induced insulin resistance causes diabetes. Rodents usually develop diabetes without showcasing the same islet pathology that researchers see in humans (islet amyloidosis) (Kaplan & Wagner, 2006). Questions surrounding the relevance of animal models to the human diabetic condition remain unanswered.

Of main concern is the difference between the specific physiological or pathophysiological mechanisms in humans and rodents. Examples that Kaplan & Wagner (2006) give are the differences between the percentage energy of the resting metabolic rate needed by the brain (20 % in humans and 3 % in rodents), the role of gender in human diabetes, and factors such as insulin resistance and T2D development from psychosocial stress in humans (Franconi, et al., 2008). These variables could possibly influence the physiology, onset and development of diabetes in rodents and humans.

Considering all of this, there is no model of T2D that will encompass all of the characteristics of the disease in humans (Chatzigeorgiou, et al., 2009). These animal

models do, however, represent many of the pathophysiological conditions that we see in diabetic humans and are thus used in T2D research.

2.6. Pathophysiology of Diabetes

Some pathophysiological mechanisms in diabetes include weakened insulin secretion from the pancreatic β cells, increased secretion of glucagon from pancreatic α cells, amplified production of hepatic glucose and inhibited glucose uptake in peripheral tissues (Defronzo, 2009). As previously mentioned, diabetes is also a major risk factor for CVD. The pathophysiological effects of diabetes have harmful effects on the macro- and microvasculature (Muhlestein, et al., 2003). Diabetes also cause chronic inflammation and an increase in oxidative stress. The over-activation of the inflammatory response causes an accumulation of leukocytes while endothelium abnormalities cause hypercoagubility (Dokken, 2008). These factors and their pathophysiological significance will be explained in detail.

2.6.1. Macrovasculature

The following factors contribute to the atherogenicity and macrovascular disease seen in diabetic patients. Dyslipidemia, increased triglycerides and decreased HDL cholesterol are associated with atherosclerosis (Fagot-Campagna, et al., 2000). These are all conditions that can arise in diabetic patients, along with an abnormal structure of the lipoprotein particle. The LDL cholesterol in diabetic patients is very susceptible to atherosclerosis because of their small and dense form (Rosenson, 2004). Because these small LDL particles can penetrate and attach to the arterial wall, they are more atherogenic and prone to oxidation (Chan, 1998). This is due to the addition of new properties to the LDL particle that the immune system does not recognize and classifies as ‘foreign.’ This induces a variety of biological responses that attracts leukocytes to the blood vessel which allows the leukocytes to ingest lipids and stimulate the proliferation of leukocytes, endothelial cells and smooth muscle cells. These factors all contribute to the formation of atherosclerotic plaque.

LDL particles in diabetic patients also become easily glycated, which allows them to promote atherogenesis (this is because glycation lengthens the LDL particle’s half-life) (Napoli, et al., 1997). Hypertriglyceridaemia is also present in diabetic blood and can

cause increased production of small LDL particles and decreased HDL cholesterol transport to the liver (Duell, et al., 1991; Shen, 2007).

Endothelial dysfunction can promote atherosclerosis (Celermejer, 1997). Normally, healthy endothelium displays vasodilatory, anti-atherogenic and anti-inflammatory properties (Dokken, 2008). As soon as these properties are affected and compromised, atherosclerosis is promoted. This leads to the conclusion that insulin deficiency and insulin resistance promotes dyslipidaemia (Dokken, 2008).

2.6.2. Microvasculature

Microvascular disease in diabetes come in the following forms: retinopathy, nephropathy, neuropathy and damage to the vasculature of the brain, heart and peripherals (Dokken, 2008). Usually damages to the microvasculature are not related to lipid levels or atherosclerosis, but to cellular and molecular mechanisms. (1) Central and (2) local regulatory mechanisms control the micro-circulation (Lewis, 1998). The (1) central regulation involves the autonomic sympathetic and parasympathetic nerves; and are the central regulators of vascular smooth muscle function (McCorry, 2007). Local products of metabolism and substances produced by endothelial cells (such as vasodilators and vasoconstrictors) are, on the other hand, part of the (2) local regulatory mechanism. The vascular smooth muscle unceasingly receives signals (from the regulatory system), nitric oxide (from the endothelium) and metabolic products. These factors all contribute to the microvascular flow and help the adjustment to the metabolic needs of the tissue (Lewis, 1998).

Defects in the endothelium, local metabolism and autonomic nervous system arise in diabetes (Smith, et al., 1981). Diabetic autonomic neuropathy (DAN) is a condition accompanied by the diminished autoregulation of blood flow in vascular beds, resulting in the high cardiovascular mortality (Ewing, et al., 1980; Taskiran, et al., 2002; Dokken, 2008). Diabetic patients also have decreased NO levels (as mentioned in *'1.2. Insulin Resistance'*) and increased endothelin-1 (ET-1, a vasoconstrictor), causing a hyper-constricted state (Brownlee, 2001; Koh, et al., 2005). Hypertension and limited blood flow to the tissues are results of this.

The thickening of the basement membrane of the capillary is another sign of diabetic microvascular disease, weakening the selectivity and amount of the transport of the different metabolic products and nutrients between tissue and blood (Hayden, et al., 2005). Exercise-stimulated delivery and transport of oxygen from the capillaries, in the skeletal muscle, are delayed in diabetic patients. Therefore, T2D patients normally have poor exercise tolerance (Bauer, et al., 2007).

Interdependent mechanisms (such as pressure, flow, size and charge specificity) regulate the transport of substances and hormones from the circulation to the tissue interstitium (through the micro vessel walls) (Tooke, 1989; Hayden, et al., 2005). Thickening of the basement membrane, however, increases the permeability of the microvasculature. This is because of the physical changes in the normal electrical charge around the pores between endothelial cells. These alterations allow large molecules to pass through the microvasculature. In diabetic patients, microvascular disease (and microalbuminuria) can be picked up by a transcapillary leak of albumin in the kidney (Weir, 2007).

2.6.3. Inflammation

Tissue injury and pathogen exposure initiate an inflammatory response in the body (Pickup, et al., 1997). This is how the body heals and fights off infection. The activation of leukocytes and a family of chemokines and cytokines all regulate this response. Inflammation is beneficial and healthy, but a chronic activation can be harmful. It has been said that diabetes is a low-level and chronic state of inflammation (Wellen & Hotamisligil, 2005). This constant immune activation may lead to the insulin resistance in prediabetic and diabetic persons, as well as the increased cardiovascular risk (Festa, et al., 2000).

The reduced NO and increased ET-1 levels in diabetic patients (as discussed under '*2.6.2. Microvasculature*') can lead to the release of pro-inflammatory cytokines and enhancement of vascular permeability, apoptosis, leukocyte recruitment and ROS production. This can, therefore, intensify and aggravate the injury (Chung & Barnes, 1999; Woods, et al., 1999).

Obesity is related to increased adipokine levels (IL-6, IL-1β, TNF-α and plasminogen activator inhibitor 1 (PAI-1)) that are also associated with the inflammatory response (Trayhurn & Wood, 2005). As fat mass increases, so do these pro-inflammatory cytokines; apart from adiponectin that is decreased in obesity (Arita, et al., 1999). Adiponectin levels have an inverse relationship with cardiovascular disease.

2.6.4. Oxidative Stress

Reactive oxidative species (ROS) and its production are stimulated by pro-inflammatory cytokines (*'2.6.3 Inflammation')* (Watts & Koller, 2004). ROS molecules are molecules that have an unpaired electron in the outer orbital, making it highly reactive to other molecules (Panth, et al., 2016). The ROS molecule must obtain a stable state and electron pair, causing it to either donate an electron or take up a proton from these other compounds. When ROS binds to other compounds, the function and structure of the tissue changes. This bonding between compounds can be damaging and because ROS molecules are reactive, they can directly impair cell components such as plasma membranes, lipids, proteins and organelles (Watts & Koller, 2004).

ROS production is a normal process of the immune system (Nourooz-Zadeh, et al., 1997). ROS becomes dangerous when oxidative stress persists. This is a state where the production of ROS exceeds the anti-oxidant properties of the cells. In diabetic patients, the chronic oxidative stress is allegedly associated with: the excess fatty acids and glucose seen in the hyperglycaemic state, and the mitochondrial dysfunction seen in insulin resistance (Nourooz-Zadeh, et al., 1997; Petersen, et al., 2004).

Complications seen in insulin resistance and diabetes are related to mitochondrial dysfunction (Sohal & Sohal, 1991; Nishikawa & Araki, 2007). ATP is produced by the mitochondria via oxidative phosphorylation (refer to *'2.2.1.1. Oxidative Phosphorylation'*) and the ETC has two sites that generate ROS. It has been said that the increase in blood glucose levels in diabetes increases ROS production (Nishikawa & Araki, 2007).

Chronic hyperglycaemia induces diabetic complications by four mechanisms; (1) polyol pathway activation, (2) increased advanced glycosylation end products, (3)

protein kinase C activation and (4) hexosamine pathway activation (Brownlee, 2005). Hyperglycaemia-induced mitochondrial ROS production activates these four hyperglycaemic damage pathways, confirming the important role of oxidative stress in the pathophysiology of the cardiovascular consequences linked to diabetes (Brownlee, 2005; Dokken, 2008).

It has been previously mentioned that insulin resistance in diabetes over-activates the inflammatory response (Dokken, 2008). Leukocytes, or white blood cells, are part of the inflammatory response and immune system. Even though mitochondria are the major source of ROS, activated leukocytes can also produce ROS. Leukocytes can thus also contribute to the diabetic related oxidative stress.

2.6.5. Hypercoagulability

Hypercoagulability is another pathophysiological effect seen in diabetes (Dokken, 2008). Thrombotic deaths occur mostly when an atherosclerotic plaque ruptures and occlude a major artery by a thrombus (blood clot) (Gu, et al., 1998). The vascular endothelium is the first defense against any thrombotic event and because diabetes contributes to extensive endothelial dysfunction, this defense is weakened (Weyrich, et al., 2002).

Platelet hyperactivity is seen in a diabetic patient's blood by the (1) increased circulating platelet aggregates, (2) increased platelet aggregation, (3) increased platelet coagulation products in the plasma (products such as β-thromboglobulin, platelet factor IV, thromboxane B_2), and (4) increased coagulation activation markers (prothrombin I and II and thrombin-anti-thrombin complexes) (Carr, 2001). There are also increased levels of clotting factors such as fibrinogen, factors VII, VIII, XI, XII, kallikrein and von Willebrand factor (vWF). The anticoagulant mechanisms (the fibrinolytic systems) are seen to be weakened in diabetic persons because of the irregular clot structures that are resistant to fibrinolysis. The increased PAI-1 levels are also a factor contributing to these inhibited anticoagulant mechanisms (Carr, 2001).

2.6.6. Heart Failure

Chronic heart failure can result from any structural or functional defect in the heart that prevents the ventricle to fill and eject blood properly (Hunt, et al., 2001). Systolic heart failure is dysfunction in the contractility of the heart (left ventricular ejection fraction of less than 45 %) and diastolic heart failure is classified as dysfunction in the ability of the heart to relax and fill up with blood (Dokken, 2008; Gutierrez & Blanchard, 2004).

Diabetic patients may suffer from heart failure due to the myocardial damage that occurs after an ischaemic or thrombotic event. Endothelial dysfunction and hypercoagulable blood are factors that can cause heart failure in a diabetic patient (Gutierrez & Blanchard, 2004; Dokken, 2008).

There have, however, been cases where heart failure was not due to thrombotic events, but other pathophysiological factors (for example diabetic cardiomyopathy (DCM)) (Dokken, 2008). DCM is a myocardial disease in diabetic patients that cannot be attributed to any CVD (Marwick, 2006; Dokken, 2008). Myocardial damage, in DCM, is without macrovascular damage but with microvascular dysfunction (Kawaguchi, et al., 1997). The myocardial injuries, fibrosis and hypertrophy in DCM may be caused by the microvascular damages seen in a diabetic patient's heart.

It has been repeatedly shown, by observational studies, that diets with a high intake of plant-based foods and beverages have a lower risk of chronic diseases (such as CVDs and some cancers) (McKay & Blumberg, 2006). These studies suggest that this correlation may be connected to the phytochemical constituents and the macro- and/or micronutrient content of the foods. Evidence that an aqueous fermented rooibos (FRE) extract can protect cardiomyocytes from diabetic rats against oxidative stress and ischaemia is presented by Dludla et al. (2013). They performed an ex *vivo* study where they investigated the effect of the chronic exposure to FRE on cardiomyocytes isolated from streptozotocin (STZ) induced diabetic rat hearts (Dludla, et al., 2014).

DCM is a heart disorder in diabetic people where the heart muscles are affected. The pathogenesis of DCM includes an excessive generation of free radicals. The reduction of these excessive free radicals, by the consumption of anti-oxidants, is becoming a very popular way to battle DCM. Therefore, utilizing the antidiabetic, anti-inflammatory

and free radical scavenging effects of rooibos for DCM treatment, is very appealing (Dludla, et al., 2014).

In their study, when the cardiomyocytes were exposed to an ischaemic solution, the cardiomyocytes presented with a decrease in ATP levels, metabolic activity and intracellular GSH (glutathione). A related increase in apoptosis and intracellular ROS molecules were also seen. When pre-treated with FRE, these effects were decreased and proved better than that of vitamin E (an anti-oxidant). These results affirmed that, even under stressful conditions, FRE pretreatment of cardiomyocytes reduced intracellular ROS, apoptosis and improved ATP and GSH levels. Therefore, the authors of this study stated that it makes sense to use rooibos/FRE as a supplement of plant-derived anti-oxidants to protect against increased oxidative stress (Dludla, et al., 2014).

3. Rooibos: South Africa's favourite tea

The increasing interest in the use of plant-based extracts in commercially available products is evident. Pantsi et al. (2011) noted that, according to the World Health Organization, about 80% of the world population relies on indigenous/traditional medicines for primary health needs. Many studies have revealed that the complexity and variety of compounds in medicinal plants contribute to their uses in treatment of diseases such as diabetes and cancer (Gurib-Fakim, et al., 2010; Street & Prinsloo, 2013).

Wild growing plants are under extreme pressure because of the increased demand for local and export markets (Cunningham, 1993). This creates a need for an alternative supply of plant material for medicinal purposes. The cultivation of these plants on a large scale can contribute to a growing economy and job opportunities in South Africa. *Aspalathus linearis* is regarded to be one of the 10 most prominently used plants for medicinal purposes (Street & Prinsloo, 2013).

Polyphenols have strong anti-oxidant properties and the potential to improve diabetic complications (Zang, et al., 2006). Tea is one of the population's major sources of polyphenolic dietary intake and there is a strong relationship between drinking tea and the decreased risk of CVD. Rooibos, an herbal tea unique to South Africa, produced

from *Aspalathus linearis*, has a high phenolic content and possesses anti-oxidant, anti-inflammatory and antidiabetic properties, making it a perfect potential candidate for treatment (and possibly prevention) of diabetes or CVD (Street & Prinsloo, 2013).

Not only are job opportunities for about 8000 farm labourers in South Africa provided for by rooibos, it also provides income for employees involved in upstream activities (processing, packaging and retailing) (South African Rooibos Council, 2016). Rooibos consumption around the world has reached 15 000 tons in 2015, increasing exports up to 7 000 tons per year. More than 30 countries import rooibos from South Africa; including Germany, the Netherlands, Japan, UK and USA.

3.1. Rooibos

Rooibos, produced from *Aspalathus linearis*, is an herbal tea that has many health-promoting properties with no reported harmful stimulants (Joubert & De Beer, 2007). Just like traditional rooibos, green rooibos tea also comes from *Aspalathus linearis*, but the production process, however, differs for the two teas (Bezuidenhout, 2007; Street & Prinsloo, 2013).

Normally, after harvesting, the tea is bruised and exposed to oxygen on dry-beds (Joubert & Schulz, 2006). The traditional taste and red colour comes from the oxidation of the tea leaves. Although this process provides the pleasant taste, it also causes a loss of valuable nutrients (Bezuidenhout, 2007).

3.1.1. Aspalathin

Aspalathin, a dihydrochalcone glucoside found in *Aspalathus linearis,* is a potent anti-oxidant that, when oxidized, changes to flavanones and polymeric brown products (Schulz, et al., 2003). This traditional processing decreases the anti-oxidant activity of rooibos aqueous infusions. This is assessed by evaluating rooibos' ability to scavenge superoxide anion and DPPH (2,2-diphenyl-1-picrylhydrazyl) radicals. In a study by Schulz, et al. (2003), it was reported that the amounts of aspalathin and nothofagin decreased in fermentation. They concluded that there is generally a good linear relationship between the total anti-oxidant activity and aspalathin content in

commercial unfermented rooibos tea. They also stated that green rooibos has a higher anti-oxidant capacity and ability to scavenge biologically relevant ROS.

This gives rise to an increasing interest in the development of green rooibos. Green rooibos is an unfermented product that maximises aspalathin content and anti-oxidant potential (Schulz, et al., 2003). It is well-established that foods which enhance the functioning of the body and supply protection against diseases spark great interest in consumers. Interestingly, Dr. Christo Muller of the SA-MRC stated that green rooibos increases the breakdown of sugar into energy and improves cellular metabolism (Koza, 2013). The anti-oxidants in the Afriplex GRT Extract increase insulin sensitivity and break down blood glucose levels.

As discussed in detail in the first part of this dissertation, diabetes is a very serious disease. More knowledge and insight are required on green rooibos tea's glucose control properties. This might potentially lead to improved drugs that can control this disease. Aspalathin and nothofagin (along with their structural flavonoid analogues) show moderate anti-mutagenic properties. Street and Prinsloo (2013) states that rooibos has hepato-protective properties.

Marnewick et al. (2010) performed a study on adults at risk of cardiovascular disease to investigate the effect rooibos has on biochemical and oxidative stress parameters. Their study concluded that the consumption of fermented rooibos does indeed improve the lipid profile and the redox status. Both of these factors are associated with heart disease. Tannin is commonly found in tea but is infamous for inhibiting protein and mineral absorption; as well as slowing down metabolism. Rooibos has a low tannin content and modulates the serum lipid profile by increasing HDL-cholesterol levels and decreasing the triacylglycerol and LDL-cholesterol levels (Joubert & Schulz, 2006).

McKay and Blumberg (2006) presented studies that demonstrated a significant difference in the number of polyphenols present between green and red rooibos. These studies show that green rooibos has a higher percentage of total polyphenols, flavonoids and non-flavonoids than fermented rooibos. These differences are because of the enzymatic and chemical modification caused by processing and fermentation.

Up to date, the only known natural source of aspalathin is rooibos. Rooibos is also one of two known sources of nothofagin.

Since 2007, 'green' rooibos tea has been receiving attention from many health-conscious consumers, locally and internationally (Bezuidenhout, 2007). This makes Afriplex GRT Extract a potential solution for a number of health problems.

3.1.2. Aspalathin Function and Anti-Oxidant Capacity

Aspalathin is a very powerful anti-oxidant that protects body tissues (Koza, 2013). He states that aspalathin improves lipid metabolism and has the potential to be used to protect against the development of diabetes (Koza, 2013).

According to Koza (2013), the development of new drugs for T2D should focus on treatments to improve insulin resistance with fewer side effects. He says that, with aspalathin, the onset of diabetes could possibly be delayed. Rooibos also helps prevent blood clots by reducing the amount of fat molecules (cholesterol) in the blood and this, in turn, protects the heart.

According to research supported by the Cancer Association of South Africa, six 200 ml cups of strong rooibos tea a day increases GSH (a natural anti-oxidant) by almost 100%. GSH binds and removes toxins from the body, helping to eliminate harmful substances in our systems, says Carl Albrecht (head of research at the cancer association) (Koza, 2013). Rooibos stimulates the body to produce more GSH.

4. Afriplex Green Rooibos Extract

Afriplex is a company focussing on plant extracts and natural additives. Afriplex, founded in 2000, is the acronym for African Plant Extracts and it has been their aim to add value to South African flora and local markets. Afriplex started producing a green rooibos tea in 2003. GRE serves as an improved product, better than normal rooibos tea. Danie Nel (Afriplex MD) says that green rooibos not only is a better source of nutrients than normal rooibos but contains less tannins as well (Table 1.1). Tannins are commonly found in tea and allegedly slows down the body's metabolism and ability to absorb minerals and proteins (Bezuidenhout, 2007).

Afriplex developed a process to keep the anti-oxidants intact. Instead of exposing the leaves to oxygen, an inert gas was used. This inert gas slows down the oxidation process during the drying-out stage, which produces a high-quality green rooibos tea (Bezuidenhout, 2007).

Afriplex states that health-conscious clients understand the health benefits of the green tea variant and will therefore easily make the transition from normal rooibos tea. Nel explains that South Africans are traditional rooibos tea drinkers and will therefore need to get accustomed to the green rooibos tea taste (Bezuidenhout, 2007).

Afriplex GRT Extract is a laboratory standardized extract of unfermented *Aspalathus linearis* (Burm.f.) R. Dahlgren rich in aspalathin and nothofagin, making it a potential powerful anti-oxidant. It is a red coloured powder and might have potential beneficial effects on diabetes. This aspalathin-rich product is currently being investigated for possible commercialization.

Aspalathin comprises about 14% of the Afriplex GRT Extract and gives this product, along with nothofagin, its anti-oxidative properties (Beelders, et al., 2012; Ku, et al., 2015). Another flavonoid is PPAG (phenylpropenoic acid glucoside) that has positive effects on both pancreatic β-cells and hyperglycaemia (Himpe, et al., 2016), whereas quercetin is known to improve obesity (Kuppusamy & Das, 1992; Ahn, et al., 2008; Rivera, et al., 2008). PPAG is also said to improve oxidative stress (Dludla, et al., 2014; Dludla, et al., 2017). Table 1.1 summarizes the concentrations of the different components in the Afriplex GRT Extract (Beelders, et al., 2012) (refer to Appendix B for the HPLC analysis of Afriplex GRT Extract).

Table 1.1 Concentration of flavonoids, flavonols and polyphenols in Afriplex GRT Extract (g compound/100 g soluble solids)	
PPAG	0,423265
Aspalathin	12,78348
Nothofagin	1,974419
Orientin	1,255839
Isoorientin	1,427281
Vitexin	0,338513
Isovitexin	0,298022
Q-3- ROB	1,040565
Rutin	0,496034
Hyperoside	0,398773
Isoquercitrin	0,572251852

The current study aimed to investigate the following in view of (i) the recognized high incidence of obesity, T2D and CVD, as well as (ii) the possibility that an aspalathin-rich substance may ameliorate these conditions:

- To characterize the effects of the high fat diet on the basal metabolism and signalling in the animals.
- Whether Afriplex GRT Extract ingestion has any effect on the high fat diet and control diet.
- Whether Afriplex GRT Extract ingestion can improve the insulin resistance state elicited by a high fat diet using a rat model.
- Whether Afriplex GRT Extract ingestion has any effects on myocardial mitochondrial oxidative phosphorylation potential and the process of mitophagy.

To answer these questions, a Wistar rat model of diet-induced obesity was used and compared to chow-fed control animals. Both groups were treated with Afriplex GRT Extract for a period of 6 weeks. Animals were grouped as follows:

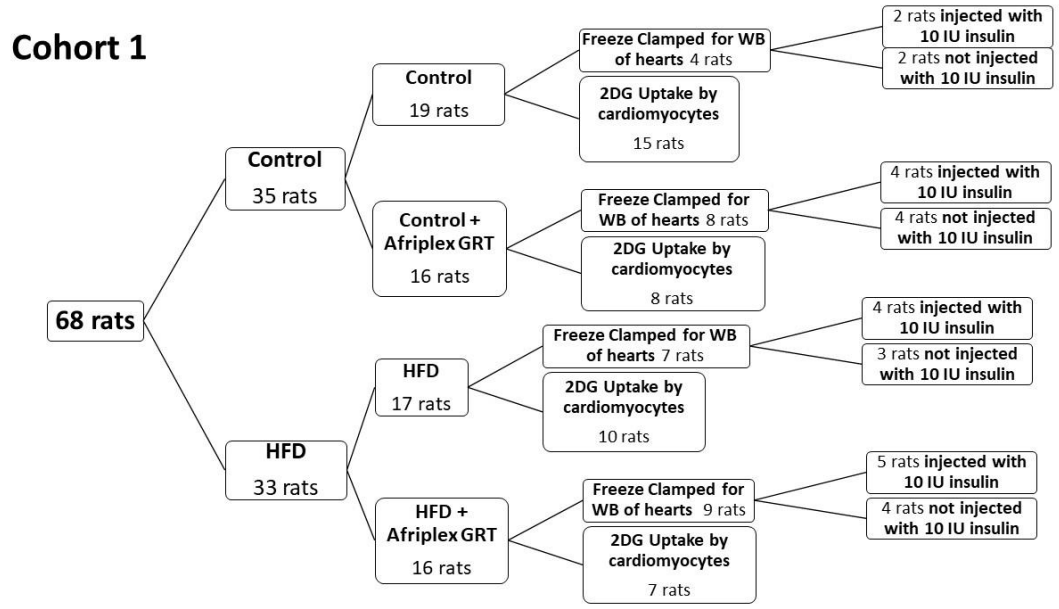

Figure 1.14 *A flow chart showing the animals distribution of cohort 1. Note that the 10 IU insulin was injected in the animal 10 minutes prior to sacrifice. WB = Western Blot.*

Please note that the discrepancies between the n-values from Figure 1.14 and the Western Blots (Figures 3.23 to 3.35) are because there were very few freeze-clamped hearts available for Western Blot analysis.

The 2DG uptake experiments were done on the cardiomyocytes from the first cohort. The cardiomyocytes were treated with insulin *ex vivo*, but no effect was seen. We thus proceeded to cohort 2 where some of the animals were injected with insulin *in vitro,* 10 minutes before sacrifice. Some of the rats were injected with insulin in order to activate the insulin signalling pathway and to decrease glucose levels. This was performed to see if the treatment with Afriplex GRT Extract affected the insulin signalling pathway in the heart.

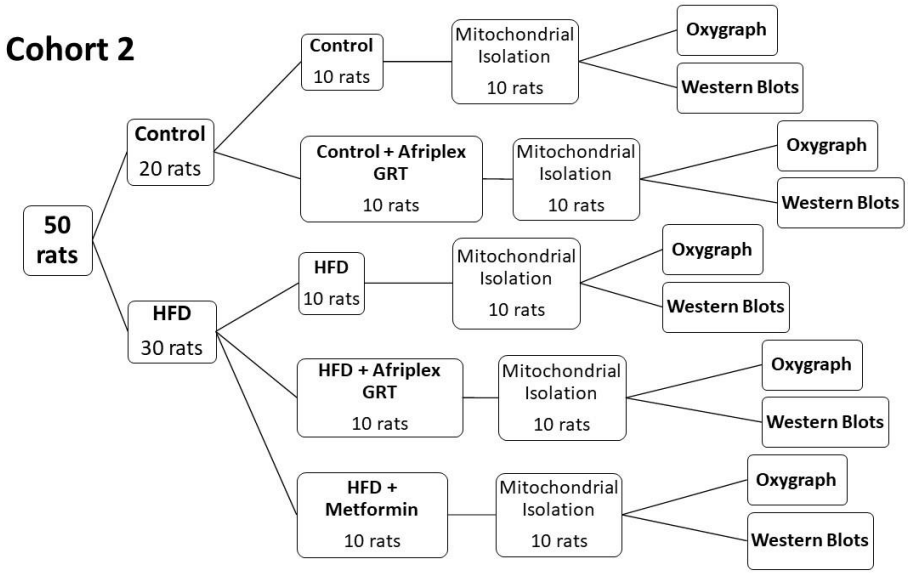

Figure 1.15 *A flow chart showing the animals distribution of cohort 2.*

In the second cohort, a group of HFD animals were treated with metformin, because it is known that metformin decreases glucose levels to treat diabetes. The control animals were not treated with metformin, because the treatment would have decreased the glucose levels and caused hypoglycaemia in the control animals.

CHAPTER 2: Materials and Methods

The following experiments were performed at the Faculty of Medicine and Health Sciences, Tygerberg Campus, Stellenbosch University.

1. Animal Treatment, Biometric Measurements and Sacrifice of Animals

Ethical clearance was obtained from the Committee for the use of animal in research of the University of Stellenbosch (SU-ACUD15/00102 (2016) and SU-ACUD16/00179 (2017)). The study was conducted under the revised South African National Standard for the Care and Use of Animals for Scientific Purposes (South African Bureau of Standards, SANS 10386, 2008).

Male Wistar rats (initial body weights of 190 ± 10 g) were fed a high fat diet (HFD) and compared to age matched controls (fed normal rat chow). The animals received separate diets for a total of 16 weeks, with free access to food and water. Body weights were measured weekly and food- and water intake daily, throughout the 16-week period. They were kept on a 12-hour day/night cycle in the Central Research Facility of the Faculty of Health Sciences of the University of Stellenbosch.

From week 11 to 16, half of each group was treated with Afriplex GRT Extract (60 mg/kg/day) in the form of jelly cubes. The jelly cubes were made from a mix containing 4 g commercially available jelly, 4 g gelatin, 25 ml boiling H_2O and the calculated amount of Afriplex GRT Extract powder (calculated according to the body weight of the animals). After the jelly and gelatin granules were dissolved, a repetitive pipette (Gilson™ Distriman™ Positive-Displacement Repetitive Pipette) was used to dispense 1 ml of the mixture into each cube on an ice-tray. The tray was placed in a fridge to set, where after one cube was given to every rat per day. The Afriplex GRT Extract jelly-cubes were prepared weekly and given to the animals daily.

The Afriplex GRT Extract dosage administered was deduced from available literature on similar extracts, since no information was available regarding the exact dosage of this specific product. A similarly prepared green rooibos extract was demonstrated to lower plasma glucose levels in rats at a dosage of 30 mg/kg (Muller, et al., 2012). In a different mouse study, this exact extract was administered at doses of 0.3 % and 0.6% of the diet (Kamakura, et al., 2015). If this is calculated according to a rat weighing

250 g, and consuming approximately 20 g food per day, the dosage would be about 250 mg/kg/day, which is very high indeed. In a personal communication between Prof. Barbara Huisamen and Dr. Christo Muller it was said that a 90 mg/kg/day dosage was used in non-human primates. When this is calculated according to the equations of Freireich EJ, et al. (1966), the dosage for a rat will be 180 mg/kg/day. Therefore, it was decided on a slightly higher dose than the initial 30 mg/kg/day (Muller, et al., 2012), but lower than the dosage used in mice or non-human primates.

In cohort 2, as a positive control, a group of HFD rats were treated with the antidiabetic substance, metformin, at 50 mg/kg/day. Body weights were monitored throughout the 16-week period. After 16 weeks, animals were sacrificed by means of an overdose of Eutha-naze (at 160mg/kg sodium pentobarbital). The body weight, fasting glucose and insulin levels were determined at sacrifice. To assure that the animals showed no response, a foot-pinch test (pedal reflex) was done before opening the chest cavity. As soon as the animal showed no pedal reflex, the chest cavity was opened and the heart was removed for further experimentation. The intraperitoneal fat (IP fat) was weighed and stored hereafter.

2. Composition of Diet

Two different diets, namely the high fat diet (HFD) and control diet, were fed to the animals for the period of 16 weeks. The high fat diet was prepared from 200 ml boiling water, 390 g normal rat chow, 100 g fructose (Sigma-Aldrich), 100 g casein (Sigma-Aldrich), 10 g cholesterol (Sigma-Aldrich), 750 g Holsum cooking fat and 790 g Nestle sweetened condensed milk. The pellets were soaked in boiling water and crushed to a smooth consistency. The other ingredients were mixed in and the food was stored in a fridge. The food was made up weekly.

3. Oral Glucose Tolerance Test and Glucose Measurement

An Oral Glucose Tolerance Test (OGTT) monitors the blood glucose level at different intervals. This procedure determines how efficiently the body metabolises sugar or carbohydrates and is thus a central marker for determining insulin sensitivity. Animals were fasted overnight. For the duration of the procedure, the animals were anaesthetized by intraperitoneal injection of 0.1 ml Eutha-naze (50 mg/kg sodium

pentobarbital). The basal glucose level of each animal was determined by pricking the tail, collecting a drop of blood and measuring with a commercially available handheld glucometer. Hereafter, 1 mg/kg of 50 % sucrose solution was gavaged to each animal. Thereafter, using the same tail prick, the blood glucose level was monitored and measured at different intervals (3 minutes, 5 minutes, 10 minutes, 15 minutes, 20 minutes, 25 minutes, 30 minutes, 45 minutes, 60 minutes, 90 minutes and 120 minutes respectively). After this metabolic insult, the animals were left to recover for a week before further experiments were conducted.

4. Biochemical Analysis: Assays

4.1. Blood Collection

After fasting the animals overnight, 1 ml blood was drawn directly from the carotid artery while the animal was under anesthesia. Blood was collected from all the groups at week 15. The blood was then centrifuged for 10 minutes at 3000 rpm (revolutions per minute) on the Damon/IEC Division Clini-Cool Centrifuge. The serum was removed and stored at -80 °C. This blood was used to determine fasting insulin levels.

4.2. Leptin Assay

For determining leptin levels, Abcam® Leptin Rat ELISA (Enzyme-Linked Immunosorbent Assay) kit was used. This kit contained a 96-well plate and all the reagents needed. The reagents and standards were prepared (according to the manufacturer's instructions) and equilibrated to room temperature before use. All the samples were analyzed in duplicate.

The 96-well plate supplied was ready to use and rinsing of the plate was not necessary. Samples were diluted 3-fold by using 1X Assay Diluent D. 100 µl of the standards, along with the samples, were pipetted into their respective wells. The wells were covered and incubated for 2 and a half hours at room temperature, while shaking gently on a shaker. During this incubation, the leptin in the samples bound to the immobilized antibody in the wells. The wells were then washed 4 times with 300 µl 1X Wash Solution, using a multi-channel pipette. After the last wash, the plate was inverted on a paper towel to decant all the remaining Wash Buffer.

After this, 100 µl of Biotinylated Leptin Antibody was added to each well and allowed to incubate for 1 hour at room temperature while gently shaking. The unbound Biotinylated Antibody was then washed away (as previously done) before adding 100 µl HRP (horse radish peroxidase)-conjugated streptavidin to each well. This was allowed to incubate for 45 minutes at room temperature while gently shaking. After washing again, 100 µl TMB (3,3',5,5'-Tetramethylbenzidine substrate) One-Step Substrate Reagent was then added and allowed to incubate for 30 minutes at room temperature while gently shaking in the dark. This reaction turned the samples a blue colour. The colour developed in proportion to the leptin levels. The colour changed to yellow as soon as 50 µl of the Stop Solution was added to each well. By using the microplate reader, the colour intensity was immediately measured at 450 nm.

The mean absorbance of each set of the duplicates of the samples and standards was calculated. For a 4-parameter logistic equation curve, the standard concentration was stipulated on the x-axis and absorbance on the y-axis. An increase in the absorbance was directly proportional to the levels of leptin in the serum samples. The standard curve was used as a reference for the determination of the samples. To set up the curve and calculate the insulin levels, an online ELISA analysis program (http://elisaanalysis.com) was used. Refer to Figure 2.1 for a summary of the protocol.

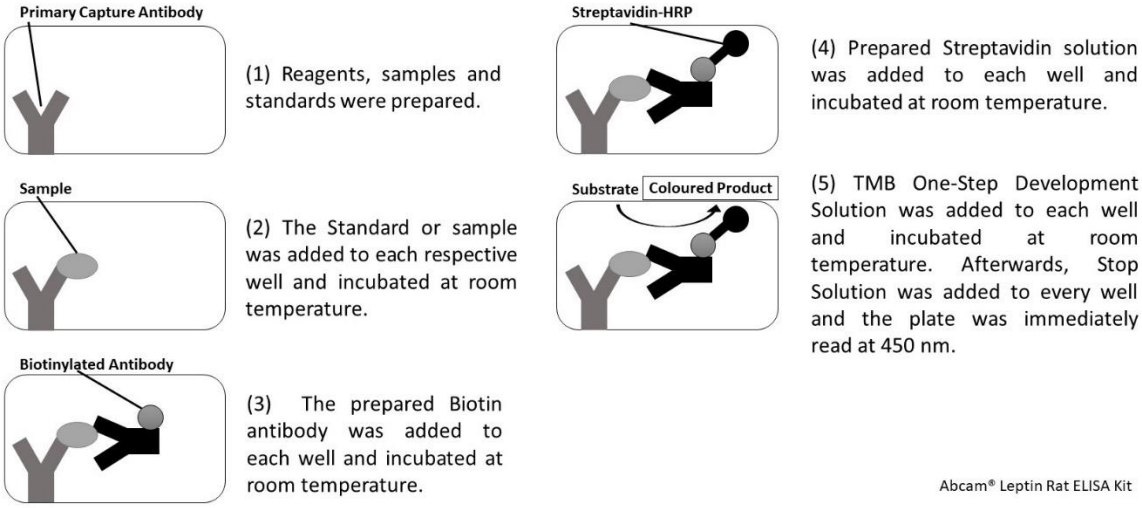

Figure 2.1 *A schematic of the Abcam Leptin Rat ELISA (adapted from the ab100773 ELISA protocol).*

4.3. Adiponectin Assay

For determining adiponectin levels, Abcam's® Adiponectin Rat ELISA kit was used. This kit contained a 96-well plate and all the reagents needed. The reagents and standards were prepared (according to the manufacturer's instructions) and equilibrated to room temperature before use. All the samples were analyzed in duplicate.

The 96-well plate supplied was ready to use and rinsing of the plate was not necessary. Samples were diluted 1:400 by using 1X Diluent N. 50 µl of the standards, along with the samples, were pipetted into their respective wells. The wells were covered and incubated for 1 hour at room temperature, while shaking gently on a shaker. During this incubation, the adiponectin in the samples bound to the immobilized antibody in the wells. The wells were then washed 5 times with 200 µl 1X Wash Buffer, using a multi-channel pipette. After the last wash, the plate was inverted on a paper towel to decant all the remaining Wash Buffer.

After this, 50 µl of Biotinylated Adiponectin Antibody was added to each well and allowed to incubate for 1 hour at room temperature while gently shaking. The unbound Biotinylated Antibody was then washed away (as previously done) before adding 50 µl 1X Streptavidin-Peroxidase Conjugate to each well. This was allowed to incubate for 30 minutes at room temperature while gently shaking. After washing again, 50 µl Chromogen Substrate was then added and allowed to incubate for 10 minutes at room temperature while gently shaking in the dark. This turned the samples a blue colour. The colour develops in proportion to the adiponectin levels. The colour changed to yellow as soon as 50 µl of the Stop Solution was added to each well. By using the microplate reader, the colour intensity was immediately measured at 450 nm and 570 nm.

The average absorbance of each set of the duplicates of the samples and standards was calculated. For a 4-parameter logistic equation curve, the standard concentration was stipulated on the x-axis and absorbance on the y-axis. An increase in the absorbance is directly proportional to the levels of adiponectin in the serum samples. The standard curve was used as a reference for the determination of the samples. To

set up the curve and calculate the insulin levels, an online ELISA analysis program (http://elisaanalysis.com) was used. Refer to Figure 2.2 for a summary of the protocol.

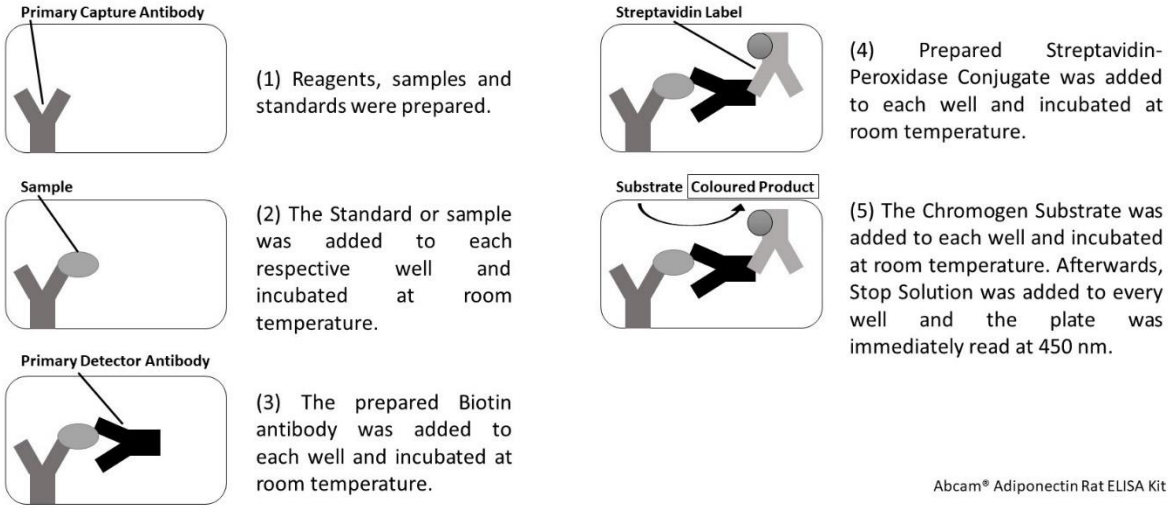

Figure 2.2 *A schematic of the Abcam Adiponectin Rat ELISA (adapted from the ab108784 ELISA protocol).*

4.4. Insulin Assay

To determine insulin levels, the RayBio® Rat Insulin ELISA kit was used. This kit contained a 96-well plate and all the reagents needed. The reagents and standards were prepared (according to the manufacturer's instructions) and equilibrated to room temperature before use. All the samples were analyzed in duplicate.

The 96-well plate supplied was ready to use and rinsing of the plate was not necessary. Of the standards and samples,100 µl was pipetted into the ready to go 96-well plates. The insulin present in the serum samples bound to the immobilized antibody. This incubation was allowed for 2 and a half hours while gently shaking. The wells were then washed 4 times with 300 µl 1X Wash Solution. After the last wash, the plate was inverted onto a paper towel to decant the remaining 1X Wash Solution.

100 µl of the prepared biotinylated anti-Rat Insulin antibody was added and incubated for 1 hour while gently shaking. Unbound biotinylated antibody was washed away as previously mentioned, before adding 100 µl of the prepared HRP-conjugated Streptavidin. Incubation for 45 minutes while gently shaking was allowed to take place before washing the wells again. 100 µl of the TMB One-Step Substrate Reagent was added and incubated for 30 minutes in the dark room while gently shaking, allowing

the samples to develop a blue colour. To stop the reaction and change the colour to yellow, 50 µl of the Stop Solution was pipetted into each well. The absorbance was then immediately measured at 450 nm.

The mean absorbance of each set of the duplicates of the samples and standards was calculated. For a 4-parameter logistic equation curve, the standard concentration was stipulated on the x-axis and absorbance on the y-axis. An increase in the absorbance was directly proportional to the levels of insulin in the serum samples. The standard curve was used as a reference for the determination of the samples. To set up the curve and calculate the insulin levels, an online ELISA analysis program (http://elisaanalysis.com) was used. Refer to Figure 2.3 for a summary of the protocol.

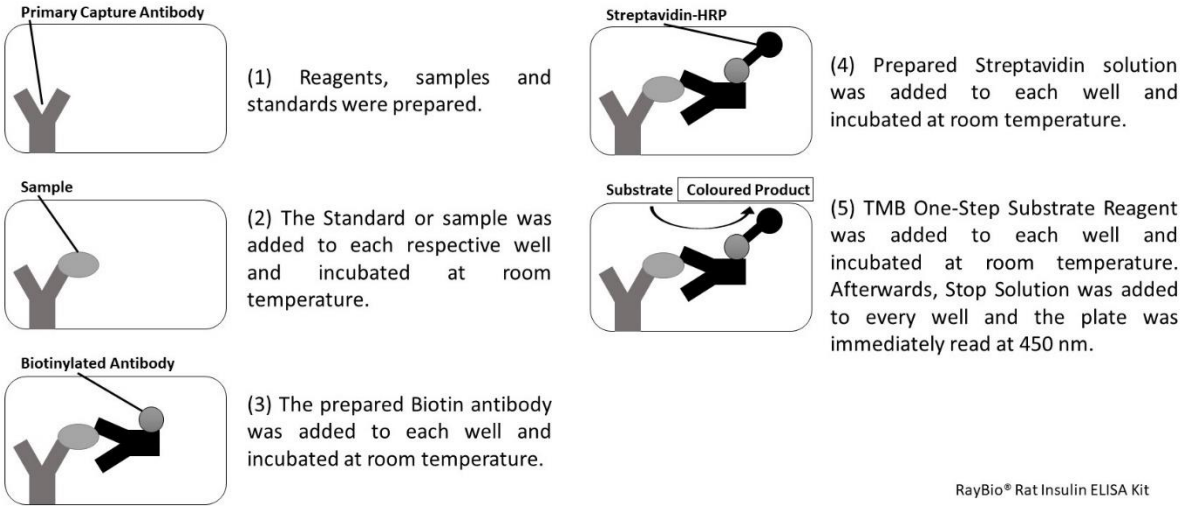

Figure 2.3 *A schematic of the RayBio Insulin Rat ELISA (adapted from the ELR-Insulin ELISA protocol).*

5. Isolation of Ventricular Cardiomyocytes

After the removal of the heart from the chest cavity, the heart was placed in ice-cold Krebs-Henseleit buffer (119 mM NaCl, 24.9 mM $NaHCO_3$, 4.75 mM KCl, 1.19 mM KH_2PO_4, 0.6 mM $MgSO_4 \cdot 7H_2O$, 0.59 mM Na_2SO_4, 1.25 mM $CaCl_2 \cdot 12H_2O$ and 10 mM glucose), after which the heart was cannulated via the aorta onto the perfusion system. The heart was retrogradely perfused with a calcium (Ca^{2+}) free Hepes buffer ('Solution A' containing: 6 mM KCl, 1 mM Na_2HPO_4, 0.2 mM NaH_2PO_4, 1.4 mM $MgSO_4$, 128 mM NaCl, 10 mm 4-(2-hydroxyethyl)-1-piperazineethanesulfonic acid (Hepes), 5.5 mM D-glucose and 2 mM pyruvate; pH 7.4) at 37 °C for 5 minutes.

Throughout the perfusion procedure, the heart was continuously gassed with 100 % oxygen (O_2). After the first 5 minutes, the hearts were perfused with Hepes digestion buffer ('Solution B' containing: 'Solution A', 0.7 % fatty acid free BSA, 1 mg/ml Worthington Collagenase Type II and 18 mM BDM (2,3-butanedione monoxime) (*an ATPase inhibitor to prevent the activation of the myosin protein and contraction*) for 15 minutes in a re-circulating manner.

Hepes, BDM, D-glucose and the Na-pyruvate were all purchased from Sigma-Aldrich (St Louis MO). Worthington Collagenase Type II was purchased from Worthington Biochemical Corporation (Lakewood, NJ). BSA and fatty acid free BSA was obtained from Roche (Cape Town).

50 µl of 100 µM $CaCl_2$ addition was started after 20 minutes and 25 minutes. The reason for the slow addition of $CaCl_2$, was to prevent Ca^{2+} overload. The indication of when the heart was fully digested was when the perfusate changed from a dripping to a free-flowing state. The heart was detached from the cannula; where after the connective tissues were removed, as well as the ventricles from the atria. The ventricular tissue was then torn apart and incubated for 15 minutes under 100 % O_2 in 50 ml post-digestion buffer ('Solution C' containing: 50 % of 'Solution A,' 50 % of 'Solution B,' 1 % BSA, 1 % fatty acid free BSA and 0.2 mM $CaCl_2$) in the IncuShaker at 37 °C and 30 rpm. After the 15 minutes of incubation, 100 mM $CaCl_2$ was added at 16, 17, 18, 19 and 20 minutes respectively. These additions were done to reach a final concentration of 1.25 mM (4 x 100 µl 100 mM $CaCl_2$ and 1 x 125 µl 100 mM $CaCl_2$). The tissue was then filtered through a 200 x 200 µm nylon net and gently spun down at 300 rpm for 3 minutes. The supernatant was aspirated and the pellet suspended in 35 ml Solution D for 5 minutes ('Solution D' containing: 'Solution A,' 2 % fatty acid free BSA and 1.25 mM $CaCl_2$). This suspension step in 2 % BSA solution was to ensure that the live cells form a loose pellet and settle under gravity. Only viable cardiomyocytes will settle into a pellet and the non-viable cells will 'float' around in the supernatant, thus the removal of the supernatant will also remove the non-viable cells. The loose pellet was resuspended in the 15 ml fresh Solution D under 100 % O_2 for 1 hour, slowly rotating in the IncuShaker at 30 rpm.

The cells were removed and left to settle under gravity for about 5 to 8 minutes. The supernatant was gently removed and the pellet resuspended in 6 ml Solution E

('Solution E' containing: 'Solution A' minus D-glucose and pyruvate, plus 2.0 % fatty acid free BSA and 1.25 mM $CaCl_2$). The cells were spun down gently at 100 rpm for 3 minutes. This washing step was repeated 3 times in fresh Solution E and the supernatant discarded after each wash. After the third wash, the cells were finally suspended in 5.5 ml fresh Solution E.

5.1. 2DG Uptake Induced By Insulin Concentrations

2DG is a glucose molecule that can be taken up but not metabolized by the cardiomyocytes, because of the hydrogen molecule it contains (instead of a 2-hydroxyl group) at position C2. The uptake of 2DG by cardiomyocytes was measured at different insulin concentrations.

The first step for this assay was to prepare the dilutions of Phloretin (Phl), insulin and 2DG. I*nsulin, deoxy-glucose and phloretin were obtained from Sigma-Aldrich (St Louis, MO). The radiolabelled 2DG was purchased from PerkinElmer South Africa (Pty) Ltd.*

The phloretin was prepared from 100 µl Phl stock (64 mM stock solution in DMSO) and 900 µl Solution E. 2DG was made up from 580 µl deoxy-glucose (45.6 mM stock solution) and 20 µl radioactive (tritiated) deoxy-glucose. Insulin was made up in a concentration of 100 nM in Solution E.

The cells were incubated at 37°C in Solution E in a total volume of 750 uL in a 24-well plate in a bench top incubator (IncuShaker). Phloretin, at a concentration of 400 uM, was initially only added to the designated phloretin samples to act as a control for carrier-mediated glucose uptake. Each dilution was made up in duplicate. After 20 minutes, 75 µl of the different insulin concentrations (100 nM, 10 nM, 1 nM) were added to their respective samples. At 35 minutes, glucose uptake was initiated by adding 25 µl of the 2DG to all the samples. After a further 30 min of incubation, to terminate glucose uptake, Phloretin was added to all the samples (except the Phloretin marked samples).

Plastic pasteur pipettes were used to transfer the contents from each of the flat-bottomed tubes over to Eppendorf tubes. The Eppendorf tubes were spun down at 14500 rpm for 90 seconds in a mini-centrifuge (Eppendorf® Minispin®). The

supernatant was aspirated and the pellet washed with ~250 µl Hepes buffer (without substrates), twice. After this, the supernatant was finally removed and the Eppendorf tubes were dried using an ear-bud. The pellet was dissolved in 500 µL 1N NaOH in the waterbath at 60°C for ~15-30 minutes.

To render a concentration of 0.5 N NaOH, 500 µl dH_2O was added to the pellet. These samples were used for Lowry protein determination (refer to Chapter 2, Section 6) and counting of the radio-activity accumulation using a scintillation counter.

For the 2DG uptake measurement in the scintillation counter, 100 µl of the dissolved sample in 0.5 N NaOH was added to 3 ml scintillation fluid (in duplicate). A blank was prepared with only scintillation fluid and another vial was prepared with scintillation fluid and 25 µl of the radiolabelled 2DG mixture. This was included to determine the specific activity of the 1100 pmol (picomol) 2DG in 25 uL. The vials were left to stand in a dark room overnight. This was done to minimize chemiluminescence production after adding the alkaline solution to the scintillation fluid. The radioactivity was counted in a Beckman® scintillation counter as disintegrations per minute (DPM). From the Lowry assay, the total protein values (mg/mL) were calculated and used with the DPM values to calculate glucose uptake in pmol 2DG/mg protein/30 mins. The Phloretin samples' average (expressed as pmol 2DG/mg protein/30 mins) were subtracted from every sample to correct for background 2DG uptake.

6. Lowry Protein Determination

The Lowry protein determination procedure is designed to determine protein concentrations of 0.01 mg/mL to 1.0 mg/mL (Lowry, et al., 1951). This procedure uses the Folin reaction. Initially, the proteins are pre-treated with copper ions in an alkali solution. These proteins reduce the phosmolybdic-phosphotungstic acid in the Folin Ciocalteus reagent, causing a blue colour to appear (Schagger, et al., 1994). The protein levels are then calculated from the amount of reduced Folin-Ciocalteu reagent in the solution. The reading absorbance is at 759 nm and a standard curve of selected known Bovine Serum Albumin (BSA) concentrations were used to calculate the protein concentrations in each sample.

The BSA standards were prepared from a BSA solution in H_2O with a known concentration. The OD was determined spectrophotometrically at 280 nm, using the molar extinction coefficient of BSA (1.51) to calculate the exact concentration of the stock standard. This stock was then used to prepare the working standards in 0.5 N NaOH, as indicated in Table 2.1.

Table 2.1 ***BSA Standards***

Standard 1	1 ml undiluted BSA in 200 ml 0.5 N NaOH
Standard 2	2 ml undiluted BSA in 200 ml 0.5 N NaOH
Standard 3	2 ml undiluted BSA in 100 ml 0.5 N NaOH

Stock solutions included 2% Na-K-Tartrate in dH_2O, 1% $CuSO_4.5H_2O$ in dH_2O, 2% Na_2CO_3 in dH_2O, Folin-Ciocalteu (kept at 4 °C) and BSA standard solutions. The Na-K-Tartrate-$CuSO_4$ solution was made up of 98 ml 2% Na_2CO_3, 1 ml 1% $CuSO_4.5H_2O$ and 1 ml 2% Na-K-Tartrate. For the Folin Ciocult dilution (1:3), 4 ml Folin-Ciocalteu was mixed with 8 ml dH_2O to make up 12 ml.

For the blank, 50 µl of 0.5 N NaOH was pipetted into a Lucham tube. 50 µl of each of the three BSA standards (assayed in triplicate) was pipetted into their designated Lucham tubes. For the samples, 50 µl of each were pipetted into their designated tubes. The samples were assayed in duplicate.

After preparation, 1 ml Na-K-Tartrate-$CuSO_4$ was added to each tube at time intervals of 10 seconds. Every tube was vortexed after addition. Ten minutes after the first addition of Na-K-Tartrate-$CuSO_4$, 100 µl of the Folin-Ciocalteu dilution was added to each tube, also with time intervals of 10 seconds between additions. The tubes were also vortexed after addition. When done, the tubes were left on the bench for 30 minutes to allow full colour development before reading the OD values on the spectrophotometer at 750 nm. The blank was set with the 0.5 N NaOH sample.

The standard curve was set up in an Excel sheet by plotting the OD values on the Y-axis and the standard protein concentrations (mg/ml) on the X-axis. This standard curve was used to determine the total protein amount (mg/ml) of every sample.

7. Mitochondrial Isolation

Polarographic measurement of mitochondrial respiration was used to determine the oxidative phosphorylation potential of the hearts. This was carried out by measuring the oxygen tension using the Hansatech Clark-type oxygen electrode (Hansatech Instruments).

Reagents included 0.18 M KCl, 0.01 M Ethylenediaminetetraacetic acid (EDTA), lysis buffer and 10 % Trichloroacetic acid (TCA).

Procedure:

The heart ventricles were longitudinally cut after sacrifice. Each half was minced separately into small pieces in Sorvall tubes containing ice cold KE buffer (0.18 M KCl and 0.01 M EDTA, pH 7.4) and rinsed to remove all traces of blood. In two bursts, the hearts were homogenised on ice with the Heidolph silent crusher M homgenizer for 4 seconds at 12000 rpm. The homogenates were centrifuged (Sorvall SS34 rotor) for 10 min at 4 °C at 2500 rpm to pellet the nuclei and larger remaining debris. The supernatant was decanted and centrifuged for another 10 min at 12500 rpms at 4 °C to sediment the mitochondria into a pellet. After this step, two separate Sorvall tubes with pellets were available. The supernatant was gently removed from both pellets. The one pellet was carefully removed and suspended in 0.26 ml KE buffer for oxidative phosphorylation determination (Hansatech Clark-type oxygen electrode) (referred to as Suspension 1). Using a Glass-Teflon homogenizer (Teflon® pestle PYREX® Potter-Elvehjem tissue grinders), the pellet was gently homogenized. The other pellet was gently suspended, homogenized (Teflon® pestle PYREX® Potter-Elvehjem tissue grinders) and stored away in 200 µl standard lysis buffer at -80 °C (refer to *'8.1 Lysate Preparation'*) for Western Blot analysis (*'8. Western Blots'*) (referred to as Suspension 2).

Of Suspension 1, 50 µl was precipitated in 1 mL 10% TCA for the Lowry assay (*'6. Lowry Protein Determination'*). For the oxygraph, 100 µl of the mitochondrial suspension was used and the rest was stored away at -80 °C for determination of the citrate synthase activity.

7.1. Mitochondrial Oxidative Phosphorylation

Reagents included 2 substrate media; glutamate (with malate) and palmitoyl-L-carnitine (with malate). The glutamate (carbohydrate) medium consisted of 2 ml 1.25 M sucrose, 1 ml 100 mM Tris-HCl (pH 7.4 with 2 M Tris), 1 ml 85 mM KH_2PO_4, 1 ml 50 mM glutamate (pH 7.4 with 2 M Tris), 1 ml 20 mM malate (pH 7.4 with 2 M Tris) and dH_2O. The palmitoyl-L-carnitine (fatty acid) medium consisted of all the ingredients for glutamate medium, but instead of glutamate, 1 ml 45 mM palmitoyl-L-carnitine was added. The pH was again adjusted to 7.4 before dH_2O was added up to 10 ml. The media were kept at room temperature.

Other reagents included 50% KCl, $Na_2S_2O_4$ (Merck Pty Ltd) and adenosine-5'-diphosphate monopotassium salt hydrate (ADP) (Sigma-Aldrich). ADP was prepared by dissolving 0.02 g in 5 ml dH_2O and the final concentration was determined with an Ultra Violet (UV) spectrophotometer at 259 nm (ADP molar extinction coefficient: 15,4).

7.1.1. Oxygraph setup:

One drop of 50% KCl (an electrolyte) was applied to the cathode and 3 drops on the anode beneath the dome. A paper spacer (Rizla) was first placed over the cathode and dome, and then an oxygen permeable membrane over the paper spacer. The paper spacer and membrane were secured with an O-ring using an applicator shaft. The electrode disk was sealed into the oxygen electrode chamber with an outer O-ring (refer to Figure 2.4 and Figure 2.5 for a visual representation of the oxygraph instrument used in this study (Hansatech Instruments, 2017)).

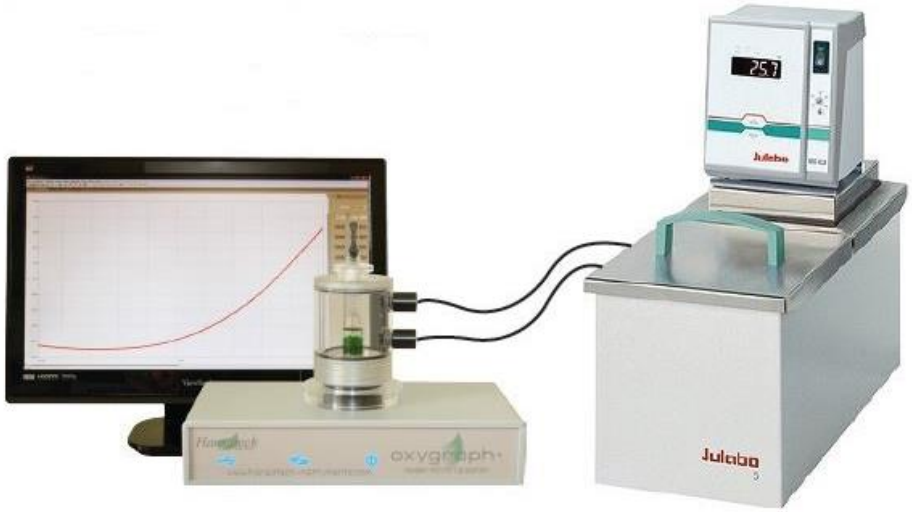

Figure 2.4 *The Oxygraph System (Hansatech Instruments) (adapted from Hansatech Instruments (2017)).*

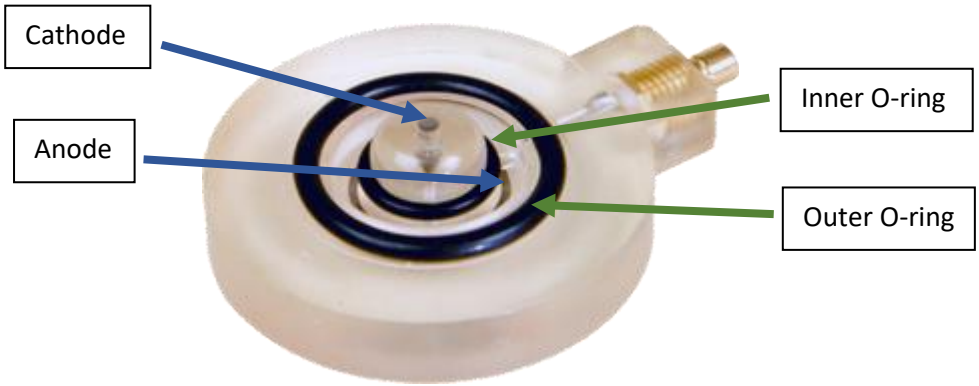

Figure 2.5 *The S1 electrode from the Oxygraph System (Hansatech Instruments) (adapted from Hansatech Instruments (2017)).*

The system was calibrated before every experiment by adding 650 µl of the respective incubation medium (glutamate or palmitoyl-L-carnitine) and a small magnetic stirrer to the oxygraph chamber. The temperature was set to 25 °C and the speed of the magnetic stirrer to 100. The oxygraph was calibrated in the liquid phase. After the plateau of ambient oxygen saturation of the medium was reached, a few grains of $Na_2S_2O_4$ was added to the chamber to remove all oxygen within the chamber (zero oxygen levels). Once the plateau was reached again, the settings of 100% and 0% oxygen were stored and the chamber rinsed thoroughly with dH_2O before replacing with fresh 650 µl of incubation medium for the experiment.

Procedure:

The chamber was filled with 650 µl of the respective incubation medium. 100 µl of the mitochondria suspension in KE buffer (Suspension 1) was added to the chamber. The

system was the closed and allowed to record for several seconds (this was state 2, where respiration of mitochondria took place in the presence of the substrate alone). After a few seconds, 50 µl of ADP was added to the chamber using a Hamilton syringe. This represented state 3, where mitochondria can convert the ADP to ATP. As soon as a curve started to form (this was where the mitochondria returned to their normal respiration state 4 after the mitochondria converted all ADP to ATP), it was allowed to run for about 60 seconds before 50 µl of 10x ADP concentration (± 3500 nM) was added to the chamber. This enabled the mitochondria to convert as much ADP to ATP as possible, until all the oxygen in the chamber was consumed. As soon as the oxygen levels reached zero, the recording was stopped and the mitochondria were subjected to anoxia for 20 minutes. After the 20 minutes, a Pasteur pipet was used to re-oxygenate the medium to ~50% of the initial concentration. Measurement of the re-oxygenation state 3 respiration was thus performed.

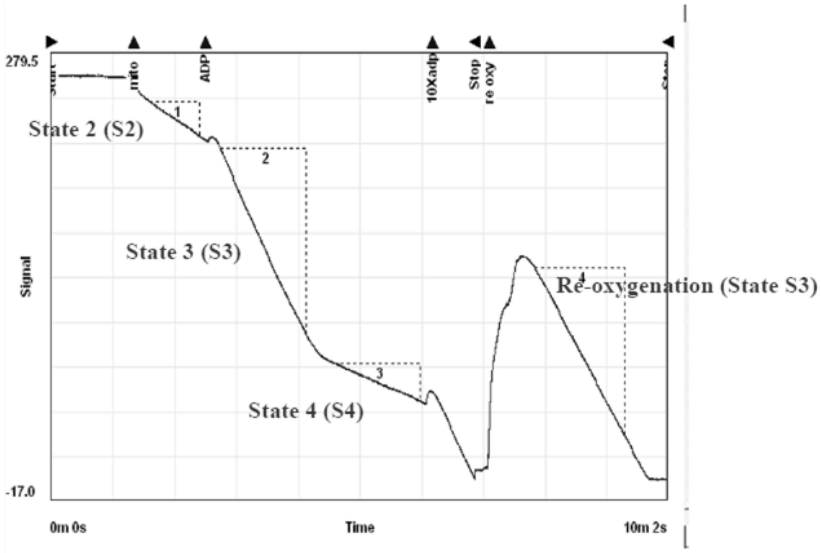

Figure 2.6 *An illustration of the mitochondrial registration generated by the oxygraph. The labels represent the three states mitochondrial respiration. State 2 is the respiration of mitochondria in the presence of the substrate alone, where State 3 represents the mitochondrial respiration in the presence of ADP (oxidative phosphorylation). State 4 represents the mitochondrial respiration after all ADP was converted to ATP. Re-oxygenation (State 3) represents the mitochondrial respiration after the mitochondria were subjected to 10x concentrated ADP and 20 minutes hypoxia.*

Several parameters were obtained or calculated from the graph generated by the oxygraph (Table 2.2). Along with these parameters, the protein determination from the Lowry Assay were used to determine the mitochondrial function. Standardizing the measured parameters to protein content allows for comparison between samples.

Table 2.2 *Mitochondrial Respiration Parameters*	
Parameter	***Definition/Calculation***
ADP/O (coupling efficiency of the mitochondria)	Ratio of ATP production to total oxygen uptake during State 3: nmoles ATP ÷ nAtom of oxygen consumed
QO_2 (State 2)	Number of atoms oxygen used in the presence of the substrate alone / mg mitochondria protein / min
QO_2 (State 3)	Number of atoms oxygen used in the presence of ADP / mg mitochondria protein / min
QO_2 (State 4)	Number of atoms oxygen used in the absence of ADP / mg mitochondria protein / min
Respiration Control Index (RCI)	QO_2 (S3) ÷ QO_2 (S4)
Oxidative Phosphorylation rate (Sate 3)	QO_2 (S3) x ADP/O (nmoles ATP produced / mg mitochondria protein / min)
Percentage recovery after re-oxygenation	% recovery after 20 mins hypoxia and re-oxygenation (measured against QO_2 (State 3))

8. Western Blots

8.1. Lysate Preparation

A standard lysis buffer was prepared in a 50-ml tube using 10X concentrated stock solutions as follows: 3 ml 200 mM Tris-HCl/10 mM EGTA, 300 µl 100 mM EDTA, 4.5 ml 1 M NaCl. 3 ml 10 mM Na_3VO_4 (prepared weekly with 0.018g Na_3VO_4 in 10 ml dH_2O), 3 ml 10 % Triton X-100. The following was added: 0.006 g β-glycerophosphate, 0.03 g tetra-Na-pyrophosphate, 30 µl Leupeptin, 30 µl Aprotinin (final concentration 10 µg/ml each) and 90 µl 100 mM PMSF. The solution was then filled up with dH_2O to a total volume of 30 ml.

8.1.1. Lysate preparation from whole heart tissue:

Lysates were prepared from freeze clamped ventricles. A small piece of the freeze clamped heart was broken off and submerged in the lysis buffer in the lysate preparation tube. The Heidolph Silent Crusher M homogenizer was used to homogenise the sample at 20 rpm for 4 seconds. The aggregate of the homogeniser was rinsed with dH_2O between samples. Once all samples were homogenised, each sample was homogenised again.

The lysate was allowed to stand for 15 - 30 minutes on ice before the sample was transferred to Eppendorf tubes which were centrifuged for 20 minutes at 15000 rpm in the Sigma 1-14K Refrigerated Microfuge. The supernatant of each sample was then removed and transferred into a new Eppendorf tube. Samples were constantly kept on ice. Protein determination was done by the method of Bradford (kindly refer to *'8.1.3 Bradford Protein Determination'*) (Bradford, 1976).

8.1.2. Lysate preparation from the mitochondrial suspension in 200 µl standard lysis buffer:

The samples were taken from storage and thawed on ice. Four to five Zirconium Oxide Beads was then added to the thawed samples for homogenisation. The samples, along with the beads, were then placed in a Bullet Blender® (Next Advanced Inc., USA) at 4 °C for 3 minutes at a speed of 5. After homogenisation, the samples were allowed to stand on ice for 15 minutes for full lysis. After this, the homogenates were centrifuged (Sigma 1-14K Refrigerated Microfuge) at 4 °C for 20 minutes at 15000 rpms. The Bradford method was also used for protein determination of these samples (kindly refer to *'8.1.3 Bradford Protein Determination'*) (Bradford, 1976).

8.1.3. Bradford Protein Determination:

Bradford solution (0.6 mM Coomasie Brilliant Blue G-250in 95 % ethanol and 50 % (v/v) phosphoric acid) was diluted 1:5 and filtered through a double layer of Whatman filter paper. For the standard curve, a BSA stock solution (5 mg/ml dH_2O) was used and diluted in a 1:4 ratio (100 µl BSA stock in 400 µl dH_2O). For the standard curve, the diluted BSA was further diluted in duplicate in the following series (Table 2.3):

Table 2.3 *Bradford Standards*

Diluted BSA	***dH_2O***
0 µl	100 µl
5 µl	95 µl
10 µl	90 µl
20 µl	80 µl
40 µl	60 µl
60 µl	40 µl
80 µl	20 µl

For the 1:10 dilution of the lysate samples, 50 µl of it was added to 450 µl dH_2O in an Eppendorf and vortexed. Of this dilution, 5 µl was added to 95 µl dH_2O in the respective reaction tube. The samples were all assayed in duplicate.

To each tube, 900 µl of the filtered Bradford reagent was added and vortexed. After the tubes were left to stand for 20 minutes, the optical density (OD) was read on the spectrophotometer at 595 nm (Spectronic® 20 Genesys™ Spectrophotometer, Thermo Fisher Scientific Inc., RSA). The 0 µl BSA standard was used as the blank. The standard ODs were then used to draw up a standard curve and calculate the protein concentrations in each sample. These calculations were done using an Excel sheet. The samples were diluted with lysis buffer to contain equal amounts of protein per volume unit after which a 3x Laemmli sample buffer was added in a 1:2 (v/v) ratio to the sample (Laemmli, 1970). The 3x Laemmli buffer consisted of 0.125 M Tris-HCl (pH 6.8), 4 % SDS, 20 % glycerol, 10 % β-mercaptoethanol and 0.0004 % bromophenol blue. Dilutions were usually made to yield in a protein concentration of 50 ug/15 uL volume to load on the SDS PAGE gel. Samples were boiled for 5 minutes and then stored in -80 °C.

8.2. Protein Separation

8.2.1. Precast Gel Preparation

For protein separation, 26-well Criterion™ TGX (Tris-Glycine,eXtended) Stain-Free™ Precast Gels (Bio-Rad Laboratories Inc., USA) with a gradient of 4-15 % were used. Gels were placed in a Criterion™ Cell system (Bio-Rad Laboratories Inc., USA). The system was filled with running buffer until the maximum level. The samples were then loaded into the wells with a Hamilton syringe. For the proteins under 100 kDa, PageRuler™Prestained Protein Ladder (Thermo Fisher Scientific Inc., RSA) was used. For proteins larger than 100 kDa, HiMark™ Pre-Stained High Molecular Weight Protein Standard was used. After the protein ladder, samples were added to the next lanes of the gel. For the insulin signalling proteins (GLUT4, Akt/PKB, AMPK, ERK and ATM), autophagy proteins (BNIP3, Beclin-1, LC3-II) and stress-responsive protein (Sesn2), 15 µl of the sample (containing 50 µg of protein) was added to the respective wells. These samples were added in the following sequence: control samples (C); controls injected with insulin before sacrifice (C I); controls treated with Afriplex GRT Extract (CT); controls treated with Afriplex GRT Extract and injected with insulin before sacrifice (CT I); high fat diet rats (HFD); HFD rats injected with insulin before sacrifice (HFD I); HFD rats treated with Afriplex GRT Extract (HFDT) and, lastly, HFD rats treated with Afriplex GRT Extract and injected with insulin before sacrifice (HFDT I).

For the mitophagy proteins (p62, PINK1, Parkin), 12 µl of the sample (containing 30 µg of protein) was added to the respective wells. The samples were loaded as follows: C, HFD, CT, HFDT, metformin (Met). Note that the sequences will be displayed along with the blots in *'Chapter 3: Results.'*

Gels were run for 10 minutes at 100 V and 200 mA, followed by 50 minutes at 200 V and 200 mA. After the proteins were separated, the gels were activated in the ChemiDoc™ MP System (Bio-Rad Laboratories Inc., USA) and the image stored.

8.3. Protein Transfer

After the proteins have been separated and the gels activated, the proteins were transferred to polyvinylidene fluoride (PVDF) membranes with wet transfer using the Criterion™ Blotter (Bio-Rad Laboratories Inc., USA). The proteins were allowed to transfer for 35 minutes at 200 V and 200 mA. The membranes were then visualized on the Bio-Rad ChemiDoc™ MP System to establish transfer and document the amount of proteins transferred. After visualizing the membranes, they were blocked on a shaker (lab rotor V1.00) with a 5 % fat free milk TBS-Tween solution (containing Tris-buffered saline (TBS) and 0.1 % Tween 20) for 2 hours to ensure blocking of non-specific binding sites. After blocking, the membranes were washed with TBS-Tween solution for 30 minutes (3 x 10 minutes at a time, replacing with fresh TBS-Tween solution every wash). After washing, the membranes were probed overnight (at 4 °C on the lab rotor V1.00) with their respective primary antibody, diluted 1:1000. The following table is a summary of the primary antibodies blotted for in this study and the conditions utilized to enable optimal visualization of the band of interest (Table 2.4).

Table 2.4 *Antibody Summary (Criterion™ Stain-Free Pre-Cast gels were used for all blots)*				
Protein	**Molecular Size (kDa)**	**Primary Antibody (AB)**	**Secondary Antibody (AB)**	**Exposure Method**
GLUT4	45 - 54	7,5 µl/5 ml primary SignalBoost™	1,25 µl/2.5 ml TBS-Tween/2.5 ml 2.5 % milk (anti-mouse 2° AB)	ChemiDoc™ MP System
Akt/PKB	60	7,5 µl/7,5 ml TBS-Tween	1,25 µl/5 ml TBS-Tween	ChemiDoc™ MP System
tAMPK + pAMPK	62	7,5 µl/7,5 ml TBS-Tween	1,25 µl/5 ml TBS-Tween	ChemiDoc™ MP System
tERK + pERK	42 + 44	7,5 µl/7,5 ml TBS-Tween	1,25 µl/5 ml TBS-Tween	ChemiDoc™ MP System
tATM + pATM	370	7,5 µl/5 ml primary SignalBoost™	1,25 µl/5 ml TBS-Tween Signalboost™	ChemiDoc™ MP System
Sesn2	54 – 56	7,5 µl/7,5 ml TBS-Tween	1,25 µl/5 ml TBS-Tween	ChemiDoc™ MP System
p62	62	7,5 µl/7,5 ml TBS-Tween	1,25 µl/5 ml TBS-Tween	ChemiDoc™ MP System
PINK1	50 + 60	7,5 µl/7,5 ml TBS-Tween	1,25 µl/5 ml TBS-Tween	ChemiDoc™ MP System
Parkin	52	7,5 µl/3.75 ml TBS-Tween/3.75 5 % milk	1,25 µl/2.5 ml TBS-Tween.	ChemiDoc™ MP System
LC3	14 + 16	7,5 µl/7,5 ml TBS-Tween	1,25 µl/5 ml TBS-Tween	ChemiDoc™ MP System
Beclin-1	60	7,5 µl/7,5 ml TBS-Tween	1,25 µl/5 ml TBS-Tween	ChemiDoc™ MP System
BNIP3	22 – 28 50 – 55	7,5 µl/7,5 ml TBS-Tween	1,25 µl/5 ml TBS-Tween	ChemiDoc™ MP System

8.4. Immunodetection of Protein using Secondary Antibody

After the membranes were probed overnight with primary antibody, they were washed with TBS-Tween (3 x 10 minutes with fresh TBS-Tween every wash) for 30 minutes. Hereafter, all the membranes (except GLUT4) were incubated for an hour at room temperature in diluted secondary anti-rabbit immunoglobulin G, HRP-conjugated secondary antibody (Cell Signaling Technology, Inc). GLUT4 was incubated in anti-mouse immunoglobulin G, HRP-conjugated secondary antibody (Cell Signaling Technology, Inc). After the one-hour incubation, the membranes were washed again (3 x 10 minutes with fresh TBS-Tween every wash) for 30 minutes.

The membranes were visualized by incubating them in BioRad Clarity™ Enhanced Chemiluminescence (ECL) substrate for 5 minutes and then exposing in the Bio-Rad ChemiDoc™ MP System.

8.5. Visualization and Normalization on Bio-Rad ChemiDoc™ MP System

The exposure times varied for the different antibodies. Exposure times were set to run with intervals of seconds prior to exposing in the Bio-Rad ChemiDoc™ MP System. The system also shows when any band is overexposed. The images were saved and quantified for analysis of the blots.

The best image of the exposed membrane without any band overexposed, was normalised to the density of the protein bands against the total protein per lane transferred to the respective PVDF membrane image saved previously (see *'8.3 Protein Transfer'*). This system negates the use of loading controls. All blots were analyzed using the BioRad ChemiDoc™ ImageLab 5.0 series software.

9. Statistical Analysis

For statistical analysis of all the data, GraphPad Prism 5 was used. The values were expressed as Mean ± Standard Error of the Mean (SEM). For analysis between protein markers with one variable (arbitrary densitometry units), One-way Analysis of Variance (ANOVA) was used followed by a Bonferroni post-hoc test. Between groups with two factors/variables (such as arbitrary densitometry units of tERK and pERK at 42 kDa and 44 kDa), a 2-way ANOVA was used to determine the differences. For OGTT analysis, a 2-way ANOVA with repeated measures was used for significant differences. A *p-value* of less than 0.05 was considered significant.

CHAPTER 3: Results

1. Biometric Data

1.1. Body Weights

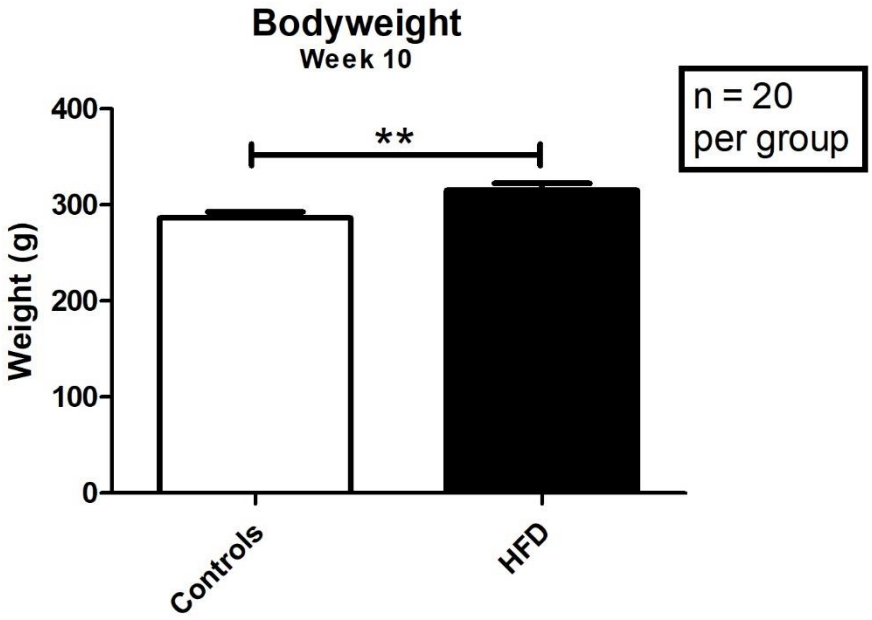

Figure 3.1 *A t-test of the bodyweights, at week 10, of the control groups versus that of the HFD groups (*p<0.05; **p<0.001; ***p<0.0001).*

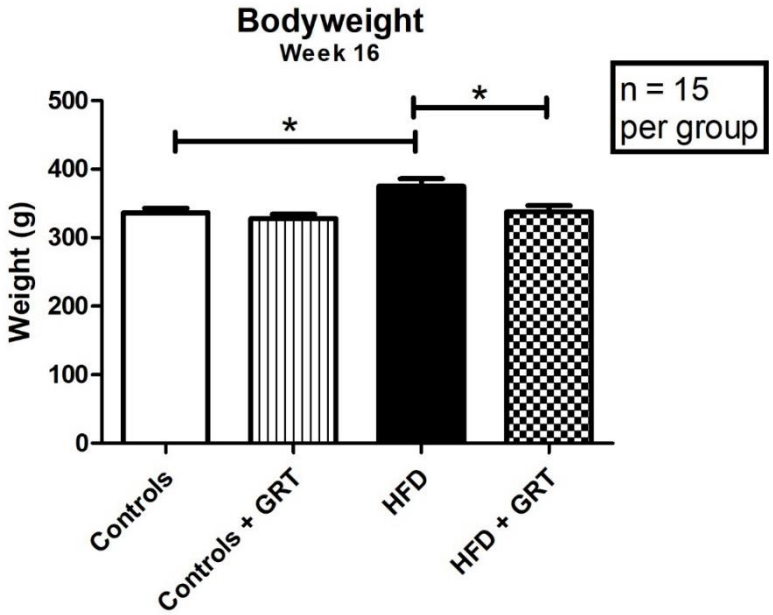

Figure 3.2 *A 1-way ANOVA of the bodyweights, at week 16, of the control groups (with and without Afriplex GRT Extract) versus that of the HFD groups (with and without Afriplex GRT Extract) (*p<0.05; **p<0.001; ***p<0.0001).*

Body weights of the HFD groups were significantly increased by week 10, indicating that the HFD caused obesity (p = 0.0055) (Figure 3.1). At week 16, the HFD groups still had significantly higher body weights than that of the control groups (p = 0.0011) (Figure 3.2). The Afriplex GRT Extract resulted in lower body weight in the HFD groups indicating lower body weight gain over this period (p = 0.0011) (Figure 3.2).

1.2. Food and Water Intake

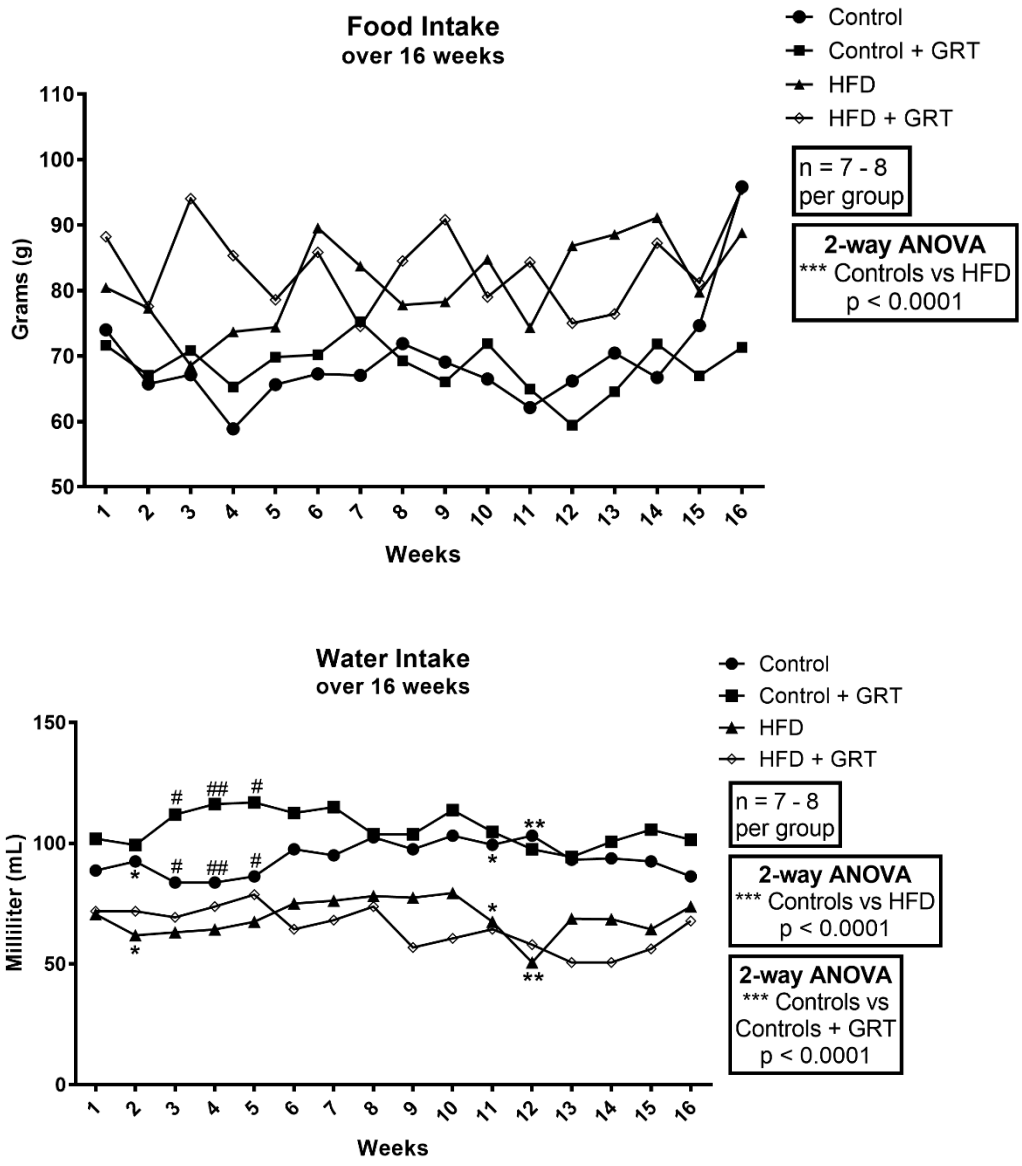

Figure 3.3 *2-way ANOVAs of the food and water intake of the control groups (with and without Afriplex GRT Extract) versus that of the HFD groups (with and without Afriplex GRT Extract) over a period of 16 weeks (*p<0.05; **p<0.001; ***p<0.0001; # p<0.05; ## p<0.001).*

A 2-way ANOVA indicated that the HFD animals had significantly more food intake than the control animals over the 16-week period (p < 0.0001) (Figure 3.3). In

another 2-way ANOVA, the water intake was less in the HFD animals than that of the control animals ($p < 0.0001$), especially at weeks 2 ($p < 0.05$), 11 ($p < 0.05$) and 12 ($p < 0.001$)). Whereas the Afriplex GRT Extract significantly increased water intake in the control animals ($p < 0.0001$) (Figure 3.3), especially at weeks 3 ($p < 0.05$), 4 ($p < 0.01$) and 5 ($p < 0.05$).

1.3. Liver Weight

Figure 3.4 *A 2-way ANOVA of the liver weights, after 16 weeks, of the control groups (with and without Afriplex GRT Extract) versus that of the HFD groups (with and without Afriplex GRT Extract) (*p<0.05; **p<0.001; ***p<0.0001).*

The HFD groups displayed significantly higher liver weight than the controls ($p < 0.0001$). The Afriplex GRT Extract attenuated this increase in the liver weights in the HFD groups ($p < 0.05$). A 2-way ANOVA indicated that the effect of the diet was overall very significant ($p < 0.0001$).

1.4. Intraperitoneal (IP) Fat Weight

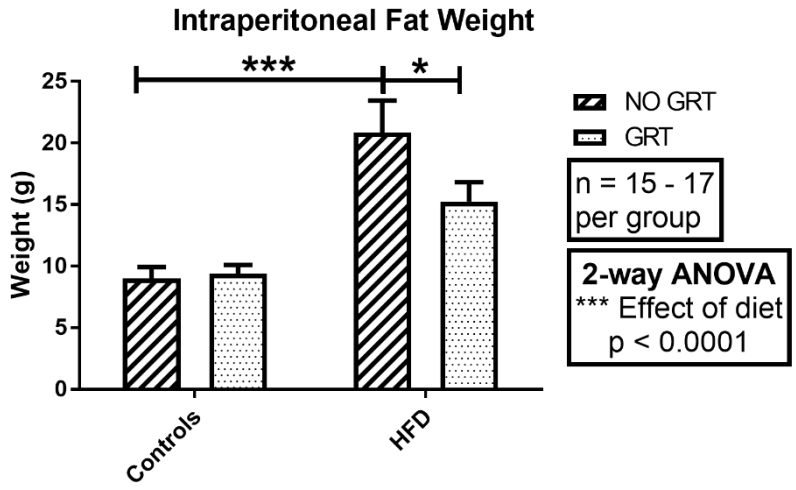

Figure 3.5 *A 2-way ANOVA of the intraperitoneal fat weights, after 16 weeks, of the control groups (with and without Afriplex GRT Extract) versus that of the HFD groups (with and without Afriplex GRT Extract) (*p<0.05; **p<0.001; ***p<0.0001).*

The HFD groups displayed significantly higher IP fat weight than the controls (Figure 3.5) ($p < 0.0001$). The Afriplex GRT Extract resulted in lower IP fat gain in the HFD groups ($p < 0.05$). No effect was seen on the control groups. A 2-way ANOVA indicated that the effect of the diet was overall very significant ($p < 0.0001$).

1.5. Oral Glucose Tolerance Tests

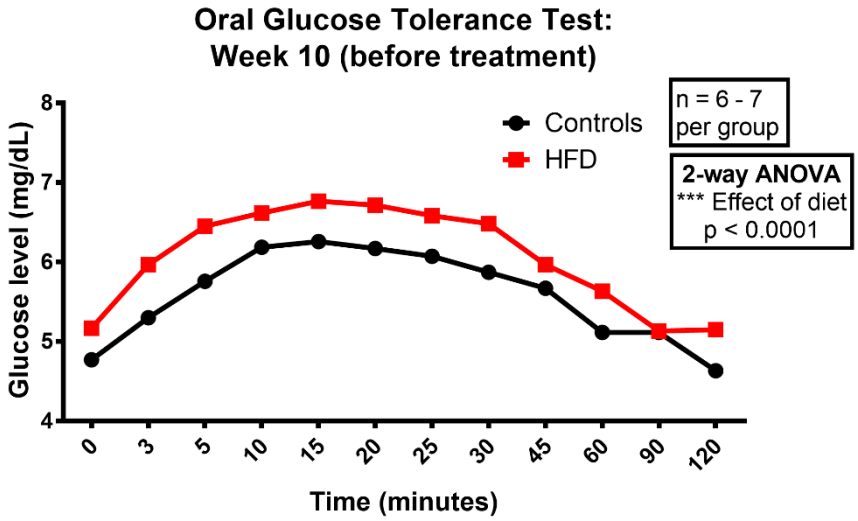

Figure 3.6 *A 2-way ANOVA of the OGTT results, at week 10, of the control groups versus that of the HFD groups (*p<0.05; **p<0.001; ***p<0.0001).*

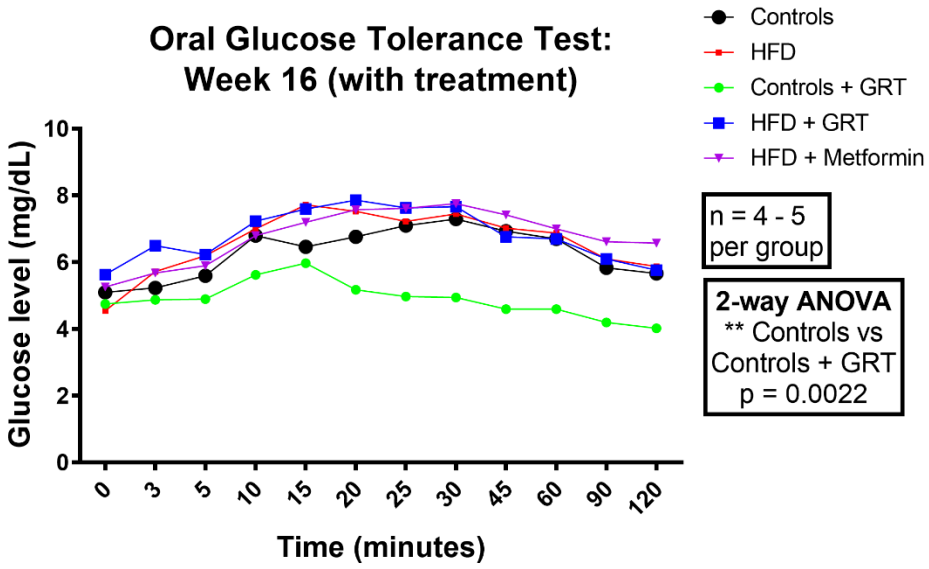

Figure 3.7 *A 2-way ANOVA of the OGTT results, at 16 weeks, of the control groups (with and without Afriplex GRT Extract) versus that of the HFD groups (with and without Afriplex GRT Extract) versus HFD groups with metformin (*p<0.05; **p<0.001; ***p<0.0001).*

At weeks 10 and 15, animals were fasted overnight to investigate their glucose tolerance. To do this, an OGTT was performed (refer to Chapter 2*, '3. Oral Glucose Tolerance Test and Glucose Measurement'*).

At week 10, there was significantly increased blood glucose levels in the HFD group compared to the control group. A 2-way ANOVA indicated that the effect of the diet

was very significant ($p < 0.0001$) (Figure 3.6). This was expected, because a high fat diet is known to impair oral glucose tolerance and cause a higher OGTT curve. At week 16 (Figure 3.7), the HFD group's glucose levels were slightly higher than that of the controls, not significantly though. A 2-way ANOVA indicated that the Afriplex GRT Extract significantly decreased the glucose levels in the control groups ($p = 0.0022$), especially at minutes 25, 30, 45 and 120 ($p < 0.05$).

There were no significant differences seen between the HFD groups and metformin treated HFD groups.

1.6. Basal Glucose Levels

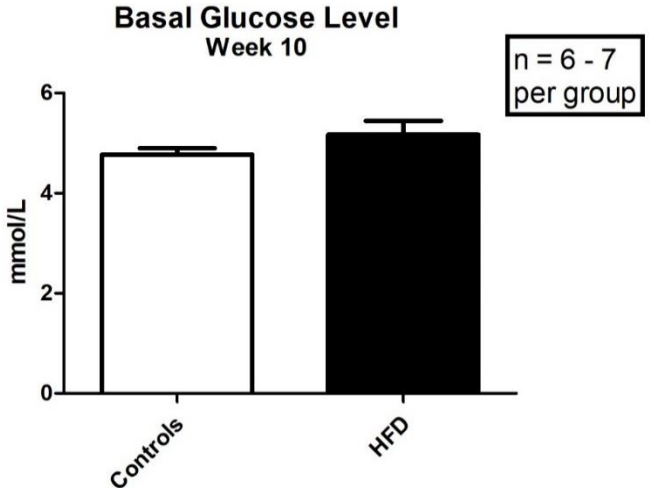

Figure 3.8 *A t-test of the basal glucose level, at week 10, of the control groups versus that of the HFD groups (*p<0.05; **p<0.001; ***p<0.0001).*

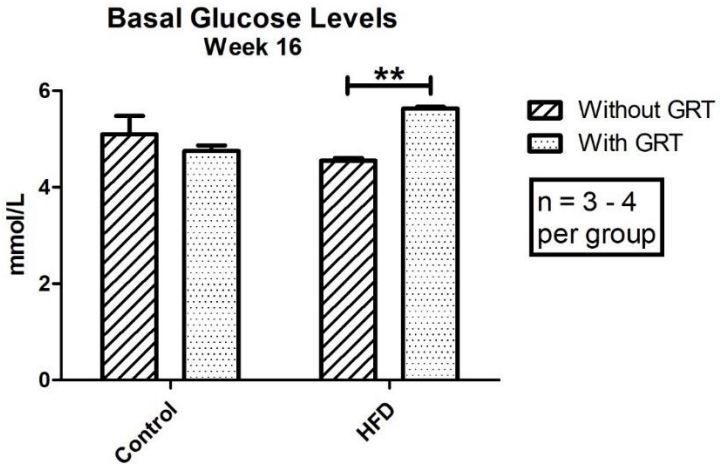

Figure 3.9 *A 2-way ANOVA of the basal glucose level, at week 15, of the control groups (with and without Afriplex GRT Extract) versus that of the HFD groups (with and without Afriplex GRT Extract) (*p<0.05; **p<0.001; ***p<0.0001).*

At week 10 (Figure 3.8), the controls showed a lower, though not significant, basal glucose level than that of the HFD groups. At week 16 (Figure 3.9), there was a significantly higher basal glucose level in the HFD group treated with Afriplex GRT Extract than that of the non-treated HFD groups ($p < 0.01$).

1.7. Urine Volume

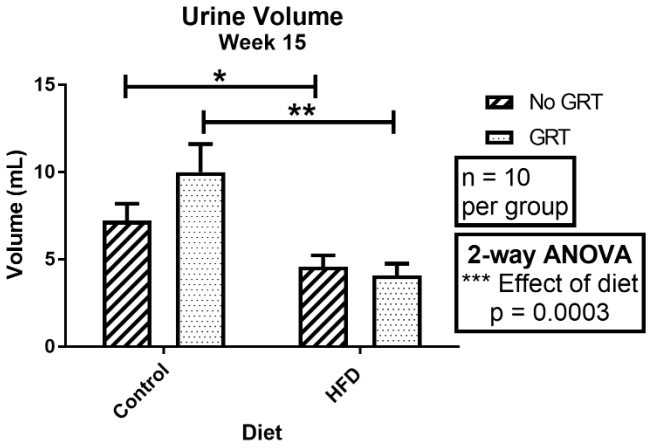

Figure 3.10 *A 2-way ANOVA of the urine volumes at week 15 of the control groups (with and without Afriplex GRT Extract) versus that of the HFD groups (with and without Afriplex GRT Extract) (*p<0.05; **p<0.001; ***p<0.0001).*

The urine volume of the HFD groups were significantly lower than that of the controls ($p = 0.0410$). The same effect was seen on the groups treated with Afriplex GRT Extract ($p = 0.0016$). The Afriplex GRT Extract did not have significant effect on any of the groups, however a 2-way ANOVA indicated that the overall effect of the diet was significant ($p = 0.0003$).

1.8. ELISA Assays

1.8.1. Leptin

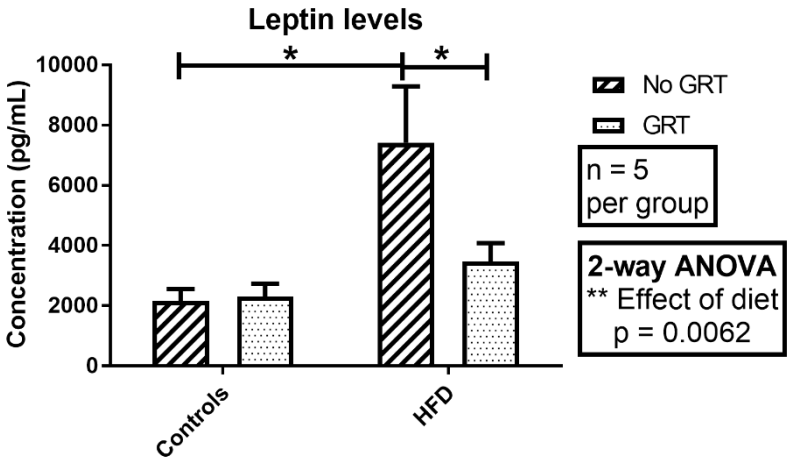

Figure 3.11 *A 2-way ANOVA of the leptin levels of the control groups (with and without Afriplex GRT Extract) versus that of the HFD groups (with and without Afriplex GRT Extract) (*p<0.05; **p<0.001; ***p<0.0001).*

The leptin levels were significantly increased in the HFD groups compared to the controls (Figure 3.11) ($p < 0.5$). The Afriplex GRT Extract group presented with significantly lower leptin levels in the HFD fed animals, while having no effect in the controls ($p < 0.05$). A 2-way ANOVA indicated that the overall effect of the diet was significant ($p = 0.0062$).

1.8.2. Adiponectin

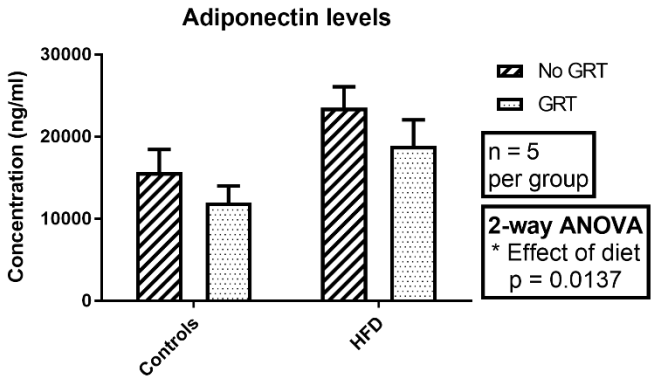

Figure 3.12 *A 2-way ANOVA of the adiponectin levels of the control groups (with and without Afriplex GRT Extract) versus that of the HFD groups (with and without Afriplex GRT Extract) (*p<0.05; **p<0.001; ***p<0.0001).*

The Afriplex GRT Extract had no significant effect on the adiponectin levels in either of the groups. The diet did, however, have an overall significant effect on the adiponectin levels ($p = 0.0137$).

1.8.3. Insulin

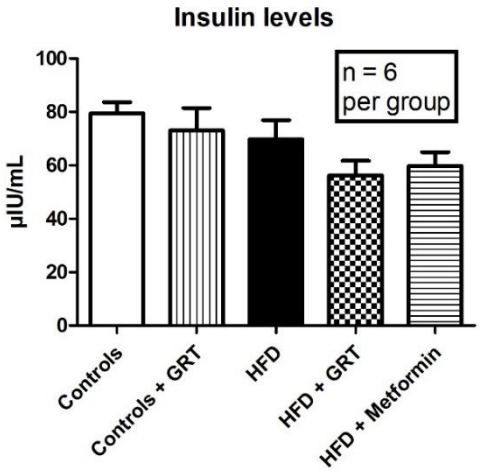

Figure 3.13 *A 2-way ANOVA of the insulin levels of the control groups (with and without Afriplex GRT Extract) versus that of the HFD groups (with and without Afriplex GRT Extract) (*p<0.05; **p<0.001; ***p<0.0001).*

There were no significant differences seen in the insulin levels between the different groups.

1.9. HOMA IR index

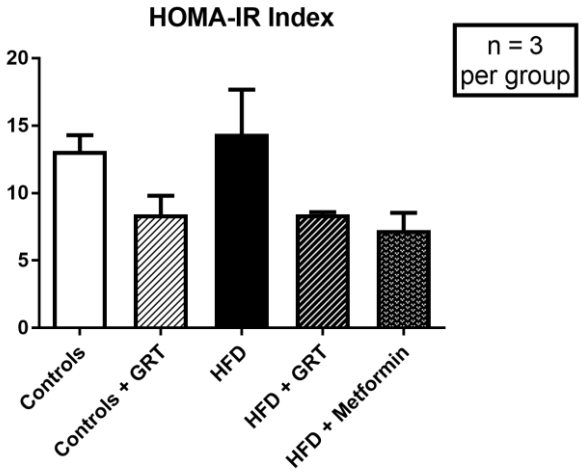

Figure 3.14 *A 2-way ANOVA of the HOMA IR Index values between the control groups (with and without Afriplex GRT Extract) versus that of the HFD groups (with and without Afriplex GRT Extract) (*p<0.05; **p<0.001; ***p<0.0001).*

A 2-way ANOVA indicated that the Afriplex GRT Extract and metformin had a very significant effect overall (p = 0.006). The low n-value is due to the limited fasting serum and fasting insulin values that were available. There was thus borderline significance seen, where Afriplex GRT Extract improved insulin resistance in the control animals (p = 0.07), and the metformin improved insulin resistance in HFD animals (p = 0.06).

2. 2DG Uptake Levels induced by Insulin

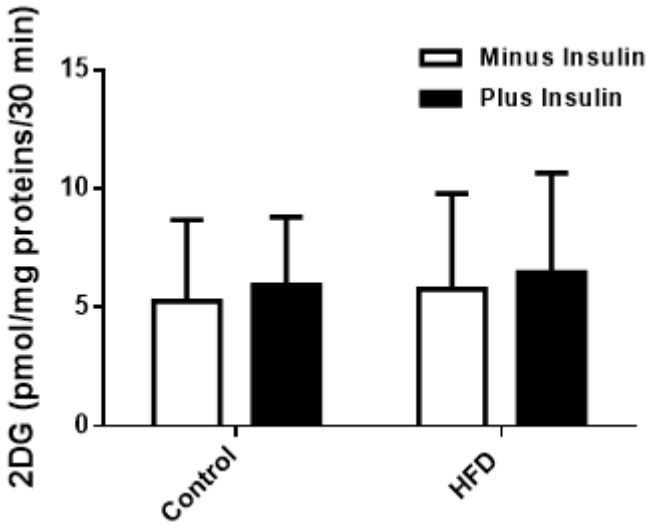

Figure 3.15 *A 2-way ANOVA of the 2DG Uptake Levels in cardiomyocytes at an Insulin Concentration of 100 nM between the control groups (with and without Afriplex GRT Extract) versus that of the HFD groups (with and without Afriplex GRT Extract) (*p<0.05; **p<0.001; ***p<0.0001).*

2DG uptake levels in cardiomyocytes prepared from the control and HFD animals were measured in response to treatment with 100 nM insulin stimulation. No significant differences were observed (n = 5 - 6 per group).

3. The effect of the HFD and Afriplex GRT™ Extract on mitochondrial energetics.

The mitochondria were prepared immediately after excision of the hearts from the chest cavity of the animal.

3.1. ADP/O Ratio

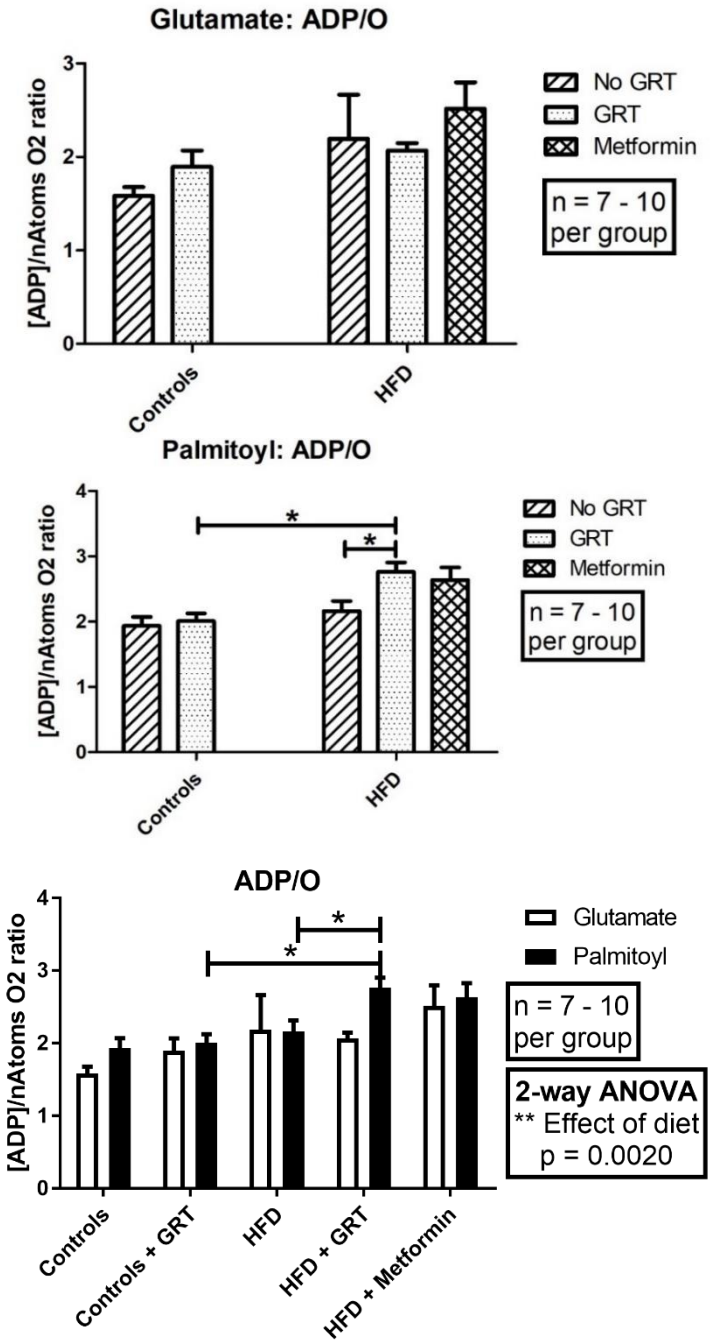

Figure 3.16 *A 2-way ANOVA of the ADP/O Ratio of mitochondria in glutamate plus malate or palmitoyl-L-carnitine plus malate substrate media (*p<0.05; **p<0.001; ***p<0.0001).*

The mitochondria from the Afriplex GRT Extract treated HFD animals had a significantly higher ADP/O ratio (in the palmitoyl-L-carnitine media) than that of the Afriplex GRT Extract control groups ($p < 0.05$). The Afriplex GRT Extract also increased the ADP/O ratio in the mitochondria of the HFD groups ($p < 0.05$). There were no significant differences between the controls and Afriplex GRT Extract treated controls.

3.2. QO2 (States 2, 3 and 4)

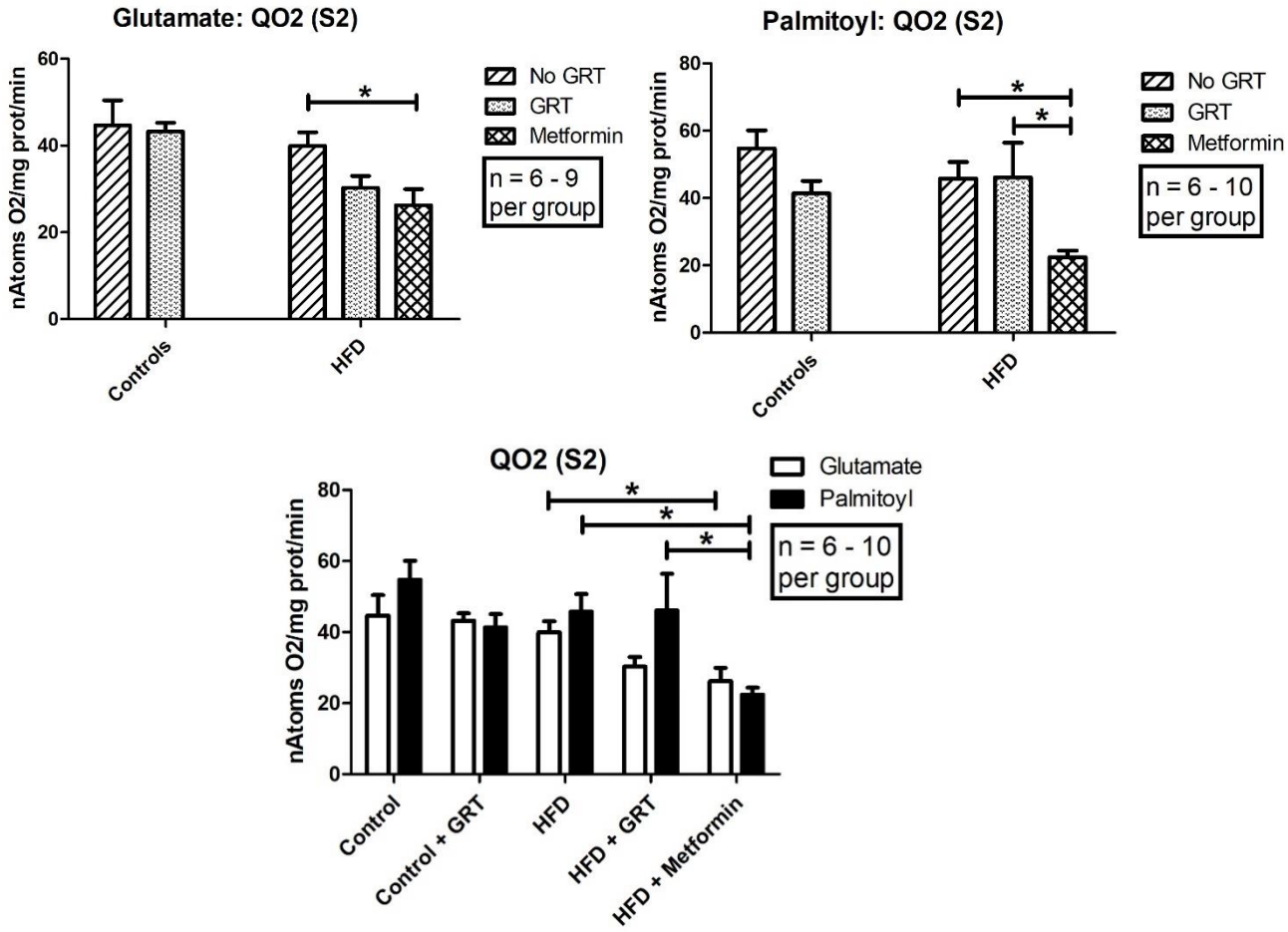

Figure 3.17 *A 2-way ANOVA of the QO2 (State 2) Respiration of mitochondria in glutamate plus malate or palmitoyl-L-carnitine plus malate substrate media (*p<0.05; **p<0.001; ***p<0.0001).*

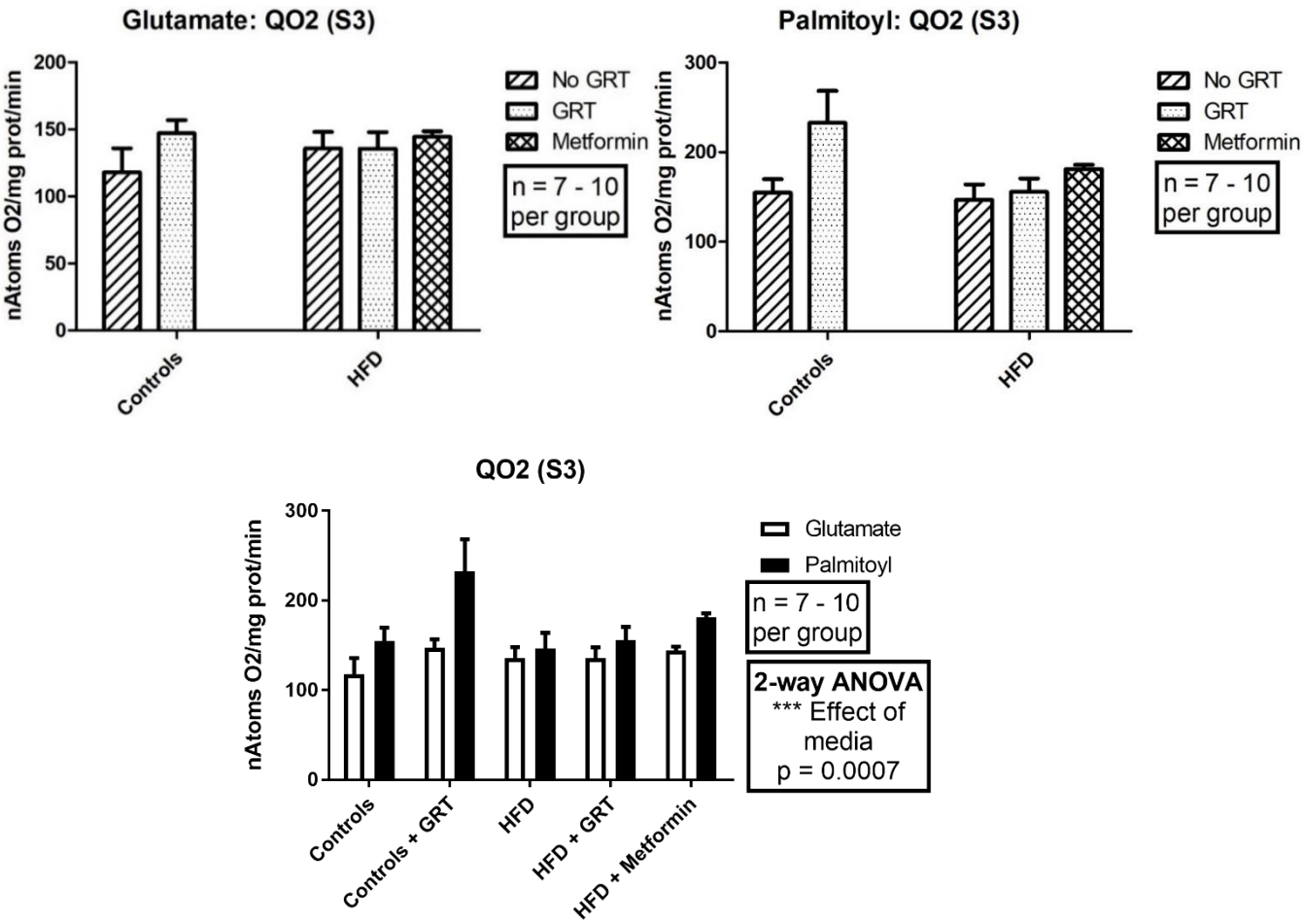

Figure 3.18 *A 2-way ANOVA of the QO2 (State 3) Respiration of mitochondria in glutamate plus malate or palmitoyl-L-carnitine plus malate substrate media (*p<0.05; **p<0.001; ***p<0.0001).*

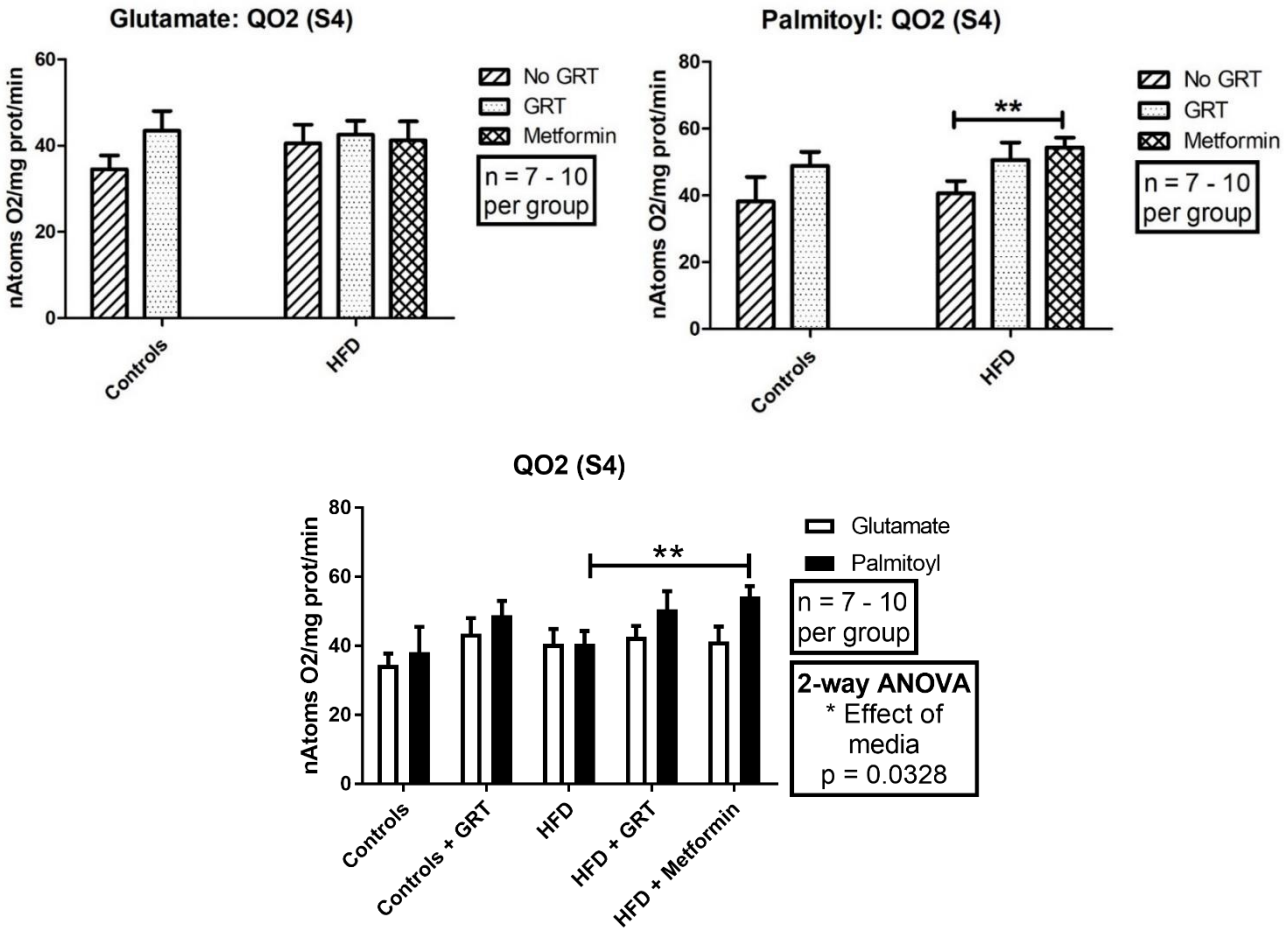

Figure 3.19 *A 2-way ANOVA of the QO2 (State 4) Respiration of mitochondria in glutamate plus malate or palmitoyl-L-carnitine plus malate substrate media (*p<0.05; **p<0.001; ***p<0.0001).*

There was significantly increased state 2 respiration in the non-treated HFD animals compared to the metformin treated HFD animals (in both glutamate and palmitoyl-L-carnitine media) (Figure 3.17) ($p < 0.05$). In addition, in the palmitoyl-L-carnitine media, the Afriplex GRT Extract treated HFD groups also had a higher state 2 respiration than that of the metformin treated HFD animals ($p < 0.05$). There was an increased state 4 respiration in the metformin treated HFD groups compared to that of non-treated HFD groups (in the palmitoyl-L-carnitine media) (Figure 3.19) ($p < 0.01$). In both states 3 (Figure 3.18) and 4, a 2-way ANOVA indicated that the media had a significant effect (in state 3, $p = 0.0007$; in state 4, $p = 0.0328$). In the palmitoyl-L-carnitine media, the state 3 and state 4 respiration rates were higher compared to the mitochondria in the glutamate media.

3.3. RCI Values

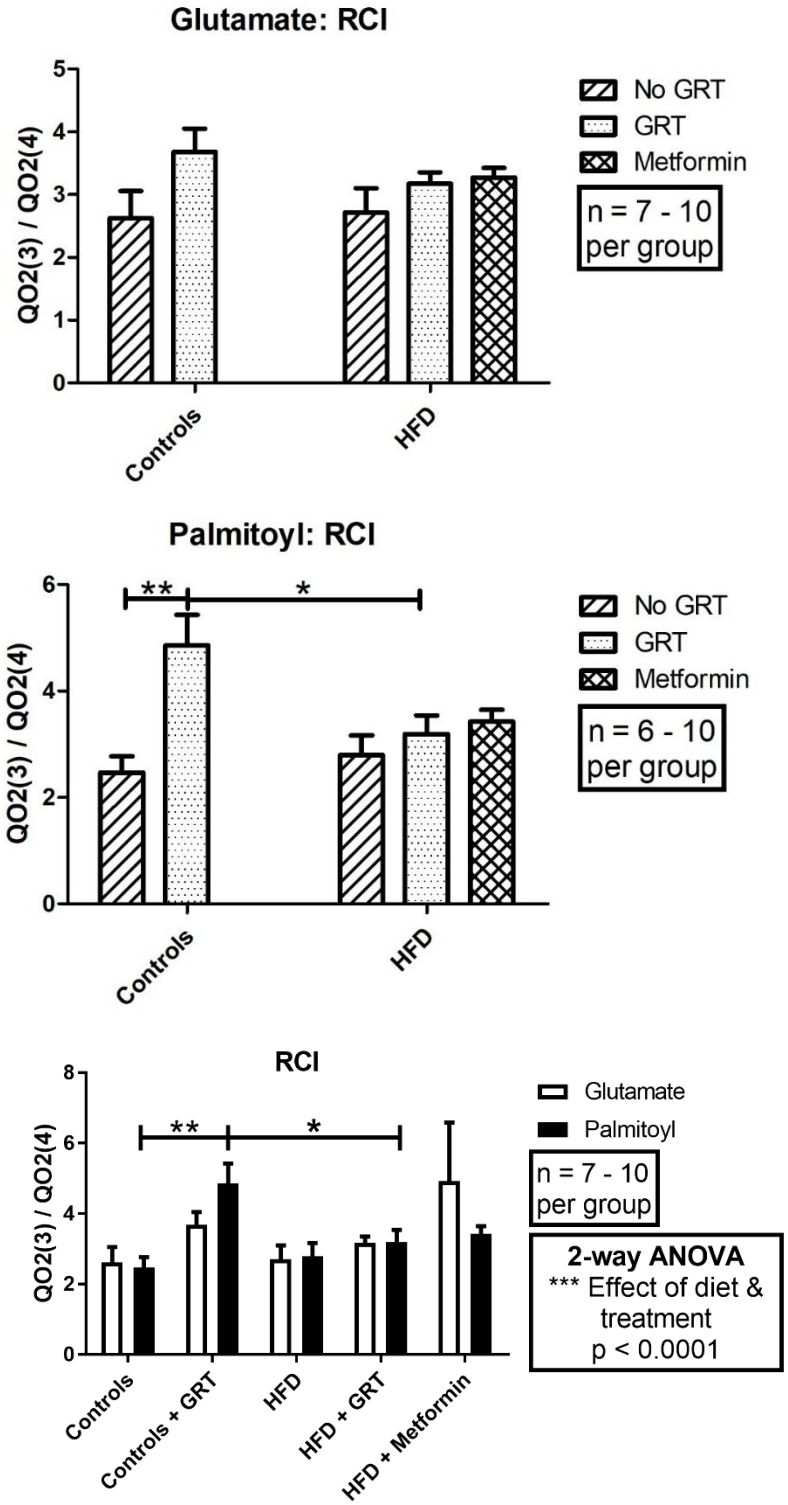

Figure 3.20 *A 2-way ANOVA of the Respiratory Control Index of mitochondria in glutamate plus malate or palmitoyl-L-carnitine plus malate substrate media (*p<0.05; **p<0.001; ***p<0.0001).*

The Afriplex GRT Extract significantly increased the RCI values in the control groups (in the palmitoyl-L-carnitine media) ($p < 0.01$). In addition, the Afriplex GRT Extract treated HFD groups had lower RCI rates than that of the Afriplex GRT Extract treated

control groups ($p < 0.05$). The treatment had an overall significant effect on the RCI value ($p < 0.0001$).

3.4. Oxidative Phosphorylation

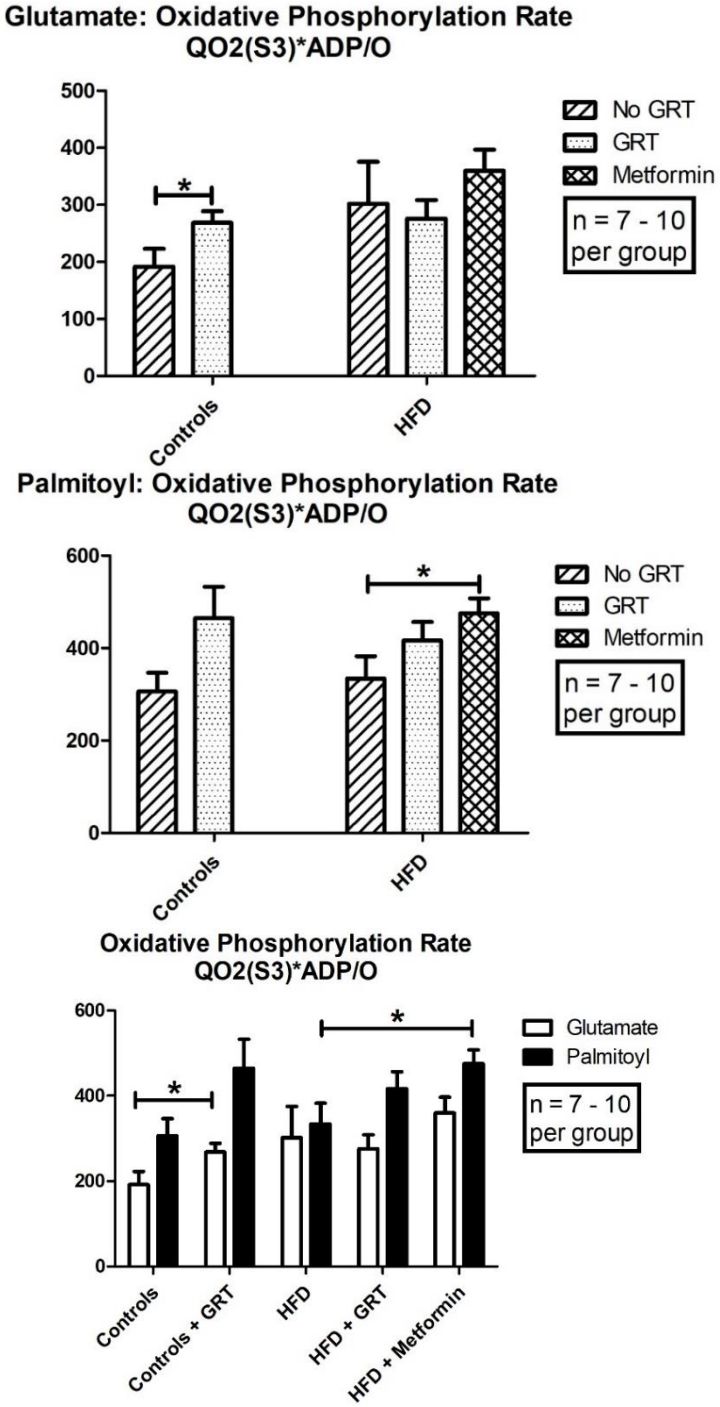

Figure 3.21 *A 2-way ANOVA of the Oxidative phosphorylation rate of mitochondria (State 3) in glutamate plus malate or palmitoyl-L-carnitine plus malate substrate media (*p<0.05; **p<0.001; ***p<0.0001).*

In the glutamate media, the Afriplex GRT Extract improved the oxidative phosphorylation rate in the control groups ($p < 0.05$). In the palmitoyl-L-carnitine media, metformin increased oxidative phosphorylation rate in the HFD groups ($p < 0.05$).

3.5. Percentage recovery in state 3 respiration after re-oxygenation of mitochondria

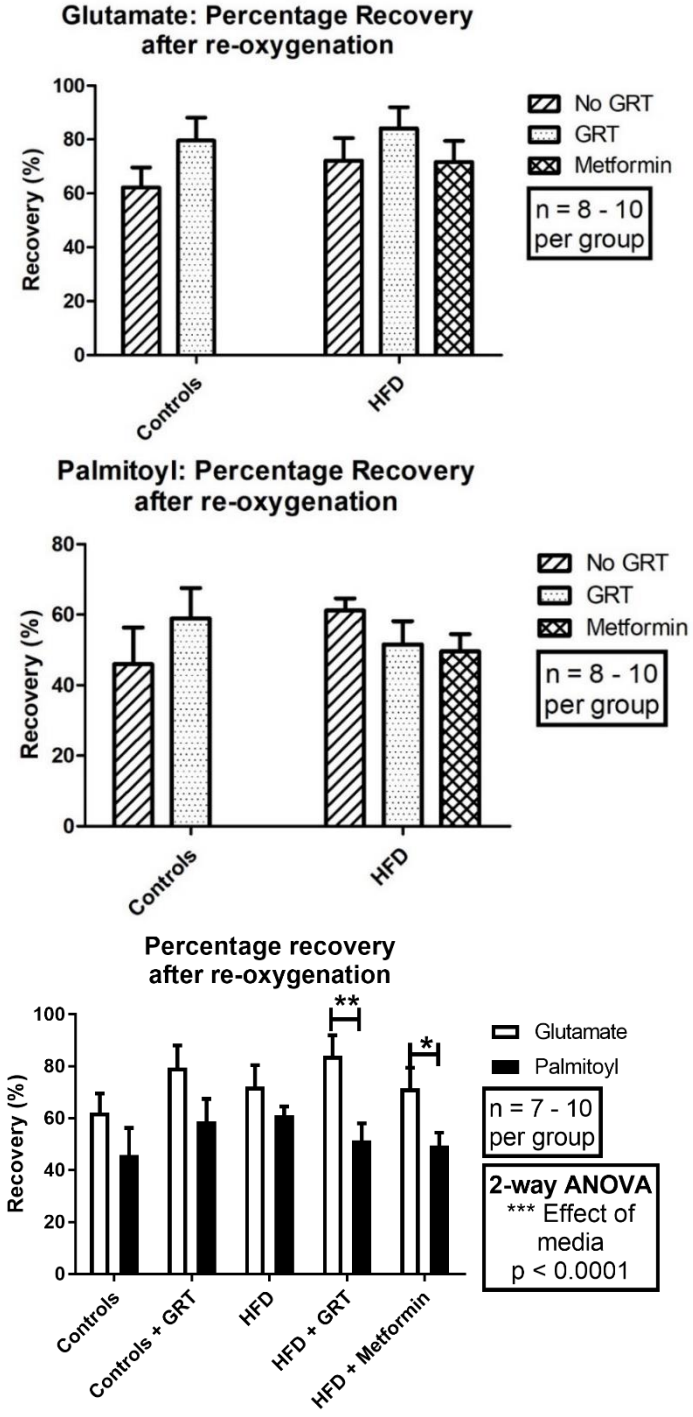

Figure 3.22 *A 2-way ANOVA of the percentage recovery after re-oxygenation in glutamate plus malate or palmitoyl-L-carnitine plus malate substrate media (*p<0.05; **p<0.001; ***p<0.0001).*

In a 2-way ANOVA, the overall effect of the media was significant ($p < 0.0001$) (Figure 3.22). In the Afriplex GRT Extract treated HFD groups, recovery was significantly improved in the glutamate media compared to the palmitoyl-L-carnitine media ($p < 0.001$). In the metformin treated HFD groups, there was also a significantly improved recovery in the glutamate media than in the palmitoyl-L-carnitine media ($p < 0.05$). No significant differences were seen otherwise.

4. Western Blot Data

Note: The .JPEG images of every blot can be found on the CD-ROM attached. See Appendix A for the methods by which the calculations of the Western blots were performed.

4.1. Insulin Signalling Proteins

The tissue in this section was prepared from hearts that were immediately freeze-clamped after being removed from the animals from cohort 1. The lysates were prepared from the cytosolic fraction, thus allowing us to observe the effects seen on baseline levels. The animals were not fasted before sacrifice.

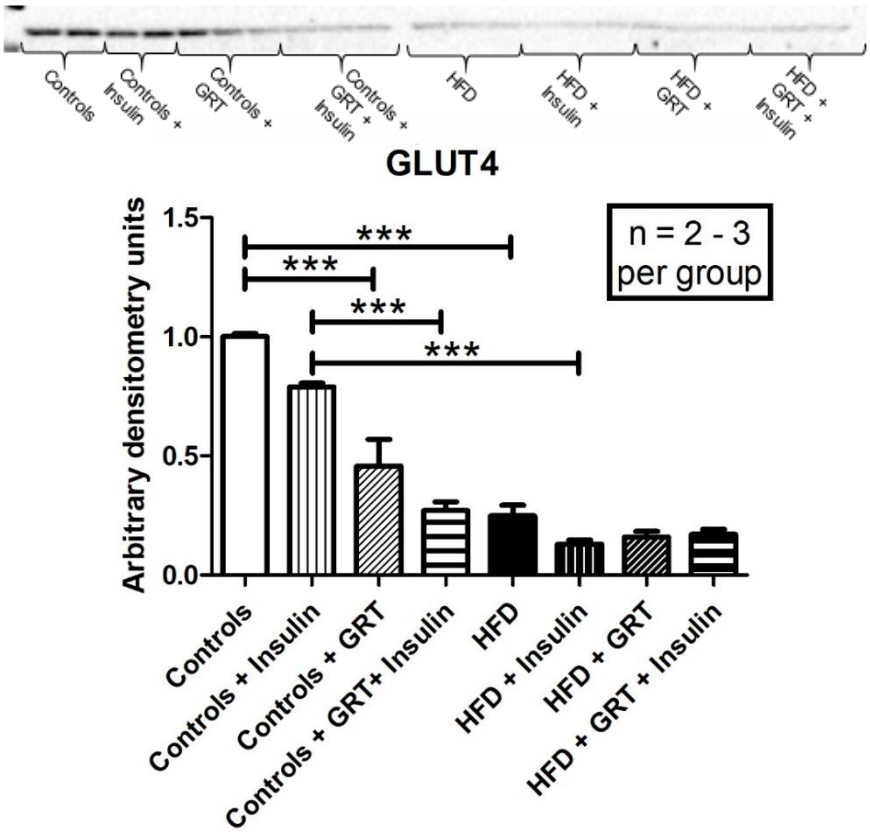

Figure 3.23 *A 1-way ANOVA of the GLUT4 expression between control groups (with and without Afriplex GRT Extract), control groups (with and without insulin injection), HFD groups (with and without Afriplex GRT Extract) and HFD groups (with and without insulin injection) (*p<0.05; **p<0.001; ***p<0.0001).*

The HFD groups presented with significantly lower cytosolic GLUT4 levels in the cytosolic compartment than the controls and the same effect was seen in control groups and HFD groups injected with insulin before sacrifice ($p < 0.0001$) (Figure 3.23). Afriplex GRT Extract treatment also significantly decreased cytosolic GLUT4 levels in the cytosolic compartment in the controls and this was also seen in those injected with insulin. Afriplex GRT Extract had no effect on the GLUT4 levels in the hearts of the HFD animals.

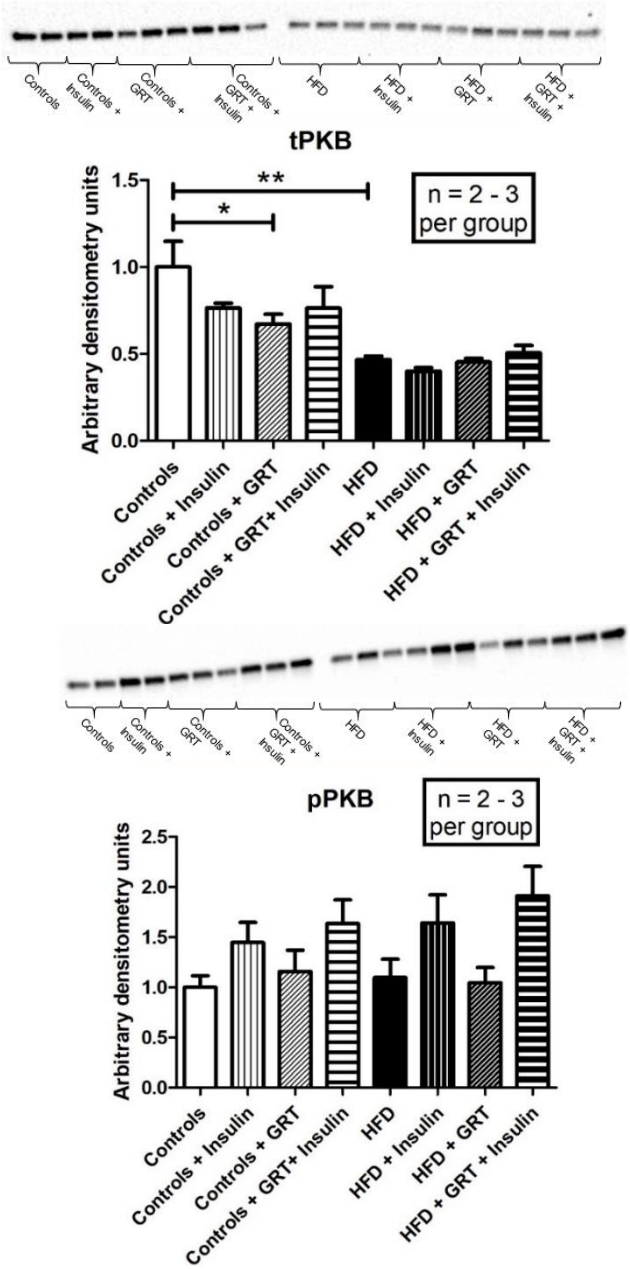

Figure 3.24 *A 1-way ANOVA of the total and phosphorylated PKB expression between control groups (with and without Afriplex GRT Extract), control groups (with and without insulin injection), HFD groups (with and without Afriplex GRT Extract) and HFD groups (with and without insulin injection) (*p<0.05; **p<0.001; ***p<0.0001).*

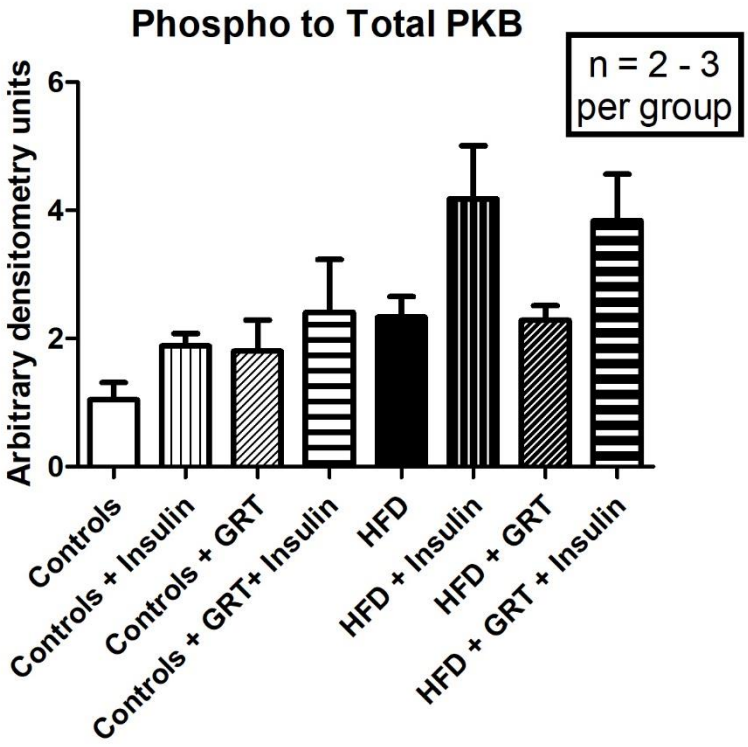

Figure 3.25 *A 2-way ANOVA of the ratio of phosphorylated vs total levels of PKB expression between control groups (with and without Afriplex GRT Extract), control groups (with and without insulin injection), HFD groups (with and without Afriplex GRT Extract) and HFD groups (with and without insulin injection) (*p<0.05; **p<0.001; ***p<0.0001).*

The HFD groups had significantly lower total PKB levels than the controls ($p < 0.001$) (Figure 3.24). Afriplex GRT Extract also significantly decreased total PKB expression in the controls ($p < 0.05$). No significant differences were found between the phosphorylated PKB levels of the groups. There were also no significant differences between the ratio of phosphorylated PKB versus total PKB in the groups (Figure 3.25), but insulin treatment seemed to have increased phosphorylated PKB expression in all the groups. It is very interesting that the HFD hearts reacted on insulin treatment despite the low total PKB levels.

Please note: In the blot from Figure 3.24, the gel was not placed straight in the ChemiDoc in the Gel Activation step. This explains why the bands seem to increase in size across the blot.

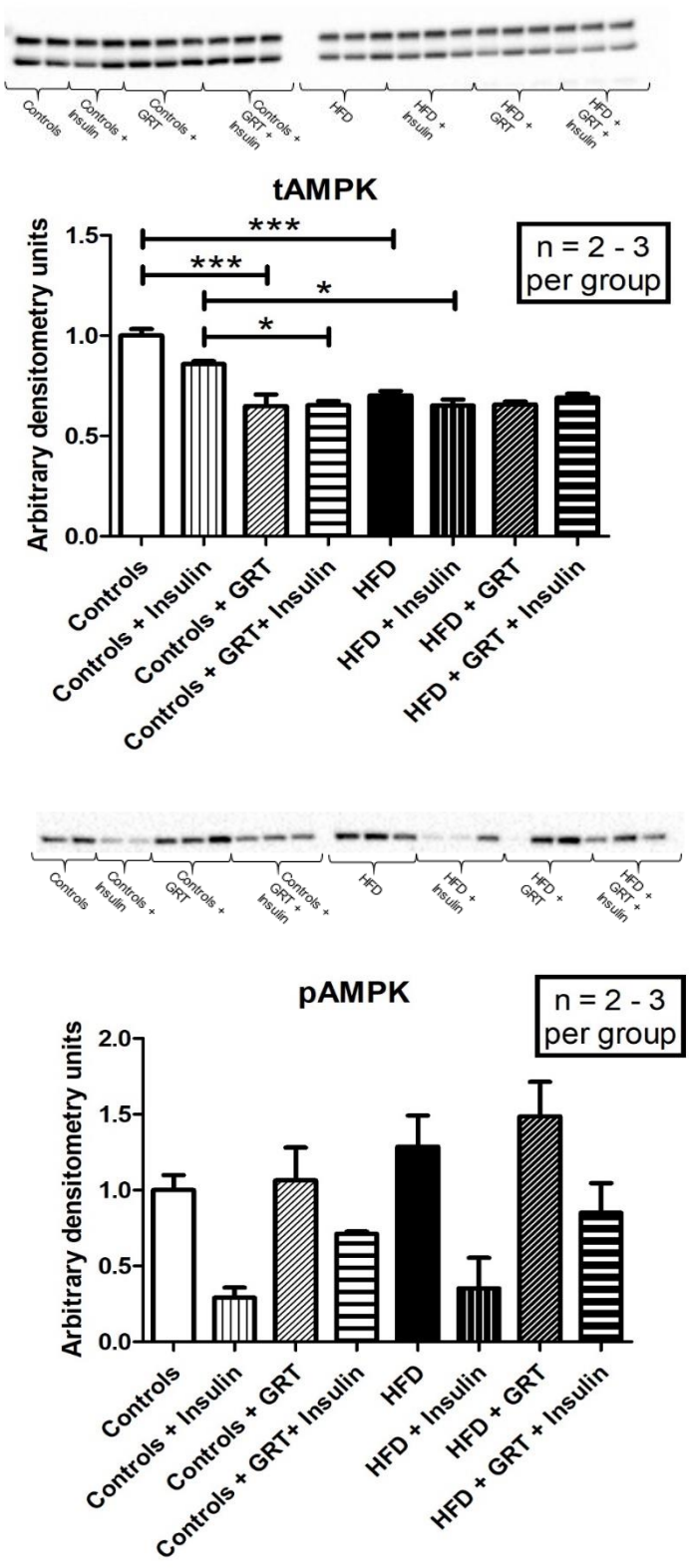

Figure 3.26 *A 1-way ANOVA of the total and phosphorylated AMPK expression between control groups (with and without Afriplex GRT Extract), control groups (with and without insulin injection), HFD groups (with and without Afriplex GRT Extract) and HFD groups (with and without insulin injection) (*p<0.05; **p<0.001; ***p<0.0001).*

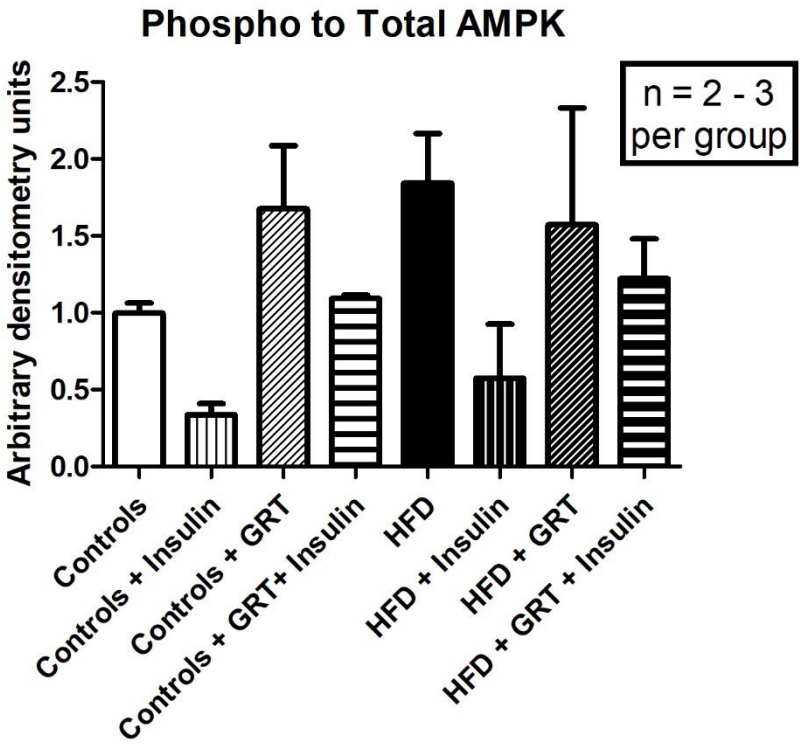

Figure 3.27 *A 1-way ANOVA of the ratio of phosphorylated vs total levels of AMPK expression between control groups (with and without Afriplex GRT Extract), control groups (with and without insulin injection), HFD groups (with and without Afriplex GRT Extract) and HFD groups (with and without insulin injection) (*p<0.05; **p<0.001; ***p<0.0001).*

The HFD groups had significantly lower total AMPK levels than the controls ($p < 0.0001$) and the same effect was seen in the controls groups and HFD groups injected with insulin before sacrifice ($p < 0.05$) (Figure 3.26). Afriplex GRT Extract also significantly decreased total AMPK expression in the controls (with and without the insulin injection before sacrifice). No significant differences were found between the phosphorylated AMPK levels of the groups. There were also no significant differences between the ratio of phosphorylated AMPK versus total AMPK in the groups (Figure 3.27).

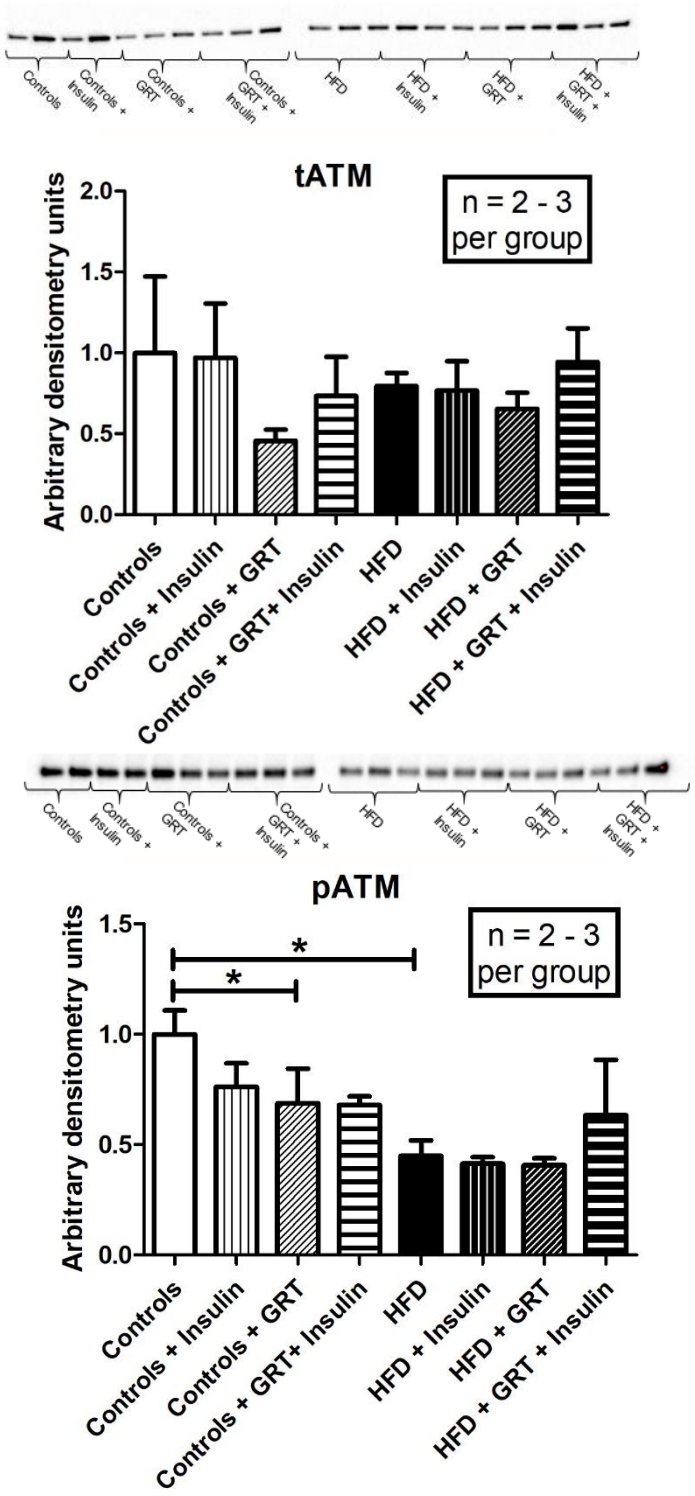

Figure 3.28 *A 1-way ANOVA of the total and phosphorylated ATM expression between control groups (with and without Afriplex GRT Extract), control groups (with and without insulin injection), HFD groups (with and without Afriplex GRT Extract) and HFD groups (with and without insulin injection) (*p<0.05; **p<0.001; ***p<0.0001).*

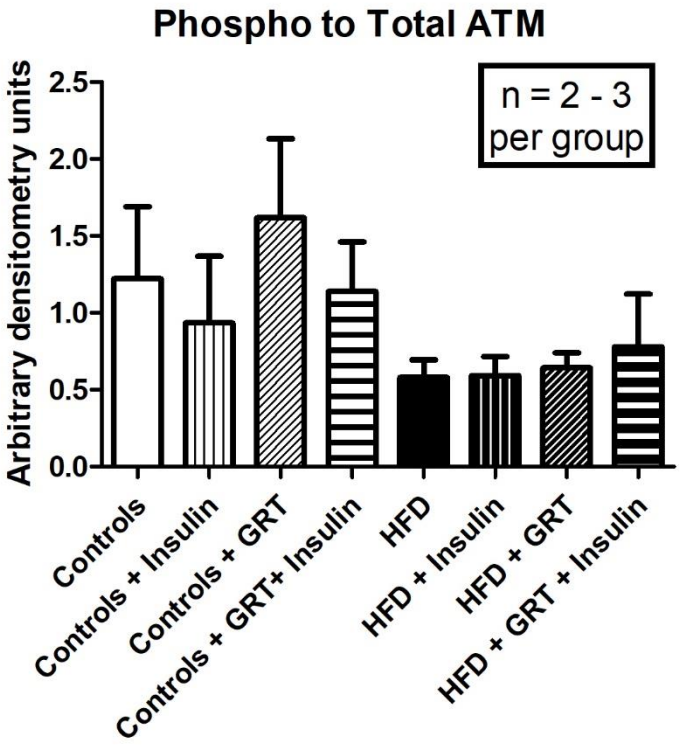

Figure 3.29 *A 1-way ANOVA of the ratio of phosphorylated vs total levels of ATM expression between control groups (with and without Afriplex GRT Extract), control groups (with and without insulin injection), HFD groups (with and without Afriplex GRT Extract) and HFD groups (with and without insulin injection) (*p<0.05; **p<0.001; ***p<0.0001).*

The HFD significantly decreased baseline phosphorylated ATM ($p < 0.05$) (Figure 3.28). In addition, Afriplex GRT Extract significantly decreased phosphorylated ATM expression in the control groups ($p < 0.05$). No significant differences were found otherwise.

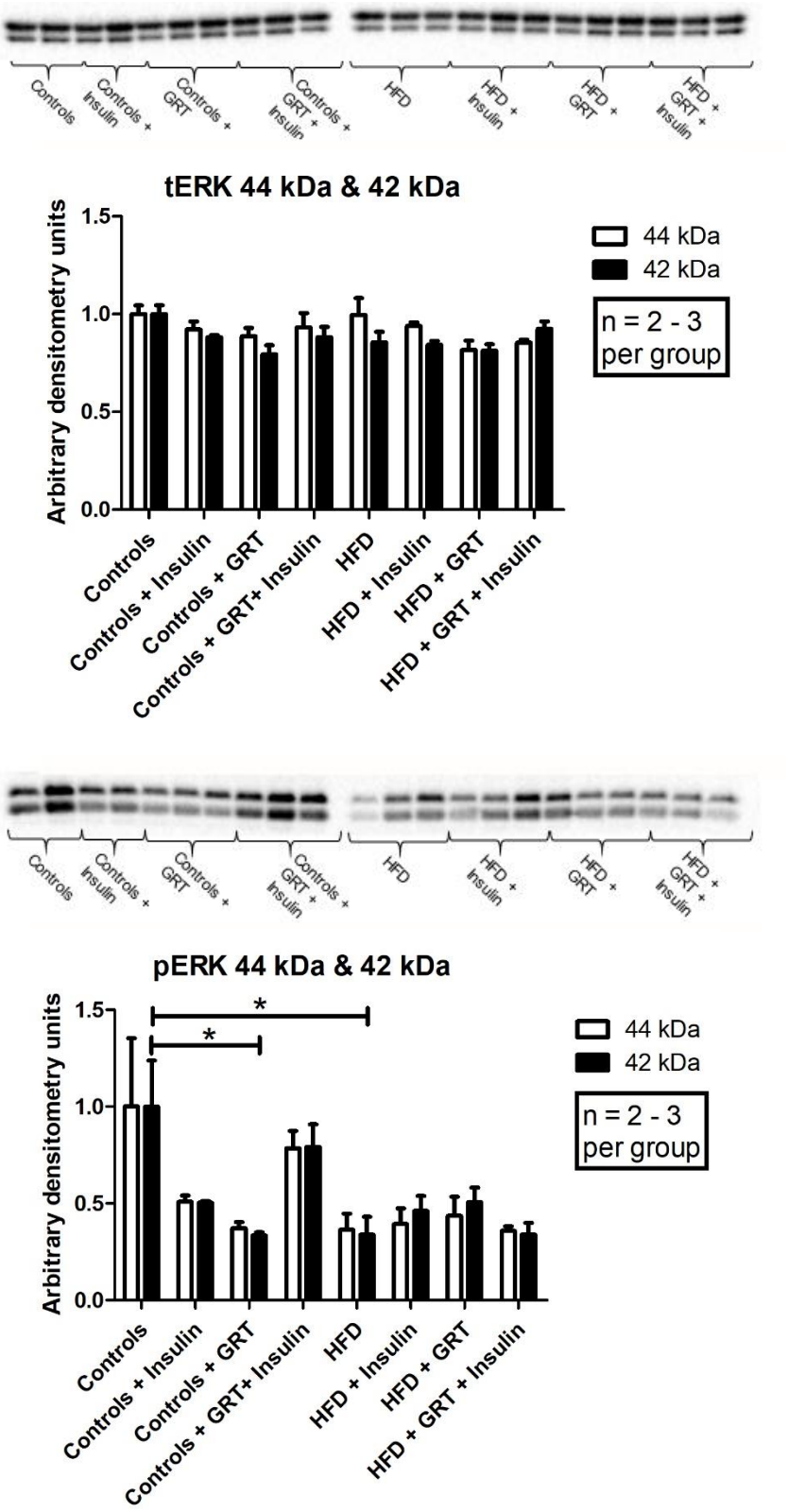

Figure 3.30 *A 2-way ANOVA of the total and phosphorylated ERK (at 42 kDa and 44 kDa) expression between control groups (with and without Afriplex GRT Extract), control groups (with and without insulin injection), HFD groups (with and without Afriplex GRT Extract) and HFD groups (with and without insulin injection) (*p<0.05; **p<0.001; ***p<0.0001).*

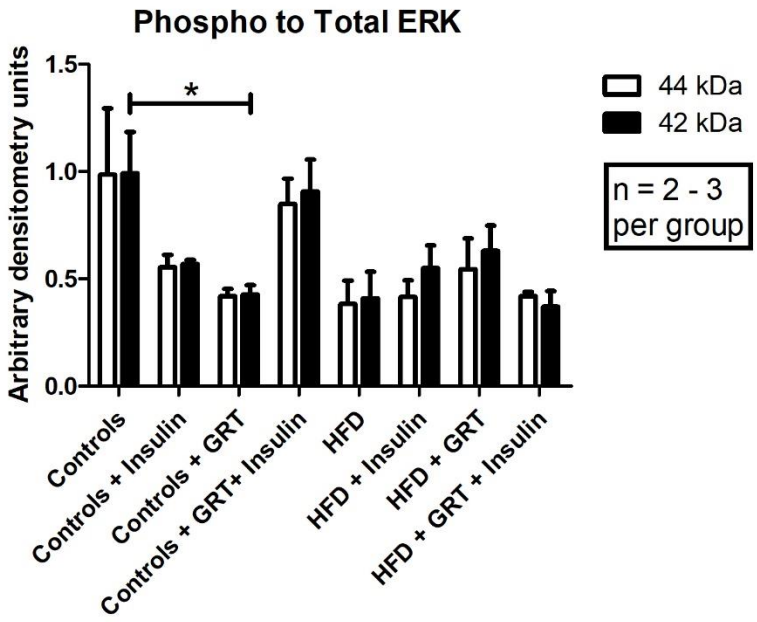

Figure 3.31 *A 2-way ANOVA of the ratio of phosphorylated vs total levels of ERK (at 42 kDa and 44 kDa) expression between control groups (with and without Afriplex GRT Extract), control groups (with and without insulin injection), HFD groups (with and without Afriplex GRT Extract) and HFD groups (with and without insulin injection) (*p<0.05; **p<0.001; ***p<0.0001).*

The HFD groups had significantly lower phosphorylated ERK levels than the controls ($p < 0.05$) (Figure 3.30). Afriplex GRT Extract also significantly decreased phosphorylated ERK expression in the controls, as well as the ratio of phosphorylated ERK to total ERK ($p < 0.05$) (Figure 3.31). No significant differences were found between the total ERK levels of the groups.

4.2. Stress Responsive Proteins

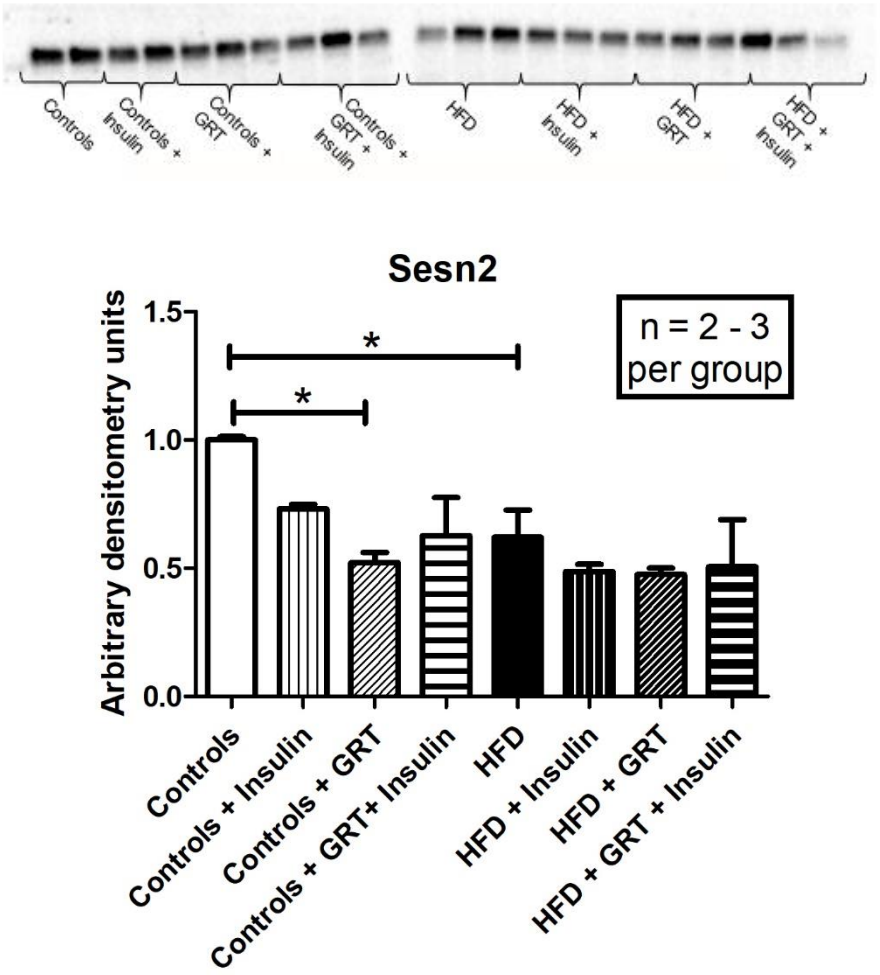

Figure 3.32 *A 1-way ANOVA of the Sesn2 expression between control groups (with and without Afriplex GRT Extract), control groups (with and without insulin injection), HFD groups (with and without Afriplex GRT Extract) and HFD groups (with and without insulin injection) (*p<0.05; **p<0.001; ***p<0.0001).*

Sesn2 levels were significantly decreased in the HFD groups ($p < 0.05$). The Afriplex GRT Extract also significantly decreased Sesn2 expression in the controls ($p < 0.05$).

4.3. Proteins associated with autophagy, measured in the cytosolic compartment of the cell

The tissue in this section was prepared from hearts that were immediately freeze-clamped after being removed from the animals from cohort 1. The lysates were prepared from the cytosolic fraction, thus allowing us to observe the effects seen on baseline levels. The animals were not fasted before sacrifice.

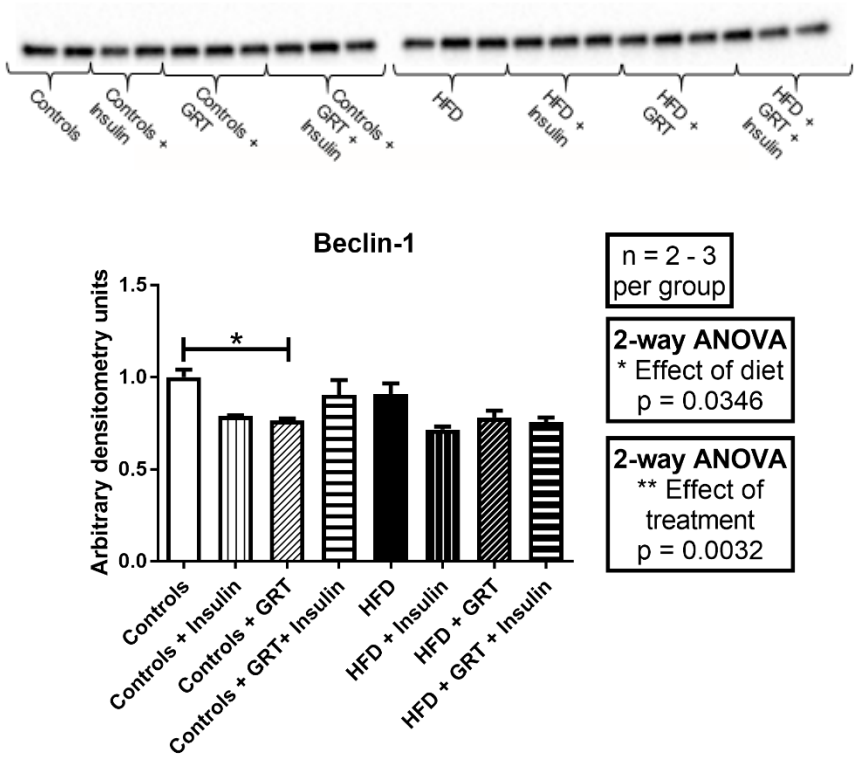

Figure 3.33 *A 1-way ANOVA of the Beclin-1 expression between control groups (with and without Afriplex GRT Extract), control groups (with and without insulin injection), HFD groups (with and without Afriplex GRT Extract) and HFD groups (with and without insulin injection) (*p<0.05; **p<0.001; ***p<0.0001).*

Cytosolic Beclin-1 expression was significantly lower in the controls treated with Afriplex GRT Extract than those not treated. A 2-way ANOVA indicated that the HFD ($p = 0.0346$) and the Afriplex GRT Extract ($p = 0.0032$) decreased Beclin-1 expression.

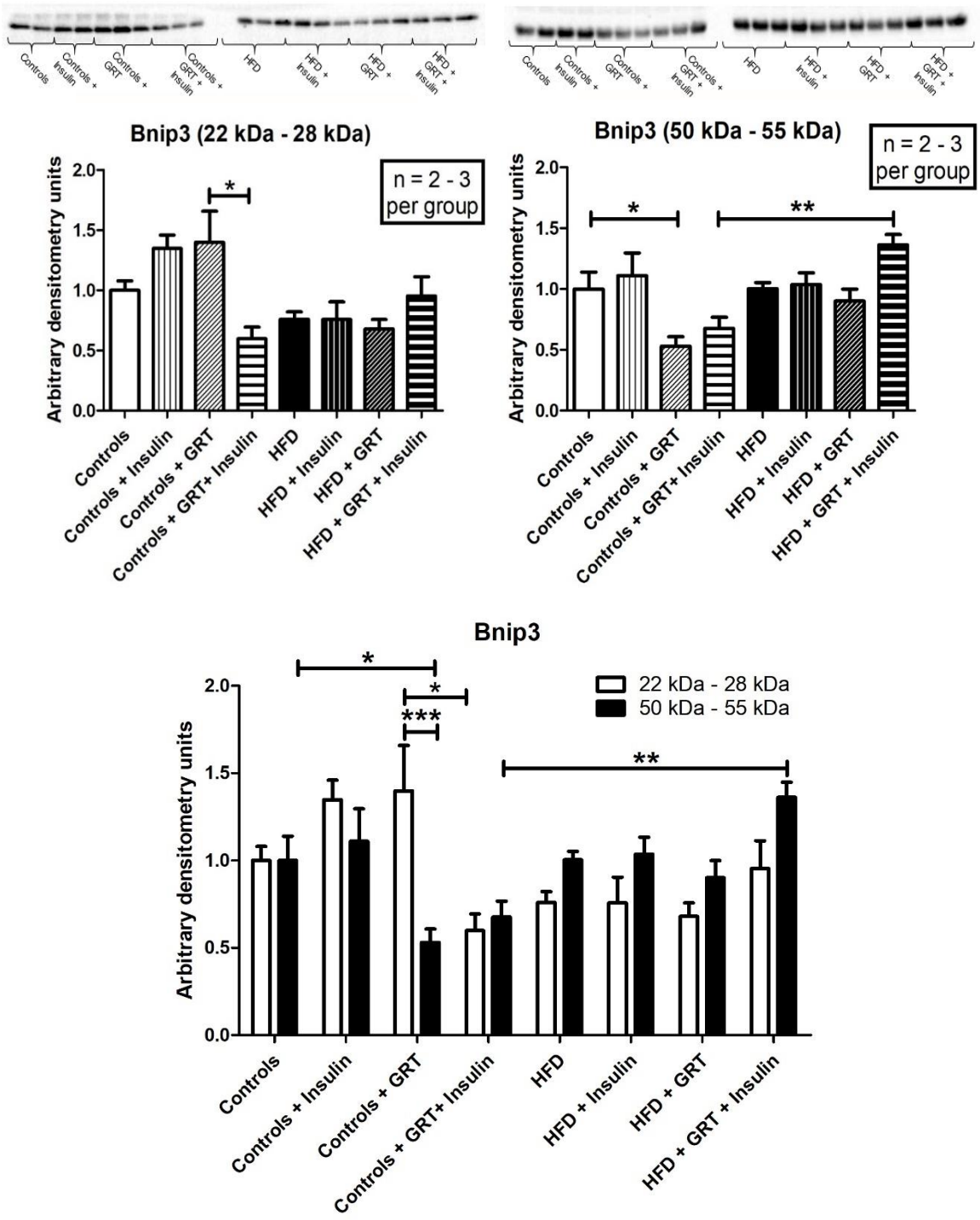

Figure 3.34 *A 1-way ANOVA of the BNIP3 (at 22 – 28 kDa and 50 – 55 kDa) expression between control groups (with and without Afriplex GRT Extract), control groups (with and without insulin injection), HFD groups (with and without Afriplex GRT Extract) and HFD groups (with and without insulin injection) (*p<0.05; **p<0.001; ***p<0.0001).*

According to a 2-way ANOVA, the HFD resulted in lower levels of BNIP3 (p = 0.0019). In addition, the 22 – 28 kDa BNIP3 expression was lowered in the controls treated with Afriplex GRT Extract and injected with insulin compared to that of the controls only

treated with Afriplex GRT Extract ($p = 0.0124$). Futhermore, a 1-way ANOVA indicated that the 50-55 kDa homodimers of BNIP3 was lower in the hearts of the control animals treated with Afriplex GRT Extract ($p < 0.05$). Animals on the HFD, treated with Afriplex GRT Extract then injected with insulin, had significantly higher BNIP3 homodimer (50 – 55 kDa) levels than the Afriplex GRT Extract treated control groups injected with insulin ($p < 0.001$).

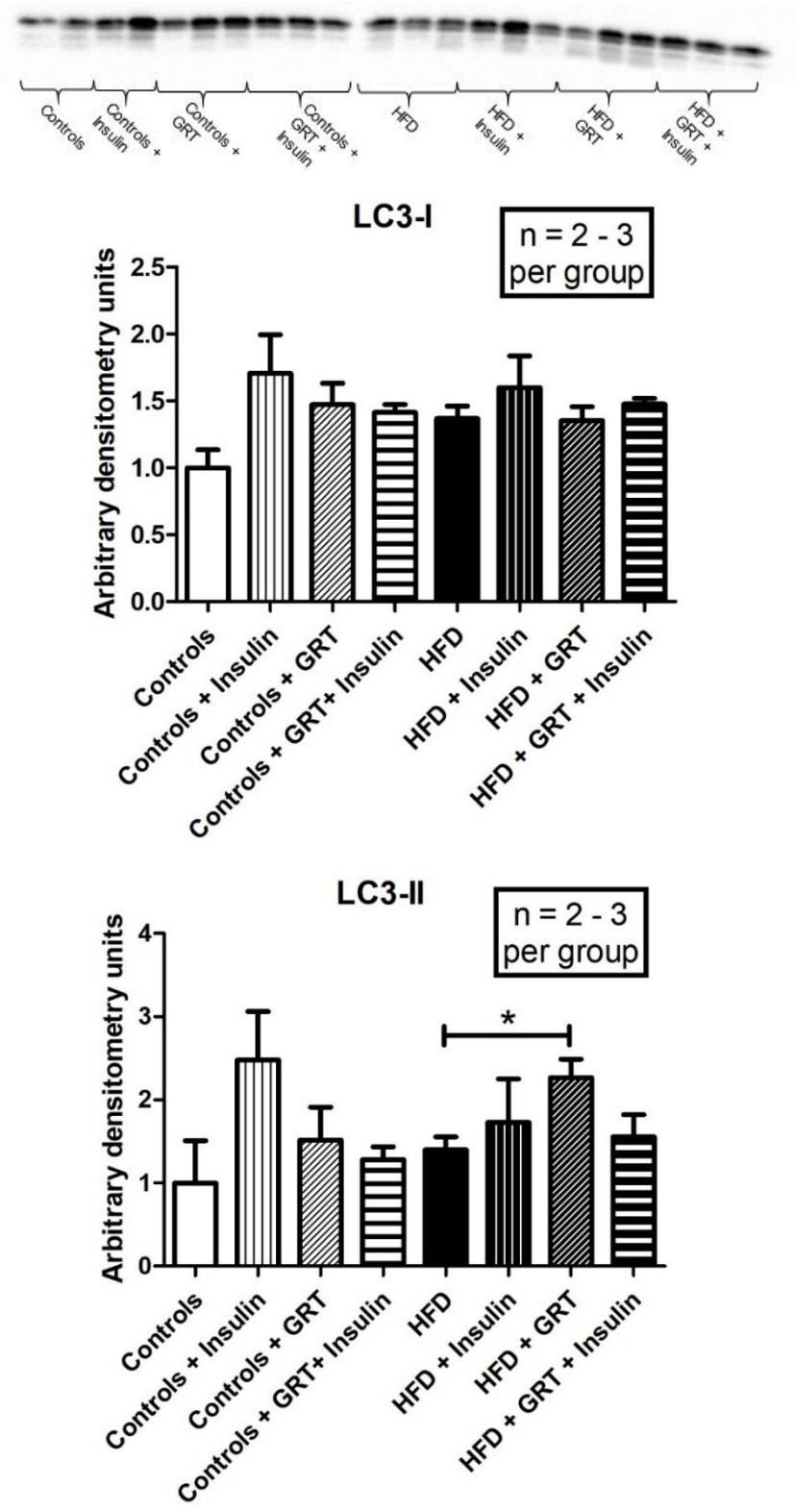

***Figure* 3.35** *A 1-way ANOVA of the LC3-I and LC3-II expression between control groups (with and without Afriplex GRT Extract), control groups (with and without insulin injection), HFD groups (with and without Afriplex GRT Extract) and HFD groups (with and without insulin injection) (*p<0.05; **p<0.001; ***p<0.0001).*

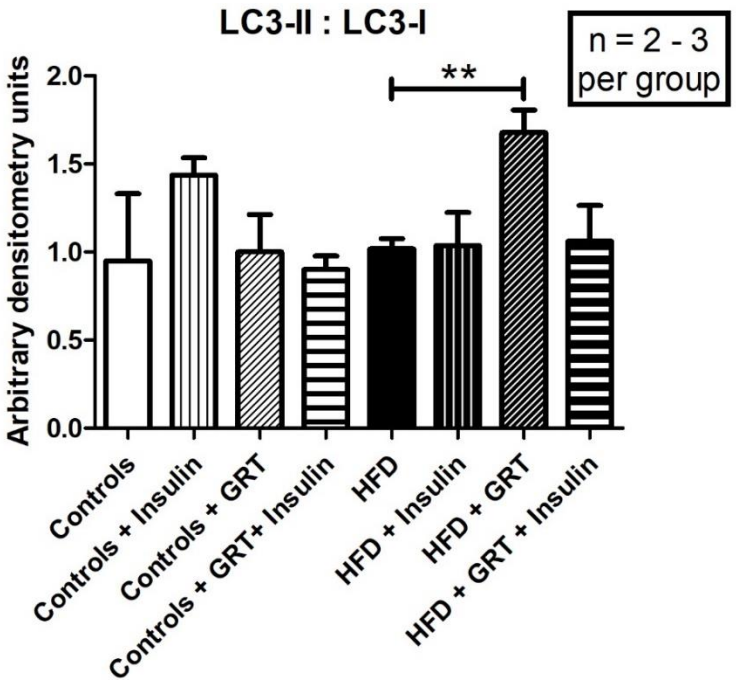

Figure 3.36 *A 1-way ANOVA of the ratio of LC3-II vs LC3-I expression between control groups (with and without Afriplex GRT Extract), control groups (with and without insulin injection), HFD groups (with and without Afriplex GRT Extract) and HFD groups (with and without insulin injection) (*p<0.05; **p<0.001; ***p<0.0001).*

There was an increase in LC3-II expression in Afriplex GRT Extract treated HFD groups, compared to the non-treated HFD group (Figure 3.35) ($p < 0.001$). The LC3-II to LC3-I ratio of the Afriplex GRT Extract treated HFD groups was significantly higher than that of normal HFD groups ($p < 0.001$).

Please note: the blot in Figure 3.35 seems as if the bands are decreasing in size across the blot. This can be explained by the fact that, when placing the gel on to the transfer paper before the transfer step, the gel was placed askew.

4.4. Mitophagy Proteins

The lysates used in this section was prepared from hearts from cohort 2 that were prepared immediately after removal from the chest cavity.

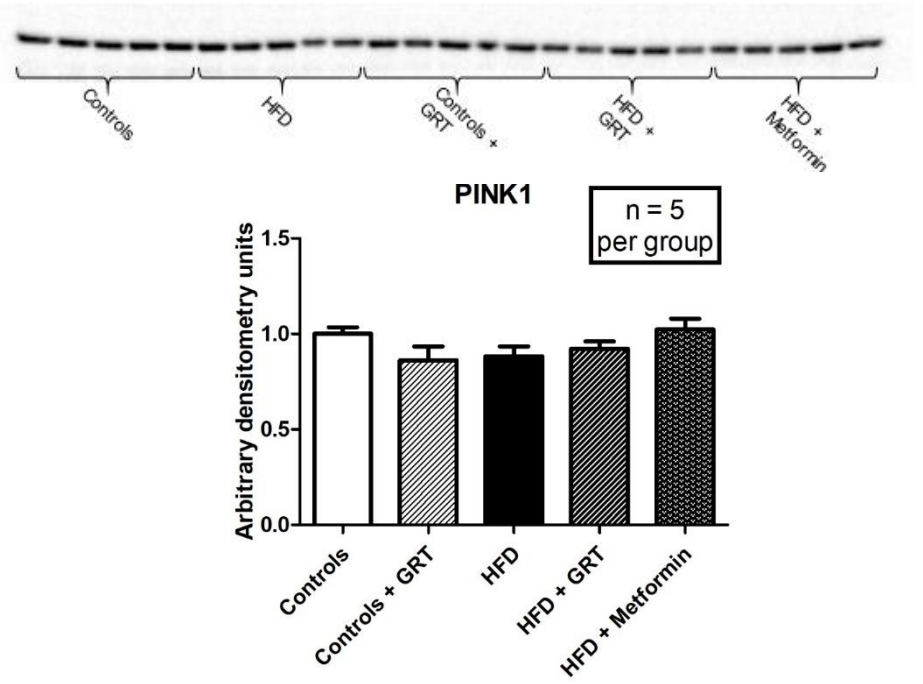

Figure 3.37 *A 1-way ANOVA of the PINK1 expression of between control groups (with and without Afriplex GRT Extract), HFD groups (with and without Afriplex GRT Extract) and HFD treated with metformin (*p<0.05; **p<0.001; ***p<0.0001).*

No significant differences in mitochondrial PINK1 expression were found between either of the groups (Figure 3.37).

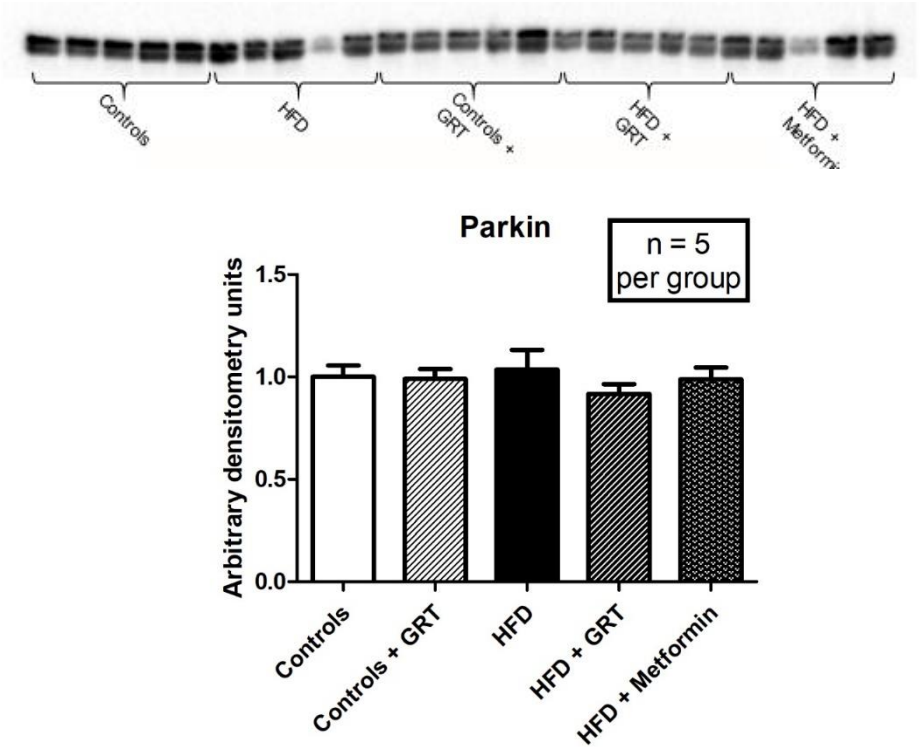

Figure 3.38 *A 2-way ANOVA of the Parkin expression of between control groups (with and without Afriplex GRT Extract), HFD groups (with and without Afriplex GRT Extract) and HFD treated with metformin (*p<0.05; **p<0.001; ***p<0.0001).*

No significant differences were found between the groups (Figure 3.38).

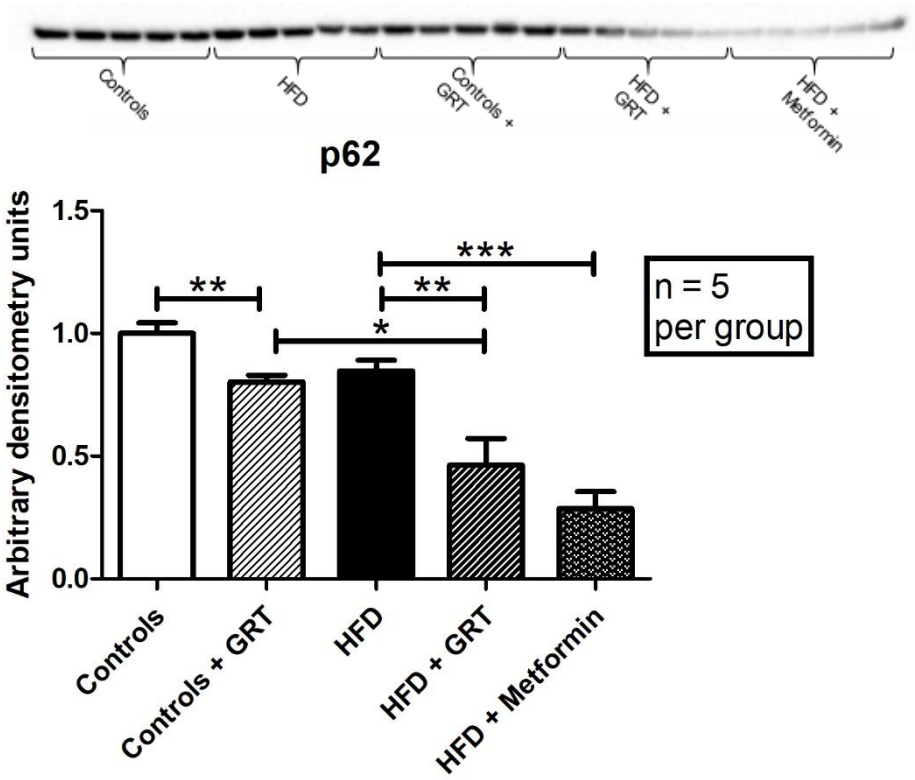

Figure 3.39 *A 2-way ANOVA of the p62 expression of between control groups (with and without Afriplex GRT Extract), HFD groups (with and without Afriplex GRT Extract) and HFD treated with metformin (*p<0.05; **p<0.001; ***p<0.0001).*

The Afriplex GRT Extract also decreased p62 levels in the control and HFD groups ($p < 0.001$) (Figure 3.39). Levels of mitochondrial p62 were significantly decreased in the Afriplex GRT Extract treated HFD groups compared to that of Afriplex GRT Extract treated control groups ($p < 0.05$). Expression of p62 was also decreased in HFD groups treated with metformin (positive control) compared to non-treated HFD groups ($p < 0.0001$).

CHAPTER 4: Discussion and Conclusion

1. Body Weight, IP Fat Weight, Liver Weight and Urine Volume

Generally, increased consumption of fats, cholesterol, sugar and carbohydrates are associated with an increase in bodyweight. This increase is attributed to the imbalance that originates when energy intake is more than energy outflow (Spiegelman & Flier, 2001; The Heart and Stroke Foundation South Africa, 2016). As previously mentioned, this imbalance is associated with development of insulin resistance.

The high fat diet (HFD) used in our study has been previously tested and established in our laboratory (Huisamen, et al., 2013). This HFD is aimed to induce obesity and insulin resistance in the animals. The biometric parameters of the animals were characterized, before experimentation, to ensure that the animals fed with the HFD developed both insulin resistance and obesity. This was done by performing OGTTs on the animals at week 10, to ensure insulin resistance in the HFD animals. The body weights were also monitored weekly and compared to the controls.

The diet fed to the HFD groups significantly increased the bodyweight gain in comparison to control fed animals, demonstrating the success of the diet regime to induce obesity in the animals (Figure 3.1 and 3.2). Along with the bodyweights, increased liver weights and IP fat gain was also seen in the HFD groups, again showing that the diet regime resulted in central obesity as well as having effects on the liver (Figure 3.4 and 3.5) (Hariri & Thibault, 2010; Gao, et al., 2015).

Ingestion of Afriplex GRT Extract, for a period of 6 weeks, resulted in significantly lowered weight gain as well as lesser IP fat weight gain by the HFD groups (Figure 3.2 and Figure 3.5). In addition, the Afriplex GRT Extract counteracted the increase in the liver weights in the HFD groups demonstrating that the product changed the metabolic profile of the animals resulting in a healthier profile with diminished central obesity.

Afriplex GRT Extract contains a fair amount of quercetin (0.5 %) and, in previous studies, quercetin has been shown to cause weight-loss and to have anti-obesity properties (Kuppusamy & Das, 1992; Ahn, et al., 2008; Rivera, et al., 2008). Ahn, et al. (2008) states that quercetin improves obesity through the AMPK and MAPK signalling pathways and Hoon, et al. (2013) have shown that quercetin suppresses adipogenesis. The quercetin in the Afriplex GRT Extract could account for the lowered

weight gain and overall obesity improvement in the treated animals (Figure 3.2, 3.4 and 3.5).

The food intake of the HFD animals were significantly more than that of the control animals throughout the 16-week period, explaining the higher bodyweight seen in these animals (Figure 3.3). However, the HFD groups also ingested significantly less water than the control groups, especially from week 11. This could be because the normal rat-chow diet (of the control animals) was simply less moist than that of the HFD (which contained 200 ml water in the diet composition).

In addition, the Afriplex GRT Extract treated control animals ingested significantly more water than the non-treated controls, especially from weeks 3 to 5 of the treatment period, indicating that Afriplex GRT Extract caused increased thirst (Figure 3.3). Thirst can be either physiological or a subjective desire to drink fluids. Animals or humans drink fluid to either maintain body fluid homeostasis or as a result of social factors (an example could be competitive behaviour between the animals, causing them to fight for the water) (McKinley & Johnson, 2004). Thus, this study's results could indicate that Afriplex GRT Extract somehow influences the body's fluid content, causing the animals to have an increased thirst and urinate more frequently (almost in a way that caffeine has diuretic properties).

Urine volume was measured at week 15 after the animals were subjected to a 24-hour period in a metabolic cage. The HFD animals presented with a significantly lower urine volume than the control animals indicating increased water retention (Figure 3.10). The Afriplex GRT Extract had no significant effect on the urine volume of the HFD animals, but a strong tendency to increased urine volume can be seen in Afriplex GRT Extract treated control animals compared to non-treated controls. It has been said that rooibos is able to reduce fluid retention by its diuretic properties (Bredenkamp, 2006; Balance Me Beautiful, 2017). This could also be the explanation for the effect on urine volume in Afriplex GRT Extract treated controls.

Water retention can also be an explanation for the increased bodyweights in HFD animals. Extreme thirst or hunger and water retention are symptoms of insulin resistance (Zhou, et al., 2014; Roland & Marcin, 2017). The latter suggests that the low urine volume in the HFD animals could confirm insulin resistance, but it does not fit the observation that HFD animals drank less water than the control animals. The

HFD animals might have, however, simply drank less water because their diet was moister than the normal control diet. The low water intake could be the reason for the lower urine volume, thus it cannot be confirmed that the HFD animals had water retention. Further studies are necessary to elaborate on this.

The ADH (antidiuretic hormone) regulates water balance in the body and an increase in fluid loss results in decreased blood pressure (Rice & Luo, 2017). The low urine output in the HFD animals could also indicate that the HFD animals might have exhibited high blood pressure, confirming insulin resistance in these animals (Vallance & Norman, 2001; Hoshiyama, et al., 2003). Aldosterone- and angiotensin levels are two hormones that maintain blood pressure and could thus have been measured to confirm if the HFD animals exhibited high blood pressure.

2. Glucose Levels, Insulin Levels and HOMA IR Index

2.1. OGTT Data and Basal Glucose Levels

An increased fasting basal glucose level can be an indication of insulin resistance (Cefalu, 2001), but at week 10 of the HFD period, this was not seen (Figure 3.8). However, the results obtained from the OGTT assays showed that animals on the HFD presented with significantly higher plasma glucose levels after ingestion of a glucose load at week 10 (Figure 3.6). This confirms that the animals on the HFD were insulin resistant and unable to effectively utilize the glucose load. This was expected, seeing as an increased glucose level indicates insulin resistance. Insulin resistant humans have higher plasma glucose levels than normal. Ingestion of Afriplex GRT Extract significantly increased the basal glucose levels after week 15 in the HFD groups and did not improve the OGTT generated curves (Figure 3.7 and 3.9), showing that Afriplex GRT Extract did not improve whole body insulin resistance in the HFD animals.

On the other hand, the OGTT data demonstrated that ingestion of Afriplex GRT Extract improved the ability of the animals on a normal control diet to handle a glucose load by week 15 (Figure 3.7). This may be because Afriplex GRT Extract was able to improve the peripheral glucose utilization of these animals but not in the HFD animals. Afriplex GRT Extract did not increase insulin secretion by the pancreatic β-cells, indicated by the fasting insulin levels measured in the animals.

The results obtained in our study, using a high fat diet-induced obesity and insulin resistant model, contrast with the data reported by Kamakura, et al. (2015), who

demonstrated that insulin resistance was improved in obese diabetic mice using a different green rooibos extract, and Kawano, et al. (2009), who demonstrated a hypoglycaemic effect on db/db mice treated with aspalathin.

2.2. Insulin levels and HOMA IR Index

Validating the OGTT results, a 2-way ANOVA of the HOMA-IR indicated that the Afriplex GRT Extract improved insulin resistance in the control animals (Figure 3.14). More specifically, the Afriplex GRT Extract had a borderline significant effect on the control animals, where the HOMA-IR was improved by this product. Metformin also had a borderline significant effect on the HFD animals, where insulin resistance was improved. The term 'borderline significance' is used because of the low n-value that was due to the limited fasting serum and fasting insulin values that were available.

3. Leptin and Adiponectin Levels

In the HFD animals the significantly increased leptin levels were expected because of the central obesity in the animals (Figure 3.11) (Li & Wu, 2012). The increased leptin levels in the HFD animals confirm once again that obesity was induced via the HFD regime as leptin levels are proportional to fat mass (Maffei, et al., 1995; Trayhurn & Bing, 2006).

Leptin is a hunger inhibiting hormone and ghrelin an appetite-increasing hormone (Brennan & Mantzoros, 2006). Ghrelin levels are increased when the stomach is empty, thus increasing appetite (Klok, et al., 2007). Leptin, on the other hand, is secreted to inhibit appetite when the stomach satiated. In obesity, T2D and insulin resistance there is increased leptin levels because of the increased fat mass. Along with the increased leptin levels, leptin resistance develops that cause obese patients to fail to control their hunger (Considine, et al., 1996).

The Afriplex GRT Extract did, however, significantly decrease the leptin levels in the HFD groups, probably because of the loss of IP fat (Figure 3.11). No significant differences were seen with Afriplex GRT Extract and the adiponectin levels, but the diet had a significant effect overall, according to a 2-way ANOVA (Figure 3.12). This was not expected. Adiponectin is produced by adipocytes and inversely related to fat mass, in contrast to leptin (Maffei, et al., 1995; Hu, et al., 1996). Adiponectin improves insulin sensitivity by AMPK activation (Yamauchi, et al., 2002). Low adiponectin levels are associated with obesity and is a known risk factor for cardiovascular disease

(Sattar, et al., 2006; Goyal, et al., 2014). The high adiponectin levels in the HFD is interesting and should be further explored especially in view of the obesity paradox (Carnethon, et al., 2012).

4. 2DG Uptake

The 100 nM insulin concentration was not sufficient to elicit a glucose response in the cardiomyocytes (Figure 3.15). This lack of effect was also seen in a study by Smit, et al. (2017), where aspalathin had no effect on the 2DG uptake of heart cells from obese and insulin resistant rats, compared to the marked stimulation observed in cardiomyocytes from young, control rats. They argue that aspalathin is dependent on the PI3K signalling pathway in order to have any effect (Smit, et al., 2017). This leads us to the speculation that the animals from this study might have been too old and that they were already insulin resistant by the time of sacrifice. Comparison to a young, control rat would have been beneficial to provide confirmation on the latter.

5. Mitochondrial Respiration

5.1. Mitochondrial Function

Mitochondria play a pivotal role in cell physiology and pathology (Bournat & Brown, 2010). Because of its widespread role in fat- and glucose metabolism, it is important to investigate the functionality of mitochondria to potentially provide answers for the effects seen in this study.

Certain parameters of mitochondrial function were determined using an oxygraph. As these analyses were performed on mitochondria isolated from fresh hearts, using differential centrifugation, the changes observed must be of such a nature that they are retained through the isolation procedure.

The HFD did not have any significant effect on the mitochondrial function with regards to the mitochondrial respiration studies.

State 2 respiration of mitochondria is recorded with no ADP present in the incubation medium and reflects the oxygen consumed by the mitochondria under these conditions. Metformin increased the state 2 respiration in cardiac myocyte mitochondria from HFD animals in both glutamate and a fatty acid medium, palmitoyl-

L-carnitine (Figure 3.17). According to Owen, et al. (2000) and Zhou, et al. (2001), this is the mechanism whereby metformin activates AMPK.

A 2-way ANOVA indicated that the mitochondrial state 3 respiration was overall higher when their cardiac myocyte mitochondria were incubated in the palmitoyl-L-carnitine media (Figure 3.18). This was expected, since Cole, et al. (2011) also demonstrate that state 3 respiration rates were increased in a palmitoyl-L-carnitine media and unchanged in glutamate and pyruvate substrates. In state 4, the mitochondria from HFD hearts treated with metformin presented with an increased respiration rate in comparison to the non-treated HFD animals, but only in the fatty acid medium (Figure 3.19). This higher respiration rate means that the metformin might have caused uncoupled mitochondria or an oxygen leak, because metformin is known to inhibit complex I in the ETC (Owen, et al., 2000).

Ingestion of Afriplex GRT Extract significantly improved the ADP/O ratio in the HFD groups (Figure 3.16) and the RCI values in the control groups in the palmitoyl-L-carnitine media (Figure 3.20). The increased ADP/O ratio shows that Afriplex GRT Extract improved coupling efficiency and mitochondrial oxygen utilization in the HFD animals (Brand & Nicholls, 2011). The increased RCI value in the Afriplex GRT Extract treated control animals indicates that Afriplex GRT Extract ingestion also improved the coupling function of the mitochondria in the control animals. These mitochondria now displayed a higher capacity for substrate oxidation and formation of ATP.

The oxidative phosphorylation rate may be the best indication of mitochondrial function in these studies, since the calculation includes both ADP/O ratio and state 3 respiration. Afriplex GRT Extract ingestion improved the oxidative phosphorylation rate in the control groups but not in the HFD animals when incubated in a carbohydrate or a fatty acid medium (Figure 3.21). This may indicate that one of the ETC complex proteins that allows the flow of electrons through the ETC, may be compromised in the HFD animals. Further studies on the individual proteins may shed light on this.

Metformin was able to improve the oxidative phosphorylation rate of mitochondria from the HFD animals when incubated in the palmitoyl-L-carnitine media. As it has been shown that metformin inhibits complex I of the ETC chain thereby activating AMPK (Owen, et al., 2000), this could mean that the mitochondria were able to have an improved import of fatty acids through the CPT-1 complex in the presence of a fatty

acid substrate. CPT-1 is indirectly activated by AMPK through the inhibition of acetyl CoA carboxylase, thereby lifting the inhibitory effects of malonyl-CoA on CPT-1 (Stanley, et al., 2005). Furthermore, it has been demonstrated that this activation of AMPK can reverse the inhibitory effects of metformin on complex I and accelerate β-oxidation (González-Barroso, et al., 2012).

The ability of the isolated mitochondria to withstand an anoxic period followed by re-oxygenation was tested (Figure 3.22). The results showed that in all groups incubation of mitochondria in the fatty acid medium significantly reduced their ability to withstand anoxia and then regain state 3 respiration (Figure 3.22). This is an indication of mitochondrial dysfunction in the presence of fatty acids as substrate medium (Weinberg, et al., 2000). In addition, no significant differences were found between the groups in the percentage recovery after exposure to hypoxia followed by re-oxygenation. These results suggest that the contractile recovery after ischaemia during reperfusion was better in the glutamate medium than with palmitoyl-L-carnitine medium, and previous studies have demonstrated that the contractile recovery after ichaemia of the heart is improved in glucose substrates rather than fatty acids substrates (Kjekshus & Mjos, 1972; Burkhoff, et al., 1991; Korvald, et al., 2000).

5.2. Mitophagy Proteins

Please note that these Western blot analyses were done on the lysates prepared from the isolated myocardial mitochondria. Mitochondrial lysates were prepared immediately after excision of the heart from the chest cavity, thus the mitochondria were in normal conditions and should not be expected to exhibit changes in mitophagy.

No significant differences were found in the PINK1 and Parkin levels between either of the groups (Figure 3.37 and 3.38). A possible explanation for this could be that, because the mitochondria were isolated immediately after excision of the hearts, they (the mitochondria) were under normal conditions where one would not expect upregulation of mitophagy.

The Afriplex GRT Extract did, however, significantly decrease mitochondrial p62 levels in the control and HFD groups, indicating that the Afriplex GRT Extract treatment could potentially have compromised autophagosome formation in the mitophagy process and therefore decreased mitophagy (Figure 3.39). Expression of p62 was also decreased because of the metformin treatment. This correlates with the fact that,

among other mechanisms, metformin activates autophagy by downregulating p62 levels (Komatsu, et al., 2007; Nazim, et al., 2016). Interestingly, low p62 levels has also been recorded in type 2 diabetes, indicating increased autophagy (Kobayashi, et al., 2012).

In this study, autophagy flux was not determined by using substances that will inhibit any step on the process. This could have been done by using chloroquine to block the autophagosome to lysosome flux (shortcoming) (Redmann, et al., 2017). The p62 expression data from this study was simply a 'snapshot' and what we see are the p62 proteins in the cytosolic pool. We could thus not see p62 accumulation. No conclusion can really be drawn from these results, but the increased LC3-II levels and decreased p62 levels in the Afriplex GRT Extract treated HFD groups (versus not treated with Afriplex GRT Extract) suggest that p62 was already associated with the autophagosome membrane and taken out of the cytosolic pool to activate mitophagy (Figure 3.35).

The increased LC3-II levels show that Afriplex GRT Extract increased mitophagy and autophagy in the HFD animals, but this was not substantiated by the other markers of mitophagy; namely Beclin-1, PINK1, Parkin or p62 levels of the mitochondria from HFD (treated and non-treated) animals. This leads us to speculate that there is a different pathway that resulted in the increased autophagy and mitophagy seen in the Afriplex GRT Extract treated HFD animals. Since the ULK1 pathway could have regulated these effects, ULK1 expression and phosphorylation could have been investigated to potentially answer these questions (Wu, et al., 2014).

6. Effects on the Insulin Signalling Pathway Proteins, Sestrin2, autophagy proteins and mitophagy proteins.

Please note that these Western blots were done with the lysates prepared from the freeze-clamped hearts.

6.1. Insulin Signalling Pathway Proteins

Indicating diet-induced insulin resistance, the HFD groups all had lower GLUT4 (Figure 3.23), total PKB (Figure 3.24), total AMPK (Figure 3.26), phosphorylated ATM (Figure 3.28) and phosphorylated ERK expression (Figure 3.30). This correlates with what was seen in previous publications (Mueckler, 2001; Brozinick Jr, et al., 2003;

Rotter, et al., 2003; Chakraborty, et al., 2010) (refer to Figure 4.1 below to see a schematic summarizing the effects seen of the HFD, used in this study, on the insulin pathway). Furthermore, lower GLUT4 levels in the HFD animals confirm that the diet regime induced obesity, as it has previously been shown that GLUT4 expression is suppressed in obese rats (Garvey, et al., 1991; Kahn & Pedersen, 1993). There were no differences seen between the HFD animals and the insulin injected HFD animals and this could be because the animals were already too old and insulin resistant.

The Afriplex GRT Extract, on the other hand, significantly decreased GLUT4 (Figure 3.23), total PKB (Figure 3.24), total AMPK (Figure 3.26), phosphorylated ATM (Figure 3.28) and phosphorylated ERK levels (Figure 3.30) in the control groups (refer to Figure 4.2 below to see a schematic summarizing the effects seen of the Afriplex GRT Extract on the insulin pathway). This indicated that Afriplex GRT Extract might have detrimental effects on the insulin signalling pathway and further investigation needs to be done. This data is contradicting to the biometrical data and OGTT results which suggested that Afriplex GRT Extract improved whole-body insulin resistance in control animals.

Bearing in mind that these blots represent protein levels in the cytosolic compartment, the significantly lowered GLUT4 expression in the Afriplex GRT Extract treated controls could indicate that the Afriplex GRT Extract might have been able to stimulate GLUT4 translocation out of the cytosol and to the membrane for glucose uptake. Fractionation of the cytosolic and membrane compartments in future may confirm that the GLUT4 did, in fact, translocate to the membrane and induce glucose uptake.

On the other hand, decreased glucose uptake in Afriplex GRT Extract treated controls could indicate that the Afriplex GRT Extract ‘forced’ the animals to utilize the fatty acids rather than glucose as energy source. PGC1α and PPARγ levels could have been measured to potentially explain or confirm the latter, because of their pivotal roles in fatty acid and glucose metabolism (Liang & Ward, 2006; Puigserver & Spiegelman, 2003). Phosphorylation of PDK4 levels could also have been investigated, because it inhibits the PDH complex and can thus be used to see if the HFD had any effect (PGC1α and PDK4 expression would have been upregulated).

When glucose is ingested, CPT-1 is downregulated and PDH upregulated to allow for glucose metabolism to form acetyl-CoA that will enter the citric acid cycle. Overload

glucose suppresses CPT-1 by signal transduction. Glucose metabolism causes decreased PGC1α and PPARγ. The opposite happens when fatty acids are ingested, causing CPT-1 to be upregulated and PDH downregulated to allow β-oxidation of the fatty acids, forming the acetyl-CoA. Fatty acid overload can lead to excess citrate that inhibits the PDH complex by activation of transcription factors (PGC1α and PPARγ). CD36 activates PDK4 and suppresses GLUT4. These are just a few of the many factors that control the uptake of either glucose or fatty acids into the mitochondria to utilize as energy substrate.

PKB is a central mediator in insulin signalling. The lowered total PKB expression indicates that both the HFD and Afriplex GRT Extract compromised the insulin signalling of the animals (Figure 3.24) (Whiteman, et al., 2002). However, injection of the animals with insulin before sacrifice resulted in enhanced phosphorylation of PKB indicating that insulin can still exert an effect on the stimulation of the protein. This was especially noticeable in the phospho/total ratio observed.

Total AMPK expression was decreased in the control animals treated with Afriplex GRT Extract (Figure 3.26). The decreased phosphorylated AMPK levels and increased phosphorylated PKB levels in the groups injected with insulin correspond with literature and was expected. Insulin induces AMPK's direct phosphorylation by Akt/PKB, thus inhibiting AMPK (Hawley, et al., 2014; Jeon, 2016). Since AMPK can activate AS160 and increase GLUT4 expression, the decreased AMPK levels in Afriplex GRT Extract treated controls could explain the decreased GLUT4 levels (Jeon, 2016).

The phosphorylated ERK levels were significantly decreased in the control animals treated with the Afriplex GRT Extract, leading us to speculate that the Afriplex GRT Extract could potentially have negatively altered nuclear transcription and cellular function (Figure 3.30) (Adcock & Caramori, 2009).

Below are two diagrams that summarize the effects resulting from the HFD and from the effects of Afriplex GRT Extract treatment on control animals. Afriplex GRT Extract had no significant effect on the HFD animals, therefore there is no figure for the HFD animals in comparison to Afriplex GRT Extract treated HFD animals.

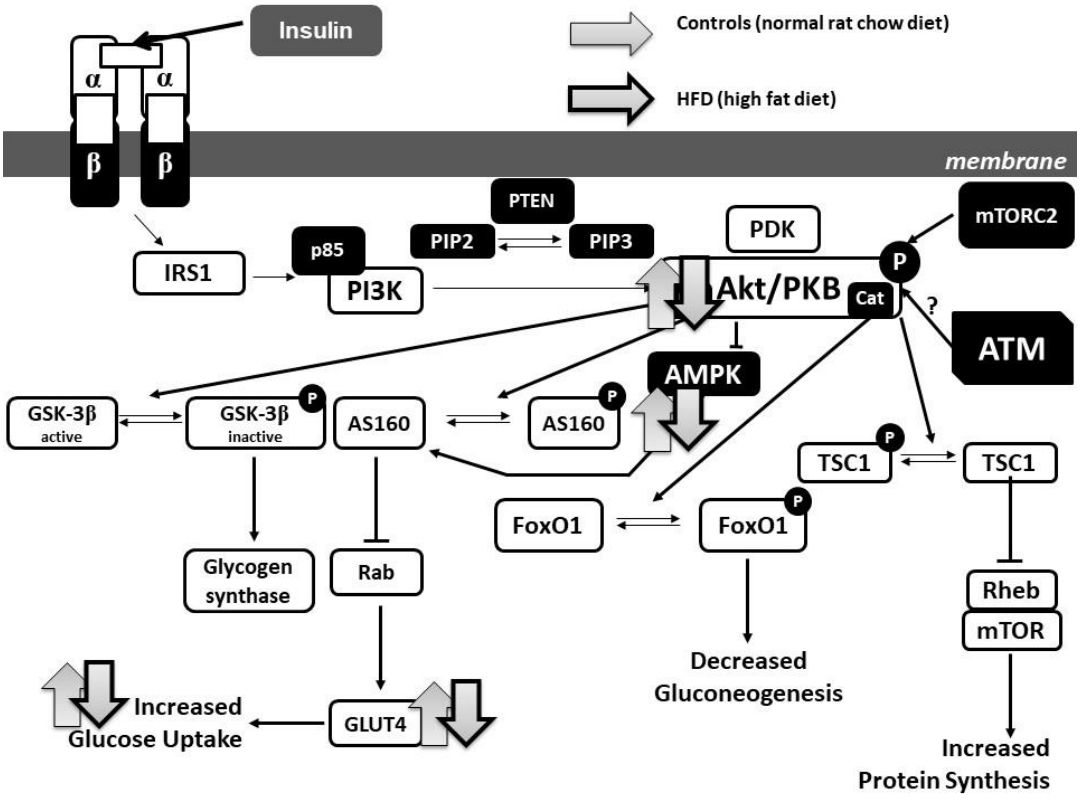

Figure 4.1 *A schematic summary of the effects of the HFD on the PI3K-dependent pathway.*

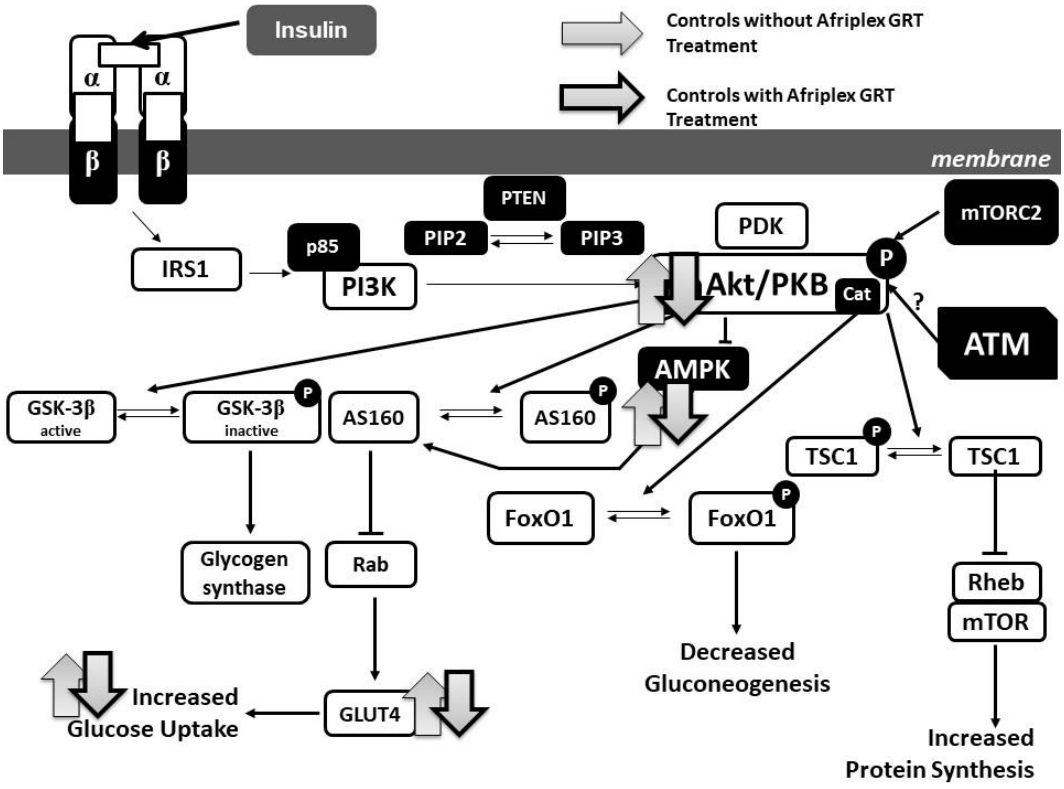

Figure 4.2 *A schematic summary of the effects of Afriplex GRT Extract on the PI3K-dependent pathway in control animals.*

6.2. Stress-responsive Protein, Sesn2

It has been proven, by previous studies, that Sesn2 levels are downregulated in obesity (Nourbakhsh, et al., 2017). Similarly, Sesn2 levels were significantly decreased in the HFD groups in comparison to the control groups, corroborating the previous findings (Figure 3.32).

The Afriplex GRT Extract decreased the Sesn2 levels in the control animals. The low Sesn2 levels could indicate that the Afriplex GRT Extract either (i) reduced oxidative stress (confirming the anti-oxidant capability of the aspalathin-rich product), or (ii) simply impaired the ability of the animals to handle oxidative stress and protect the heart.

(i) Sesn2 expression is induced by oxidative stress, hypoxia of DNA damage (Lee, et al., 2013; Rhee & Bae, 2015). This statement leads to the conclusion that a decreased Sesn2 level indicates decreased oxidative stress. This would agree with the proven fact that rooibos has anti-oxidant properties (Schulz, et al., 2003; Koza, 2013), as well as the capability to ameliorate oxidative stress (Dludla, et al., 2017). Dludla, et al. (2014) argues that PPAG can prevent oxidative stress and apoptosis. Quercetin and rutin are also appealing flavonols in rooibos that have anti-obesity properties (Kuppusamy & Das, 1992; Ahn, et al., 2008; Rivera, et al., 2008).

(ii) On the contrary it is known that, through AMPK activation, Sesn2 is able to protect the muscle and heart (Budanov, et al., 2010). Sesn2 activates AMPK, thus inhibiting mTORc1 and consequently preventing autophagy. Increased Sesn2 levels are conventionally seen in oxidative stress since it is a stress-inducible protein that is known to inhibit ROS (Pasha, et al., 2017). The low expression of Sesn2 in hearts from the obese animals could therefore indicate that they have a compromised ability to react against stress.

Further research should be done to establish which of these possibilities could be the answer.

6.3. Autophagy Proteins

Increased Beclin-1 expression is associated with increased autophagy. Beclin-1 can associate with Bcl-2, which is an anti-apoptotic protein. This association inhibits autophagy (Marquez & Xu, 2012). The Beclin-1 and Bcl-2 complex plays a significant

role in the switch between autophagy and apoptosis. Afriplex GRT Extract significantly decreased Beclin-1 expression in the control groups (Figure 3.33), indicating that Bcl-2 was not able to effectively associate with Beclin-1 to decrease autophagy (Liang, et al., 1998). Hence, this could mean that Afriplex GRT Extract potentially decreased autophagy in the normal control animals.

The Afriplex GRT Extract treated controls injected with insulin had higher BNIP3 (22 kDa – 28 kDa) levels than that of the Afriplex GRT Extract treated controls not injected with insulin (Figure 3.34). A decrease in BNIP3 indicates decreased autophagy. Afriplex GRT Extract treated HFD animals (injected with insulin) had increased BNIP3 homodimer (50 – 55 kDa) expression than that of the Afriplex GRT Extract treated controls (also injected with insulin). Not much can be concluded from these results, but the reduced BNIP3 homodimer levels in the Afriplex GRT Extract controls indicate that the Afriplex GRT Extract upregulated the drive from autophagy to apoptosis (Kubli, et al., 2008). The BNIP3 homodimer also associates with Bcl-2, pulling Bcl-2 away from the mitochondria and dissociating Bcl-2 from Bax. This leaves Bax, which has pro-apoptotic potential, to induce apoptosis (Walls, et al., 2009; Marquez & Xu, 2012). Further research should investigate Bax and Bcl-2 levels.

Along with Beclin-1, BNIP3 and p62 expression, LC3-II expression must also be determined to confirm whether autophagy was actually inhibited or activated. Afriplex GRT Extract increased LC3-II and LC3-II to LC3-I ratio of expression in the HFD groups, thus increasing mitophagy (Figure 3.35 and 3.36). In the glutamate media, the oxidative phosphorylation rate was significantly increased in the Afriplex GRT Extract treated controls. The increased LC3-II levels indicate increased mitophagy, thus increased mitophagic removal of depolarized mitochondria. This could explain the improved oxidative phosphorylation rate, mitochondrial function and coupling efficiency seen in Afriplex GRT Extract treated groups.

7. Conclusion

We can conclude that the high fat diet induced insulin-resistance, as these animals exhibited increased leptin levels, body weight, IP fat weight gain and liver weight gain. According to protein expression, Afriplex GRT Extract did not improve the insulin resistance in the HFD groups; and had a negative effect on insulin pathway mediating proteins in the control groups. On the contrary, Afriplex GRT Extract significantly increased basal serum glucose levels and the overall metabolic profile as indicated in the HFD groups (compared to non-treated HFD animals), which is in contrast to the worsened insulin resistance reflected by the protein expression levels, such as GLUT4, total PKB, total AMPK, phosphorylated ATM and phosphorylated ERK.

Afriplex GRT Extract improved coupling efficiency, mitochondrial function and oxidative phosphorylation. Most of the improvements were seen in the control animals and not the HFD animals. This could be because aspalathin only influences control animals and not insulin resistant animals. Smit, et al. (2017) stated that aspalathin increased glucose uptake in cardio-myocytes of young, control rats; but could not increase glucose uptake in cells from rats on a high-caloric diet (Smit, et al., 2017). The high fat diet had no effect on mitochondrial oxidative phosphorylation capacity.

The most significant changes with regards to mitophagy proteins, were observed in the expression of p62 in mitochondria from hearts of HFD animals. The reduced p62 in Afriplex GRT Extract treated groups could not fully provide an answer since these results only display a ‘snapshot’ of the p62 levels in the cytosol. We suggest that the lower p62 levels indicate that these p62 proteins had already associated to the autophagosome and increased depolarized mitochondria removal. This explains the improved oxidative phosphorylation seen in the mitochondrial respiration data, primarily in controls.

The decreased Sesn2 levels bring this product and its anti-oxidant capacity in to question. As mentioned earlier, Afriplex GRT Extract has a high aspalathin and PPAG content that allows Afriplex GRT Extract to display anti-oxidant effects (Dludla, et al. (2017). This validates our speculation that the lowered Sesn2 expression seen in Afriplex GRT Extract treated animals indicate that this product has strong anti-oxidant potential and ultimately improved oxidative stress.

Afriplex GRT Extract seemed to have decreased autophagy in controls according to the Beclin-1 levels, having no effect in cardiomyocytes from the HFD hearts. However, the extract upregulated apoptosis, according to BNIP3 homodimer formation, in the HFD hearts. It has been shown that BNIP3 homodimers have the ability to associate directly with LC3 to induce mitophagy without the linkage formed by the association with p62. BNIP3 may also result in the depolarization of the membrane potential of mitochondria, thereby driving mitophagy. Afriplex GRT Extract did increase LC3-II levels in the HFD group, confirming upregulated mitophagy. The increased mitophagy in the treated HFD groups might therefore have been driven and regulated by a different pathway, e.g. the ULK mediated pathway.

We can conclude that Afriplex GRT Extract improved overall mitochondrial function and the obesity profile, but conversely had a negative effect on the insulin signalling pathway intermediates. There were also no detrimental effects observed with the dosage of Afriplex GRT Extract used.

CHAPTER 5: Limitations and Future Research

- The small n-value from the first cohort of rats that were used in Western Blots was a big limitation.
- Another limitation would be that we did not send a sample of our high fat diet away for diet composition analyses.
- Future research could look in to the p62 accumulation by blocking the autophagosome to autophagolysosome flux by using chloroquine. Furthermore, the apoptotic proteins BCl2 and Bax should be analysed.
- ULK1 expression determination might have answered and confirmed the increased autophagy and mitophagy seen in Afriplex GRT Extract treated animals (with regards to the LC3-II levels).
- It would be interesting to analyse the ETC complex proteins in both their expression levels as well as their activity. This can be done using specific antibodies to determine expression levels as well as different inhibitors of the complex I to complex V proteins to determine their individual contribution to ATP production.
- In addition, the actual ATP that was produced by state 3 respiration may be determined by isolating the residual ADP and the ATP formed to determine the levels by HPLC methods.

CHAPTER 6: Appendices

Appendix A – The Methods by which the calculations of the Western blots were performed.

Gel (used for GLUT4 expression):

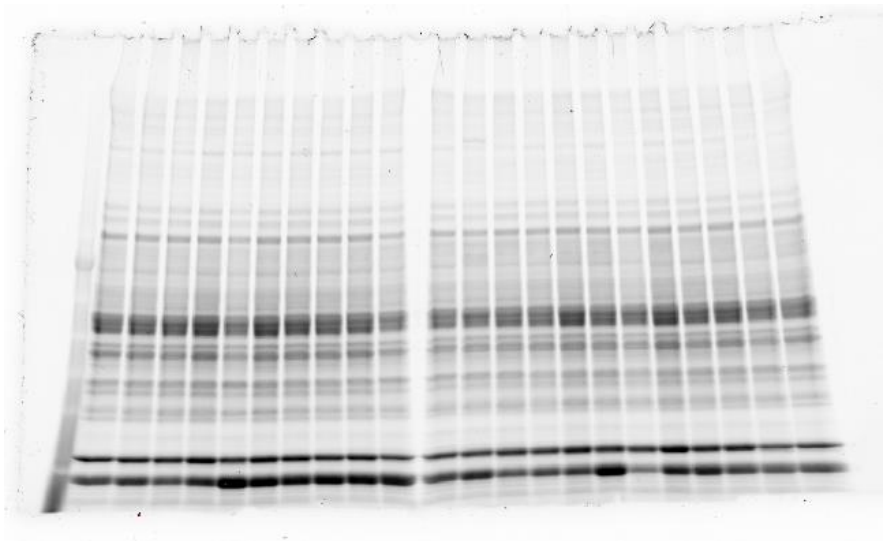

Membrane (used for GLUT4 expression):

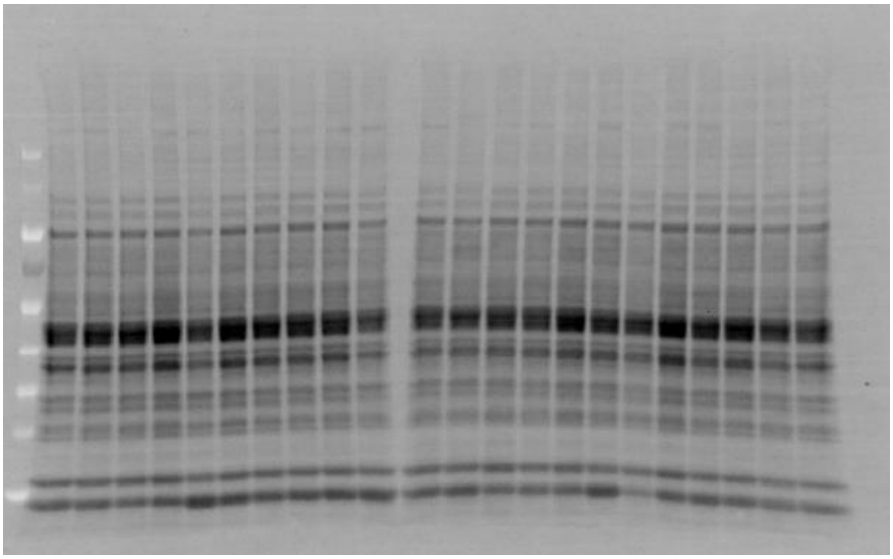

Blot (used for GLUT4 expression):

BioRad ChemiDoc™ ImageLab 5.0 series software used to analyse blots:

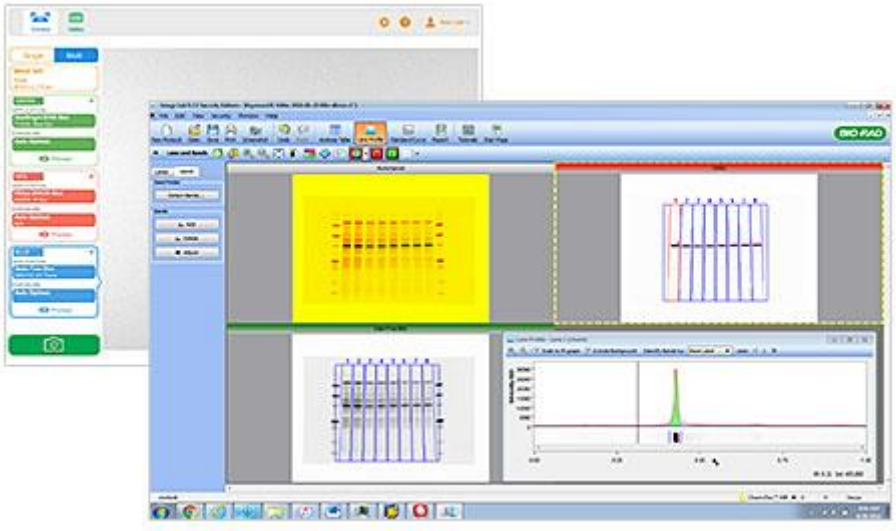

(BioRad, 2017)

Appendix B – Certificate of Analysis of Afriplex GRT Extract

Afriplex PHARMACEUTICALS

CERTIFICATE OF ANALYSIS

Product Name: Afriplex GRT Extract
Product Code: CPE--03287
Product Batch Number: 730330
Product Manufacturing date: September 2015
Product Expiry Date: August 2017

CHARACTERISTIC	SPECIFICATION	RESULTS
Analytical parameters		
Definition	Needle-like leaves and fine stems	Conforms
Characteristics	Reddish brown fine powder. Aroma is typical to Rooibos	Conforms
Appearance	Appearance complies	Conforms
Identification (FT-IR)	≥ 95.00 %	First Reference
Loss on Drying	≤ 5.0 % (m/m)	2.2 % (m/m)
Bulk Density	0.20 - 0.45 g/ ml	0.32 g/ ml
Extract Yield	> 15 % (g/ 100g)	16.84 %
Soluble Solids content	> 2 % (g/ 100g)	2.12 %
Aspalathin Content	> 15 % (g/ 100g)	12.36 %
Pesticides	Meets Ph. Eur. requirements	Conforms
Heavy Metal parameters		
Heavy Metals	≤ 10 ppm	Conforms
Cadmium	≤ 1.0 ppm	< 0.01 ppm
Lead	≤ 3.0 ppm	0.07 ppm
Mercury	≤ 0.1 ppm	0.02 ppm
Arsenic	≤ 1.0 ppm	0.09 ppm
Microbial parameters		
Total aerobic count	< 2 000 cfu/ g	65 cfu/ g
Total combined yeast and mould count	< 100 cfu/ g	No growth
Escherichia coli	Absent/ g	No growth
Coliforms	Absent/ g	No growth
Salmonella	Absent/ 25 g	Absent

STORAGE REQUIREMENTS
Store in a cool dry place protected from temperature extremes and direct light.

PAARL, 23 September 2015

Quality Control Department

Appendix C – Turnitin Report

Please note that the whole thesis was submitted, excluding the Appendices and References.

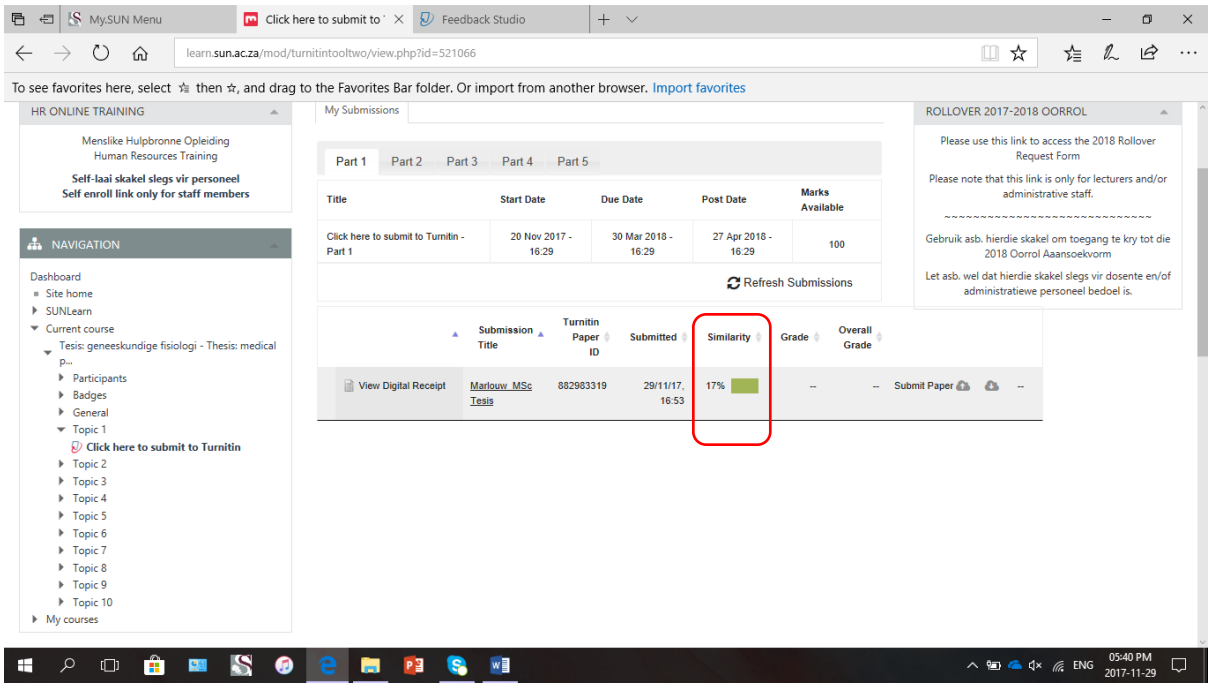

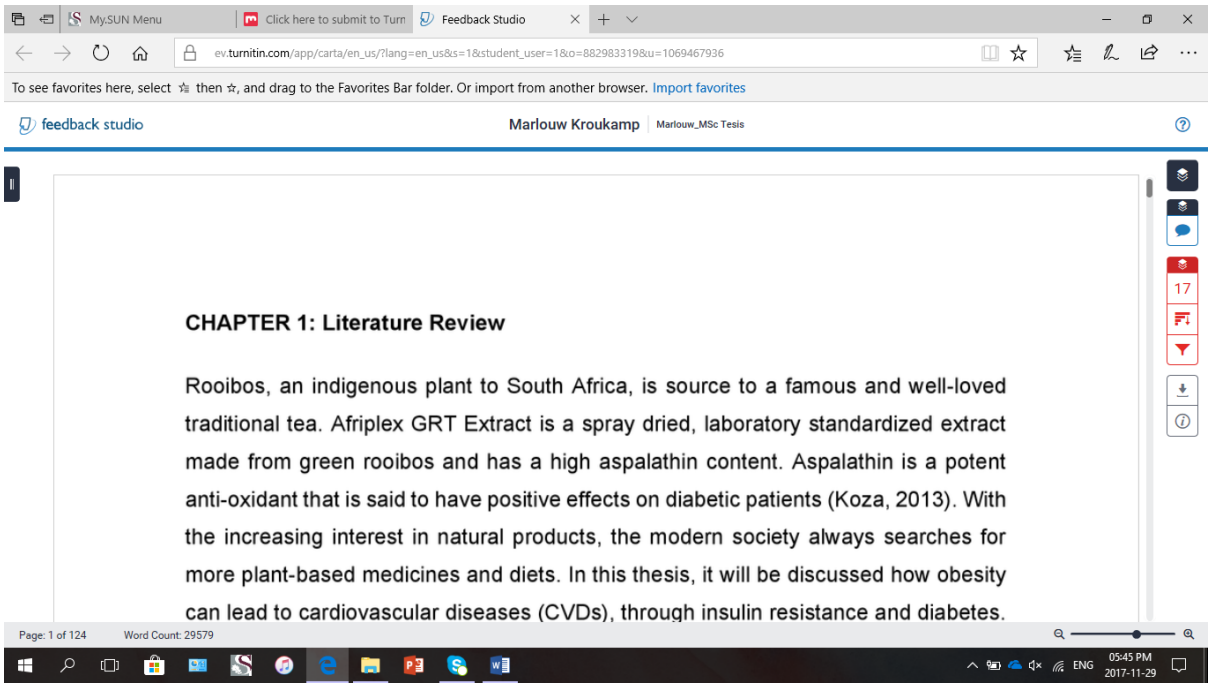

CHAPTER 7: References

Accili, D. & Arden, K. C., 2004. FoxOs at the Crossroads of Cellular Metabolism, Differentiation, and Transformation. Cell, Volume 117, pp. 421-426.

Acheson, K. J. et al., 1988. Glycogen storage capacity and de novo lipogenesis during massive carbohydrate overfeeding in man. The American Society for Clinical Nutrition, 48(2), pp. 240-247.

Adrian, G. S., McCammon, M. T., Montgomery, D. L. & Douglas, M. G., 1986. Sequences required for delivery and localization of the ADP/ATP translocator to the mitochondrial inner membrane. Molecular Cell Biology, 6(2), pp. 626-634.

Ahn, J. et al., 2008. The anti-obesity effect of quercetin is mediated by the AMPK and MAPK signaling pathways. Biochemical and Biophysical Research Communications, 373(4), pp. 545-549

Akira, S., Taga, T. & Kishimoto, T., 1993. Interleukin-6 in biology and medicine. Advances in Immunology, Volume 54, pp. 1-78.

Alberts, B. et al., 2002. Molecular Biology of the Cell. 4th ed. New York: Garland Science. The Mitochondrion. Available from: https://www.ncbi.nlm.nih.gov/books/NBK26894/.

American Diabetes Association, 2006. Standards of medical care in diabetes--2006. Diabetes Care, Volume 29, pp. Suppl 1:S4-42.

American Heart Association, 2015. Cardiovascular Disease & Diabetes. [Online] Available at: http://www.heart.org/HEARTORG/Conditions/Diabetes/WhyDiabetesMatters/Cardiovascular-Disease-Diabetes_UCM_313865_Article.jsp/#.Vr2c-I9OJMs [Accessed 12 February 2016].

Arita, Y. et al., 1999. Paradoxical decrease of an adipose-specific protein, adiponectin, in obesity. Biochemical and Biophysical Research Communications, Volume 257, pp. 79-83.

Aronoff, S. L., Berkowitz, K., Shreiner, B. & Want, L., 2004. Glucose Metabolism and Regulation: Beyond Insulin and Glucagon. Diabetes Spectrum, 17(3), pp. 183 - 190.

Ashrafi, K., 2007. Obesity and the regulation of fat metabolism. WormBook, ed. The C. elegans Research Community, 9 March.Volume doi/10.1895/wormbook.1.130.1, http://www.wormbook.org.

Ashwell, M., Mayhew, L., Richardson, J. & Rickayzen, B., 2014. Waist-to-Height Ratio Is More Predictive of Years of Life Lost than Body Mass Index. PLoS One, 9(9), p. e10348.

Aulston, B. D., Odero, G. L., Aboud, Z. & Glazner, G. W., 2013. Alzheimer's Disease and Diabetes. [Online] Available at: http://www.intechopen.com/books/understanding-alzheimer-s-disease/alzheimer-s-disease-and-diabetes [Accessed 4 March 2016].

Bacha, T. E., Luz, M. & Da Poian, A., 2010. Dynamic Adaptation of Nutrient Utilization in Humans. Nature Education, 3(9), p. 8.

Bae, S. H. et al., 2013. Sestrins activate Nrf2 by promoting p62-dependent autophagic degradation of Keap1 and prevent oxidative liver damage. Cell Metabolism, 17 (doi:10.1016/j.cmet.2012.12.002), pp. 73-84.

Balance Me Beautiful, 2017. The Beautiful Relationship Between Rooibos Tea and Weight Loss. [Online] Available at: http://www.balancemebeautiful.com/rooibos-tea-for-weight-loss/ [Accessed 8 11 2017].

Balarini, C. M. & Braga, V. A., 2016. Editorial: New Translational Insights on Metabolic Syndrome: Obesity, Hypertension, Diabetes and Beyond. Frontiers in Physiology, Volume 7, p. 229.

Basso, E., Fante, L., Fowlkes, J., Petronilli, V., Forte, M. A., & Bernardi, P. (2005). Properties of the permeability transition pore in mitochondria devoid of cyclophilin D. Journal of Biological Chemistry, 280, 18558-18561.

Bauer, T. A., Reusch, J. E., Levi, M. & Regensteiner, J. G., 2007. Skeletal muscle deoxygenation after the onset of moderate exercise suggests slowed microvascular blood flow kinetics in type 2 diabetes. Diabetes Care, Volume 30, pp. 2880-2885.

Baumann, C. A. et al., 2000. CAP defines a second signalling pathway required for insulin-stimulated glucose transport. PubMed, 407(6801), pp. 202-207.

Beelders, T. et al., 2012. Comprehensive two-dimensional liquid chromatographic analysis of rooibos (Aspalathus linearis) phenolics. Journal of Seperation Science, 35(14), pp. 1808-1820.

Behrends, C. & Fulda, S., 2012. Receptor Proteins in Selective Autophagy. International Journal of Cell Biology, Volume 2012, pp. 1-9.

Bell, D. S., 2003. β-Cell rejuvenation with thiazolidinediones. The American Journal of Medicine, Volume 2003, pp. 35-44.

Berg, J. M., Tymoczko, J. L. & Stryer, L., 2002. Biochemistry. 5 ed. New York: W. H. Freeman & Company.

Beutner, G., Rück, A., Riede, B., & Brdiczka, D. (1998). Complexes between porin, hexokinase, mitochondrial creatine kinase and adenylate translocator display properties of the permeability transition pore. Implication for regulation of permeability transition by the kinases. Biochimica et Biophysica Acta, 1368, 7-18.

Bevan, P., 2009. Insulin Signalling. Journal of Cell Science, 114(8), pp. 1429-1430.

Bezuidenhout, G., 2007. Green rooibos tea gains market popularity. [Online] Available at:http://www.engineeringnews.co.za/article/green-rooibos-tea-gains-market-popularity-2007-08-10 [Accessed 10 November 2016].

BioRad, 2017. Image Lab™ Software. [Online] Available at: http://www.bio-rad.com/en-ch/product/image-lab-software [Accessed 28 11 2017].

Bonen, A. et al., 2004. Regulation of fatty acid transport by fatty acid translocase/CD36. Proceedings of the Nutrition Society, 2004(63), pp. 245-249.

Bonen, A. & McDermott, M. H., 1990. Glycogenesis and glyconeogenesis in skeletal muscle: effects of pH and hormones. American Journal of Physiology - Endocrinology and Metabolism, 258(4), pp. E693-E700.

Boucher, J., Kleinridders, A. & Kahn, C. R., 2014. Insulin Receptor Signaling in Normal and Insulin-Resistant States. Cold Spring Harbor Perspectives Biology, 6(1), p. a009191.

Boundless, 2016. ATP and Muscle Contraction. [Online] Available at: https://www.boundless.com/biology/textbooks/boundless-biology-textbook/the-musculoskeletal-system-38/muscle-contraction-and-locomotion-218/atp-and-muscle-contraction-826-12069/ [Accessed 10 August 2017].

Bournat, J. C. & Brown, C. W., 2010. Mitochondrial Dysfunction in Obesity. Current Opinion in Endocrinology, Diabetes and Obesit., 17(5), p. 446–452.

Bradford, M. M., 1976. A rapid and sensitive method for the quantitation of microgram quantities of protein utilizing the principle of protein-dye binding. Analytical Biochemistry, 72(1-2), pp. 248-254.

Brand, M. D. & Nicholls, D. G., 2011. Assessing mitochondrial dysfunction in cells. Biochemical Journal, Volume 435, pp. 297-312.

Bredenkamp, A., 2006. Remarkable Rooibos Tea: The Red Tea from South Africa. [Online] Available at: http://www.newlands.ca/about%20Rooibos.htm [Accessed 8 11 2017].

Brennan, A. M. & Mantzoros, C. S., 2006. Drug Insight: the role of leptin in human physiology and pathophysiology—emerging clinical applications. Nature Clinical Practice Endocrinology & Metabolism, Volume 2, pp. 318-327.

Brochu-Gaudreau, K. et al., 2010. Adiponectin action from head to toe. Endocrinology, 2010(37), pp. 11-32.

Brownlee, M., 2001. Biochemistry and molecular cell biology of diabetic complications. Nature, Volume 414, pp. 813-820.

Brownlee, M., 2005. The pathobiology of diabetic complications: a unifying mechanism. Diabetes, Volume 54, pp. 1615-1625.

Brozinick Jr, J. T., Roberts, B. R. & Dohm, G. L., 2003. Defective signaling through Akt-2 and -3 but not Akt-1 in insulin-resistant human skeletal muscle: potential role in insulin resistance. Diabetes, Volume 52, pp. 935-941.

Budanov, A. V. & Karin, M., 2008. p53 target genes Sestrin1 and Sestrin2 connect genotoxic stress and mTOR signaling. Cell, Volume 134, pp. 451-460.

Budanov, A. V., Lee, J. H. & Karin, M., 2010. Stressin' Sestrins take an aging fight. EMBO Molecular Medicine, Volume 2, pp. 388-400.

Budanov, A. V. et al., 2004. Regeneration of peroxiredoxins by p53-regulated Sestrins, homologs of bacterial AphD. Science, 304(doi:10.1126/science.1095569), pp. 596-600.

Burkhoff, D. et al., 1991. G. Influence of metabolic substrate on rat heart function and metabolism at different coronary flows. American Journal of Physiology-Heart and Circulatory Physiology, Volume 261, p. H741–H750.

Burton, T. R. & Gibson, S. B., 2009. The role of Bcl-2 family member BNIP3 in cell death and disease: NIPping at the heels of cell death. Cell Death & Differentiation, 16(4), pp. 515-523.

Calleja, V. et al., 2007. Intramolecular and intermolecular interactions of protein kinase B define its activation in vivo. Public Library of Science Biology, 5(4), p. 95.

Carnethon, M. R. et al., 2012. Association of Weight Status with Mortality in Adults With Incident Diabetes. JAMA, 308(6), pp. 581-590.

Carr, M. E., 2001. Diabetes: a hypercoagulable state. Journal of Diabetes and its Complications, Volume 15, pp. 44-54.

Cefalu, W. T., 2001. Insulin resistance: cellular and clinical concepts. Experimental Biology and Medicine (Maywood), 226(1), pp. 13-26.

Cefalu, W. T., 2006. Animal models of type 2 diabetes: Clinical presentation and pathophysiological relevance to the human condition. ILAR Journal, Volume 47, pp. 186-198.

Celermejer, D., 1997. Endothelial dysfunction: does it matter? Journal of the American College of Cardiology, Volume 30, pp. 325-333.

Cell Signaling Technology, 2016. Insulin Receptor Signaling Pathway. [Online] Available at: http://www.cellsignal.com/contents/science-pathway-research-cellular-metabolism/insulin-receptor-signaling-pathway/pathways-irs [Accessed 8 March 2016].

Cell Signaling Technology, 2016. PI3K / Akt Signaling Pathway. [Online] Available at: http://www.cellsignal.com/contents/science-pathway-research-pi3k-akt-signaling-resources/pi3k-akt-signaling-pathway/pathways-akt-signaling [Accessed 8 March 2016].

Center for Young Women's Health, 2016. PCOS: Preparing for Your Oral Glucose Tolerance Test. [Online] Available at: http://youngwomenshealth.org/2014/02/25/oral-glucose-tolerance-test/ [Accessed 15 3 2017].

Chakraborty, A. et al., 2010. Inositol pyrophosphates inhibit Akt signaling, thereby regulating insulin sensitivity and weight gain. Cell, 143(6), pp. 897-910.

Chan, A. C., 1998. Vitamin E and atherosclerosis. J Nutr 128:1593–1596, 1998. Journal of Nutrition, Volume 128, pp. 1593-1596.

Chance, B. & Williams, G. R., 1955. Respiratory Enzymes in Oxidative Phosphorylation: I. Kinetics of Oxygen Utilization. Journal of Biological Chemistry, Volume 217, pp. 383-393.

Chan, D. C., 2006. Mitochondria: dynamic organelles in disease, aging, and development. Cell, 125(7), pp. 1241-1252.

Chandrasekera, P. C. & Pippin, J. J., 2013. Of Rodents and Men: Species-Specific Glucose Regulation and Type 2 Diabetes Research. Altex, 31(2), pp. 157-176.

Chatterjee, S. & Davies, M. J., 2015. Current management of diabetes mellitus and future directions in care. The BMJ, Volume 91, pp. 612-621.

Chatzigeorgiou, A., Halapas, A., Kalafatakis, K. & Kamper, E., 2009. The use of animal models in the study of diabetes mellitus. In Vivo, Volume 23, pp. 245-258.

Chen, Y. & Dorn, G. W., 2013. PINK1-phosphorylated mitofusin 2 is a Parkin receptor for culling damaged mitochondria. Science, 340(6131), pp. 471-475.

Chiara, F., Castellaro, D., Marin, O., Petronilli, V., Brusilow, W. S., Juhaszova, M., . . . Rasola, A. (2008). Hexokinase II detachment from mitochondria triggers apoptosis through the

permeability transition pore independent of voltage-dependent anion channels. PLoS ONE, 3, e1852.

Chipuk, J. E., 2008. How do BCL-2 proteins induce mitochondrial outer membrane permeabilization? Trends in Cell Biology, 18(4), pp. 157-164.

Chung, K. F. & Barnes, P. J., 1999. Cytokines in asthma. Thorax, Volume 54, pp. 825-857.

Clarke, S. J., McStay, G. P. & Halestrap, A. P., 2002. Sanglifehrin A acts as a potent inhibitor of the mitochondrial permeability transition and reperfusion injury of the heart by binding to cyclophilin-D at a different site from cyclosporin A. Journal of Biological Chemistry, 277(38), pp. 34793-34799.

Cole, M. A. et al., 2011. A high fat diet increases mitochondrial fatty acid oxidation and uncoupling to decrease efficiency in rat heart. Basic Research in Cardiology, 106(3), pp. 447-457.

Cong, L. N. et al., 1997. Physiological role of Akt in insulin-stimulated translocation of GLUT4 in transfected rat adipose cells. Molecular Endocrinology, 11(13), pp. 1881-90.

Considine, R. V. et al., 1996. Serum immunoreactive-leptin concentrations in normal-weight and obese humans. The New England Journal of Medicine, 334(5), p. 292–295.

Consoli, A. & Formoso, G., 2013. Do thiazolidinediones still have a role in treatment of type 2 diabetes mellitus? Diabetes, Obesity and Metabolism, Volume 15, pp. 967-977.

Cory, S. & Adams, J. M., 2002. The Bcl2 family: regulators of the cellular life-or-death switch. Nature Reviews Cancer, Volume 2, pp. 647-656.

Crompton, M., Ellinger, H. & Costi, A., 1988. Inhibition by cyclosporin A of a Ca2+-dependent pore in heart mitochondria activated by inorganic phosphate and oxidative stress. Biochemical Journal, 255(1), pp. 357-360.

Cross, D. A. et al., 1995. Inhibition of glycogen synthase kinase-3 by insulin mediated by protein kinase B. Nature, 378(6559), pp. 785-789.

Cunningham, A. B., 1993. African Medicinal Plants: Setting priorities at the interface between conservation and primary health care. People and Plants Working Paper, p. 25.

Cuyàs, E., Corominas-Faja, B., Joven, J. & Menendez, J. A., 2014. Cell cycle regulation by the nutrient-sensing mammalian target of rapamycin (mTOR) pathway. Methods in Molecular Biology, Volume 1170, pp. 113-114.

Deacon, C. F., Mannucci, E. & Ahrén, B., 2012. Glycaemic efficacy of glucagon-like peptide-1 receptor agonists and dipeptidyl peptidase-4 inhibitors as add-on therapy to metformin in subjects with type 2 diabetes-a review and meta analysis. Diabetes, Obesity and Metabolism, Volume 14, pp. 762-767.

Deepa, S. S. & Dong, L. Q., 2009. APPL1: role in adiponectin signaling and beyond. American Journal of Physiology. Endocrinology and Metabolism, 296(1), pp. 22-36.

Defronzo, R. A., 2009. Banting lecture. from the triumvirate to the ominous octet: a new paradigm for the treatment of type 2 diabetes mellitus. Diabetes, Volume 58, pp. 773-795.

Department of Health and Human Services USA, n.d. Body Mass Index: Considerations for Practitioners. [Online] Available at: https://www.cdc.gov/obesity/downloads/BMIforPactitioners.pdf [Accessed 20 February 2017].

Depre, C., Vanoverschelde, J. L. & Taegtmeyer, H., 1999. Glucose for the heart. Circulation, 99(4), pp. 578-588.

Desvergne, B. & Wahli, W., 1999. Peroxisome proliferator-activated receptors: nuclear control of metabolism. Endocrine Reviews, 20(5), pp. 649-688.

Dludla, P. V. et al., 2013. The cardioprotective effect of an aqueous extract of fermented rooibos (Aspalathus linearis) on cultured cardiomyocytes derived from diabetic rats. Phytomedicine, 21(5), pp. 595-601.

Dludla, P. V. et al., 2017. Hyperglycemia-induced oxidative stress and heart disease-cardioprotective effects of rooibos flavonoids and phenylpyruvic acid-2-O-β-D-glucoside. Nutrition & Metabolism, 14(45), pp. 1-18.

Dokken, B. B., 2008. The Pathophysiology of Cardiovascular Disease and Diabetes: Beyond Blood Pressure and Lipids. Diabetes Spectrum, 21(3), pp. 160-165.

Dong, B. et al., 2017. Sestrin 2 attenuates neonatal rat cardiomyocyte hypertrophy induced by phenylephrine via inhibiting ERK1/2. Molecular and Cellular Biochemistry, Volume 433, pp. 113-123.

Duell, P. B., Oram, J. F. & Bierman, E. L., 1991. Nonenzymatic glycosylation of HDL and impaired HDL-receptor-mediated cholesterol efflux. Diabetes, Volume 40, pp. 377-348.

Duke, T. A., 1999. Molecular model of muscle contraction. Proceedings of the National Academy of Sciences of the United States of America, 96(6), p. 2770–2775.

Eder, K., Baffy, N., Falus, A. & Fulop, A. K., 2009. The major inflammatory mediator interleukin-6 and obesity. Inflammation Research, Volume 58, pp. 727-736.

Egan, D. F. et al., 2011. Phosphorylation of ULK1 (hATG1) by AMP-activated protein kinase connects energy sensing to mitophagy. Science, 331(6016), pp. 456-461.

Eskelinen, E., 2005. Maturation of Autophagic Vacuoles in Mammalian Cells. Autophagy, 1(1), pp. 1-10.

Ethicon, 2016. Obesity, the Metabolic Disease. [Online] Available at: http://www.ethicon.com/healthcare-professionals/specialties/obesity/obesity-overview [Accessed 29 February 2016].

Evans, R. M., Barish, G. D. & Wang, Y. X., 2004. PPARs and the complex journey to obesity. Nature Medicine, 10(4), pp. 355-361.

Ewing, D. J., Campbell, D. & Clarke, B. F., 1980. The natural history of diabetic autonomic neuropathy. QJM: An International Journal of Medicine, Volume 49, p. 95–108.

Exton, J. H. & Park, C. R., 1968. Control of Gluconeogenesis in Liver II. Effects of glucagon, catecholamines, and adenosine 3',5'-monophosphate on gluconeogenesis in the perfused rat liver. Journal of Biological Chemistry, Volume 243, pp. 4189-4196.

Fagot-Campagna, A. et al., 2000. Prevalence of lipid abnormalities, awareness, and treatment in US adults with diabetes [Abstract]. Diabetes, 49(Suppl. 1), p. A78.

Feng, Y. & Klionsky, D. J., 2017. Autophagic membrane delivery through ATG9. Cell Research, Volume 27, pp. 161-162.

Festa, A. et al., 2000. Chronic subclinical inflammation as part of the insulin resistance syndrome. Circulation, Volume 102, pp. 42-47.

Fink, S. L. & Cookson, B. T., 2005. Apoptosis, Pyroptosis, and Necrosis: Mechanistic Description of Dead and Dying Eukaryotic Cells. Infection & Immunity, 73(4), pp. 1907-1916.

Formiguera, X. & Cantón, A., 2004. Obesity: Epidemiology and Clinical Aspects. Best Practice & Research Clinical Gastroenterology, 18(6), pp. 1125-1146.

Franconi, F. et al., 2008. Are the available experimental models of type 2 diabetes appropriate for a gender perspective? Pharmacological Research, Volume 57, pp. 6-18.

Freireich, E. J. et al., 1966. Quantitative comparison of toxicity of anticancer agents in mouse, rat, hamster, dog, monkey, and man. Cancer Chemotherapy Reports, 50(4), pp. 219-244.

Friedman, J. M. & Halaas, J. L., 1998. Leptin and the regulation of body weight in mammals. Nature, Volume 395, pp. 763-770.

Fulda, S. & Debatin, K. M., 2006. Review Article: Extrinsic versus intrinsic apoptosis pathways in anticancer chemotherapy. Oncogene, Volume 25, pp. 4798-4811.

Fulda, S., Gorman, A. M., Hori, O. & Samali, A., 2010. Review Article: Cellular Stress Responses: Cell Survival and Cell Death. International Journal of Cell Biology, pp. 1-Gambino, et al., 201123.

Galluzzi, L. & Kroemer, G., 2013. Common and divergent functions of Beclin 1 and Beclin 2. Cell Research, 2013(23), pp. 1341-1342.

Gambino, R., Musso, G. & Cassader, M., 2011. Redox Balance In The Pathogenesis Of Non-Alcoholic Fatty Liver Disease: Mechanisms And Therapeutic Opportunities. Antioxidants and Redox Signaling, 15(5), pp. 1325-1365.

Gao, M., Ma, Y. & Liu, D., 2015. High-Fat Diet-Induced Adiposity, Adipose Inflammation, Hepatic Steatosis and Hyperinsulinemia in Outbred CD-1 Mice. PLoS One, 10(3), p. e0119784.

Gargani, Y. et al., 2012. Metabolism of Red Blood Cells. In: D. Horton-Szar, ed. 4th Edition Crash Course: Haematology and Immunology. Manchester, UK: Mosby Elsevier, p. 18.

Garvey, W. T. et al., 1991. Pretranslational suppression of a glucose transporter protein causes insulin resistance in adipocytes from patients with non-insulin-dependent diabetes mellitus and obesity. Journal of Clinical Investigation, Volume 87, pp. 1072-1081.

Glick, D. et al., 2012. BNip3 Regulates Mitochondrial Function and Lipid Metabolism in the Liver. Molecular and Cellular Biology, 32(13), p. 2570–2584.

Golding, S. E. et al., 2009. Improved ATM kinase inhibitor KU-60019 radiosensitizes glioma cells, compromises insulin, AKT and ERK prosurvival signaling, and inhibits migration and invasion. Molecular Cancer Therapy, 8(10), pp. 2894-2902.

González-Barroso, M. M. et al., 2012. Fatty acids revert the inhibition of respiration caused by the antidiabetic drug metformin to facilitate their mitochondrial β-oxidation. Biochimica et Biophysica Acta, Volume 1817, pp. 1768-1775.

Goyal, A., Kameswara, R. & Zonszein, J., 2014. Is There a Paradox in Obesity? Cardiology in Review, 22(4), pp. 163-170.

Gu, K., Cowie, C. C. & Harris, M. L., 1998. Mortality in adults with and without diabetes in a national cohort of the US population. Diabetes Care, Volume 21, p. 1971–1993.

Gurib-Fakim, A., Brendler, T., Philips, L. D. & Eloff, J. N., 2010. Green Gold: Success Stories Using Southern African Plant Species. s.l.:AAMPS Publishing.

Gutierrez, C. & Blanchard, D. G., 2004. Diastolic heart failure: challenges of diagnosis and treatment. American Family Physician, Volume 69, pp. 2609-2616.

Halaby, M. J., Hibma, J. C., He, J. & Yang, D. Q., 2008. ATM protein kinase mediates full activation of Akt and regulates glucose transporter 4 translocation by insulin in muscle cells. Cell Signalling, 20(8), pp. 1555-1563.

Halestrap, A. P., 2009. What is the mitochondrial permeability transition pore? Journal of Molecular and Cellular Cardiology, 46(6), pp. 821-831.

Halestrap, A. P. & Richardson, A. P., 2015. The mitochondrial permeability transition: a current perspective on its identity and role in ischaemia/reperfusion injury. Journal of Molecular and Cellular Cardiology, Volume 78, pp. 129-141.

Hamacher-Brady, A., 2012. Autophagy Regulation and Integration with Cell Signalling. Antioxidants & Redox Signaling, 17(5), pp. 756-765.

Hansatech Instruments, 2017. Oxygraph Plus System. [Online] Available at: http://www.hansatech-instruments.com/products/introduction-to-oxygen-measurements/complete-systems/2079-2/ [Accessed 3 10 2017].

Hara, K. et al., 2002. A genetic variation in the PGC-1 gene could confer insulin resistance and susceptibility to Type II diabetes. Diabetologia, Volume 45, p. 740–743.

Hardin, J., Bertoni, G. P. & Kleinsmith, L. J., 2015. Becker's World of the Cell. 9 ed. United Kingdom: Benjamin Cummings.

Hariri, N. & Thibault, L., 2010. High-fat diet-induced obesity in animal models. Nutrition Research Reviews, Volume 23, pp. 270-299.

Hashimoto, T., Hussien, R. & Brooks, G. A., 2006. Colocalization of MCT1, CD147, and LDH in mitochondrial inner membrane of L6 muscle cells: evidence of a mitochondrial lactate oxidation complex. American Journal of Physiology-Endocrinology and Metabolism, 290(6), p. E1237–E1244.

Hawley, S. A. et al., 2014. Phosphorylation by Akt within the ST loop of AMPK-alpha1 downregulates its activation in tumour cells. Biochemical Journal, Volume 459, pp. 275-287.

Hayden, M. R., Sowers, J. R. & Tyagi, S. C., 2005. The central role of vascular extracellular matrix and basement membrane remodeling in metabolic syndrome and type 2 diabetes: the matrix preloaded. Cardiovascular Diabetology, Volume 4, pp. 9-29.

Hebebrand, J. et al., 2017. A Proposal of the European Association for the Study of Obesity to Improve the ICD-11 Diagnostic Criteria for Obesity Based on the Three Dimensions Etiology, Degree of Adiposity and Health Risk. Obesity Facts, 10(4), pp. 284-307.

Hemmings, B. A. & Restuccia, D. F., 2012. PI3K-PKB/Akt Pathway. Cold Spring Harbor Laboratory Press, p. doi: 10.1101/cshperspect.a011189.

Hengartner, M. O., 2000. Review Article: The biochemistry of apoptosis. Nature, Volume 407, pp. 770-776.

Hers, H. G., 1976. The control of glycogen metabolism in the liver. Annual Review of Biochemistry, Volume 45, pp. 167-189.

Hers, I., Vincent, E. E. & Tavaré, J. M., 2011. Akt signalling in health and disease. Cellular Signalling, 23(10), pp. 1515-27.

Himpe, E. et al., 2016. Phenylpropenoic Acid Glucoside from Rooibos Protects Pancreatic Beta Cells against Cell Death Induced by Acute Injury. PLoS One, 11(6), p. e0157604.

Holloszy, J. O., Oscai, L. B. & Mole, P. A., 1970. Mitochondrial citric acid cycle and relative enzymes: adaptive response to exercise. Biomedical and Biophysical Research Communications, 40(6), pp. 1368-1373.

Holloway, G. P. et al., 2010. Fatty acid transport in skeletal muscle: role in energy provision and insulin resistance. Clinical Lipidology, 5(5), pp. 731-745.

Hoon, J., Do, H. J., Kim, O. Y. & Shin, M. J., 2013. Antiobesity effects of quercetin-rich onion peel extract on the differentiation of 3T3-L1 preadipocytes and the adipogenesis in high fat-fed rats. Food and Chemical Toxicology: An International Journal Published for the British Industrial Biological Research Association, Volume 58, p. 347–354.

Hoshiyama, M. et al., 2003. Effect of high glucose on nitric oxide production and endothelial nitric oxide synthase protein expression in human glomerular endothelial cells. Nephron. Experimental Nephrology, 95(2), pp. 62-68.

Høyer-Hansen, M. et al., 2007. Control of Macroautophagy by Calcium, Calmodulin-Dependent Kinase Kinase-b, and Bcl-2. Molecular Cell, Volume 25, p. 193–205.

Hu, E., Liang, P. & Spiegelman, B. M., 1996. AdipoQ is a novel adipose-specific gene dysregulated in obesity. Journal of Biological Chemistry, 271(18), pp. 10697-10703.

Hu, F., 2008. Measurements of Adiposity and Body Composition. In: Obesity Epidemiology. New York City: Oxford University Press, pp. 53-83.

Huisamen, B., George, C. & Dietrich, D., 2013. Cardioprotective and anti-hypertensive effects of Prosopis glandulosa in rat models of pre-diabetes. Cardiovascular Journal of Africa, 24(2), pp. 10-16.

Hunt, S. A. et al., 2001. ACC/AHA Guidelines for the evaluation and management of chronic heart failure in the adult: executive summary. Circulation, Volume 104, pp. 2996-3007.

Ichim, G. & Tait, S. W., 2016. A fate worse than death: apoptosis as an oncogenic process. Nature Reviews Cancer, Volume 16, pp. 539-548.

Itakura, E., Kishi, C., Inoue, K. & Mizushima, N., 2008. Beclin 1 forms two distinct phosphatidylinositol 3-kinase complexes with mammalian Atg14 and UVRAG. Molecular Biology of the Cell, 19(12), pp. 5360-5372.

Jeon, S., 2016. Regulation and function of AMPK in physiology and diseases. Experimental & Molecular Medicine, Volume 48, p. oi:10.1038/emm.2016.81.

Jin, S. M. et al., 2010. Mitochondrial membrane potential regulates PINK1 import and proteolytic destabilization by PARL. Journal of Cell Biology, 191(5), pp. 933-942.

Johnson, J. A., 2015. The safety of sulfonylurea therapy in type 2 diabetes: have we reached the practical limits of our evidence base? Diabetologia, Volume 58, pp. 1-3.

Joubert, E. & De Beer, D., 2007. Rooibos (Aspalathus linearis) beyond the farm gate: from herbal tea to potential phytopharmaceutical. South African Journal of Botany, 77(4), pp. 869-886.

Joubert, E. & Schulz, H., 2006. Production and quality aspects of rooibos tea and related products. Journal of Applied Botany and Food Quality, 80(2), pp. 138-144.

Jung, C. H. et al., 2009. ULK-Atg13-FIP200 Complexes Mediate mTOR Signaling to the Autophagy Machinery. Molecular Biology of the Cell, 20(7), pp. 1992-2003.

Kahn, B. B. & Pedersen, O., 1993. Suppression of GLUT4 expression in skeletal muscle of rats that are obese from high fat feeding but not from high carbohydrate feeding or genetic obesity. Endocrinology, 132(1), pp. 13-22.

Kamakura, R. et al., 2015. Antidiabetic effect of green rooibos (Aspalathus linearis) extract in cultured cells and type 2 diabetic model KK-Ay mice. Cytotechnology, 67(4), pp. 699-710.

Kang, R., Zeh, H. J., Lotze, M. T. & Tang, D., 2011. The Beclin 1 network regulates autophagy and apoptosis. Cell Death & Differentiation, 18(4), pp. 571-580.

Kaplan, J. R. & Wagner, J. D., 2006. Type 2 diabetes-an introduction to the development and use of animal models. ILAR Journal, Volume 47, pp. 181-185.

Karunakaran, U. & Jeoung, N. H., 2010. O-GlcNAc Modification: Friend or Foe in Diabetic Cardiovascular Disease. Korean Diabetes Journal, 34(4), pp. 211-219.

Katayama, M., Kawaguchi, T., Berger, M. S. & Pieper, R. O., 2007. DNA damaging agent-induced autophagy produces a cytoprotective adenosine triphosphate surge in malignant glioma cells. Cell Death and Differentiation, 14(3), pp. 548-558.

Kawaguchi, M. et al., 1997. A comparison of ultrastructural changes on endomyocardial biopsy specimens obtained from patients with diabetes mellitus with and without hypertension. Heart & Vessels, Volume 12, pp. 267-274.

Kawano, A. et al., 2009. Hypoglycemic effect of aspalathin, a rooibos tea component from Aspalathus linearis, in type 2 diabetic model db/db mice. Phytomedicine, 16(5), pp. 437-443.

Kim, J., Kundu, M., Viollet, B. & Guan, K., 2011. AMPK and mTOR regulate autophagy through direct phosphorylation of Ulk1. Nature Cell Biology, Volume 13, pp. 132-141.

Kim, J. H. et al., 2005. Peroxisome proliferator-activated receptor gamma coactivator 1 alpha promoter polymorphisms are associated with early-onset type 2 diabetes mellitus in the Korean population. Diabetologia, 48(7), pp. 1323-1330.

Kirkin, V., Lamark, T., Johansen, T. & Dikic, I., 2009. NBR1 cooperates with p62 in selective autophagy of ubiquitinated targets. Autophagy, 5(5), pp. 732-733.

Kjekshus, J. K. & Mjos, O. D., 1972. Effect of free fatty acids on myocardial function and metabolism in the ischemic dog heart. Journal of Clinical Investigation, Volume 51, p. 1767–1776.

Klingenberg, M., 2008. The ADP and ATP transport in mitochondria and its carrier. Biochimica et Biophysica Acta (BBA) - Biomembranes, 1778(10), pp. 1978-2021.

Klionsky, D. J., Abdalla, F. C., Zuckerbraun, B. & et al., 2012. Guidelines for the use and interpretation of assays for monitoring autophagy. Autophagy, 8(4), pp. 445-544.

Klok, M. D., Jakobsdottir, S. & Dent, M. L., 2007. The role of leptin and ghrelin in the regulation of food intake and body weight in humans: a review. Obesity Reviews, 8(1), pp. 21-34.

Kobayashi, S., Xu, X., Chen, K. & Liang, Q., 2012. Suppression of autophagy is protective in high glucose-induced cardiomyocyte injury. Autophagy, 8(4), pp. 577-592.

Koh, K. K., Han, S. H. & Quon, M. J., 2005. Inflammatory markers and the metabolic syndrome [Abstract]. Journal of the American College of Cardiology, Volume 46, pp. 1978-1985.

Kolch, W., 2000. Meaningful relationships: the regulation of the Ras/Raf/MEK/ERK pathway by protein interactions. Biochemistry, Volume 351, p. 289–305.

Komatsu, M. et al., 2007. Homeostatic levels of p62 control cytoplasmic inclusion body formation in autophagy-deficient mice. Cell, 131(6), pp. 1149-1163.

Kopelman, P. G., 2000. Obesity as a medical problem. Nature, Volume 404, pp. 635-643.

Korvald, C., Elvenes, O. P. & Myrmel, T., 2000. Myocardial substrate metabolism influences left ventricular energetics in vivo. American Journal of Physiology-Heart and Circulatory Physiology, Volume 278, p. H1345–H1351.

Koza, L., 2013. Green rooibos takes fight to diabetes. Mail & Guardian, 11 October, p. 40.

Kruppa, A. J., Kendrick-Jones, J. & Buss, F., 2016. Myosins, Actin and Autophagy. Traffic., 17(8), pp. 878-890.

Kubli, D. A. et al., 2008. Bnip3 functions as a mitochondrial sensor of oxidative stress during myocardial ischemia and reperfusion. American Journal of Physiology-Heart and Circulatory Physiology, 295(5), pp. H2025-H2031.

Kuppusamy, U. R. & Das, N. P., 1992. Effects of flavonoids on cyclic AMP phosphodiesterase and lipid mobilization in rat adipocytes. Biochemical Pharmacology, 44(7), pp. 1307-1315.

Laemmli, U. K., 1970. Cleavage of Structural Proteins during the Assembly of the Head of Bacteriophage T4. Nature, 227(doi:10.1038/227680a0), pp. 680-685.

Lamb, C. A., Yoshimori, T. & Tooze, S. A., 2013. The autophagosome: origins unknown, biogenesis complex. Nature Reviews Molecular Cell Biology, 14(12), pp. 759-774.

Lastya, A., Saraswati, M. R. & Suastika, K., 2014. The low level of glucagon-like peptide-1 (GLP-1) is a risk factor of type 2 diabetes mellitus. BMC Research Notes, 7(849), pp. https://doi.org/10.1186/1756-0500-7-849.

Lavin, M. F. & Shiloh, Y., 1997. The genetic defect in ataxia-telangiectasia. Annual Review of Immunology, Volume 15, pp. 177-202.

Lazarou, M., 2015. Keeping the immune system in check: a role for mitophagy. Nature, 2015(93), pp. 3-10.

Lazarou, M., Jin, S. M., Kane, L. A. & Youle, R. J., 2012. Role of PINK1 binding to the TOM complex and alternate intracellular membranes in recruitment and activation of the E3 ligase Parkin. Developmental Cell, 22(2), pp. 320-333.

Lee, J. H., Budanov, A. V. & Karin, M., 2013. Sestrins orchestrate cellular metabolism to attenuate aging. Cell Metabolism, 18 (doi:10.1016/j.cmet.2013.08.018), pp. 792-801.

Lehman, J. J. et al., 2000. Peroxisome proliferator-activated receptor gamma coactivator-1 promotes cardiac mitochondrial biogenesis. Journal of Clinical Investigation, Volume 106, pp. 847-856.

Lesnefsky, E. J. et al., 2001. Mitochondrial dysfunction in cardiac disease: ischemia--reperfusion, aging, and heart failure. Journal of Molecular and Cellular Cardiology, 33(6), pp. 1065-1089.

Leto, D. & Saltiel, A. R., 2012. Regulation of glucose transport by insulin: traffic control of GLUT4. Nature Reviews Molecular Cell Biology, 13(doi:10.1038/nrm3351), pp. 383-396.

Leung, A. W., Varanyuwatana, P. & Halestrap, A. P., 2008. The mitochondrial phosphate carrier interacts with cyclophilin D and may play a key role in the permeability transition. Journal of Biological Chemistry, 283(39), pp. 26312-26323.

Lewis, D. H., 1998. The effect of trauma on the regulation of the microcirculation [Abstract].. Pathophysiology, 5(Suppl. 1), p. 191.

Liang, H. & Ward, W. F., 2006. PGC-1α: a key regulator of energy metabolism. Advances in Physiology Education, 30(4), pp. 145-151.

Liang, X. H. et al., 1998. Protection against fatal Sindbis virus encephalitis by beclin, a novel Bcl-2-interacting protein. Journal of Virology, Volume 72, pp. 8586-8596.

Li, L. & Wu, L. L., 2012. Adiponectin and interleukin-6 in inflammation-associated disease. Vitamins and Hormones, 2012(90), pp. 375-395.

Lim, G. E. & Brubaker, P. L., 2006. Glucagon-Like Peptide 1 Secretion by the L-Cell. Diabetes, Volume 55 (Supplement 2), pp. S70-S77.

Liu, L. et al., 2012. Mitochondrial outer-membrane protein FUNDC1 mediates hypoxia-induced mitophagy in mammalian cells. Nature Cell Biology, 14(2), pp. 177-185.

Liu, K., Paterson, A. J., Chin, E. & Kudlow, J. E., 2000. Glucose stimulates protein modification by O-linked GlcNAc in pancreatic β cells: Linkage of O-linked GlcNAc to β cell death. Proceedings of the National Academy of Sciences of the United States of America, 97(6), pp. 2820-2825.

Liu, L. et al., 2011. Age-associated differences in the inhibition of mitochondrial permeability transition pore opening by cyclosporine A: Age-associated differences in mPTP modulated by cyclosporine A. Acta Anaesthesiologica Scandinavica, 55(5), pp. 622-630.

Lizcano, J. M. & Alessi, D. R., 2002. The insulin signaling pathway. Current Biology, Volume 12, pp. 236-238.

Lopaschuk, G. D. et al., 2010. Myocardial fatty acid metabolism in health and disease. Physiological Reviews, 90(1), pp. 207-258.

Lowry, O. H., Rosebrough, N. J., Farr, A. L. & Randall, R. J., 1951. Protein measurement with the folin phenol reagent. The Journal of Biological Chemistry, Volume 193, pp. 265-275.

Lymn, R. W. & Taylor, E. W., 1971. Mechanism of Adenosine Triphosphate Hydrolysis by Actomyosin. Biochemistry, 10(25), pp. 4617-4624.

Madiraju, A. K., Erion, D. M., Rahimi, Y. & et al., 2014. Metformin suppresses gluconeogenesis by inhibiting mitochondrial glycerophosphate dehydrogenase. Nature, Volume 510, pp. 542-546.

Maffei, M. et al., 1995. Leptin levels in human and rodent: measurement of plasma leptin and ob RNA in obese and weight-reduced subjects. Nature Medicine, 1(11), pp. 1155-1161.

Majeski, A. E. & Dice, J. F., 2004. Mechanisms of chaperone-mediated autophagy. The International Journal of Biochemistry & Cell Biology, 36(12), pp. 2435-2444.

Malviya, N., Jain, S. & Malviya, S., 2010. Antidiabetic potential of medicinal plants. Acta Poloniae Pharmaceutica - Drug Research, 67(2), pp. 113-118.

Manning, B. D. & Cantley, L. C., 2007. Akt/PKB Signaling: Navigating Downstream. Cell, 129(7), p. 1261–1274.

Marathe, C. S., Rayner, C. K., Jones, K. L. & Horowitz, M., 2011. Effects of GLP-1 and Incretin-Based Therapies on Gastrointestinal Motor Function. Experimental Diabetes Research, Volume 2011, p. http://dx.doi.org/10.1155/2011/279530.

Marnewick, J. L. et al., 2010. Effects of rooibos (Aspalathus linearis) on oxidative stress and biochemical parameters in adults at risk for cardiovascular disease. Journal of Ethnopharmacology, 133(1), pp. 46-52.

Marquez, R. T. & Xu, L., 2012. Bcl-2:Beclin 1 complex: multiple, mechanisms regulating autophagy/apoptosis toggle switch. American Journal of Cancer Research, 2(2), pp. 214-221.

Marwick, T. H., 2006. Diabetic heart disease. Heart, Volume 92, pp. 296-300.

Matthews, D. R. et al., 1985. Homeostasis model assessment: insulin resistance and beta-cell function from fasting plasma glucose and insulin concentrations in man. Diabetologia, 28(7), pp. 412-419.

McCorry, L. K., 2007. Physiology of the Autonomic Nervous System. American Journal of Pharmaceutical Education, 71(4), p. 78.

McGarry, J. D. & Brown, N. F., 1997. The mitochondrial carnitine palmitoyl transferase system: From concept to molecular analysis. European Journal of Biochemistry, Volume 244, pp. 1-14.

McKay, D. L. & Blumberg, J. B., 2006. A Review of the Bioactivity of South African Herbal Teas: Rooibos (Aspalathus linearis) and Honeybush (Cyclopia intermedia). Phytotherapy Research, 23 August, 21(1), pp. 1-16.

McKinley, M. J. & Johnson, A. K., 2004. The Physiological Regulation of Thirst and Fluid Intake. Physiology, 19(1), pp. 1-6 DOI: 10.1152/nips.01470.2003.

McKnight, N. C. & Zhenyu, Y., 2013. Beclin 1, an Essential Component and Master Regulator of PI3K-III in Health and Disease. Current Pathobiology Reports, 1(4), pp. 231-238.

Meyer, G. et al., 2013. The Cellular Autophagy Markers Beclin-1 and LC3B-II are Increased During Reperfusion in Fibrillated Mouse Hearts. Current Pharmaceutical Design, 19(39), p. DOI: 10.2174/13816128193913112712251O.

Michael, L. F. et al., 2001. Restoration of insulin-sensitive glucose transporter (GLUT4) gene expression in muscle cells by the transcriptional coactivator PGC-1. Proceedings of the National Academy of Sciences of the United States of America, Volume 98, p. 3820–3825.

Michalik, L. et al., 2006. International union of pharmacology. LXI. Peroxisome proliferator-activated receptors. Pharmacology Reviews, 58(4), pp. 726-741.

Mihaylova, M. & Shaw, R. J., 2012. The AMP-activated protein kinase (AMPK) signaling pathway coordinates cell growth, autophagy, & metabolism. Nature Cell Biology, 13(9), p. 1016–1023.

Mizushima, N. et al., 2003. Mouse Apg16L, a novel WD-repeat protein, targets to the autophagic isolation membrane with the Apg12-Apg5 conjugate. Journal of Cell Science, Volume 116, pp. 1679-1688.

Molina, J. R. & Adjei, A. A., 2006. The Ras/Raf/MAPK Pathway. Journal of Thoracic Oncology, 1(1 DOI: http://dx.doi.org/10.1016/S1556-0864(15)31506-9), pp. 7-9.

Moore, C. X. & Cooper, G. J., 1991. Co-secretion of amylin and insulin from cultured islet beta-cells: modulation by nutrient secretagogues, islet hormones and hypoglycaemic agents. Biochemical and Biophysical Research Communications, Volume 179, pp. 1-9.

Mootha, V. K. et al., 2003. PGC-1alpha-responsive genes involved in oxidative phosphorylation are coordinately downregulated in human diabetes. Nature Genetics, Volume 34, p. 267–273.

Morgunov, I. & Srere, P., 1998. Interaction between citrate synthase and malate dehydrogenase. Journal of Biological Chemistry, 273(45), pp. 29540-29544.

Morris, R. D. et al., 1989. Obesity and heredity in the etiology of non-insulin-dependent diabetes mellitus in 32,662 adult white women. American Journal of Epidemiology, 130(1), pp. 112-121.

Mueckler, M., 1990. Family of glucose-transporter genes. Implications for glucose homeostasis and diabetes. Diabetes, 39(1), pp. 6-11.

Mueckler, M., 2001. Insulin resistance and the disruption of Glut4 trafficking in skeletal muscle. Journal of Clinical Investigation, 107(10), p. 1211–1213.

Muhlestein, J. B. et al., 2003. Effect of fasting glucose levels on mortality rate in patients with and without diabetes mellitus and coronary artery disease undergoing percutaneous coronary intervention. American Heart Journal, Volume 146, pp. 351-358.

Muller, C. J. F. et al., 2012. Acute assessment of an aspalathin-enriched green rooibos (Aspalathus linearis) extract with hypoglycemic potential. Phytomedicine, 15(20 (1)), pp. 32-39.

Murphy, E. & Steenbergen, C., 2008. Mechanisms underlying acute protection from cardiac ischemia-reperfusion injury. Physiology Reviews, Volume 88, pp. 581-609.

Nagoshi, T. et al., 2011. Optimization of Cardiac Metabolism in Heart Failure. Current Pharmaceutical Design, 17(35), pp. 3846-3853.

Nakatogawa, H., 2013. Two ubiquitin-like conjugation systems that mediate membrane formation during autophagy. Essays in Biochemistry, Volume 55, pp. 39-50.

Napoli, C. et al., 1997. Glycosylation enhances oxygen radical-induced modifications and decreases acetylhydrolase activity of human low-density lipoprotein. Basic Research in Cardiology, Volume 92, pp. 96-105.

Näslund, E. et al., 1999. GLP-1 slows solid gastric emptying and inhibits insulin, glucagon, and PYY release in humans. American Journal of Physiology, 277(3), pp. 910-916.

National Institute of Diabetes and Digestive and Kidney Diseases, 2009. Prediabetes & Insulin Resistance. [Online] Available at: https://www.niddk.nih.gov/health-information/diabetes/overview/what-is-diabetes/prediabetes-insulin-resistance [Accessed 14 March 2017].

Nazim, U. M. et al., 2016. Activation of autophagy flux by metformin downregulates cellular FLICE–like inhibitory protein and enhances TRAIL- induced apoptosis. Oncotarget, 7(17), pp. 23468-23481.

Nelson, D. L. & Cox, M. M., 2004. Lehninger Principles of Biochemistry. 4th ed. s.l.:W. H. Freeman.

Neubauer, N. & Kulkarni, R. N., 2006. Molecular approaches to study control of glucose homeostasis. ILAR Journal, Volume 47, pp. 199-211.

Newmeyer, D. D. & Ferguson-Miller, S., 2003. Mitochondria: releasing power for life and unleashing the machineries of death. Cell, Volume 112, pp. 481-490.

Nishikawa, T. & Araki, E., 2007. Impact of mitochondrial ROS production in the pathogenesis of diabetes mellitus and its complications. Antioxidants & Redox Signaling, Volume 9, pp. 343-353.

Nordlie, R. C., Foster, J. D. & Lange, A. J., 1999. Regulation of glucose production by the liver. Annual Review of Nutrition, Volume 19, pp. 379-406.

Nordqvist, C., 2013. Why BMI is inaccurate and misleading. [Online] Available at: http://www.medicalnewstoday.com/articles/265215.php [Accessed 11 04 2017].

Nourbakhsh, M. et al., 2017. Evaluation of Plasma TRB3 and Sestrin 2 Levels in Obese and Normal-Weight Children. Child Obesity, 13(5), pp. 409-414.

Nourooz-Zadeh, J. et al., 1997. Relationships between plasma measures of oxidative stress and metabolic control in NIDDM. Diabetologia, Volume 40, pp. 647-653.

Okuno, D., Iino, R. & Noji, H., 2011. JB Review Rotation and structure of FoF1-ATP synthase. The Journal of Biochemistry, 149(6), pp. 655-664.

Opie, L. H., 2004. Heart Physiology: From Cell to Circulation. 4 ed. Lippingcott Williams and Wilkins.

Orton, R. J. et al., 2005. Computational modelling of the receptor-tyrosine-kinase-activated MAPK pathway. Biochemical Journal, 392(Part 2), p. 249–261.

Owen, M. R., Doran, E. & Halestrap, A. P., 2000. Evidence that metformin exerts its anti-diabetic effects through inhibition of complex 1 of the mitochondrial respiratory chain. Biochemical Journal, 348(Part 3), pp. 607-614.

Pan American Health Organization, 2012. Obesity as a Precursor to Diabetes. [Online] Available at: http://www.paho.org/hq/index.php?option=com_content&view=article&id=6718%3A2012-obesity-as-precursor-diabetes&catid=4475%3Adiabetes-content2&Itemid=39448&lang=en [Accessed 16 2 2017].

Panth, N., Paudel, K. R. & Parajuli, K., 2016. Reactive Oxygen Species: A Key Hallmark of Cardiovascular Disease. Advances in Medicine, Article ID 9152732(http://dx.doi.org/10.1155/2016/9152732).

Pantsi, W. G. et al., 2011. Rooibos (Aspalathus linearis) offers cardiac protection against ischaemia/reperfusion in the isolated perfused rat heart. Phytomedicine, 18(14), pp. 1220-1228.

Parikh, N. H., Parikh, P. K. & Koth, C., 2014. Indigenous plant medicines for health care: treatment of Diabetes mellitus and hyperlipidemia. Chinese Journal of Natural Medicines, 12(5), pp. 335-344.

Parmigiani, A. et al., 2014. Sestrins inhibit mTORC1 kinase activation through the GATOR complex. Cell Reports, 9 (doi:10.1016/j.celrep.2014.10.019), pp. 1281-1291.

Pasha, M. et al., 2017. Sestrin2 as a Novel Biomarker and Therapeutic Target for Various Diseases. Oxidative Medicine and Cellular Longevity, Volume 2017, p. Article ID 3296294.

Petersen, K. F. et al., 2004. Impaired mitochondrial activity in the insulin-resistant offspring of patients with type 2 diabetes. The New England Journal of Medicine, Volume 350, pp. 664-671.

Pickup, J. C., Mattock, M. B., Chusney, G. D. & Burt, D., 1997. NIDDM as a disease of the innate immune system: association of acute-phase reactants and interleukin-6 with metabolic syndrome X. Diabetologia, Volume 40, pp. 1286-1292.

Pouliot, M. C. et al., 1994. Waist circumference and abdominal sagittal diameter: best simple anthropometric indexes of abdominal visceral adipose tissue accumulation and related cardiovascular risk in men and women. The American Journal of Cardiology, 73(7), pp. 460-468.

Puigserver, P. & Spiegelman, B. M., 2003. Peroxisome proliferator-activated receptor-gamma coactivator 1 alpha (PGC-1 alpha): transcriptional coactivator and metabolic regulator. Endocrine Reviews, Volume 24, p. 78–90.

Quinsay, M. N., Thomas, R. L., Lee, Y. & Gustafsson, A. B., 2010. Bnip3-mediated mitochondrial autophagy is independent of the mitochondrial permeability transition pore. Autophagy, 6(7), pp. 855-862.

Radziuk, J., McDonald, T. J., Rubenstein, D. & Dupre, J., 1978. Initial splanchnic extraction of ingested glucose in normal man. Metabolism, 27(6), pp. 657-669.

Redmann, M. et al., 2017. Inhibition of autophagy with bafilomycin and chloroquine decreases mitochondrial quality and bioenergetic function in primary neurons. Redox Biology, Volume 11, pp. 73-81.

Reggiori, F. & Klionsky, D. J., 2002. Autophagy in the Eukaryotic Cell. Eukaryotic Cell., 1(1), pp. 11-21.

Rhee, S. G. & Bae, S. H., 2015. The antioxidant function of Sestrins is mediated by promotion of autophagic degradation of Keap1 and Nrf2 activation and by inhibition of mTORC1. Free Radical Biology and Medicine, 88(Part B), pp. 205-211.

Rinaldi, S. et al., 2016. A Comprehensive Review of the Literature Supporting Recommendations from the Canadian Diabetes Association for the Use of a Plant-Based Diet for Management of Type 2 Diabetes. Canadian Journal of Diabetes, Volume 40, pp. 471-477.

Rice, S. C. & Luo, E. K., 2017. Antidiuretic Hormone (ADH) Test. [Online] Available at: https://www.healthline.com/health/adh#overview1 [Accessed 27 11 2017].

Richardson, A. P., & Halestrap, A. P. (2016). Quantification of active mitochondrial permeability transition pores using GNX-4975 inhibitor titrations provides insights into molecular identity. Biochemical Journal, 473(9), 1129-1140.

Rines, A. K. & Ardehali, H., 2014. Assessment of Mitochondrial Function in Isolated Cells. Oxford, UK: John Wiley & Sons, Ltd.

Rivera, L. et al., 2008. Quercetin ameliorates metabolic syndrome and improves the inflammatory status in obese Zucker rats. Obesity (Silver Spring, Md.), 16(9), pp. 2081-2087.

Rogatzki, M. J., Ferguson, B. S., Gladden, L. B. & Goodwin, M. L., 2015. Lactate is always the end-product of glycolysis. Frontiers in Neuroscience, 9(22), p. doi: 10.3389/fnins.2015.00022.

Roland, J., 2016. Symptoms of Insulin Resistance. [Online] Available at: http://www.healthline.com/health/diabetes/insulin-resistance-symptoms#Overview1 [Accessed 05 05 2017].

Roland, J. & Marcin, J., 2017. Signs of Insulin Resistance. [Online] Available at: https://www.healthline.com/health/diabetes/insulin-resistance-symptoms#2 [Accessed 8 11 2017].

Rondinone, C. M. et al., 1997. Insulin receptor substrate (IRS) 1 is reduced and IRS-2 is the main docking protein for phosphatidylinositol 3-kinase in adipocytes from subjects with non-insulindependent diabetes mellitus. Pharmacology, Volume 94, pp. 4171-4175.

Rosenson, R. S., 2004. Clinical role of LDL and HDL subclasses and apolipoprotein measurement. ACC Current Journal Reviews, Volume May, pp. 33-37.

Rother, K. I., 2007. Diabetes Treatment — Bridging the Divide. The New England Journal of Medicine, 356(15), pp. 1499-1501.

Rotter, V., Nagaev, I. & Smith, U., 2003. Interleukin-6 (IL-6) induces insulin resistance in 3T3-L1 adipocytes and is, like IL-8 and tumor necrosis factor-alpha, overexpressed in human fat cells from insulin-resistant subjects. Journal of Biological Chemistry, 278(46), pp. 45777-45784.

Ruderman, N. B., Carling, D., Prentki, M. & Cacicedo, J. M., 2013. AMPK, insulin resistance, and the metabolic syndrome. The Journal of Clinical Investigation, 123(7), pp. 2764-2772.

Saito, T. & Sadoshima, J., 2015. The Molecular Mechanisms of Mitochondrial Autophagy/ Mitophagy in the Heart. Circulation Research, 116(8), p. 1477–1490.

Sakamoto, K. & Holman, G. D., 2008. Emerging role for AS160/TBC1D4 and TBC1D1 in the regulation of GLUT4 traffic. American Journal of Physiology - Endocrinology and Metabolism, 295(1), pp. E29-E37.

Saltiel, A. R. & Kahn, C. R., 2001. Insulin signalling and the regulation of glucose and lipid metabolism. Nature, 414(6865), pp. 799-806.

Sattar, N. et al., 2006. Adiponectin and coronary heart disease: a prospective study and meta-analysis. Circulation., 114(7), pp. 623-629.

Schagger, H., Cramer, W. A. & Vonjagow, G., 1994. Analysis of Molecular Masses and Oligomeric States of Protein Complexes by Blue Native Electrophoresis and Isolation of Membrane Protein Complexes by Two-Dimensional Native Electrophoresis. Analytical Biochemistry, 217(2), pp. 220-230.

Scheepers, A., Joost, H.-G. & Schürmann, A., 2004. The Glucose Transporter Families SGLT and GLUT: Molecular Basis of Normal and Aberrant Function. Journal of Parenteral and Enteral Nutrition, 28(5), pp. 364-371.

Schulz, H., Joubert, E. & Schütze, W., 2003. Quantification of quality parameters for reliable evaluation. [Online] Available at: https://www.researchgate.net/publication/225603036_Quantification_of_quality_parameters_for_reliable_evaluation_of_green_rooibos_Aspalathus_linearis [Accessed 15 February 2016].

Sharifi, M. N., Mowers, E. E., Drake, L. E. & Macleod, K. F., 2015. Measuring Autophagy in Stressed Cells. Methods in Molecular Biology, Volume 1292, pp. 129-150.

Shen, G. X., 2007. Lipid disorders in diabetes mellitus and current management. Current Pharmaceutical Design, Volume 3, pp. 17-24.

Shen, H. M. & Mizushima, N., 2014. At the end of the autophagic road: an emerging understanding of lysosomal functions in autophagy. Trends in Biochemical Science, 39(2), pp. 61-71.

Shibata, R., Ouchi, N. & Murohara, T., 2009. Adiponectin and cardiovascular disease. Circulation Journal, 73(4), pp. 608-614.

Sileikyte, J., Petronilli, V., Zulian, A., Dabbeni-Sala, F., Tognon, G., Nikolov, P., . . . Ricchelli, F. (2011). Regulation of the inner membrane mitochondrial permeability transition by the outer membrane translocator protein (peripheral benzodiazepine receptor). Journal of Biological Chemistry, 286, 1046-1053.

Shires, S. E. & Gustaffson, B., 2015. Mitophagy and Heart Failure. Journal of Molecular Medicine, 93(3), pp. 253-262.

Smith, S. E., Smith, S. A. & Brown, P. M., 1981. Cardiac autonomic dysfunction in patients with diabetic retinopathy. Diabetologia, Volume 21, pp. 525-528.

Smit, S. E., Johnson, R., Van Vuuren, M. A. & Huisamen, B., 2017. Myocardial Glucose Clearance by Aspalathin Treatment in Young, Mature, and Obese Insulin-Resistant Rats. Planta Medica, pp. DOI: 10.1055/s-0043-117415.

Sohal, R. S. & Sohal, B. H., 1991. Hydrogen peroxide release by mitochondria increases during aging. Mechanisms of Ageing and Development, Volume 57, pp. 187-202.

Song, G., Ouyang, G. & Bao, S., 2005. The activation of Akt/PKB signaling pathway. Journal of Cellular and Molecular Medicine, 9(1), pp. 59-71.

South African Rooibos Council, 2016. ROOIBOS INDUSTRY FACT SHEET 2016. [Online] Available at: http://sarooibos.co.za/wp/wp-content/uploads/2016/10/20160930-SARC-Fact-Sheet-final.pdf [Accessed 20 7 2017].

Spero, D., 2016. What Is Normal Blood Sugar Level? Diabetes Self-Management - David Spero's Blog, 13 January.

Spiegelman, B. M. & Flier, J. S., 2001. Obesity and the Regulation of Energy Balance. Cell, Volume 104, pp. 531-543.

Srere, P. A., 1969. Citrate Synthase. Methods in Enzymology, Volume 13, pp. 3-11.

Stanley, W., Recchia, F. A. & Lopaschuk, G. D., 2005. Myocardial Substrate Metabolism in the Normal and Failing Heart. Physiological Reviews, Volume 85, pp. 1093-1129.

Stefan, J., 2015. The heart: our first organ. [Online] Available at: http://www.eurostemcell.org/heart-our-first-organ [Accessed 10 6 2017].

Street, R. A. & Prinsloo, G., 2013. Commercially Important Medicinal Plants of South Africa: A Review. Journal of Chemistry, 2013(Article ID: 205048), pp. 1-16.

Stryer, L., 1995. Oxidative Phosphorylation. In: Biochemistry. New York: W.H. Freeman and Company, pp. 537-549.

Sumiyoshi, M., Sakanaka, M. & Kimura, Y., 2006. Chronic Intake of High-Fat and High-Sucrose Diets Differentially Affects Glucose Intolerance in Mice. The Journal of Nutrition, 136(3), pp. 582-587.

Su, Y. et al., 2012. Voltage-dependent Anion Channels (VDACs) Recruit Parkin to Defective Mitochondria to Promote Mitochondrial Autophagy. The Journal of Biological Chemistry, 287(48), p. 40652–40660.

Szabó, I., De Pinto, V., & Zoratti, M. (1993). The mitochondrial permeability transition pore may comprise VDAC molecules. II. The electrophysiological properties of VDAC are compatible with those of the mitochondrial megachannel. Federation of Euopean Biochemical Societies, 330(2), 206-210.

Tabák, A. G. et al., 2012. Prediabetes: A high-risk state for developing diabetes. Lancet, 379(9833), pp. 2279-2290.

Tahrani, A. A., Barnett, A. H. & Bailey, C. J., 2013. SGLT inhibitors in management of diabetes. Lancet Diabetes Endocrinology, Volume 1, pp. 140-151.

Tanida, I., Ueno, T. & Kominami, E., 2008. LC3 and Autophagy. Methods in Molecular Biology, Volume 445, pp. 77-88.

Taskiran, M. et al., 2002. Decreased myocardial perfusion reserve in diabetic autonomic neuropathy. Diabetes, Volume 51, pp. 3306-3310.

The Heart and Stroke Foundation South Africa, 2016. National Obesity Week: South Africa's weighty problem. [Online] Available at: http://www.heartfoundation.co.za/media-releases/national-obesity-week-south-africa%E2%80%99s-weighty-problem [Accessed 16 2 2017].

Thorens, B. & Mueckler, M., 2009. Glucose transporters in the 21 Century. American Journal of Physiology. Endocrinology and Metabolism., Volume 298, pp. E141-5. 10.1152/ajpendo.00712.2009.

Tooke, J. E., 1989. Microcirculation and diabetes. British Med Bull, Volume 45, pp. 206-223.

Torpy, J. M., Cassio, L. & Glass, R. M., 2007. Chronic Stress and the Heart. JAMA., 298(14 doi:10.1001/jama.298.14.1722), p. 1722.

Tran, H., Brunet, A., Griffith, E. C. & Greenberg, M. E., 2003. The many forks in FOXO's road. Science's STKE: signal transduction knowledge environment, 2003(172).

Trayhurn, P. & Bing, C., 2006. Appetite and energy balance signals from adipocytes. Philosophical Transactions of the Royal Society B: Biological Sciences, 361(1471), pp. 1237-1249.

Trayhurn, P. & Wood, I. S., 2005. Signalling role of adipose tissue: adipokines and inflammation in obesity. Biochemical Society Transactions, Volume 33, pp. 1078-1081.

Tsai, M. et al., 2016. Dual functions of a small regulatory subunit in the mitochondrial calcium uniporter complex. eLife 2016;5:e15545 doi: 10.7554/eLife.15545. [Online] Available at: https://elifesciences.org/articles/15545#digest [Accessed 11 July 2017].

Tzagoloff, A., 1982. The Electron Transfer Chain; Cytochrome Oxidase; Oxidative Phosphorylation. In: Mitochondria. New York: Plenum Press, pp. 39-156.

Unger, R. H., Aguilar-Parada, E., Muller, W. A. & Eisentraut, A. M., 1970. Studies of Pancreatic Alpha Cell Function in Normal and Diabetic Subjects. Journal of Clinical Investigation, Volume 49, pp. 837-848.

Vallance, P. & Norman, C., 2001. Endothelial function and nitric oxide: clinical relevance. Heart, 85(3), pp. 342-350.

Van Den Brom, C. E. et al., 2013. Diabetes, perioperative ischaemia and volatile anaesthetics: consequences of derangements in myocardial substrate metabolism. Cardiovascular Diabetology, 12(42), p. http://www.cardiab.com/content/12/1/42.

Vander Heiden, M. G., Li, X. X., Gottleib, R. B., Hill, C. B., Thompson, M., & Colombini, M. (2001). Bcl-xL promotes the open configuration of the voltage-dependent anion channel and metabolite passage through the outer mitochondrial membrane. Journal of Biological Chemistry, 276, 19414-19419.

Varanyuwatana, P., & Halestrap, A. P. (2012). The roles of phosphate and the phosphate carrier in the mitochondrial permeability transition pore. Mitochondrion, 12, 120-125.

Varshavsky, A., 1996. The N-end rule: functions, mysteries, uses. Proceedings of the National Academy of Sciences of the United States of America, 93(22), pp. 12142-12149.

Voet, D., Voet, J. G. & Pratt, C. W., 2006. Fundamentals of Biochemistry: Life at the Molecular Level. 4th Edition ed. New York: John Wiley and Sons.

Vos, M., Verstreken, P. & Klein, C., 2015. Stimulation of electron transport as potential novel therapy in Parkinson's disease with mitochondrial dysfunction. Biochemical Society Transactions, 43(2), pp. 275-279.

Walls, K. C. et al., 2009. bcl-2/Adenovirus E1B 19 kDa Interacting Protein-3 (BNIP3) Regulates Hypoxia-Induced Neural Precursor Cell Death. Journal of Neuropathology & Experimental Neurology, 68(12), pp. 1326-1338.

Wang, Y. et al., 2005. Comparison of abdominal adiposity and overall obesity in predicting risk of type 2 diabetes among men. The American Journal of Clinical Nutrition, 81(3), pp. 555-563.

Ward, C., 2016. Metabolic pathways [internet]. Diapedia 5105765817 rev. no. 25., 19 January.Volume Available from: https://doi.org/10.14496/dia.5105765817.25.

Watson, R. T. & Pessin, J. E., 2006. Bridging the GAP between insulin signaling and GLUT4 translocation. Trends in Biochemical Sciences, 31(4), pp. 215-222.

Watts, R. L. & Koller, W. C., 2004. Mitochondria in movement disorders. In: Movement Disorders. 2nd ed. New York: McGraw Hill, pp. 61-86.

WebMD, 2016. Heart Disease and Stress: What's the Link? [Online] Available at: http://www.webmd.com/heart-disease/guide/stress-heart-disease-risk [Accessed 23 3 2017].

Weinberg, J. M., Venkatachalam, M. A., Roeser, N. F. & Nissim, I., 2000. Mitochondrial dysfunction during hypoxia/reoxygenation and its correction by anaerobic metabolism of citric

acid cycle intermediates. Proceedings of the National Academy of Sciences of the United States of America, 97(6), p. 2826–2831.

Weir, M., 2007. Microalbuminuria and cardiovascular disease. Clinical Journal of the American Society of Nephrology, Volume 2, p. 581–590.

Wellen, K. E. & Hotamisligil, G. S., 2005. Inflammation, stress, and diabetes. The Journal of Clinical Investigation, 115(5 doi: 10.1172/JCI200525102), pp. 1111-1119.

Weyrich, A. S., Prescott, S. M. & Zimmerman, G. A., 2002. Platelets, endothelial cells, inflammatory chemokines, and restenosis: signaling in the vascular play book. Circulation, Volume 106, pp. 1433-1435.

White, M. F., 1997. The insulin signalling system and the IRS proteins. Diabetologia, Issue 40, p. S2–S17.

Whiteman, E. I., Cho, H. & Bimbaum, M. J., 2002. Role of Akt/protein kinase B in metabolism. Trends in Endocrinology and Metabolism, Volume 13, p. 444–451.

WHO Fact Sheet No: 311, 2016. Obesity and Overweight. [Online] Available at: http://www.who.int/mediacentre/factsheets/fs311/en/ [Accessed 14 February 2017].

Williams, S. B. et al., 1998. Acute hyperglycemia attenuates endothelium-dependent vasodilation in humans *in vivo*. Circulation, Volume 97, pp. 1695-1998.

Woodcock, E. A. & Matkovich, S. J., 2005. Cardiomyocytes structure, function and associated pathologies. The International Journal of Biochemistry & Cell Biology, 37(9), pp. 1746-1751.

Woods, M. et al., 1999. Endothelin-1 is induced by cytokines in human vascular smooth muscle cells: evidence for intracellular endothelin-converting enzyme. Molecular Pharmacology, Volume 55, pp. 902-909.

World Health Organization, 2008. Waist Circumference and Waist-Hip Ratio. [Online]

Available at: http://apps.who.int/iris/bitstream/10665/44583/1/9789241501491_eng.pdf [Accessed 14 04 2017].

Wullschleger, S., Loewith, R. & Hall, M. N., 2006. TOR signaling in growth and metabolism. Cell, Volume 124, pp. 471-484.

Wu, W. et al., 2014. ULK1 translocates to mitochondria and phosphorylates FUNDC1 to regulate mitophagy. EMBO Reports, 15(5), pp. 566-575.

Yamano, K. & Youle, R. J., 2013. PINK1 is degraded through the N-end rule pathway. Autophagy, 9(11), pp. 1758-1769.

Yamauchi, T. et al., 2002. Adiponectin stimulates glucose utilization and fatty-acid oxidation by activating AMP-activated protein kinase. Nature Medicine, 8(11), pp. 1288-1295.

Yang, Y. et al., 2014. Sestrin2 decreases renal oxidative stress, lowers blood pressure, and mediates dopamine D2 receptor-induced inhibition of reactive oxygen species production. Hypertension, 64(doi:10.1161/HYPERTENSIONAHA.114.03840), pp. 825-832.

Yoon, J. C. et al., 2001. Control of hepatic gluconeogenesis through the transcriptional coactivator PGC-1. Nature, Volume 413, p. 131–138.

Yorimitsu, T. & Klionsky, D. J., 2005. Autophagy: molecular machinery for self-eating. Cell Death Differentiation, 12(Suppl. 2), pp. 1542-1552.

Zang, M. et al., 2006. Polyphenols stimulate AMP-activated pro-tein kinase, lower lipids, and inhibit accelerated atherosclerosis in diabetic LDL receptor-deficient mice. Diabetes, Volume 55, pp. 2180-2191.

Zhou, G. et al., 2001. Role of AMP-activated protein kinase in mechanism of metformin action. Journal of Clinical Investigation, 108(8), pp. 1167-1174.

Zhou, M., Wang, A. & Yu, H., 2014. Link between insulin resistance and hypertension: What is the evidence from evolutionary biology? Diabetology & Metabolic Syndrome, 6(12), pp. https://doi.org/10.1186/1758-5996-6-12.

Zhu, Y. et al., 2013. Cardiac PI3K-Akt Impairs Insulin-Stimulated Glucose Uptake Independent of mTORC1 and GLUT4 Translocation. Molecular Endocrinology, 27(1), pp. 172-184.